PROBLEMS IN ORTHOTROPIC ELASTICITY

by

NICOLAS MOUTAFIS

A thesis submitted for the degree
of Doctor of Philosophy

Department of Civil Engineering,
The University of Aston in Birmingham

July 1975

ΣΤΟΥΣ ΓΟΝΕΙΣ ΜΟΥ

SUMMARY.

This thesis deals with the solution of certain problems in 2-dimensional, linear orthotropic elasticity theory, which are of particular interest to engineering.

The types of problems analysed, can be classified according to their geometrical configuration, into the following four categories: Layered half-plane; quarter-plane; infinite strip, and, half-plane with irregular boundary.

Solutions to problems related to the layered half-plane have been obtained using a Fourier integral approach, whereas solutions to problems related to the quarter-plane and the half-plane with irregular boundary, have been obtained using a superposition technique. This technique is an extension of the method used by Hetènyi (1960) to obtain a solution for the isotropic quarter-plane. In the case of problems related to the infinite strip, both of the above methods of solution have been used.

Salient numerical results have been presented to the problems cited earlier. In addition, the solutions of certain quarter-plane and half-plane problems have been verified experimentally through a series of laboratory conducted tests.

ACKNOWLEDGEMENTS.

I would like to express my gratitude to my supervisor Dr.A.P.S.Selvadurai, for his continuous guidance, advice and help throughout my research.

I would also like to thank the Departmental Superintendent Mr.W.Parsons and the technicians of the Department for their assistance with the experimental work. Their help is greatly appreciated.

Finally, I thank my fiancèe, Miss D.L.Epifaniou, for drawing some of the graphs, but mainly for her continuous encouragement and support.

LIST OF SYMBOLS

C_i	:	Constants.
D	:	Distance.
E_i	:	Young's modulus in i direction.
G_{ij}	:	Modulus of rigidity between i and j directions.
H	:	Distance.
P	:	Concentrated force/unit thickness.
T_x, T_y, T_z	:	Force/unit area, in x,y,z directions respectively.
W	:	Strain Energy function.
X,Y,Z	:	Orthogonal coordinate axes.
a	:	Distance; unit length.
b	:	Thickness.
c_{ij}	:	Elastic compliances.
k_1 k_2	:	Orthotropic elastic constants.
ℓ	:	Half-width of distributed loads.
ℓ_{ij}	:	Elastic compliances.
n_i	:	Direction cosines.
p	:	Stress applied normal to a plane.
q	:	Stress applied tangential to a plane.
u,v,w	:	Displacements in X,Y,Z directions respectively.
v_i	:	Volume fraction.
x,y,z	:	Orthogonal coordinates.
$\bar{x}, \bar{y}, \bar{z}$	:	Orthogonal dimensionless coordinates.
γ_{ij}	:	Shear strain between i and j directions.
ε_i	:	Direct strain in i-direction.
μ	:	Refractive index.
ν_{ij}	:	Poisson's ratio = strain induced in j-direction/ strain in direction.
ρ_1, ρ_2	:	Constants.
σ_i	:	Direct stress in i-direction.
τ_{ij}	:	Shear stress in the i-direction on a plane specified by its normal in the j-direction.

LIST OF SYMBOLS (contd)

Φ : Stress function.

ϕ : Angle.

ψ : Load parameter.

Ω : Constant.

ASSUMPTIONS

a) Compressive stresses are denoted as positive.

b) Clockwise shear stresses on an element, are denoted as positive.

c) Displacements in the positive coordinate directions are denoted as positive.

CONTENTS

Page No.

CHAPTER 9 (contd)

CHAPTER I

INTRODUCTION

The theory of anisotropic elasticity is a mathematical model devised to describe physical response of certain materials, which exhibit directional elastic characteristics. This theory, which is based on the generalized Hooke's law of proportionality between stress and strain, has been summarized and presented in three classical books on Elasticity, by Love (1906), Green and Zerna (1954) and Lekhnitskii (1963).

In the first two books, the authors presented a general account of the theory of elasticity with special references to anisotropy, whereas Lekhnitskii dealt exclusively with the anisotropic elasticity theory and its applications. A brief summary of the theory is given in Chapter 2 of this thesis.

A special case of anisotropy, is orthotropy. In this case, the directional elastic characteristics are assumed to be symmetric about three mutually perpendicular planes. Since most naturally occurring or artificial engineering materials are orthotropic, the theory of orthotropic elasticity has received considerable attention. Many investigators have employed the theory of orthotropic elasticity to obtain solutions to 3-dimensional or 2-dimensional problems of engineering interest. Various methods of solution have been used, ranging from simple analytical, to Fourier integral or numerical methods. At this stage we shall not list the numerous important contributions. A historical background will be presented for specific problems in the introductions to the ensuing chapters.

This thesis deals with the solution of certain problems in 2-dimensional orthotropic elasticity. In particular, problems related to the layered half plane, the quarter plane, the infinite strip and the half-plane with an irregular boundary are considered.

The development of a solution to the above problems, re-

quires the solution of a number of fundamental problems which are related to the orthotropic infinite-plane and the orthotropic half-plane. A collection of such problems and their solutions is presented in Chapters 3 and 4. These solutions are not meant to be original in any way. Most of the information has been drawn from the works of Green and Taylor (1939), Green (1939), Conway (1953, 1955) and Lekhnitskii (1963). However, since these solutions form the basis of the subsequent work, they are included in the thesis.

In Chapter 5, problems related to the layered half-plane are considered. The half-plane is assumed to consist of 'n' orthotropic elastic layers and the interfaces between the layers are assumed to be either rough (perfect continuity) or perfectly smooth (frictionless interface). The method of solution to layered half-plane problems, is based on a Fourier integral representation of boundary loads. The special case of a 2-layer half-plane is examined in detail and numerical results are presented for the stress distributions along the interface when the layered half-plane is subjected on its boundary to a normal concentrated force. The numerical results are presented for a range of orthotropic materials and the effect of orthotropy on the stress distributions are considered.

In Chapter 6, a method of solution is developed for problems related to the orthotropic elastic quarter-plane. This method is based on a superposition technique developed by Hetènyi, for the solution of the isotropic elastic quarter-plane. The solution is presented in a general form, for an arbitrary loading system, which may be applied at the boundaries or at the interior of the quarter-plane. Numerical results for the stresses, are presented for the cases in which a concentrated force is applied normal to a boundary of the quarter-plane, or at the interior.

In Chapter 7, we concentrate on problems related to the

orthotropic infinite strip. A method of solution is developed for the problem in which the infinite strip is subjected to an arbitrary self-equilibrating loading system, acting at its boundaries or at the interior. This method is based on the repeated superposition of known solutions to orthotropic half-plane problems, so that the resulting stress field satisfies the traction boundary conditions of the infinite strip. This procedure leads to a sequence of infinite integrals of recursive pattern. Numerical results are presented for the case of an orthotropic infinite strip which is subjected at its interior to two equal and opposite concentrated forces acting a small distance apart, in the longitudinal or in the transverse direction.

The problem of an infinite strip which is subjected on its boundaries to equal and opposite loading systems, is dealt with separately, using a Fourier integral technique. Due to the symmetry of loading, this problem is equivalent to that of an elastic layer resting on a smoothrigid bed. Green's (1939) method of solution, for problems of this type, is employed to obtain numerical results for the stress distributions along the axes of symmetry, when the infinite strip is subjected to concentrated or partially distributed uniform loads. The way in which the orthotropy of the material affects the stress distributions is examined in detail, by considering a number of orthotropic materials.

In Chapter 8, we consider the problem of an orthotropic elastic half-plane with an irregular boundary in the form of a 'step', which is subjected to an arbitrary loading system. The proposed method of solution to this type of problem, is an extension of the superposition technique used by Hetènyi for the solution of the isotropic elastic quarter-plane. The method consists of successive reversals of stress on certain planes of an orthotropic half-plane and the superposition of the corresponding solutions, so that after a number of reversals, the resulting stress field satisfies the

traction boundary conditions of the irregular half-plane.

In Chapter 9, we describe the experimental work that was carried out, with the objective of investigating the applications of various solutions, in predicting stress or strain fields in real orthotropic materials. The work consisted of a series of tests under plane strain and plane stress conditions, using a laminated rubber and a glass reinforced polyester resin as orthotropic materials.

The problems considered in this thesis, are of particular interest to Civil Engineering since they represent cases which may be encountered in Civil Engineering practice. For example, the use of fibre-reinforced composites as structural materials in the construction and aerospace industries and the treatment of many types of rocks or soils as anisotropic materials, present a variety of problems. The analysis of these problems, using the theory of anisotropic elasticity, results in a better assessment of the behaviour of the materials under load and consequently in a more economical design.

CHAPTER 2

THEORY OF ANISOTROPIC ELASTICITY.

2.1) Introduction.

In this chapter, we shall describe the fundamental concepts of the theory of anisotropic elasticy and its applications to real materials.

The theory of elasticity is essentially a mathematical model devised to describe physical response of materials, and is based on laws of proportionality between stress and strain. The relation between stress and stain can either be linear (directly proportional) or non-linear, but we shall limit our discussion on the former case.

The development of the theory requires that:

a) At any point in an elastically deforming body, the stresses are in a state of equilibrium.

b) The displacements are continuous within the boundaries of the body.

Additionally, the bodies to which the theory is applicable, are assumed to be continuous homogeneous media; and that all elastic deformations take place under isothermal or adiabatic conditions.

2.2) State of stress in a body.

The state of stress at a given point of a body is uniquely determined by six stress components on three mutually perpendicular planes passing through that point.

Assuming the planes to be perpendicular to the Cartesian coordinate axes X,Y,Z:

a) the normal stresses in the X,Y,Z directions are denoted by σ_x, σ_y, σ_z respectively; and are assumed to be positive if compressive and negative if tensile; and

b) the shear stresses on XY, YZ, ZX planes are denoted by τ_{xy}, τ_{yz}, τ_{zx} respectively.

The stress components satisfy the equilibrium eqnations, which in the absence of body forces reduce to:

$$\begin{aligned} \frac{\partial \sigma_x}{\partial x} + \frac{\partial \tau_{xy}}{\partial y} + \frac{\partial \tau_{zx}}{\partial z} &= 0, \\ \frac{\partial \tau_{xy}}{\partial x} + \frac{\partial \sigma_y}{\partial y} + \frac{\partial \tau_{yz}}{\partial z} &= 0, \\ \frac{\partial \tau_{zx}}{\partial x} + \frac{\partial \tau_{yz}}{\partial y} + \frac{\partial \sigma_z}{\partial z} &= 0. \end{aligned} \qquad 2.2\text{-}1$$

At points on the boundaries of a body, the stress components should be in equilibrium with the externally applied loads. This condition is expressed by the following relations:

$$\begin{aligned} T_x &= n_x \sigma_x + n_y \tau_{xy} + n_z \tau_{zx}, \\ T_y &= n_x \tau_{xy} + n_y \sigma_y + n_z \tau_{yz}, \\ T_z &= n_x \tau_{zx} + n_y \tau_{yz} + n_z \sigma_z, \end{aligned} \qquad 2.2\text{-}2$$

where T_x, T_y, T_z denote the components of external forces per unit area in the X,Y, Z directions respectively, and n_x, n_y, n_z are the direction cosines of the outward normal to the boundary at the point considered.

The displacement of a point in a body undergoing

2.2) contd.

elastic deformation is represented by three components u,v,w in the positive X,Y,Z directions respectively.

The state of deformation in the neighbourhood of a given point, is characterized by six components of strain, which can be expressed in terms of displacements u,v,w. In the case of small strains, when the derivatives of displacements are small compared with unity, the relations are:

$$\varepsilon_x = \frac{\partial u}{\partial x}, \qquad \gamma_{xy} = \frac{\partial u}{\partial y} + \frac{\partial v}{\partial x},$$
$$\varepsilon_y = \frac{\partial v}{\partial y}, \qquad \gamma_{yz} = \frac{\partial v}{\partial z} + \frac{\partial w}{\partial y}, \qquad 2.2\text{-}3$$
$$\varepsilon_z = \frac{\partial w}{\partial z}, \qquad \gamma_{zx} = \frac{\partial w}{\partial x} + \frac{\partial u}{\partial z},$$

where ε_x, ε_y, ε_z are the normal strains in the X,Y,Z directions, and γ_{xy}, γ_{yz}, γ_{zx} are the shear strains on XY, YZ, ZX planes.

For the integrability of equations (2.2-3), the strain components should satisfy the compatibility conditions expressed by the following six relations:

$$\frac{\partial^2 \varepsilon_x}{\partial y^2} + \frac{\partial^2 \varepsilon_y}{\partial x^2} = \frac{\partial^2 \gamma_{xy}}{\partial x \partial y}, \qquad 2.2\text{-}4$$

$$\frac{2\partial^2 \varepsilon_x}{\partial y \partial z} = \frac{\partial}{\partial x}\left[- \frac{\partial \gamma_{yz}}{\partial x} + \frac{\partial \gamma_{xz}}{\partial y} + \frac{\partial \gamma_{xy}}{\partial z} \right].$$

The other four equations can be obtained by interchanging the subscripts x,y,z in cyclic order.

2.3) Stress-strain relations and energy function.

The effects of the elastic properties of the body on the stress and strain distribution, are introduced by the stress-strain relations. The relations are based on the generalized Hooke's law, that each component of strain is a linear function of the six components of stress. Thus 36

2.3) contd.

independent constants of proportionality are necessary for the most general linear relation between stress and strain.

In matrix form the relations are:

$$\begin{bmatrix} \varepsilon_x \\ \varepsilon_y \\ \varepsilon_z \\ \gamma_{yz} \\ \gamma_{zx} \\ \gamma_{xy} \end{bmatrix} = \begin{bmatrix} c_{11} & c_{12} & c_{13} & \cdots & c_{16} \\ c_{21} & & & & \vdots \\ c_{31} & & & & \vdots \\ \vdots & & & & \vdots \\ c_{61} & \cdots & \cdots & \cdots & c_{66} \end{bmatrix} \begin{bmatrix} \sigma_x \\ \sigma_y \\ \sigma_z \\ \tau_{yz} \\ \tau_{zx} \\ \tau_{xy} \end{bmatrix} \qquad 2.3\text{-}1$$

The 36 constants c_{ij} (for $i = 1 \ldots 6, j = 1 \ldots 6$) will be referred to as elastic compliances. Existence of a strain energy function W, such that

$$\sigma_x = \frac{\partial W}{\partial \varepsilon_x}, \quad \sigma_y = \frac{\partial W}{\partial \varepsilon_y} \quad \ldots \text{ etc},$$

gives

$$c_{ij} = c_{ji}, \qquad 2.3\text{-}2$$

thus reducing the number of independent elastic compliances to 21.

For an elastic material, the form of the compliance matrix c_{ij} changes with the choice of the reference coordinate system.

The energy function can be employed as a criterion for the distinction of materials into isotropic and anisotropic categories. If the strain energy function remains unchanged for a rigid body transformation of the reference coordinate system, the material of the body is said to be isotropic, otherwise is called anisotropic.

2.4) Elastic Symmetry

When a body possesses symmetry of internal structure, its elastic properties expressed by means of its elastic compliances, should show this symmetry, and the stress-strain

2.4) contd.

relations for the symmetric cases should be identical.

To obtain relations between the elastic compliances, introduced by the elastic symmetry of the body, one has to consider the strain energy function. For the symmetric cases, the strain energy per unit volume should be the same; and for the equality to be fulfilled some of the elastic compliances must be equal to zero.

We shall limit our discussion to only the following cases of elastic symmetry:

1) Orthotropic symmetry,

2) Transversely isotropic symmetry,

3) Isotropic symmetry.

2.4.1) Three planes of elastic symmetry (orthotropy).

An orthotropic material is one which possesses three orthogonal planes of symmetry. If the axes of orthotropy (perpendicular to the planes) coincide with the reference coordinate axes X,Y,Z, the stress strain relations (2.3-1) reduce to:

$$\begin{bmatrix} \varepsilon_x \\ \varepsilon_y \\ \varepsilon_z \\ \gamma_{yz} \\ \gamma_{zx} \\ \gamma_{xy} \end{bmatrix} = \begin{bmatrix} c_{11} & c_{12} & c_{13} & & & \\ c_{21} & c_{22} & c_{23} & & & \\ c_{31} & c_{32} & c_{33} & & & \\ & & & c_{44} & & \\ & & & & c_{55} & \\ & & & & & c_{66} \end{bmatrix} \begin{bmatrix} \sigma_x \\ \sigma_y \\ \sigma_z \\ \tau_{yz} \\ \tau_{zx} \\ \tau_{xy} \end{bmatrix}. \qquad 2.4\text{-}1$$

It is convenient for purpose of comparison to introduce the following definitions of the elastic compliances c_{ij}; we shall write (2.4-1) as:

2.4.1) contd.

$$\begin{bmatrix} \varepsilon_x \\ \varepsilon_y \\ \varepsilon_z \end{bmatrix} = \begin{bmatrix} \frac{1}{E_x} & -\frac{\nu_{yx}}{E_y} & -\frac{\nu_{zx}}{E_z} \\ -\frac{\nu_{xy}}{E_x} & \frac{1}{E_y} & -\frac{\nu_{zy}}{E_z} \\ -\frac{\nu_{xz}}{E_x} & -\frac{\nu_{yz}}{E_y} & \frac{1}{E_y} \end{bmatrix} \begin{bmatrix} \sigma_x \\ \sigma_y \\ \sigma_z \end{bmatrix}, \qquad 2.4\text{-}2a$$

and

$$\begin{bmatrix} \gamma_{yz} \\ \gamma_{zx} \\ \gamma_{xy} \end{bmatrix} = \begin{bmatrix} \frac{1}{G_{yz}} & & \\ & \frac{1}{G_{zx}} & \\ & & \frac{1}{G_{xy}} \end{bmatrix} \begin{bmatrix} \tau_{yz} \\ \tau_{zx} \\ \tau_{xy} \end{bmatrix}, \qquad 2.4\text{-}2b$$

where

E_i : Young's modulus in i-direction,

ν_{ij} : Poisson's ration - Ratio of strain induced in j-direction by strain in i-direction,

G_{ij} : Modulus of rigidity between i and j directions.

From the symmetry requirement (2.3-2), it follows that:

$$\frac{\nu_{xy}}{E_x} = \frac{\nu_{yx}}{E_y} \; ; \; \frac{\nu_{zx}}{E_z} = \frac{\nu_{xz}}{E_x} \; ; \; \frac{\nu_{zy}}{E_z} = \frac{\nu_{yz}}{E_y}. \qquad 2.4\text{-}3$$

The engineering elastic constants must satisfy the following conditions (see B.M.Lempriere (1968)).

$$E_x, E_y, E_z, G_{xy}, G_{yz}, G_{zx} > 0 \; , \qquad 2.4\text{-}4a$$

$$\left| \nu_{ij} \right| < (E_i/E_j)^{\frac{1}{2}} \; , \qquad 2.4\text{-}4b$$

$$\nu_{xy} \cdot \nu_{yz} \cdot \nu_{zx} < \tfrac{1}{2} \, . \qquad 2.4\text{-}4c$$

For orthotropic bodies, nine independent elastic compliances or engineering constants are necessary to describe its elastic behaviour.

2.4.2) One axis of elastic symmetry (transverse isotropy).

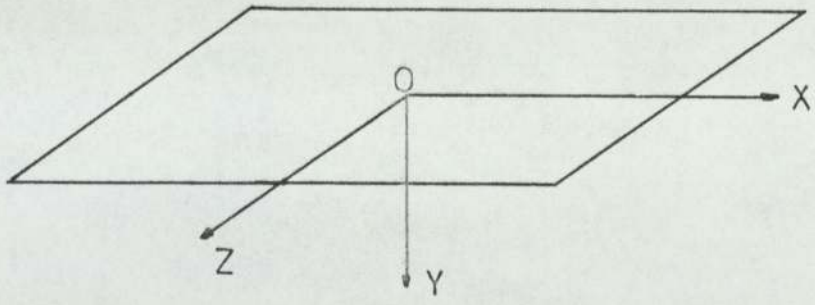

Fig.2.1

A transversely isotropic material is one for which there exists a preferred plane (XZ) (see Fig.2.1), and the form of the strain energy function remains unchanged for rotation of the reference coordinate system about an axis (Y) normal to this plane. Consequently, all directions in the preferred plane are equivalent with respect to their elastic properties.

For a transversely isotropic material therefore, the stress-strain relations (2.3-1) reduce to:

$$\begin{bmatrix} \varepsilon_x \\ \varepsilon_y \\ \varepsilon_z \end{bmatrix} = \begin{bmatrix} \frac{1}{E_x} & -\frac{\nu_{yx}}{E_y} & -\frac{\nu_{xz}}{E_x} \\ -\frac{\nu_{xy}}{E_x} & \frac{1}{E_y} & -\frac{\nu_{xy}}{E_x} \\ \frac{\nu_{xz}}{E_x} & -\frac{\nu_{yx}}{E_y} & \frac{1}{E_x} \end{bmatrix} \begin{bmatrix} \sigma_x \\ \sigma_y \\ \sigma_z \end{bmatrix}, \qquad 2.4\text{-}5a$$

and

$$\begin{bmatrix} \gamma_{yz} \\ \gamma_{zx} \\ \gamma_{xy} \end{bmatrix} = \begin{bmatrix} \frac{1}{G_{xy}} & & \\ & \frac{1}{G_{zx}} & \\ & & \frac{1}{G_{xy}} \end{bmatrix} \begin{bmatrix} \tau_{yz} \\ \tau_{xz} \\ \tau_{xy} \end{bmatrix}. \qquad 2.4\text{-}5b$$

Again, for symmetry of ε_{ij}:

$$\frac{\nu_{xy}}{E_x} = \frac{\nu_{yx}}{E_y}. \qquad 2.4\text{-}6$$

2.4.2) contd.

In the plane of isotropy:

$$E_x = E_z \text{ and } G_{xz} = \frac{E_x}{2(1+\nu_{xz})}, \qquad 2.4\text{-}7$$

thus reducing the number of independent elastic constants to five.

For transversely isotropic materials, equation (2.4-4a) should be satisfied and additionally:

$$-1 < \nu_{xz} \leq 1 - \frac{2\nu^2_{xy} E_x}{E_y}. \qquad 2.4\text{-}8$$

2.4.3) Complete symmetry (isotropy).

For an isotropic material, the strain energy function is independent of the choice of the reference coordinate system, and only two elastic constants are necessary for a full description of the elastic behaviour of the material.

The stress-strain relations are:

$$\begin{bmatrix} \varepsilon_x \\ \varepsilon_y \\ \varepsilon_z \end{bmatrix} = \begin{bmatrix} \frac{1}{E} & -\frac{\nu}{E} & -\frac{\nu}{E} \\ -\frac{\nu}{E} & \frac{1}{E} & -\frac{\nu}{E} \\ -\frac{\nu}{E} & -\frac{\nu}{E} & \frac{1}{E} \end{bmatrix} \begin{bmatrix} \sigma_x \\ \sigma_y \\ \sigma_z \end{bmatrix}, \qquad 2.4\text{-}9a$$

and

$$\begin{bmatrix} \gamma_{yz} \\ \gamma_{zx} \\ \gamma_{xy} \end{bmatrix} = \begin{bmatrix} \frac{1}{G} & & \\ & \frac{1}{G} & \\ & & \frac{1}{G} \end{bmatrix} \begin{bmatrix} \tau_{yz} \\ \tau_{zx} \\ \tau_{xy} \end{bmatrix}, \qquad 2.4\text{-}9b$$

where

$$G = \frac{E}{2(1+\nu)}. \qquad 2.4\text{-}9c$$

For isotropic materials, equation (2.4-8) reduces to:

$$-1 < \nu < 0.5. \qquad 2.4\text{-}10$$

2.5) Plane stress and plane strain.

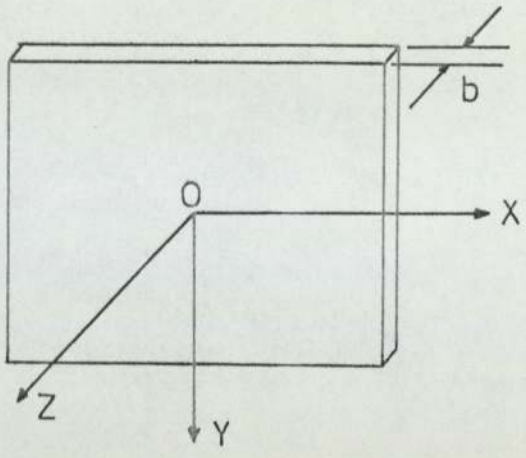

Fig.2.2

Plane stress or plane strain is assumed to exist in a certain plane (say XY plane; see Fig.2.2).

For plane stress conditions, the components of stress are taken to be the average values of the stresses over the thickness 'b' of the plate. The value of σ_z is negligible as compared with σ_x, σ_y, τ_{xy} and therefore is assumed to be equal to zero.

For plane strain conditions, the displacement w in the Z-direction is zero; therefore:

$$\varepsilon_z = 0.$$

For an orthotropic body under plane stress conditions, the stress-strain relations (2.4-1) reduce to:

$$\begin{bmatrix} \varepsilon_x \\ \varepsilon_y \\ \gamma_{xy} \end{bmatrix} = \begin{bmatrix} \frac{1}{E_x} & -\frac{\nu_{yx}}{E_y} & 0 \\ -\frac{\nu_{xy}}{E_x} & \frac{1}{E_y} & 0 \\ 0 & 0 & \frac{1}{G_{xy}} \end{bmatrix} \begin{bmatrix} \sigma_x \\ \sigma_y \\ \tau_{xy} \end{bmatrix}, \qquad 2.5\text{-}1$$

and for plane strain conditions:

2.5) contd.

$$\varepsilon_x = \frac{1-\nu_{zx}\nu_{xz}}{E_x}\sigma_x - \frac{\nu_{yx}+\nu_{zx}\nu_{yz}}{E_y}\sigma_y ,$$

$$\varepsilon_y = -\frac{\nu_{xy}+\nu_{zy}\nu_{xz}}{E_x}\sigma_x + \frac{1-\nu_{zy}\nu_{yz}}{E_y}\sigma_y , \qquad 2.5\text{-}2$$

$$\gamma_{xy} = \frac{1}{G_{xy}}\tau_{xy} .$$

Equations (2.5-1) and (2.5-2) can be expressed in the following form:

$$\begin{bmatrix}\varepsilon_x\\ \varepsilon_y\\ \gamma_{xy}\end{bmatrix} = \begin{bmatrix}\ell_{11} & \ell_{12} & 0\\ \ell_{21} & \ell_{22} & 0\\ 0 & 0 & \ell_{66}\end{bmatrix}\begin{bmatrix}\sigma_x\\ \sigma_y\\ \tau_{xy}\end{bmatrix} \qquad 2.5\text{-}3$$

where ℓ_{ij} can take their appropriate values (from equations 2.5-1, 2.5-2) depending on whether the body is under plane stress or plane strain conditions. By writing the stress-strain relations in the form (2.5-3), we establish mathematical equivalence between the plane stress and plane strain conditions.

For a transversely isotropic body, ℓ_{ij} for plane stress are specified by equation (2.5-1), and for plane strain are given by:

$$\ell_{11} = \frac{1-\nu_{xz}^2}{E_x} , \qquad \ell_{12} = -\frac{\nu_{yx}(1+\nu_{xz})}{E_y} , \qquad 2.5\text{-}4$$

$$\ell_{22} = \frac{1-\nu_{xy}\nu_{yx}}{E_y} , \qquad \ell_{66} = \frac{1}{G_{xy}} . \qquad 2.5\text{-}4$$

For an isotropic body under plane stress, we have:

$$\ell_{11} = \ell_{22} = \frac{1}{E} , \quad \ell_{12} = -\frac{\nu}{E} , \quad \ell_{66} = \frac{2(1+\nu)}{E} , \qquad 2.5\text{-}5$$

and for plane strain conditions:

$$\ell_{11} = \ell_{22} = \frac{1-\nu^2}{E} , \quad \ell_{12} = -\frac{\nu(1+\nu)}{E} , \quad \ell_{66} = \frac{2(1+\nu)}{E} . \qquad 2.5\text{-}6$$

The 2-Dimensional equations of equilibrium (2.2-1) (valid for plane stress and plane strain), take the form:

2.5) contd.

$$\frac{\partial \sigma_x}{\partial x} + \frac{\partial \tau_{xy}}{\partial y} = 0,$$

$$\frac{\partial \tau_{xy}}{\partial x} + \frac{\partial \sigma_y}{\partial y} = 0, \qquad 2.5\text{-}7$$

and the compatibility equation is:

$$\frac{\partial^2 \varepsilon_x}{\partial y^2} + \frac{\partial^2 \varepsilon_y}{\partial x^2} = \frac{\partial^2 \gamma_{xy}}{\partial x \partial y} . \qquad 2.5\text{-}8$$

2.6) Differential equation in 2-Dimensional elasticity and constants k_1 and k_2.

We introduce a stress function $\Phi(x,y)$, such that, the stress components given by:

$$\sigma_x = \frac{\partial^2 \Phi}{\partial y^2} , \quad \sigma_y = \frac{\partial^2 \Phi}{\partial x^2} , \quad \tau_{xy} = - \frac{\partial^2 \Phi}{\partial x \partial y} , \qquad 2.6\text{-}1$$

identically satisfy the equations of equilibrium (2.5-7).

Using these equations (2.6-1) and the stress-strain relations (2.5-3), the compatibility condition (2.5-8) can be reduced to the form:

$$\ell_{22} \frac{\partial^4 \Phi}{\partial x^4} + (2\ell_{12} + \ell_{66}) \frac{\partial^4 \Phi}{\partial x^2 \partial y^2} + \ell_{11} \frac{\partial^4 \Phi}{\partial y^4} = 0. \qquad 2.6\text{-}2$$

Assuming that $\ell_{22} \neq 0$, the above equation can be expressed in the following form:

$$\left(\frac{\partial^2 \Phi}{\partial x^2} + k_1^2 \frac{\partial^2 \Phi}{\partial y^2} \right) \left(\frac{\partial^2 \Phi}{\partial x^2} + k_2^2 \frac{\partial^2 \Phi}{\partial y^2} \right) = 0, \qquad 2.6\text{-}3$$

where

$$k_1^2 . k_2^2 = \frac{\ell_{11}}{\ell_{22}} \text{ and } k_1^2 + k_2^2 = \frac{2\ell_{12} + \ell_{66}}{\ell_{22}} . \qquad 2.6\text{-}4$$

The constants k_1 and k_2 may take real or imaginary values (Green & Taylor (1939), Leknilskii (1963)), but for the present discussion we shall assume that they are real and positive, as this is the case for a large number of materials (see Table 2.1).

Making the substitutions:

2.6) contd.

$$\rho_1 = \frac{2\ell_{12}+\ell_{66}}{2\ell_{22}} \quad \text{and} \quad \rho_2 = \frac{\ell_{11}}{\ell_{22}}, \qquad 2.6\text{-}5$$

we have:

$$\left.\begin{matrix} k_1^2 \\ k_2^2 \end{matrix}\right\} = \rho_1 \pm \sqrt{\rho_1^2 - \rho_2}, \qquad 2.6\text{-}6$$

with $\rho_1 > 0$ and $\rho_1^2 \geq \rho_2$.

For plane stress conditions, ρ_1 and ρ_2 can be expressed in terms of the engineering elastic constants in the following form:

$$\rho_1 = \frac{E_y - 2\nu_{yx} G_{xy}}{2G_{xy}}, \quad \rho_2 = \frac{E_y}{E_x}. \qquad 2.6\text{-}7$$

For isotropy,

$\rho_1 = \rho_2 = 1$, and from equation (2.6-6)

$$k_1 = k_2 = 1. \qquad 2.6\text{-}8$$

It can be shown that equation (2.6-8) is also valid for plane strain conditions.

The variation of k_1^2 and k_2^2 with ρ_1, ρ_2 is shown in Fig.2.3. From these graphical results, we make the following observations:

i) A material can exhibit anisotropy, with either one of k_1 or k_2 being equal to unit independently.

ii) For a given value of ρ_1, there are upper and lower limits for k_1^2 and k_2^2, such that

$$\rho_1 \leq k_1^2 \leq 2\rho_1, \quad 0 \leq k_2^2 \leq \rho_1. \qquad 2.6\text{-}9$$

iii) Since the parameters k_1 and k_2 (or ρ_1 and ρ_2) are independent of each other, a straight forward comparison between orthotropic materials as to their relative degree of anisotropy cannot be made. Nevertheless, it can be deduced from the graphs that, the more k_1 AND k_2 deviate from unity, the more anisotropic a material becomes.

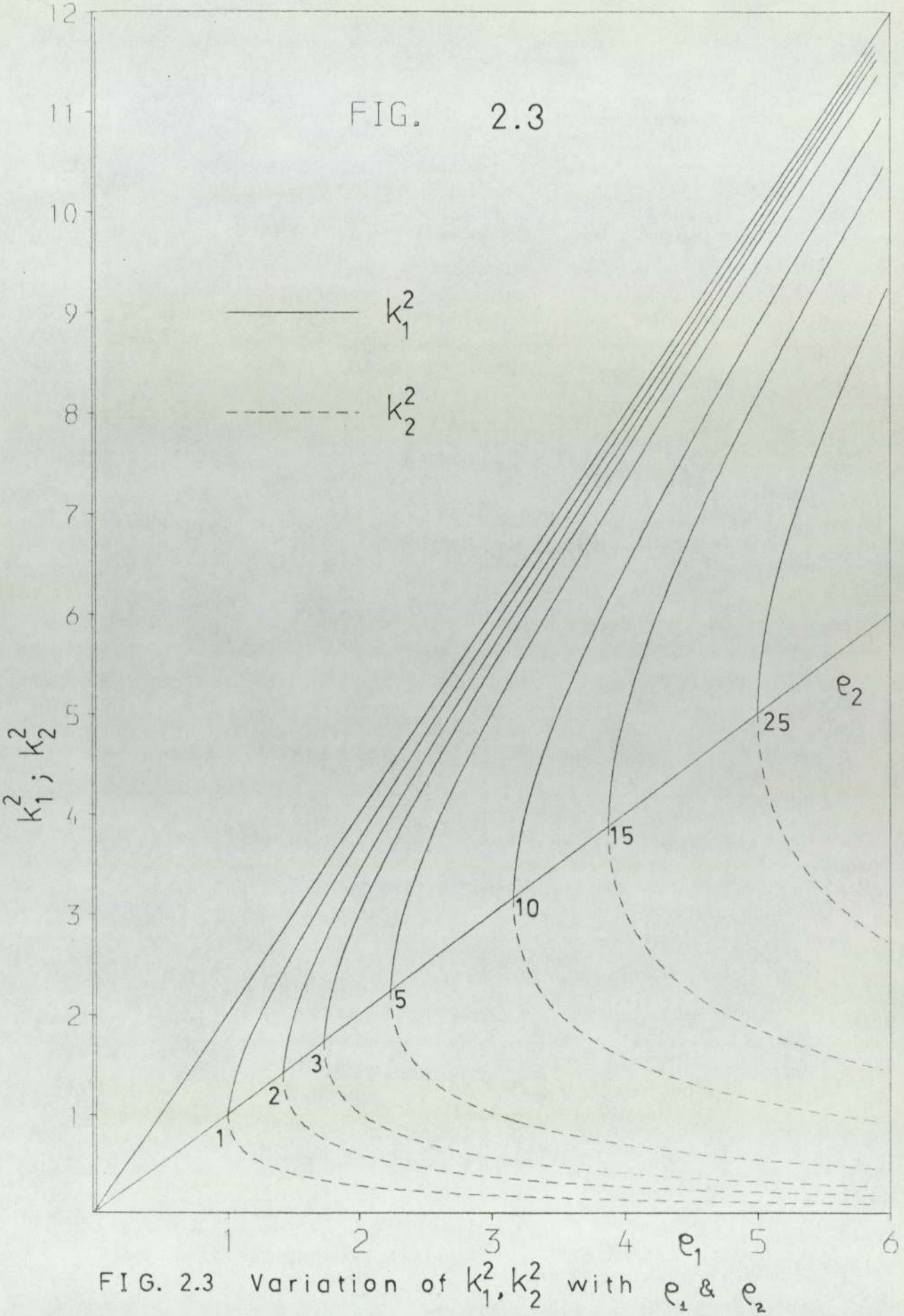

FIG. 2.3 Variation of k_1^2, k_2^2 with e_1 & e_2

TABLE 2·1

Material	E_x KN/mm^2	E_y KN/mm^2	ν_{xy}	G_{xy} KN/mm^2	k_1	k_2	Reference
Graphite Epoxy	275·88	11·03	0·25	5·51	1·3998	0·1428	Saha, etal. (1972)
Boron Epoxy	275·88	27·58	0·25	10·34	1·6055	0·1969	Saha, etal. (1972)
Glass Epoxy	53·79	17·93	0·25	8·62	1·3112	0·4403	Saha, etal. (1972)
Plywood	11·77	5·88	0·071	0·686	2·9053	0·2433	Lekhnitskii (1963)
Delta wood	29·92	4·58	0·13	2·158	1·4164	0·2762	Lekhnitskii (1963)
Pine wood	9·81	0·41	0·238	0·735	0·6676	0·3069	Lekhnitskii (1963)
Glass Polyester	21·20	8·27	0·252	3·29	1·4609	0·4275	Author's results
Laminated* Rubber	$4·60 \times 10^{-3}$	$3·90 \times 10^{-3}$	0·48	130×10^{-3}	1·3320	0·6760	Author's results

* Plain strain ; $\nu_{xz} = 048$

2.7) Transformation of the compliance matrix.

In Section 2.3, it was mentioned that the elastic compliances c_{ij} of an anisotropic body, can be defined for a specific orientation of the reference coordinate axes relative to the body.

For a new orientation, expressions for the elastic compliances can be obtained in terms of the compliances of the original system and the angles of rotation of the axes. Lekhnitskii (1963) formulates the derivation of the expressions for an orthotropic body under plane stress conditions, using the strain energy function. In terms of the engineering elastic constants, the expressions in their final form are given by Lekhnitskii (1963) and Ogorkiewicz (1973). For reference purposes are reproduced in Appendix [1].

Of particular interest is the effect on k_1 and k_2 of 90° rotation of the axes. It can be shown (see Appendix [2]), that for the new orientation of the reference axes:

$$k_1' = \frac{1}{k_2} \quad \text{and} \quad k_2' = \frac{1}{k_1} \qquad 2.7\text{-}1$$

where k_1' and k_2' are the orthotropic constants of the material for the new orientation.

2.8) Anisotropic materials.

Anisotropy, as a mathematical model for the description of physical response and behaviour of materials, generally stems from non-homogeneity in the microscale structure of the material.

Examining various anisotropic materials, either naturally occurring ones,like the different types of wood, or artificial ones, like reinforced plastics or plywood,

2.8) contd.

we observe that on the microscale are non-homogeneous. To treat them as such, is a complicated lengthy process and from an engineer's point of view, rather impractical.

The problem can be very much simplified by assuming the materials to be homogeneous on the macroscale, but with different properties in different directions, thus introducing the concept of anisotropy to explain the effects of microscale non-homogeneity.

The basic assumption of "homogeneity on the macroscale" is always open to question as to whether it is justified or not. For a specific problem, that would depend on the ratio of length parameters characteristic of the 'macro' and 'micro' scales.

On the microscale, the length parameter λ_{micro}, should represent the non-homogeneity of the material (e.g. diameter of reinforcement in composites, thickness of laminations in wood, etc.).

On the macroscale, the length parameter λ_{macro}, should generally be equal to the "unit length" of the particular problem (e.g. the width of an external load; the distance from a boundary that the load is applied, etc.).

Now, if

$$\frac{\lambda_{micro}}{\lambda_{macro}} \ll 1,$$

the assumption of homogeneity on the macroscale is usually justified.

In view of the experimental work to be undertaken, we shall limit our discussion on a certain type of non-homogeneous materials, namely orthotropic composites, that can frequently be treated as homogeneous, anisotropic and

2.5) contd.

"continuous" media.

2.9) Composite materials.

a) Reinforced b) Laminated

Fig.2.4

Two types of composite materials will be considered, and are shown diagrammatically in Fig.2.4.

a) Reinforced materials.

One material (reinforcement), in the form of rods or fibres, is embedded into another (matrix) to form a continuous medium.

b) Laminated materials.

Two or more different materials, in the form of laminas are joined together on their flat surfaces, in alternating sequence, to form a continuous medium.

In both cases, it is assumed that:

i) The constituent materials are homogeneous, isotropic and linearly elastic.

ii) The displacements are continuous over the mass of the body. This implies that there is no slippage at the interfaces between the constituent materials.

iii) The stresses are continuous in the composite body. Obviously, this assumption is not justified locally, but since average stresses are considered (being the object of the anisotropic elasticity approach to non-homogeneous materials), continuity is ensured.

2.9) contd.

iv) The longitudinal dimensions of the composite material are very large compared with the diameter of the reforcement or the thickness of the laminations.

The advantages that such combinations of materials offer are many, but is not in the scope of the present work to analyse them or to treat composite materials as such. We will concentrate on the assumption that the theory of orthotropic elasticity can predict their behaviour by treating them as homogeneous, continuous media.

2.10) Elastic constants of composite materials.

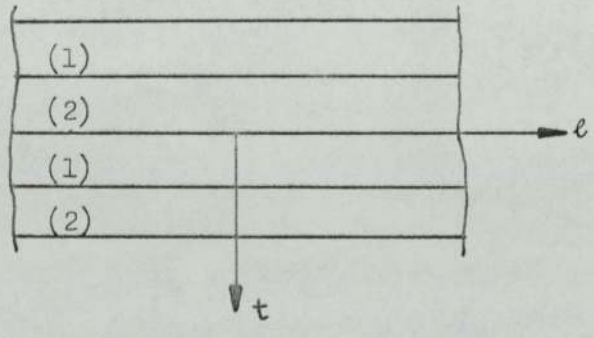

Fig.2.5

The elastic constants of orthotropic composites, can be predicted with a certain degree of accuracy from the elastic properties of the constituent materials, taking into account their geometrical configuration.

We shall limit our discussion on the case of orthotropic composites which consist of two isotropic, linearly elastic materials, denoted by the subscripts (1) and (2) (see Fig.2.5). The two principal directions, parallel and normal to the direction of the reinforcing fibres or layers, will be denoted by the subscripts 'ℓ' (longitudinal) and 't' (transverse) respectively.

2.10) contd.

There are three basic techniques for the determination of the elastic constants of a composite based on:

a) The mechanics of materials theory,

b) the theory of elasticity, and

c) bounding techniques using variational principles of the theory of elasticity.

Techniques (a) and (b) can be applied to reinforced and to laminated composites, while technique (c) is usually applied to fibre-reinforced composites which require a more rigorous approach, due to the many variables involved (e.g. type, shape and distribution of fibres in the composite).

We shall now present a summary of the formulae used in the prediction of the elastic constants of composite materials:

1) Prediction of E_ℓ.

Regardless of the theory used, it is generally accepted that the law of mixtures given by the equation:

$$E_\ell = v_1 E_1 + v_2 E_2, \qquad 2.10\text{-}1$$

where v_1 and v_2 are the volume fractions of materials (1) and (2) respectively, is a good approximation for the longitudinal modulus. Equation (2.10-1) can be derived using the mechanics of materials approach with the assumption that plane sections remain plane during deformation.

2) Prediction of E_t.

Using the mechanics of materials approach and assuming that both materials are subjected to the same

2.10) contd.

2) contd.

transverse stress σ_t, it can be shown that:

$$E_t = \frac{E_1 E_2}{E_1 v_2 + E_2 v_1} . \qquad 2.10\text{-}2$$

Ekvall (1961), introducing a biaxial slate of stress in conjunction with the mechanics of materials theory, obtained:

$$\frac{1}{E_t} = \frac{v_1}{E_1} + \frac{v_2}{E_2} - \frac{v_2}{E_2} \frac{[E_1 \nu_2/E_2)-\nu_1]^2}{[(v_1 E_1/v_2 E_2)+1]} . \qquad 2.10\text{-}3$$

Tsai (1961) developed an expression for E_t, for reinforced composites, by considering circular fibres and representing the surrounding matfix material as cylindrical inclusions.

Tsai's equation is:

$$E_t = 2[1 - \nu_1 + (\nu_1-\nu_2)v_2] \left\{ (1-C) \frac{K_1(2K_2+G_2)-G_2(K_1-K_2)v_2}{(2K_2+G_2)+2(K_1-K_2)v_2} + C \frac{K_1(2K_2+G_1)+G_1(K_2-K_1)v_2}{(2K_2+G_1)-2(K_2-K_1)v_2} \right\}, \qquad 2.10\text{-}4a$$

where
$$K_1 = E_1/2(1-\nu_1),$$
$$K_2 = E_2/2(1-\nu_2), \qquad 2.10\text{-}4b$$
$$G_1 = E_1/2(1+\nu_1),$$
$$G_2 = E_2/2(1+\nu_2),$$

and C is a contiguity factor which varies linearly between C = 0 for isolated fibres and C = 1 for fibres in contact.

3) Prediction of $\nu_{\ell t}$

Using the mechanics of materials approach, it can be shown that:

2.10) contd.

3) contd.

$$\nu_{\ell t} = v_1 \nu_1 + v_2 \nu_2 . \qquad 2.10\text{-}5$$

For reinforced composites, Rosen et al.(1964) using the variational bounding method, found that the bounds on $\nu_{\ell t}$ coincide for random arrays of fibres. Their expression is:

$$\nu_{\ell t} = \frac{v_1 E_1 L_1 + v_2 E_2 L_2 \nu_2}{v_1 E_1 L_3 + v_2 E_2 L_2} , \qquad 2.10\text{-}6a$$

where

$$L_1 = 2\nu_1(1 - \nu_2^2)v_1 + v_2(1+\nu_2)\nu_2 ,$$

$$L_2 = v_1(1 - \nu_1 - 2\nu_1^2) , \qquad 2.10\text{-}6b$$

$$L_3 = 2(1-\nu_2^2)v_1 + (1+\nu_2)v_2 .$$

Tsai (1964), using the same technique, along with the contiguity factor C, obtained the following relation:

$$\nu_{\ell t} = (1-C)\left[\frac{K_1\nu_1(2K_2+G_2)+K_2\nu_2(2K_1+G_2)v_2}{K_1(2K_2+G_2)-G_2(K_1-K_2)v_2}\right]$$

$$+ C\left[\frac{K_2\nu_2(2K_1+G_1)v_2+K_1\nu_1(2K_2+G_1)v_1}{K_1(2K_2+G_1)+G_1(K_2-K_1)v_2}\right], \qquad 2.10\text{-}7$$

where the various terms are defined by equation (2.10-4b).

4) Prediction of $G_{\ell t}$

Using the mechanics of materials approach and assuming equal shearing stresses in the constituent materials, it can be shown that:

$$G_{\ell t} = \frac{G_1 G_2}{v_1 G_2 + v_2 G_1} . \qquad 2.10\text{-}8$$

For random arrays of fibres, Rosen et al.(1964), using the variational method obtained:

$$G_{\ell t} = G_2\left[\frac{G_1(1+ v_1)+ G_2 v_2}{G_1 v_2+G_2(1 + v_1)}\right]. \qquad 2.10\text{-}9$$

Finally, Tsai (1964) developed an expression for $G_{\ell t}$, in the following form:

2.10) contd.

4) contd.

$$G_{\ell t} = (1-C)\ G_2 \left[\frac{2G_1-(G_1-G_2)v_2}{2G_2+(G_1-G_2)v_2}\right] + C\ G_1 \left[\frac{(G_1+G_2)-(G_1-G_2)v_2}{(G_1+G_2)+(G_1-G_2)v_2}\right] \qquad 2.10\text{-}10$$

5) Prediction of $\nu_{t\ell}$

The value of Poisson's ratio $\nu_{t\ell}$ can be obtained from the values of $\nu_{\ell t}$, $E_{\ell t}$ and $E_{t\ell}$, by the symmetry condition (see equation 2.4-3):

$$\nu_{t\ell} = \nu_{\ell t}\ \frac{E_{t\ell}}{E_{\ell t}}\ . \qquad 2.10\text{-}11.$$

CHAPTER 3

ORTHOTROPIC INFINITE PLANE

3.1) Introduction.

A solution to the problem of an infinite isotropic elastic plane, loaded over its thickness by a concentrated line load applied parallel to the plane, has been developed by Flamant and Boussinesq (1892). The analogous solution for the orthotropic plane has been developed by Conway (1953a).

Since Conway's solution is employed in the ensuing chapters, we shall present here a brief summary of the infinite plane problem and in particular the case of the infinite plane loaded by a concentrated force; by a moment; and by two equal and opposite concentrated forces acting a small distance apart.

3.2) Orthotropic infinite plane subjected to a concentrated force.

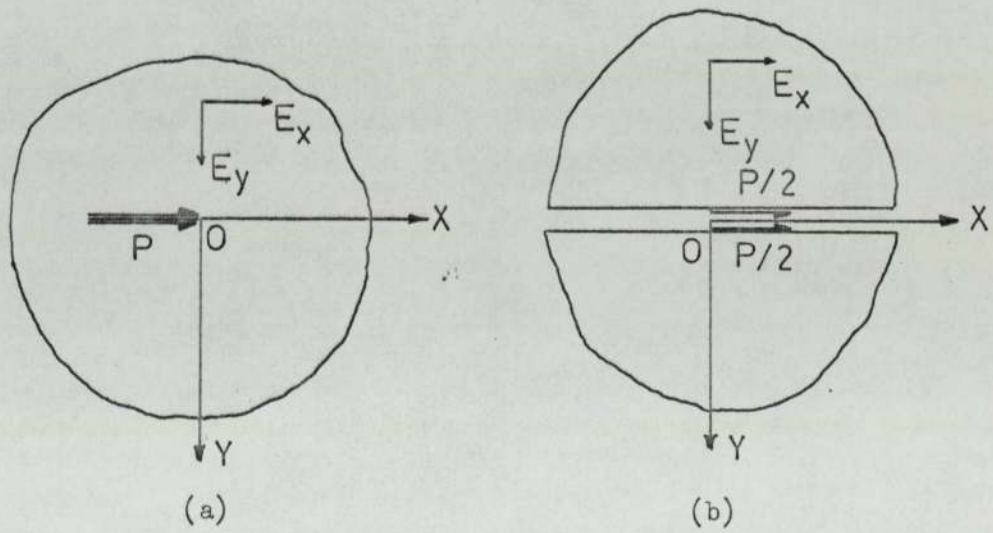

Fig.3.1

The problem of the orthotropic infinite plane subjected to a concentrated force, is shown diagrammatically in Fig.3.1a.

The force P/unit thickness, is applied at the origin of the coordinates O, in the positive X-direction.

The axes of orthotropy are assumed to coincide with the reference coordinate axes.

3.2) contd.

It may be verified that the general form of Airy's stress function:

$$\Phi = \int_0^\infty \frac{1}{\zeta^2} \left(C_1 e^{-\frac{\zeta y}{k_1}} + C_2 e^{-\frac{\zeta y}{k_2}} + C_3 e^{-\frac{\zeta y}{k_1}} + C_4 e^{\frac{\zeta y}{k_2}} \right) \sin\zeta x \, d\zeta \qquad 3.2\text{-}1$$

where $C_1 \ldots C_4$ are arbitrary constants, satisfies the general differential equation (2.6-2).

From (3.2-1), the stress components are given by:

$$\sigma_x(x,y) = \int_0^\infty \left(\frac{C_1}{k_1^2} e^{-\frac{\zeta y}{k_1}} + \frac{C_2}{k_2^2} e^{-\frac{\zeta y}{k_2}} + \frac{C_3}{k_1^2} e^{\frac{\zeta y}{k_1}} + \frac{C_4}{k_2^2} e^{\frac{\zeta y}{k_2}} \right) \sin\zeta x \, d\zeta, \qquad 3.2\text{-}2a$$

$$\sigma_y(x,y) = -\int_0^\infty \left(C_1 e^{-\frac{\zeta y}{k_2}} + C_2 e^{-\frac{\zeta y}{k_2}} + C_3 e^{\frac{\zeta y}{k_1}} + C_4 e^{\frac{\zeta y}{k_2}} \right) \sin\zeta x \, d\zeta, \qquad 3.2\text{-}2b$$

$$\tau_{xy}(x,y) = \int_0^\infty \left(\frac{C_1}{k_1} e^{-\frac{\zeta y}{k_1}} + \frac{C_2}{k_2} e^{-\frac{\zeta y}{k_2}} - \frac{C_3}{k_1} e^{\frac{\zeta y}{k_1}} - \frac{C_4}{k_2} e^{\frac{\zeta y}{k_2}} \right) \cos\zeta x \, d\zeta. \qquad 3.2\text{-}2c$$

The boundary conditions of the infinite plane require that the stresses should vanish at $y = \pm \infty$, and this implies:

$$C_3 = C_4 = 0. \qquad 3.2\text{-}3a$$

The remaining constants C_1 and C_2, can be determined by stress and displacement conditions on surface (X,0):

Considering the infinite plane as composed of two half planes $Y > 0$ and $Y < 0$ (see Fig.3.1b), each loaded by a concentrated tangential force P/2 at (0,0), the stress boundary conditions can be written in a Fourier integral form:

$$\tau_{xy}(x,o) = \lim_{c \to o} \frac{P}{2\pi} \int_0^\infty \frac{\sin \zeta c}{\zeta c} \cos\zeta x \, d\zeta. \qquad 3.2\text{-}3b$$

From symmetry, the displacement boundary condition is:

$$v(x,o) = 0. \qquad 3.2\text{-}3c$$

Equation (3.2-3b) in conjunction with (3.2-2c) gives:

3.2) contd.

$$\frac{C_1}{k_1} + \frac{C_2}{k_2} = \frac{P}{2\pi}. \qquad 3.2\text{-}4a.$$

The displacement $v(x,y)$ can be obtained from the indefinite integral:

$$v(x,y) = \int \epsilon_y \, dy = \ell_{12} \int \sigma_x \, dy + \ell_{22} \int \sigma_y \, dy,$$

and for $v(x,o) = 0$:

$$\ell_{22}(C_1 k_1 + C_2 k_2) = \ell_{12} \left(\frac{C_1}{k_1} + \frac{C_2}{k_2} \right). \qquad 3.2\text{-}4b$$

C_1 and C_2, evaluated from (3.2-4a and b) are given by:

$$\left[C_1; \; C_2 \right] = \frac{P}{2\pi(k_1^2 - k_2^2)} \left[-k_1\left(k_2^2 - \frac{\ell_{12}}{\ell_{22}}\right); \; k_2\left(k_1^2 - \frac{\ell_{12}}{\ell_{22}}\right) \right]. \qquad 3.2\text{-}5$$

Substituting the expressions for the constants $C_1 \ldots C_4$ from (3.2-3a, 3.2-5) into (3.2-2), we obtain:

$$\left[\sigma_x; \; \sigma_y; \; \tau_{xy} \right] = \frac{P}{2\pi} \frac{k_1 k_2}{(k_1^2 - k_2^2)} \left\{ \right.$$

$$\left. \left[x\left(k_1 \xi_{22} - k_2 \xi_{11}\right); \; x\left(k_1 \xi_{11} - k_2 \xi_{22}\right); \; y\left(k_1 \xi_{22} - k_2 \xi_{11}\right) \right] \right\}, \qquad 3.2\text{-}6a$$

where

$$\xi_{ij} = \frac{1 - \eta k_i^2}{k_j^2 x^2 + y^2} \quad , \text{ for } i = 1,2 \text{ and } j = 1,2,$$

and $$\eta = \frac{\ell_{12}}{\ell_{11}}. \qquad 3.2\text{-}6b$$

In the case of the concentrated force being applied in the positive Y-direction, the stresses are given by:

$$\left[\sigma_x; \; \sigma_y; \; \tau_{xy} \right] = \frac{P}{2\pi(k_1^2 - k_2^2)} \left\{ \right.$$

$$\left. \left[y(k_2 \xi_{12} - k_1 \xi_{21}); \; y(k_1^3 \xi_{21} - k_2^3 \xi_{12}); \; x(k_1^3 \xi_{21} - k_2^3 \xi_{12}) \right] \right\}, \qquad 3.2\text{-}7$$

where ξ_{ij} are defined by (3.2-6b).

3.3) Orthotropic infinite plane subjected to two equal and opposite forces acting a small distance apart.

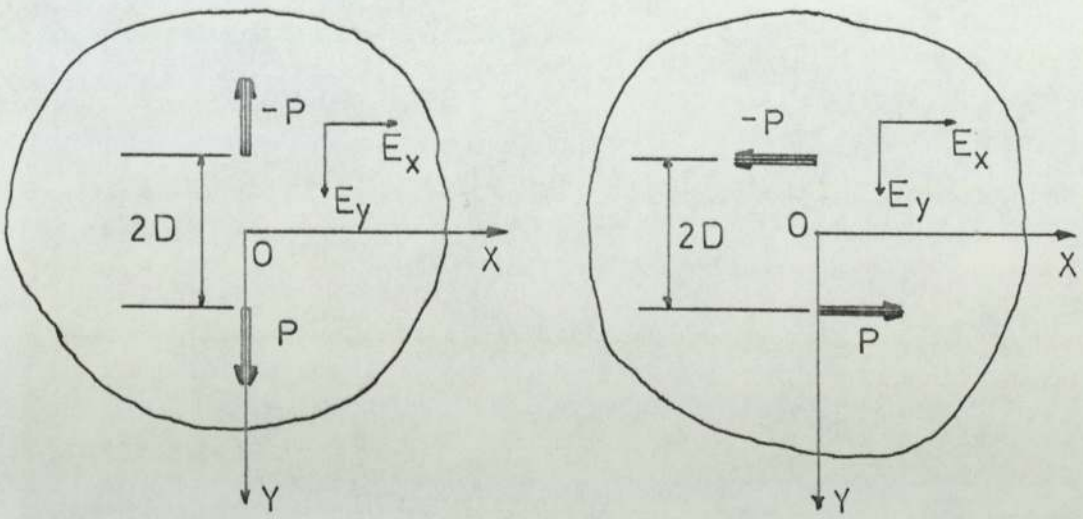

Fig.3.2

The solution to this problem (for convenience we shall refer to this as the "unit pinch" problem), shown diagrammatically in Fig.3.2a, can be obtained as a superposition of two concentrated force solutions, given in the previous section (3.2).

The stress components are given by:

$$[\sigma_x;\sigma_y;\tau_{xy}] = \frac{P}{\pi(k_1^2-k_2^2)} \left\{ \alpha_1 \, r_1\left[f_1;\ -k_1^2 f_1;\ -k_1^2 x\right] \right.$$
$$+ \alpha_1 \, r_2\left[-f_2;\ k_1^2 f_2;\ k_1^2 x\right]$$
$$+ \alpha_2 \, r_3\left[f_1;\ -k_2^2 f_1;\ -k_2^2 x\right]$$
$$\left. + \alpha_2 \, r_4\left[-f_2;\ k_2^2 f_2;\ k_2^2 x\right] \right\}, \qquad 3.3\text{-}1$$

where

$$\left.\begin{matrix} f_1 \\ f_2 \end{matrix}\right\} = y \pm D\,, \qquad \begin{aligned} \alpha_1 &= k_1(1-\eta\, k_2^2)/2\,, \\ \alpha_2 &= -\,k_2(1-\eta k_1^2)/2\,, \end{aligned}$$

3.3) contd.

$$\left.\begin{matrix} r_1 \\ r_2 \end{matrix}\right\} = \left[k_1^2x^2 + (y \pm D)^2\right]^{-1}, \qquad \left.\begin{matrix} r_3 \\ r_4 \end{matrix}\right\} = \left[k_2^2x^2 + (y \pm D)^2\right]^{-1},$$

$$\eta = \frac{\ell_{12}}{\ell_{11}} .$$

At $y = 0$,

$$\sigma_y(x,o) = -\frac{2P}{\pi(k_1^2 - k_2^2)}\left\{\alpha_1 k_1 \frac{k_1 D}{k_1^2x^2+D^2} + \alpha_2 k_2 \frac{k_2 D}{k_2^2x^2+D^2}\right\}, \qquad 3.3\text{-}2$$

and since

$$\int_o^\infty e^{-\frac{D\zeta}{k_i}} \cos\zeta x \; d\zeta = \frac{k_i D}{k_i^2x^2 + D^2} \quad \text{for } i = 1,2, \qquad 3.3\text{-}3$$

equation (3.3-2) can be written in the following form:

$$\sigma_y(x,o) = -\frac{2P}{\pi(k_1^2 - k_2^2)}\left\{\int_o^\infty \left(\alpha_1 k_1 e^{-\frac{D\zeta}{k_1}} + \alpha_2 k_2 e^{-\frac{D\zeta}{k_2}}\right) \cos\zeta x \; d\zeta\right\} \qquad 3.3\text{-}4$$

The above expression for $\sigma_y(x,o)$, will be used in section (4.7) to develop a solution to the half-plane problem loaded at the interior by a concentrated force P, normal to the boundary and at point (0,D).

When the concentrated forces are applied as shown in Fig.3.2b, the stress components are given by:

$$\begin{aligned}\left[\sigma_x;\ \sigma_y;\ \tau_{xy}\right] = \frac{P}{\pi}\frac{k_1k_2}{(k_1^2-k_2^2)}\Big\{ & \alpha_2 r_1\left[-x;\ xk_1^2\ ;\ -f_1\right] \\ & + \alpha_2 r_2\left[x;\ -xk_1^2;\ f_2\right] \\ & + \alpha_1 r_3\left[-x;\ xk_2^2;-f_1\right] \\ & + \alpha_1 r_4\left[x\ ;\ -xk_2^2;\ f_2\right]\Big\}. \end{aligned} \qquad 3.3\text{-}5$$

The expression for the shear stress τ_{xy}, for $y = 0$, can be modified, by substitution of equation (3.3-3), into the following form:

3.3) contd.

$$\tau_{xy}(x,o) = - \frac{2P\ k_1k_2}{\pi(k_1^2-k_2^2)} \left\{ \int_0^\infty \left(\frac{\alpha_2}{k_1} e^{-\frac{D\zeta}{k_1}} + \frac{\alpha_1}{k_2} e^{-\frac{D\zeta}{k_2}} \right) \cos\zeta x \, d\zeta \right\} \quad 3.3\text{-}6$$

3.4) Orthotropic infinite plane subjected to a moment.

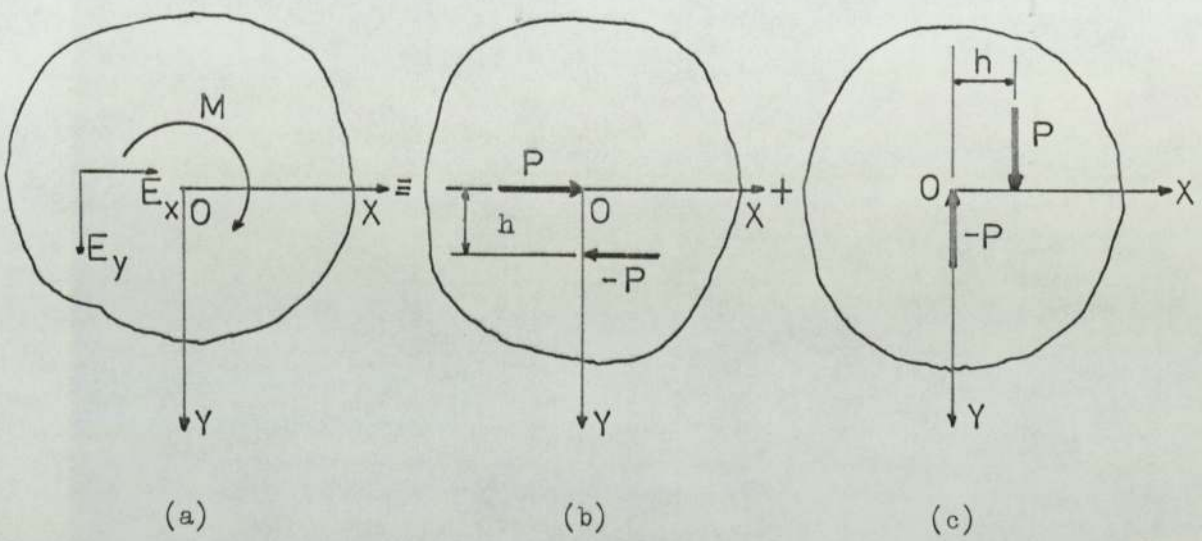

(a) (b) (c)

Fig.3.3

A solution to the problem of an orthotropic infinite plane subjected at the origin to a moment M, can be obtained from superposition of a set of concentrated force solutions (see Fig.3.3b and c).

Equal and opposite forces P and -P are applied at distances 'h' apart. The distance 'h' is decreased in such a way that as $h \to 0$, Ph remains constantly equal to $\frac{M}{2}$.

The resulting stresses are given by:

$$\sigma_y(x,y) = - \frac{M}{2\pi} xy \left[\frac{k_1}{(k_1^2x^2+y^2)^2} + \frac{k_2}{(k_2^2x^2+y^2)^2} \right], \quad 3.4\text{-}1a$$

$$\sigma_y(x,y) = \frac{M}{2\pi} xy \left[\frac{k_1^3}{(k_1^2x^2+y^2)^2} + \frac{k_2^3}{(k_2^2x^2+y^2)^2} \right], \quad 3.4\text{-}1b$$

$$\tau_{xy}(x,y) = \frac{M}{4\pi} \left[\frac{k_1(k_1^2x^2-y^2)}{(k_1^2x^2+y^2)^2} + \frac{k_2(k_2^2x^2-y^2)}{(k_2^2x^2+y^2)^2} \right] \quad 3.4\text{-}1c$$

For an isotropic material (i.e. $k_1 = k_2 = 1$),

3.4) contd.

equations (2.4-2) reduce to:

$$\left[\sigma_x;\sigma_y;\tau_{xy}\right] = \frac{M}{\pi}\left[-\frac{xy}{(x^2+y^2)^2}\;;\;\frac{xy}{(x^2+y^2)^2};\;\frac{x^2-y^2}{2(x^2+y^2)^2}\right] \qquad 3.4\text{-}2$$

CHAPTER 4

ORTHOTROPIC HALF - PLANE.

4.1) Introduction.

Problems associated with isotropic semi-infinite bodies (henceforth referred to as half-plane problems), have received considerable attention.

Flamant (1892) obtained a solution to the problem of a half-plane subjected to a concentrated force acting normal to the boundary, while Michell (1902) extended the solution to the case of a uniformly distributed load. Several cases of distributed loadings on the straight boundary have been discussed by Carothers (1920).

Similar solutions were obtained for anisotropic or orthotropic elastic bodies by Lekhnitskii (1963), Green and Taylor (1939), Okubo (1951), Brilla (1962), Conway (1953a), Aköz and Tauchert (1973) and others.

Conway (1953b) developed a solution to the orthotropic half-plane subjected to concentrated forces applied at the interior; and recently Saha et al. (1972) investigated the same problem for a generally anisotropic material.

Several cases of rigid body indentations on the straight boundary of the half-plane have been discussed by Okubo (1940), Sen (1954), Conway (1955) and Brilla (1962).

In the following sections of this chapter we shall summarize solutions to various "half-plane" problems, which will form the basis for developing solutions to a number of problems in the ensuing chapters.

Unless otherwise stated, it is assumed that the material of the half-plane is orthotropic, with the axes of orthotropy coinciding with the rectangular coordinate axes.

The general method of solution is based on the use of Fourier integrals to represent the externally applied loads (see Conway (1953a,b), Lekhnitskii (1963)).

4.1) contd.

The assumed stress function Φ is of the form:

$$\Phi(x,y) = \int_0^\infty f(\zeta,y)\ \cos\zeta x\ \ d\zeta, \qquad 4.1\text{-}1$$

where $f(\zeta,y)$ depends on the roots of the characteristic equation (2.6-4).

For k_1, k_2 real and positive (see Lekhnitskii (1963)):

$$f(\zeta,y) = \frac{1}{\zeta^2}\left(C_1\ e^{-\frac{\zeta y}{k_1}} + C_2\ e^{-\frac{\zeta y}{k_2}}\right). \qquad 4.1\text{-}2$$

4.2) Concentrated force normal to the boundary

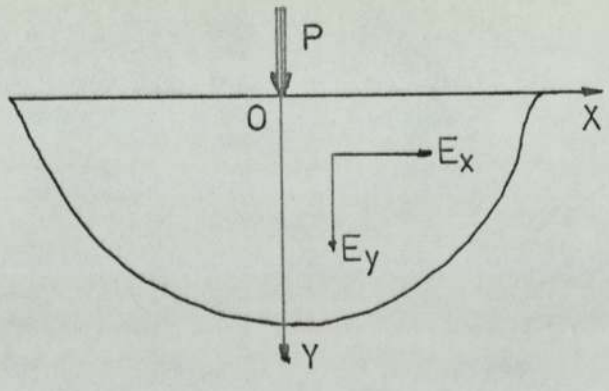

Fig.4.1

The orthotropic half-plane (occupying the region $-\infty < x < +\infty$ and $0 \leq y < +\infty$) is subjected at its free boundary to a concentrated normal force P/unit thickness, acting in the positive Y-direction (see Fig.4.1).

It may be verified that the stress function

$$\Phi = \int_0^\infty \frac{1}{\zeta^2}\left(C_1\ e^{-\frac{\zeta y}{k_1}} + C_2\ e^{-\frac{\zeta y}{k_2}}\right)\cos\zeta x\ d\zeta\ , \qquad 4.2\text{-}1$$

satisfies the governing differential equation (2.6-3).

The constants C_1 and C_2 can be determined from the following traction boundary conditions:

i) The normal stress on the free boundary is zero at all points, except point (0,0) where it is infinite. To

4.2) contd.

i) contd.

overcome the singular behaviour at the point (0,0), we may assume that the concentrated force P is equivalent to a uniformly distributed normal stress p, symmetrical about the Y-axis and of width 2c, such that the total load is given by 2pc. As $c \to 0$, the total load remains constant and equal to P.

This condition can be expressed in a Fourier integral form (see Conway 1953a):

$$\sigma_y(x,o) = \underset{c \to o}{\ell imit} \frac{P}{\pi} \int_o^\infty \frac{\sin\zeta c}{\zeta c} \cos\zeta x \, d\zeta . \qquad 4.2\text{-}3a$$

ii) The shear stress at any point on the free boundary is equal to zero,

$$\tau_{xy}(x,o) = 0. \qquad 4.2\text{-}3b$$

The components of stress can then be obtained through equation (2.6-1) in the following form:

$$\left[\sigma_x;\ \sigma_y;\tau_{xy}\right] = \frac{P(k_1+k_2)}{\pi(k_1^2x^2+y^2)(k_2^2x^2+y^2)} \left[x^2y;\ y^3;\ xy^2\right]. \qquad 4.2\text{-}4$$

The displacement v in the Y-direction can be determined by integration of the stress-strain relation for ε_y:

$$v(x,y) = \int (\ell_{12}\sigma_x + \ell_{22}\sigma_y)dy + f(x). \qquad 4.2\text{-}5a$$

The function f(x) may be shown to be a constant, and we shall assume that it represents rigid body rotation.

Therefore:

$$v(x,y) = \frac{P}{2\pi(k_1-k_2)} \left\{ \ell_1 \ell n(k_1^2x^2+y^2) - \ell_2 \ell n(k_2^2x^2+y^2) \right\} + \text{const.} \qquad 4.2\text{-}5b$$

where

4.2) contd.

$$\ell_i = \ell_{22}\, k_i^2 - \ell_{12} \quad , \text{ for } i = 1,2. \qquad 4.2\text{-}5c$$

At the boundary (y = o):

$$v(x,o) = \frac{P}{\pi(k_1-k_2)} \left\{ \ell_1 \ell n k_1 - \ell_2 \ell n k_2 + \ell_{22}(k_1^2-k_2^2)\ell n|x| \right\} + \text{const.} \qquad 4.2\text{-}6$$

A way of interpreting the arbitrary constant is to make the displacement v at a point on the boundary $x = \pm a$, $y = o$, equal to zero, such that:

$$v(x,o) = \frac{P}{\pi}\, \ell_{22}(k_1+k_2)\, \ell n \left| \frac{x}{a} \right| \qquad 4.2\text{-}7$$

4.3) Concentrated force tangential to the boundary.

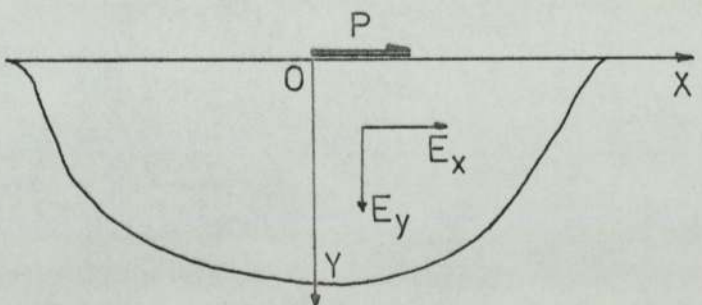

Fig.4.2

The orthotropic half-plane Y > 0 is subjected at its free boundary to a concentrated tangential force P/unit thickness, applied at the origin of the coordinate axes and in the positive X-direction (see Fig.4.2).

The assumed stress function is:

$$\Phi = \int_0^\infty \frac{1}{\zeta^2} \left(C_1\, e^{-\frac{\zeta y}{k_1}} + C_2\, e^{-\frac{\zeta y}{k_2}} \right) \sin\zeta x \, d\zeta . \qquad 4.3\text{-}1$$

Expressing the concentrated tangential force in a Fourier integral form, the boundary conditions for the half-plane are:

4.3) contd.

$$\sigma_y(x,o) = 0 \qquad 4.3\text{-}2a$$

$$\tau_{xy}(x,o) = \underset{c \to o}{\ell imit}\ \frac{P}{\pi} \int_o^\infty \frac{\sin\zeta c}{\zeta c} \cos\zeta x\, d\zeta\ , \qquad 4.3\text{-}2b$$

and the components of stress can then be obtained in the following form:

$$\left[\sigma_x;\ \sigma_y;\ \tau_{xy}\right] = \frac{P\ k_1 k_2 (k_1+k_2)}{\pi(k_1^2x^2+y^2)(k_2^2x^2+y^2)} \left[x^3;\ xy^2;\ x^2y\right]. \qquad 4.3\text{-}3$$

4.4) Uniformly distributed load normal to the boundary.

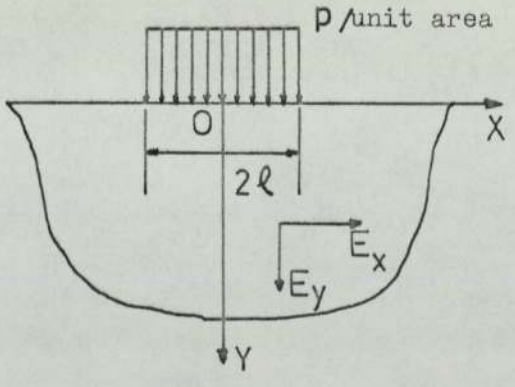

Fig.4.3

In this case, the orthotropic half-plane is subjected at its free boundary to a normal uniformly distributed load of intensity p/unit area and width 2ℓ, applied symmetrically about the Y-axis (see Fig.4.3).

A solution to this problem can be obtained by treating the uniformly distributed load as a series of closely spaced concentrated forces, and by integrating the expressions for the stresses (4.2-4) between the limits $-\ell$ and $+\ell$.

The stress components are then given by the following relations:

$$\left[\sigma_x;\sigma_y;\tau_{xy}\right] = \frac{p}{\pi(k_1-k_2)} \left[\left(\frac{T_2}{k_2} - \frac{T_1}{k_1}\right);(T_1k_1-T_2k_2);\ \tfrac{1}{2}\ \ell n\left(\frac{t_1}{t_2}\right)\right], \qquad 4.4\text{-}1$$

where

4.4) contd.

$$T_i = \tan^{-1} \frac{k_i(x+\ell)}{y} - \tan^{-1} \frac{k_i(x-\ell)}{y} \text{ , for } i = 1,2, \qquad 4.4\text{-}2a$$

and

$$t_i = \frac{t_i^+}{t_i^-} \text{ , } t_i^{\pm} = y^2+k_i^2(x\pm\ell)^2 \text{. for } i = 1,2. \qquad 4.4\text{-}2b$$

The displacement v at any point (x,y) is then given by the following relation:

$$v(x,y) = \frac{P}{\pi(k_1-k_2)} \left\{ -\left(\frac{T_2\ell_2}{k_2} - \frac{T_1\ell_1}{k_1} \right) y + \right.$$
$$+ \frac{\ell_1}{2} \left[(x+\ell)\ell n\, t_1^+ - (x-\ell)\ell n\, t_1^- \right] -$$
$$\left. - \frac{\ell_2}{2} \left[(x+\ell)\ell n + t_2^+ - (x-\ell)\ell n\, t_2^- \right] \right\} + \text{const.} \qquad 4.4\text{-}3$$

where $\ell_i = \ell_{22}\, k_i^2 - \ell_{12}$, for i = 1,2.

For y = o, equation (4.4-3) reduces to:

$$v(x,o) = \frac{P}{\pi(k_1-k_2)} \left\{ 2\ell(\ell_1 \ell nk_1 - \ell_2 \ell nk_2) + \right.$$
$$\left. (\ell_1-\ell_2) \left[(x+\ell)\ell n(x+\ell) - (x-\ell)\ell n(x-\ell) \right] \right\} + \text{const.} \qquad 4.4\text{-}4$$

The arbitrary constant in equation (4.4-4) can be eliminated by considering relative displacement $v_r(x,o)$ between points (x,o) and (o,o),

i.e. $v_r(x,o) = v(x,o) - v(o,o)$,

such that

$$v_r(x,o) = \frac{P}{\pi} \ell_{22}(k_1+k_2) \left\{ (x+\ell)\ell n|x+\ell| - (x-\ell)\ell n|x-\ell| - 2\ell\ \ell n\ell \right\} \qquad 4.4\text{-}5$$

4.5) Uniformly distributed load tangential to the boundary.

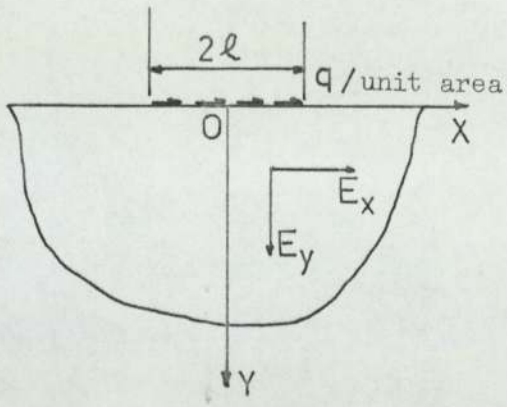

Fig.4.4

In this case, the orthotropic half-plane is subjected to a uniformly distributed shear stress of intensity q/unit area and width 2ℓ, applied symmetrically about the Y-axis (see Fig.4.4).

A solution to this problem can be obtained from the solution to the half-plane subjected to a concentrated tangential force (section 4.3), by integrating the equations for the stresses (4.3-3) between the limits $-\ell$ and $+\ell$.

Retaining the notation adopted in Section 4.4, the stress components are given by:

$$\left[\sigma_x;\sigma_y;\tau_{xy}\right] = \frac{q}{2\pi}\frac{k_1k_2}{(k_1-k_2)}\left[\left(\frac{\ell n t_2}{k_2^2}-\frac{\ell n t_1}{k_1^2}\right);\ \ell n\frac{t_1}{t_2};-2\left(\frac{T_1}{k_1}-\frac{T_2}{k_2}\right)\right] \qquad 4.5\text{-}1$$

4.6) Concentrated normal force applied through a rigid punch.

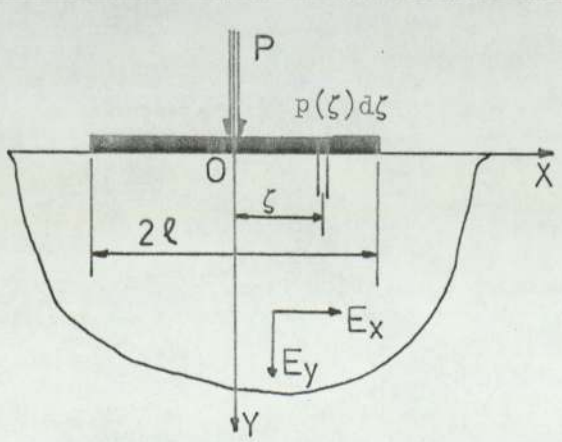

Fig.4.5

4.6) contd.

In this case, the orthotropic half-plane is subjected to a normal concentrated force P/unit thickness, applied through a rigid block of width 2ℓ (see Fig.4.5).

Let p be the pressure distribution underneath the block.

Since the block is rigid, it is assumed that:

$$v(x,o) = \text{constant, for } -\ell \leq x \leq \ell. \qquad 4.6\text{-}1$$

From equation (4.2-7):

$$v(x,o) = \frac{\ell_{22}(k_1+k_2)}{\pi} \int_{-\ell}^{\ell} p(\zeta)\, \ell n \left| \frac{x-\zeta}{a} \right| d\zeta. \qquad 4.6\text{-}2$$

Since $v(x,o)$ is constant over the loaded region of the half-plane:

$$\int_{-\ell}^{\ell} p(\zeta)\, \ell n \left| \frac{x-\zeta}{a} \right| d\zeta = \text{constant}, \qquad 4.6\text{-}3$$

Solving (4.6-3) and considering equilibrium we have:

$$p = \frac{P}{\pi\sqrt{\ell^2 - x^2}}. \qquad 4.6\text{-}4$$

The stress distribution in the half-plane can then be obtained by treating the applied stress p as a series of closely spaced concentrated forces, of magnitude $p(x)dx$, and integrating expressions (4.2-4) between the limits $-\ell$ and ℓ.

4.7) Concentrated force at the interior, acting in the positive Y-direction.

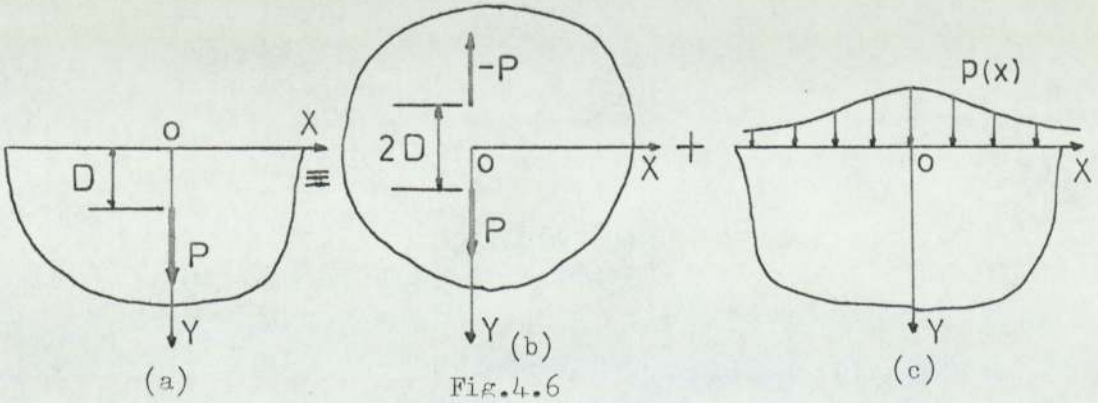

Fig.4.6

4.7) contd.

The orthotropic half-plane is subjected to a concentrated force P/unit thickness, applied at point (0,D) and in the positive Y-direction (Fig.4.6a).

Solutions to this problem have been developed by Conway (1953b) using Fourier integrals and by Saha et al. using complex variables. We shall concentrate on Conway's solution .

The infinite orthotropic plane (Fig.4.6b) is subjected to two equal and opposite forces P and -P acting along the Y-axis at points (0,D) and (0,-D) respectively. Because of symmetry of loading, the shear stresses are zero along the X-axis; and the normal stress distribution $\sigma_y^b(x,o)$ is given by equation (3.3-4).

We can nullify the normal stresses and make the X-axis a traction free boundary, by superposition to the infinite plane , of a half-plane subjected along its boundary to a normal stress distribution (see Fig.4.6c):

$$p(x) = - \sigma_y^b(x,o). \qquad 4.7\text{-}1$$

Let the indices 'b' and 'c' refer to the "infinite" and "half" plane problems respectively. Then, the stresses induced in the half-plane by an "internal" concentrated force P (Fig.4.6a) are given by:

$$\left[\sigma_x;\sigma_y;\tau_{xy}\right] = \left[\sigma_x^b;\sigma_y^b;\tau_{xy}^b\right] + \left[\sigma_x^c;\sigma_y^c;\tau_{xy}^c\right]. \qquad 4.7\text{-}2$$

The stress components $\sigma_x^b;\sigma_y^b,\tau_{xy}^b$ are given by equation (3.3-4), while $\sigma_x^c,\sigma_y^c,\tau_{xy}^c$ can be determined by considering the half-plane subjected along its boundary to a normal stress distribution p(x).

Finally:

4.7) contd.

$$\left[\sigma_x;\sigma_y;\tau_{xy}\right] = \frac{P}{\pi(k_1^2-k_2^2)}\Big\{(\alpha_1+\alpha_3)r_1\left[f_1;\ -f_1k_1^2;\ -k_1^2x\right] + \alpha_1 r_2\left[-f_2;\ f_2k_1^2;\ k_1^2x\right] + (\alpha_2-\alpha_4)r_3\left[f_1;\ f_1k_2^2;\ -k_2^2x\right] + \alpha_2 r_4\left[-f_2;\ f_2k_2^2;\ k_2^2x\right] + \alpha_3 r_5\left[-f_3;\ f_3k_2^2;\ k_1^2k_2^2x\right] + \alpha_4 r_6\left[f_4;\ f_4k_1^2;\ -k_1^2k_2^2x\right]\Big\},$$

4.7-3

where

$$\left.\begin{matrix} f_1 \\ f_2 \end{matrix}\right\} = y \pm D, \qquad f_3 = k_1(k_1y+k_2D), \qquad f_4 = k_2(k_2y+k_1D),$$

$$\left.\begin{matrix} r_1 \\ r_2 \end{matrix}\right\} = \left[k_1^2x^2+(y\pm D)^2\right]^{-1}, \qquad \left.\begin{matrix} r_3 \\ r_4 \end{matrix}\right\} = \left[k_2^2x^2+(y\pm D)^2\right]^{-1},$$

$$r_5 = \left[k_1^2k_2^2x^2+(k_2D+k_1y)^2\right]^{-1}, \quad r_6 = \left[k_1^2k_2^2x^2+(k_1D+k_2y)^2\right]^{-1},$$

$$\alpha_1 = k_1(1-\eta\, k_2^2)/2, \qquad \alpha_3 = -\frac{k_1^2(1-\eta\, k_2^2)}{k_1-k_2},$$

$$\alpha_2 = -k_2(1-\eta\, k_1^2)/2, \qquad \alpha_4 = \frac{k_2^2(1-\eta\, k_1^2)}{k_1-k_2},$$

$$\eta = \frac{\ell_{12}}{\ell_{11}}.$$

4.7-4

4.8) <u>Concentrated force at the interior acting in the positive X-direction.</u>

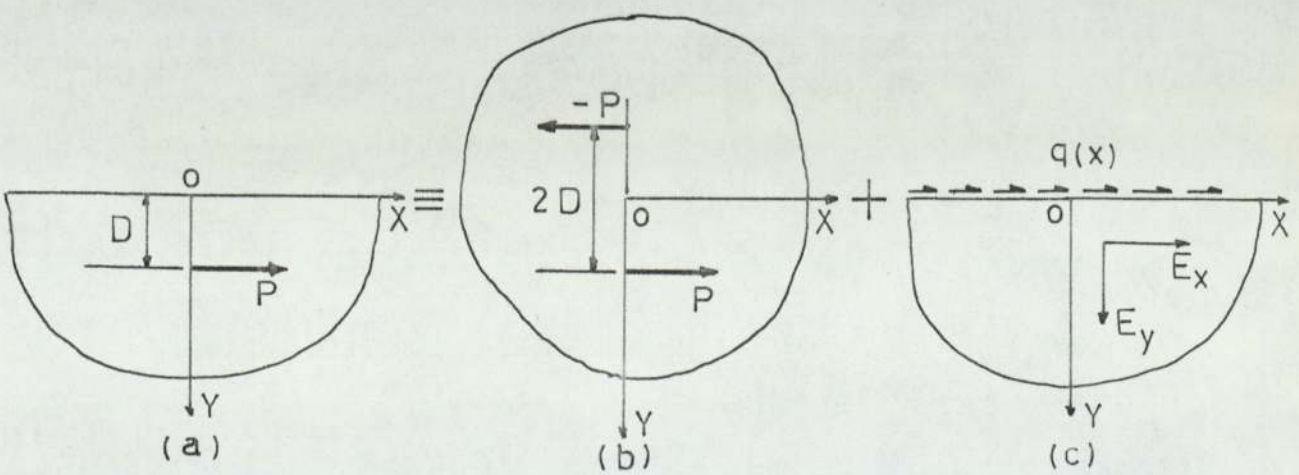

Fig.4.7

4.8) contd.

A solution to the problem of a half-plane loaded at point (0,D) by a concentrated force P/unit thickness (Fig. 4.7a), can be obtained using the method outlined in the previous section. The stress systems to be superposed are shown diagrammatically in Fig.4.7b and c.

The shear stress distribution q(x) (Fig.4.7c) is defined as being equal and opposite to $\tau_{xy}(x,o)$ of an infinite plane loaded as shown in Fig.4.7b. An expression for $\tau_{xy}(x,o)$ is given in equation (3.3-6).

Finally, the stresses induced in the half-plane by the concentrated force P (Fig.4.7a) are given by the following relations:

$$\left[\sigma_x;\sigma_y;\tau_{xy}\right] = \frac{P}{\pi}\,\frac{k_1k_2}{(k_1^2-k_2^2)}\left\{(\alpha_2-\alpha_4)r_1\left[-x\;;\;x\,k_1^2\;;\;-f_1\right]\right.$$
$$+\,\alpha_2 r_2\left[x\;;-x\,k_1^2\;;\;f_2\right]$$
$$+(\alpha_1+\alpha_3)r_3\left[-x\;;\;x\,k_2^2\;;\;-f_1\right]$$
$$+\,\alpha_1 r_4\left[x\;;-x\,k_2^2\;;\;f_2\right]$$
$$+\,\alpha_4 r_5\left[-xk_1^2;\;xk_1^2k_2^2;-f_3\right]$$
$$\left.+\,\alpha_3 r_6\left[xk_2^2;-xk_1^2k_2^2;\;f_4\right]\right\}. \qquad 4.8\text{-}1$$

4.9) Orthotropic half-plane $X > 0$.

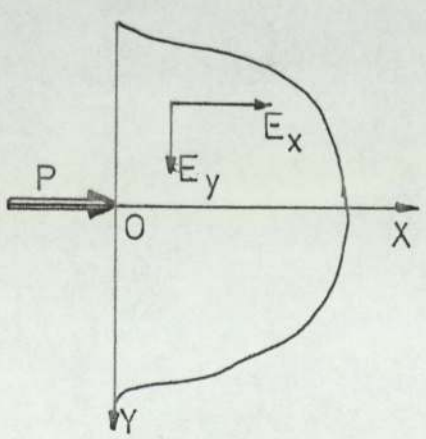

Fig.4.8

4.9) contd.

In this case, the orthotropic half-plane occupies the region $0 \leqslant x < +\infty$, $-\infty < y < +\infty$, and the concentrated force P/unit thickness is applied at the origin of the axes in the positive X-direction (See Fig.4.8).

The state of stress is defined by the stress function:

$$\Phi = \int_0^\infty \frac{1}{\zeta^2} \left(C_1 e^{-k_1 \zeta y} + C_2 e^{-k_2 \zeta y} \right) \cos \zeta y \, d\zeta, \qquad 4.9\text{-}1$$

and the corresponding stress components are given by:

$$\left[\sigma_x ; \sigma_y ; \tau_{xy} \right] = \frac{P}{\pi} \frac{k_1 k_2 (k_1 + k_2)}{(k_1^2 x^2 + y^2)(k_2^2 x^2 + y^2)} \left[x^3 ; \; xy^2 ; \; x^2 y \right]. \qquad 4.9\text{-}2$$

4.10) Uniformly distributed loads at the interior.

The expressions for the components of stress that have been developed for the problem of a half-plane subjected to concentrated forces at the interior (sections 4.7 and 4.8), can be employed to obtain solutions to the problem of a half-plane loaded at the interior by uniformly distributed stresses of finite width.

We shall limit our discussion on uniformly distributed direct/shear stresses, applied on a plane parallel to the XZ/YZ plane.

In each case, the method of solution is the same, that of integration of expressions (4.7-a) or (4.8-1) between the prescribed limits. The uniformly distributed loads are of total width $2c$, and is assumed that the centre of the load coincides with point (0,D).

The applied direct stresses are denoted by p/unit area, and the shear stresses by q/unit area.

4.10) contd.

a) Uniformly distributed direct stress applied on a plane parallel to XZ plane.

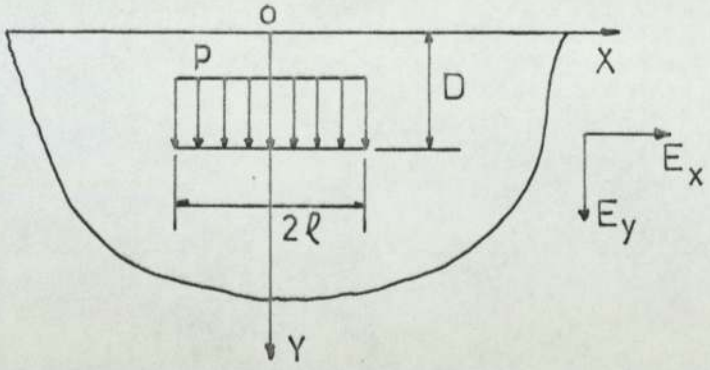

Fig.4.9

$$\left[\sigma_x;\sigma_y;\tau_{xy}\right] = \frac{p}{\pi(k_1^2-k_2^2)}\Big\{(\alpha_1+\alpha_3)\left[\frac{T^+_{11}}{k_1}\ ;\ -k_1T^+_{11}\ ;\ -\frac{L^+_{11}}{2}\right]$$

$$+\ \alpha_1\left[-\frac{T^-_{11}}{k_1}\ ;\ k_1T^-_{11}\ ;\ \frac{L^-_{11}}{2}\right]$$

$$+\ (\alpha_2-\alpha_4)\left[\frac{T^+_{22}}{k_2}\ ;\ -k_2T^+_{22}\ ;\ -\frac{L^+_{22}}{2}\right]$$

$$+\ \alpha_2\left[-\frac{T^-_{22}}{k_2}\ ;\ k_2T^-_{22}\ ;\ \frac{L^-_{22}}{2}\right]$$

$$+\ \alpha_3\left[-\frac{T^+_{12}}{k_2}\ ;\ k_2T^+_{12}\ ;\ \frac{L^+_{12}}{2}\right]$$

$$+\ \alpha_4\left[\frac{T^+_{21}}{k_1}\ ;\ -k_1T^+_{21}\ ;\ -\frac{L^+_{21}}{2}\right] \qquad 4.10\text{-}1.$$

where

$$T^{\pm}_{ij} = \tan^{-1}\frac{k_ik_j(x+\ell)}{k_iy\pm k_jD} - \tan^{-1}\frac{k_ik_j(x-\ell)}{k_iy\pm k_jD},$$

$$L^{\pm}_{ij} = \ell n\left[\frac{k_i^2k_j^2(x+\ell)^2+(k_iy\pm k_jD)^2}{k_i^2k_j^2(x-\ell)^2+(k_iy\pm k_jD)^2}\right], \qquad 4.10\text{-}2$$

for i = 1,2; j = 1,2

and α_1 ... α_4 are given by equation (4.7-4).

b) Uniformly distributed shear stress, applied on a plane parallel to XZ plane.

b) contd.

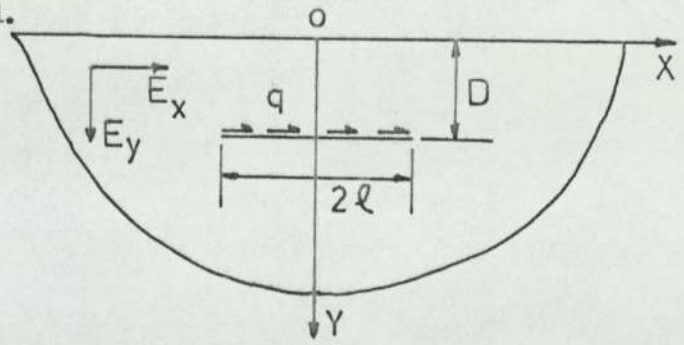

Fig.4.10

$$\left[\sigma_x;\sigma_y;\tau_{xy}\right] = \frac{q}{2\pi}\frac{k_1k_2}{(k_1^2-k_2^2)}\left\{(\alpha_2-\alpha_4)\left[-\frac{L^+_{11}}{k_1^2};\ L^+_{11};\ -\frac{2T^+_{11}}{k_1}\right]\right.$$

$$+\alpha_2\left[\frac{L^-_{11}}{k_1^2};\ -L^-_{11};\ \frac{2T^-_{11}}{k_1}\right]$$

$$+(\alpha_1+\alpha_3)\left[-\frac{L^+_{22}}{k_2^2};\ L^+_{22};\ -\frac{2T^+_{22}}{k_2}\right]$$

$$+\alpha_1\left[\frac{L^-_{22}}{k_2^2};\ -L^-_{22};\ \frac{2T^-_{22}}{k_2}\right]$$

$$+\alpha_4\left[-\frac{L^+_{12}}{k_2^2};\ L^+_{12};\ -\frac{2T^+_{12}}{k_2}\right]$$

$$\left.+\alpha_3\left[\frac{L^+_{21}}{k_1^2};\ -L^+_{21};\ \frac{2T^+_{21}}{k_1}\right]\right\}$$

4.10-3

where $L^{\pm}_{ij}$ and $T^{\pm}_{ij}$ are defined by equation (4.10-2).

c) Uniformly distributed direct stress, applied on YZ plane.

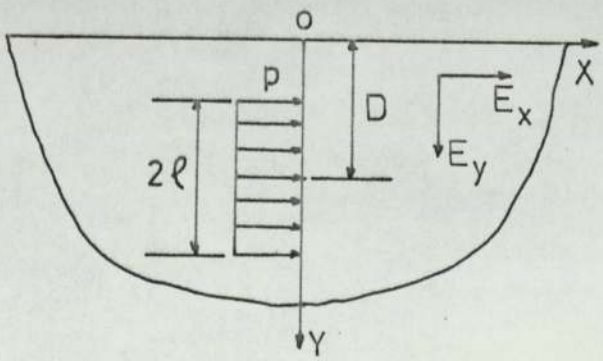

Fig.4.11

4.10) contd.

c) contd.

$$\left[\sigma_x;\sigma_y;\tau_{xy}\right] = -\frac{p}{\pi}\frac{k_1k_2}{(k_1^2-k_2^2)}\Bigg\{ (\alpha_2-\alpha_4)\left[\frac{\bar{T}^+_{11}}{k_1} - -k_1\bar{T}^+_{11}\ ;\ \frac{\bar{L}^+_{11}}{2}\right]$$

$$+\ \alpha_2\left[\frac{\bar{T}^-_{11}}{k_1}\ ;\ -k_1\bar{T}^-_{11}\ ;\ \frac{\bar{L}^-_{11}}{2}\right]$$

$$+(\alpha_1+\alpha_3)\left[\frac{\bar{T}^+_{22}}{k_2}\ ;\ -k_2\bar{T}^+_{22}\ ;\ \frac{\bar{L}^+_{22}}{2}\right]$$

$$+\ \alpha_1\left[\frac{\bar{T}^-_{22}}{k_2}\ ;\ -k_2\bar{T}^-_{22}\ ;\ \frac{\bar{L}^-_{22}}{2}\right]$$

$$+\ \alpha_4\left[\frac{k_1\bar{T}^+_{12}}{k_2^2};\ -k_1\bar{T}^+_{12};\ \frac{k_1}{k_2}\ \frac{\bar{L}^+_{12}}{2}\right]$$

$$+\ \alpha_3\left[\frac{-k_2\bar{T}^+_{21}}{k_1^2};\ k_2\bar{T}^+_{21};-\frac{k_2}{k_1}\ \frac{\bar{L}^+_{21}}{2}\right]\Bigg\}$$

4.10-4

where

$$\bar{T}^{\pm}_{ij} = \tan^{-1}\frac{k_iy\pm k_j(D+\ell)}{k_ik_jx} - \tan^{-1}\frac{k_iy\pm k_j(D-\ell)}{k_ik_jx}\ ,$$

and

$$\bar{L}^{\pm}_{ij} = \ell n\left[\frac{(k_ik_jx)^2+[k_iy\pm k_j(D+\ell)]^2}{(k_ik_jx)^2+[k_iy\pm k_j(D-\ell)]^2}\right]. \qquad 4.10\text{-}5$$

d) Uniformly distributed shear stress applied on the YZ plane.

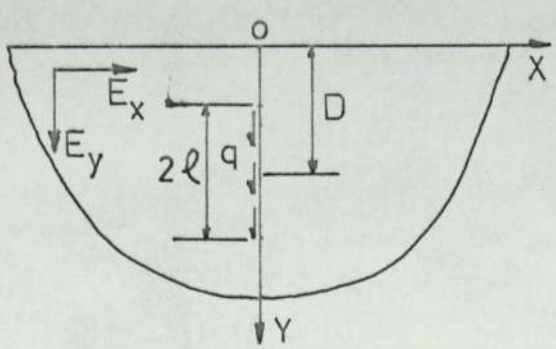

Fig.4.12

4.10) contd.

d) contd.

$$\left[\sigma_x;\ \sigma_y;\ \tau_{xy}\right] = -\frac{q}{2\pi(k_1^2-k_2^2)}\Bigg\{$$

$$(\alpha_1+\alpha_3)\left[-\bar{L}^{+}_{11}\ ;\ k_1^2\,\bar{L}^{+}_{11}\ ;\ 2k_1\,\bar{T}^{+}_{11}\right]$$

$$+\ \alpha_1\left[-\bar{L}^{-}_{11}\ ;\ k_1^2\,\bar{L}^{-}_{11}\ ;\ 2k_1\,\bar{T}^{-}_{11}\right]$$

$$+(\alpha_2-\alpha_4)\left[-\bar{L}^{+}_{22}\ ;\ k_2^2\,\bar{L}^{+}_{22}\ ;\ 2k_2\,\bar{T}^{+}_{22}\right]$$

$$+\ \alpha_2\left[-\bar{L}^{-}_{22}\ ;\ k_2^2\,\bar{L}^{-}_{22}\ ;\ 2k_2\,\bar{T}^{-}_{22}\right]$$

$$+\ \alpha_3\left[\frac{k_1}{k_2}\,\bar{L}^{+}_{12};\ -k_1k_2\,\bar{L}^{+}_{12};\ -2k_1\,\bar{T}^{+}_{12}\right]$$

$$+\ \alpha_4\left[-\frac{k_2}{k_1}\,\bar{L}^{+}_{21};\ k_1k_2\,\bar{L}^{+}_{21};\ 2k_2\bar{T}^{+}_{21}\right]\Bigg\}$$

where $\bar{T}^{\pm}_{ij}$ and $\bar{L}^{\pm}_{ij}$ are defined by equation (4.10-5).

CHAPTER 5

LAYERED ORTHOTROPIC HALF PLANE.

5.1) Introduction.

The analysis of layered elastic systems has mainly concentrated in the past, on problems related to the two-layer half-space, which is subjected on its plane boundary to axially symmetric (3-dimensional) or strip loads (2-dimensional).

The two-layer half-space was assumed to consist of two isotropic elastic materials, one in the form of a layer of finite thickness and infinite horizontal extent, overlying a second material which was assumed to correspond to an elastic half-space.

Different properties have been assigned to the layers by different investigators, who, in addition assumed that the interface between the layers was either smooth (frictionless) or rough (perfect continuity).

Biot (1935), developed expressions for the stresses and displacements in an isotropic elastic layer resting on a rigid base for line or axial loadings. Both conditions of smooth and rough interface were considered. Similar results we obtained by Pickett (1938).

Burmister (1943), established equations for the stresses in the isotropic two-layer system subjected to a radially symmetric load. He assumed a value of Poisson's ratio $\nu = 0.5$, for conditions of perfect continuity and zero friction at the interface. In 1945, Burmister (1945) extended his theory to the three-layer system.

Lemcoe (1960), derived expressions for the stresses in multi-layer systems, which were assumed to be in a state of plane strain. He presented numerical results for the stresses in a two-layer isotropic half-plane, subjected to line and strip loadings, for a given value of Poisson's ratio $\nu = 0.25$ for both materials. Lemcoe considered a

5.1) contd.

range of values for the ratio of the Young's modulii of the two materials.

Approximate solutions for surface displacements in multilayer systems due to circular uniform loads, have been developed by Ueshita and Meyerhoff (1967).

Gerrard (1967), considered the problem of an anisotropic elastic layer resting on a smooth rigid base and subjected to a strip load. He assigned different values to the elastic constants of the material and in each case, he presented numerical results for the stresses in the elastic layer.

Gerrard and Harrison (1971), formulated mathematical solutions (without mathematical evaluation) for stresses and displacements in a half-space, consisting of any number of anisotropic layers and subjected on its plane boundary to a radially symmetric uniform load.

In this chapter, we shall employ Lemcoe's method, to obtain a solution to the layered half-plane, which consists of any number of orthotropic elastic layers. Numerical results will be presented for the particular case of a two-layer half-plane, which is subjected to a line load.

5.2) Assumptions and Conditions.

The assumptions and conditions necessary for a full description of the problem can be classified into three categories:

I) Notation.

The layered half plane is assumed to consist of (n-1) layers, each of finite thickness and infinite extent, and the n^{th} layer corresponding to a half plane. In general, a layer is designated by the subscript i (i = 1,2 ... n) (see Fig.5.1).

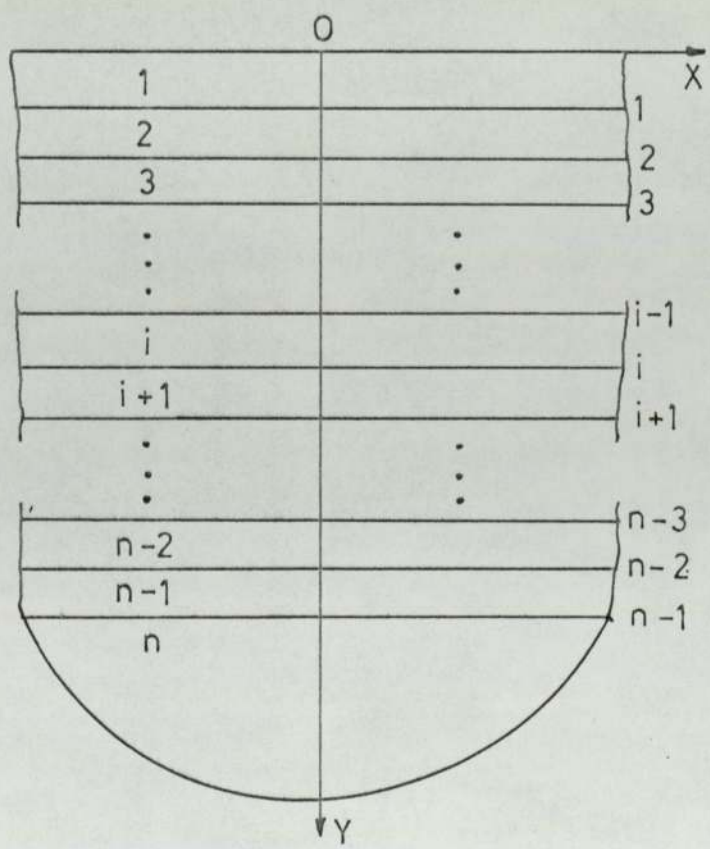

Fig.5.1 Layered half plane.

II) Properties of the material.

All layers in the half plane are assumed to be of homogeneous, orthotropic, elastic materials. The

5.2) contd.

II) contd.

axes of elastic symmetry for each material are assumed to be parallel to the coordinate axes X and Y. Their elastic properties are specified by k_1^i and k_2^i and are assumed to be different for each layer.

III) Boundary conditions.

The boundary conditions for the layered half plane can be divided into two categories:

a) Those they deal with the half plane as a whole; and

b) those they specify the conditions at the interfaces between layers.

a) The complete layered half plane should satisfy:

1) Traction or displacement boundary conditions at $y = 0$.

2) The stresses should tend to zero as $y \to \infty$.

b) The interface conditions considered are:

1) Perfect continuity.

At the i^{th} interface ($y = y_i$):

$$\left[\sigma_y^i;\ \tau_{xy}^i;\ u^i;\ v^i\right] = \left[\sigma_y^{i+1};\ \tau_{xy}^{i+1};\ u^{i+1};\ v^{i+1}\right].$$

2) Smooth interface.

At the i^{th} interface:

$$\left[\sigma_y^i;\ v^i\right] = \left[\sigma_y^{i+1};\ v^{i+1}\right],$$

and

$$\tau_{xy}^i = \tau_{xy}^{i+1} = 0.$$

5.3) Stress function.

The layered half plane is subjected at its free boundary to two sinusoidal loads:

a normal stress

$$p(x) = p_o \cos(\lambda x), \qquad 5.3\text{-}1$$

5.3) contd.

and a shear stress

$$q(x) = q_o \sin(\lambda x). \qquad 5.3\text{-}2$$

The assumed Airy's stress function (see Timoshenko & Goodier) is:

$$\Phi = f(y) \cos(\lambda x), \qquad 5.3\text{-}3$$

where f(y) is a function of y only.

The stresses are defined by:

$$\sigma_x = \frac{\partial^2 \Phi}{\partial y^2} \ , \ \sigma_y = \frac{\partial^2 \Phi}{\partial x^2} \ , \ \tau_{xy} = -\frac{\partial^2 \Phi}{\partial x \partial y} \ . \qquad 5.3\text{-}4$$

Using the assumed form of Φ (5.3-3) and the general differential equation for plane orthotropic elasticity:

$$\left(\frac{\partial^2 \Phi}{\partial x^2} + k_1^2 \ \frac{\partial^2 \Phi}{\partial y^2} \right) \left(\frac{\partial^2 \Phi}{\partial x^2} + k_2^2 \ \frac{\partial^2 \Phi}{\partial y^2} \right) = 0,$$

we obtain Φ as follows:

$$\Phi = \left(C_1 \ e^{\alpha y} + C_2 \ e^{-\alpha y} + C_3 \ e^{\beta y} + C_4 \ e^{-\beta y} \right) \cos(\lambda x), \qquad 5.3\text{-}5$$

where

$$\alpha = \frac{\lambda}{k_1} \ , \ \beta = \frac{\lambda}{k_2} \text{ and } C_1 \ldots C_4 \text{ are constants}$$

that can be determined by the boundary conditions.

5.4) Layered half plane subjected to sinusoidal loads; Perfect continuity.

The stresses in the i^{th} layer of a layered half plane, under the action of normal and shear sinusoidal stresses at the free boundary (y = 0), are given by the equation:

$$\underset{\sim}{S}^i = \underset{\sim}{E}^i \ \underset{\sim}{C}^i \ , \qquad 5.4\text{-}1a$$

where

5.4) contd.

$$\mathfrak{S}^i = \begin{bmatrix} \sigma_x^i \\ \sigma_y^i \\ \tau_{xy}^i \\ \end{bmatrix}, \qquad \mathfrak{C}^i = \begin{bmatrix} C_1^i \\ C_2^i \\ C_3^i \\ C_4^i \end{bmatrix},$$

and

$$\mathfrak{E}^i = \begin{bmatrix} & \cos(\lambda x) & \left[\alpha_i^2 e^{\alpha_i y};\ \alpha_i^2 e^{-\alpha_i y};\ \beta_i^2 e^{\beta_i y};\ \beta_i^2 e^{-\beta_i y}\right] \\ -\lambda^2 & \cos(\lambda x) & \left[\ e^{\alpha_i y};\ \ e^{-\alpha_i y};\ \ e^{\beta_i y};\ \ e^{-\beta_i y}\right] \\ \lambda & \sin(\lambda x) & \left[\alpha_i e^{\alpha_i y};-\alpha_i e^{-\alpha_i y};\ \beta_i e^{\beta_i y};-\beta_i e^{-\beta_i y}\right] \end{bmatrix}. \qquad 5.4\text{-}1b$$

The constants $\mathfrak{C}^i$ can be uniquely determined from the boundary conditions of the i^{th} layer. These are:

a) Normal and shear stress continuity, and

b) compatibility of displacements at the (i-1) and i^{th} interfaces.

Since the externally applied loads are sinusoidal, we may assume that the normal and shear stresses on any interface are also sinusoidal.

Let $p_i \cos(\lambda x)$ and $q_i \sin(\lambda x)$ be the normal and shear stresses on the i^{th} interface. For equilibrium at the boundaries of the i^{th} layer :

a) on the i^{th} interface $(y = y_i)$

$\sigma_y = p_i \cos(\lambda x)$; $\tau_{xy} = q_i \sin(\lambda x)$,

b) on the $(i-1)^{th}$ interface $(y = y_{i-1})$

$\sigma_y = p_{i-1} \cos(\lambda x)$; $\tau_{xy} = q_{i-1} \sin(\lambda x)$.

Substituting the above expressions into equation (5.4-1), four relations can be obtained between

5.4) contd.

$(p_i, q_i, p_{i-1}, q_{i-1})$ and $\mathfrak{L}^i$:

$$\begin{bmatrix} p_{i-1} \\ q_{i-1} \\ p_i \\ q_i \end{bmatrix} = \mathfrak{A}^i \ \mathfrak{L}^i , \qquad 5.4\text{-}2a$$

where

$$\underset{\sim}{\Lambda}^i = \begin{bmatrix} -\lambda^2 \left[e^{\alpha_i y_{i-1}}; \ e^{-\alpha_i y_{i-1}}; \ e^{\beta_i y_{i-1}}; \ e^{-\beta_i y_{i-1}} \right] \\ \lambda \left[\alpha_i e^{\alpha_i y_{i-1}}; -\alpha_i e^{-\alpha_i y_{i-1}}; \beta_i e^{\beta_i y_{i-1}}; -\beta_i e^{-\beta_i y_{i-1}} \right] \\ -\lambda^2 \left[e^{\alpha_i y_i} ; \ e^{-\alpha_i y_i} ; \ e^{\beta_i y_i} ; \ e^{-\beta_i y_i} \right] \\ \lambda \left[\alpha_i e^{\alpha_i y_i} ; -\alpha_i e^{-\alpha_i y_i} ; \beta_i e^{\beta_i y_i} ; -\beta_i e^{-\beta_i y_i} \right] \end{bmatrix} . \qquad 5.4\text{-}2b$$

$\underset{\sim}{\Lambda}^i$ is known (for each layer), since its elements are functions of α_i, β_i and the y-coordinates of the boundaries of the i^{th} layer.

Let

$$\mathfrak{L}^i = \begin{bmatrix} p_i \\ q_i \end{bmatrix} , \text{ and } \mathfrak{R}^i = \begin{bmatrix} \mathfrak{L}^{i-1} \\ \underset{\sim}{\mathfrak{L}}^i \end{bmatrix} .$$

Then

$$\mathfrak{R}^i = \underset{\sim}{\Lambda}^i \ \mathfrak{L}^i . \qquad 5.4\text{-}3$$

Assuming that $|\underset{\sim}{\Lambda}^i| \neq 0$, the inversion of (5.4-3) gives:

$$\mathfrak{L}^i = \mathfrak{A}^i \ \mathfrak{R}^i , \qquad 5.4\text{-}4$$

where

$$\underset{\sim}{A}^i = [\underset{\sim}{\Lambda}^i]^{-1} . \qquad 5.4\text{-}5$$

Let $\underset{\sim}{A}^i$ be partitioned according to:

$$\underset{\sim}{A}^i = [\underset{\sim}{A}^i_1 \vdots \ \underset{\sim}{A}^i_2] .$$

5.4) contd.

Then,

$$\underset{\sim}{C}^i = \left[\underset{\sim}{A}_1^i \vdots \underset{\sim}{A}_2^i \right] \begin{bmatrix} \underset{\sim}{L}^{i-1} \\ \underset{\sim}{L}^i \end{bmatrix},$$

or

$$\underset{\sim}{C}^i = \underset{\sim}{A}_1^i \; \underset{\sim}{L}^{i-1} + \underset{\sim}{A}_2^i \; \underset{\sim}{L}^i . \qquad 5.4\text{-}6$$

Considering the displacements at the i^{th} interface ($y = y_i$), for perfect continuity,

$$\left[u^i \right]_{y_i} = \left[u^{i+1} \right]_{y_i} , \text{ and } \left[v^i \right]_{y_i} = \left[v^{i+1} \right]_{y_i} . \qquad 5.4\text{-}7$$

It can be shown (see Appendix [3]), that the displacements at the i^{th} interface can be expressed in terms of the constants $\underset{\sim}{C}^i$ by the following relations:

$$\left[u^i \right]_{y_i} = \underset{\sim}{U}^i \; \underset{\sim}{C}^i \; \sin(\lambda x), \qquad 5.4\text{-}8a$$

$$\left[v^i \right]_{y_i} = \underset{\sim}{V}^i \; \underset{\sim}{C}^i \; \cos(\lambda x), \qquad 5.4\text{-}8b$$

$$\left[u^{i+1} \right]_{y_i} = \underset{\sim}{U}^{i+1} \; \underset{\sim}{C}^{i+1} \; \sin(\lambda x), \qquad 5.4\text{-}8c$$

$$\left[v^{i+1} \right]_{y_i} = \underset{\sim}{V}^{i+1} \underset{\sim}{C}^{i+1} \; \cos(\lambda x). \qquad 5.4\text{-}8d$$

Substituting equations (5.4-8) into (5.4-7) and expressing the system of the two simultaneous equations,

$$\underset{\sim}{U}^i \; \underset{\sim}{C}^i = \underset{\sim}{U}^{i+1} \; \underset{\sim}{C}^{i+1} ,$$

$$\underset{\sim}{V}^i \; \underset{\sim}{C}^i = \underset{\sim}{V}^{i+1} \; \underset{\sim}{C}^{i+1} ,$$

in matrix form:

$$\underset{\sim}{D}^i \; \underset{\sim}{C}^i = \underset{\sim}{D}^{i+1} \; \underset{\sim}{C}^{i+1} , \qquad 5.4\text{-}9a$$

5.4) contd.

where

$$\underset{\sim}{D}^i = \begin{bmatrix} U^i \\ V^i \end{bmatrix}. \qquad 5.4\text{-}9b$$

Using the appropriate expressions for $\underset{\sim}{\mathcal{C}}^i$ and $\underset{\sim}{\mathcal{C}}^{i+1}$ (equation 5.4-6), and adopting the notation:

$$\underset{\sim}{B}^i = \underset{\sim}{D}^i \underset{\sim}{A}^i, \qquad 5.4\text{-}10a$$

and

$$\underset{\sim}{B}^i = \left[\underset{\sim}{B}_1^i \vdots \underset{\sim}{B}_2^i \right], \qquad 5.4\text{-}10b$$

equation (5.4-9) can be expressed in the form:

$$\underset{\sim}{B}_1^i \underset{\sim}{L}^{i-1} + \underset{\sim}{B}_2^i \underset{\sim}{L}^i = \underset{\sim}{B}_1^{i+1} \underset{\sim}{L}^i + \underset{\sim}{B}_2^{i+1} \underset{\sim}{L}^{i+1},$$

$$\text{or} \quad \underset{\sim}{L}^{i-1} = \underset{\sim}{M}^i \underset{\sim}{L}^i + \underset{\sim}{N}^i \underset{\sim}{L}^{i+1}, \qquad 5.4\text{-}11a$$

where

$$\underset{\sim}{M}^i = \left[\underset{\sim}{B}_1^i \right]^{-1} \left[\underset{\sim}{B}_1^{i+1} - \underset{\sim}{B}_2^i \right], \qquad 5.4\text{-}11b$$

$$\text{and} \quad \underset{\sim}{N}^i = \left[\underset{\sim}{B}_1^i \right]^{-1} \underset{\sim}{B}_2^{i+1}. \qquad 5.4\text{-}11c$$

For the $(n-1)^{th}$ interface, and since $\underset{\sim}{L}^n$ is a null matrix, equation (5.4-11a) gives:

$$\underset{\sim}{L}^{n-2} = \underset{\sim}{M}^{n-1} \underset{\sim}{L}^{n-1},$$

or

$$\underset{\sim}{L}^{n-1} = \underset{\sim}{F}^{n-1} \underset{\sim}{L}^{n-2}, \qquad 5.4\text{-}12a$$

where

$$\underset{\sim}{F}^{n-1} = \left[\underset{\sim}{M}^{n-1} \right]^{-1}. \qquad 5.4\text{-}12b$$

By considering the $(n-2)^{nd}$ interface, and the result (5.4-12b), we can obtain a relation between $\underset{\sim}{L}^{n-2}$ and $\underset{\sim}{L}^{n-3}$. This takes the form:

$$\underset{\sim}{L}^{n-2} = \underset{\sim}{F}^{n-2} \underset{\sim}{L}^{n-3}. \qquad 5.4\text{-}13$$

The same procedure can be followed through all the interfaces, so that for the $(i+1)^{th}$ interface (it follows from 5.4-12a),

5.4) contd.

$$\mathcal{L}^{i+1} = \mathcal{F}^{i+1}\,\mathcal{L}^{i}. \qquad 5.4\text{-}14$$

Substituting the above equation into (5.4-11a) gives:

$$\underset{\sim}{L}^{i-1} = \left[\underset{\sim}{M}^{i} + \underset{\sim}{N}^{i}.\underset{\sim}{F}^{i+1}\right] \underset{\sim}{L}^{i}. \qquad 5.4\text{-}15$$

Inverting (5.4-15) we obtain:

$$\underset{\sim}{L}^{i} = \underset{\sim}{F}^{i}\ \underset{\sim}{L}^{i-1}\ , \qquad 5.4\text{-}16a$$

where

$$\underset{\sim}{F}^{i} = \left[\underset{\sim}{M}^{i} + \underset{\sim}{N}^{i}\ \underset{\sim}{F}^{i+1}\right]^{-1}. \qquad 5.4\text{-}16b$$

For i = n, equation (5.4-16a) gives

$$\underset{\sim}{L}^{n} = \underset{\sim}{F}^{n}\ \ \underset{\sim}{L}^{n-1}\ ,$$

but since $\underset{\sim}{L}^{n} = 0$, being the stresses at $y = \infty$, it follows that for the equation to be satisfied,

$$\underset{\sim}{F}^{n} = 0.$$

Since $\mathcal{M}^{i}$ and $\mathcal{N}^{i}$ are known for all the layers, and and since $\mathcal{F}^{n} = 0$, then $\mathcal{F}^{i}$ can be determined for each layer through equation (5.4-16b).

It follows from equation (5.4-16a) that:

$$\underset{\sim}{L}^{i} = \underset{\sim}{F}^{i}\ \underset{\sim}{F}^{i-1}\ \underset{\sim}{F}^{i-2}\ \ \cdots\cdots\ \underset{\sim}{F}^{2}\ \underset{\sim}{F}^{1}\ \underset{\sim}{L}^{o},$$

or

$$\underset{\sim}{L}^{i} = \underset{\sim}{F}^{i}\ !\ \underset{\sim}{L}^{o}. \qquad 5.4\text{-}17$$

We shall note here that for i = 0, the term $\underset{\sim}{F}^{o}$ appears, which has not been previously defined. But referring to equation (5.4-17), for i = 0 the equation becomes an identity and $\underset{\sim}{F}^{o}$ must be the unit matrix for the identity to be satisfied for all values of $\underset{\sim}{L}^{o}$.

Once the boundary loads for each layer have been specified in terms of the external loads $\underset{\sim}{L}^{o}$ (see 5.4-17), the constants $\mathcal{C}^{i}$ can be determined from equation (5.4-6):

5.4) contd.

$$\underset{\sim}{C}^{i} = \left[\underset{\sim}{A}_{1}^{i} + \underset{\sim}{A}_{2}^{i} \quad \underset{\sim}{F}^{i} \right] \underset{\sim}{F}^{i-1} \; ! \; \underset{\sim}{L}^{o}. \qquad 5.4\text{-}18$$

The above equation can be simplified by making the substitution:

$$\underset{\sim}{A}_{o}^{i} = \left[\underset{\sim}{A}_{1}^{i} + \underset{\sim}{A}_{2}^{i} \quad \underset{\sim}{F}^{i} \right] \underset{\sim}{F}^{i-1} \; ! \; , \qquad 5.4\text{-}19a$$

such that

$$\underset{\sim}{C}^{i} = \underset{\sim}{A}_{o}^{i} \; \underset{\sim}{L}^{o} \; . \qquad 5.4\text{-}19b$$

Once the constants $\underset{\sim}{C}^{i}$ have been established in terms of the external loads, the stresses at any point in the half plane can be determined from equation (5.4-1).

5.5) Layered half plane subjected to sinusoidal loads; Smooth interface.

The method of solution of this problem is identical to the procedure outlined in the previous section. Whenever possible, the notation adopted earlier has been retained.

The normal and shear stresses at the interfaces are given, as before, by:

$$p_i \cos(\lambda x) \text{ and } q_i \sin(\lambda x) = 0,$$

and the matrices $\underset{\sim}{\Lambda}^{i}$ and $\underset{\sim}{A}^{i}$ remain unaltered.

It follows that the general relationship:

$$\underset{\sim}{C}^{i} = \underset{\sim}{A}_{1}^{i} \; \underset{\sim}{L}^{i-1} + \underset{\sim}{A}_{2}^{i} \; \underset{\sim}{L}^{i} \qquad , \qquad 5.5\text{-}1$$

as defined by (5.4-6), is still valid, but since the shear stresses are zero at the interfaces, certain simplifications can be achieved.

By partitioning $\underset{\sim}{A}_{1}^{i}$ and $\underset{\sim}{A}_{2}^{i}$ according to:

$$\underset{\sim}{A}_{1}^{i} = \left[\underset{\sim}{A}_{11}^{i} \; \vdots \; \underset{\sim}{A}_{12}^{i} \right] \; ; \; \underset{\sim}{A}_{2}^{i} = \left[\underset{\sim}{A}_{21}^{i} \; \vdots \; \underset{\sim}{A}_{22}^{i} \right] ,$$

equation (5.5-1) reduces to

5.5) contd.

$$\underset{\sim}{C}^{i} = \begin{bmatrix} \underset{\sim}{A}^{i}_{11} \vdots \underset{\sim}{A}^{i}_{12} \end{bmatrix} \begin{bmatrix} p_{i-1} \\ q_{i-1} \end{bmatrix} + \begin{bmatrix} \underset{\sim}{A}^{i}_{21} \vdots \underset{\sim}{A}^{i}_{22} \end{bmatrix} \begin{bmatrix} p_{i} \\ q_{i} \end{bmatrix}, \quad 5.5\text{-}2$$

and since

$$q_{i-1} = q_{i} = 0,$$

for $i > 1$

$$\underset{\sim}{C}^{i} = \underset{\sim}{A}^{i}_{11} \; p_{i-1} + \underset{\sim}{A}^{i}_{21} \; p_{i} \; . \qquad 5.5\text{-}3$$

For $i = 1$, and since $q_{o} \neq 0$, the constants $\underset{\sim}{C}^{1}$ are given by:

$$\underset{\sim}{C}^{1} = \begin{bmatrix} \underset{\sim}{A}^{1}_{11} \vdots \underset{\sim}{A}^{1}_{12} \end{bmatrix} \begin{bmatrix} p_{o} \\ q_{o} \end{bmatrix} + \underset{\sim}{A}^{1}_{21} \; p_{1} \; . \qquad 5.5\text{-}4$$

The compatibility of displacements in the Y-direction, at the interfaces, requires that:

$$\left[v^{i} \right]_{y_i} = \left[v^{i+1} \right]_{y_i} \; . \qquad 5.5\text{-}5$$

No relation can be established between the displacements in the X-direction, since the layers are free to move relative to each other.

By means of equations (5.4-8b and c), the compatibility condition (5.5-5) can be expressed as:

$$\underset{\sim}{V}^{i} \; \underset{\sim}{C}^{i} = \underset{\sim}{V}^{i+1} \; \underset{\sim}{C}^{i+1} \; . \qquad 5.5\text{-}6$$

Upon substitution of values for $\underset{\sim}{C}^{i}$ and $\underset{\sim}{C}^{i+1}$ given by (5.5-3), we obtain:

a) For $i > 1$,

$$B^{i}_{11} \; p_{i-1} + B^{i}_{21} \; p_{i} = B^{i+1}_{11} \; p_{i} + B^{i+1}_{21} \; p_{i+1} \; , \qquad 5.5\text{-}7a$$

where

$$B^{i}_{jk} = \underset{\sim}{V}^{i} \; \underset{\sim}{A}^{i}_{jk} \quad \text{for } j = 1,2; \; k = 1,2. \qquad 5.5\text{-}7b$$

We note that B^{i}_{ik} is a scalar quantity.

5.5) contd.

a) contd.

for $B^{i}_{11} \neq 0$,

$$p_{i-1} = M^{i}\, p_{i} + N^{i}\, p_{i+1}\,, \qquad 5.598a$$

where

$$M^{i} = \frac{B^{i+1}_{11} - B^{i}_{21}}{B^{i}_{11}} \quad \text{and} \quad N^{i} = \frac{B^{i+1}_{21}}{B^{i}_{11}}\,. \qquad 5.5\text{-}8b$$

b) For i = 1,

$$B^{1}_{11}\, p_{o} + B^{1}_{12}\, q_{o} + B^{1}_{21}\, p_{1} = B^{2}_{11} p_{1} + B^{2}_{21} p_{2}\,. \qquad 5.5\text{-}9$$

From here onwards the procedure to determine the constants $\underset{\sim}{C}^{i}$ in terms of the external loads (p_o, q_o), is identical to the one followed in the previous section and therefore it will not be considered in any great detail.

It can be shown that a relation can be obtained between the normal stresses on adjacent interfaces, in the form:

For i > 1,

$$p_{i} = F^{i}\, p_{i-1}\,, \qquad 5.5\text{-}10a$$

and for i = 1, an expression for p_1 can be obtained through equation (4.5-9) in the form:

$$p_{1} = F^{1}\left[\, p_{o} + \frac{B^{1}_{12}}{B^{1}_{11}}\, q_{o}\right], \qquad 5.5\text{-}10b$$

where

$$F^{i} = (M^{i} + N^{i}\, F^{i+1})^{-1}\,. \qquad 5.5\text{-}10c$$

For i = 0, equation (5.5-10a) becomes an identity, and to be satisfied, $F^{o} = 1$.

Let

$$p_{eqv.} = p_{o} + \frac{B^{1}_{12}}{B^{1}_{11}}\, q_{o}\,, \qquad 5.5\text{-}11$$

the, it follows from equations (5.5-10a and b):

5.5) contd.

$$p_i = F^i \; ! \; p_{eqv.} \; , \qquad 5.5\text{-}12$$

and consequently the constants $\underset{\sim}{C}^i$ can be determined for all the layers through the following equation:

$$\underset{\sim}{C}^i = \underset{\sim}{A}^i_o \; p_{eqv.} \; , \qquad 5.5\text{-}13a$$

where

$$\underset{\sim}{A}^i_o = \left[\underset{\sim}{A}^i_{11} + \underset{\sim}{A}^i_{21} \; F^i \right] F^{i-1} \; ! \quad . \qquad 5.5\text{-}13b$$

5.6) Two-layer half-plane subjected to sinusoidal loads.

The 2-layer half-plane constitutes a special case of the general problem described in the previous sections (5.4 and 5.5), and is of interest to many engineering situations, particularly those involving design of pavements, embankments or continuous footings, where the interaction of two materials (structure and soil), approximately resembles the 2-layer system.

Investigations into the elastic properties of soils and rocks has shown (see Barden (1963), Berry (1961), Salamon (1968), Pickering (1970)), that various types of soil (overconsolidated or fissured clays, stratified soils) and many rocks (stratified sedimentary, folded, faulted etc.) exhibit orthotropic behaviour. Similarly, reinforced concrete can be treated as orthotropic material (Isenberg and Adham (1970)).

In view of its applications to Soil Mechanics and Civil Engineering in general, we shall consider the 2-layer half-plane problem in some detail.

The two types of interface between the layers, namely "perfect continuity" and "the smooth interface" are considered separately. In each case, a solution is

5.6) contd.

sought to the problem, where the surface of the layered half plane is subjected to external sinusoidal loads. This solution forms the basis for the treatment of half-plane problems, in which the surface of the half-plane is subjected to either concentrated or uniformly distributed loads.

In the following sections, the symbols which refer to the second layer, namely the half-plane, are denoted by a dash ('), e.g. σ'_x.

The thickness h of the top layer (see Fig.5.2), can be set equal to the unit length, such that:

$$\bar{x} = \frac{x}{h} \quad , \quad \bar{y} = \frac{y}{h}. \qquad 5.6\text{-}1$$

5.6.1) "Perfect continuity" condition.

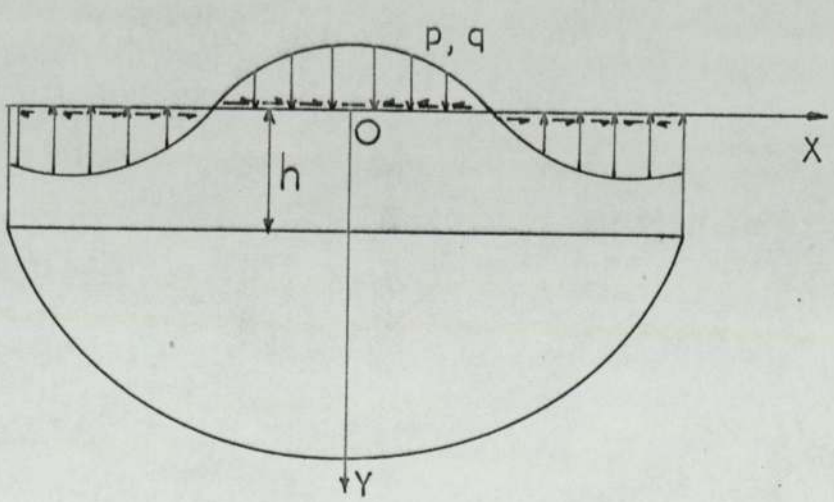

Fig.5.2

The externally applied loads are:

$$\left.\begin{aligned} \sigma_y\,(\bar{x},\,0) &= p\,\cos(\lambda\bar{x}) \\ \tau_{xy}(\bar{x},\,0) &= q\,\sin(\lambda\bar{x}) \end{aligned}\right\}, \qquad 5.6\text{-}2a$$

and the stress distribution on the interface is assumed to be composed of:

5.6.1) contd.

$$\left.\begin{aligned} \sigma_y\ (\bar{x},\ 1) &= p'\ \cos(\lambda\bar{x}) \\ \tau_{xy}(\bar{x},\ 1) &= q'\ \sin(\lambda\bar{x}) \end{aligned}\right\}, \qquad 5.6\text{-}2b$$

Equation (5.4-1) in conjunction with (5.6-2a and b) gives:

$$\begin{bmatrix} p \\ q \\ p' \\ q' \end{bmatrix} = \begin{bmatrix} -\lambda^2 & -\lambda^2 & -\lambda^2 & -\lambda^2 \\ \lambda\alpha & -\lambda\alpha & \lambda\beta & -\lambda\beta \\ -\lambda^2 e^{\alpha} & -\lambda^2 e^{-\alpha} & -\lambda^2 e^{\beta} & -\lambda^2 e^{-\beta} \\ \lambda\alpha e^{\alpha} & -\lambda\alpha e^{-\alpha} & \lambda\beta e^{\beta} & -\lambda\beta e^{-\beta} \end{bmatrix} \begin{bmatrix} C_1 \\ C_2 \\ C_3 \\ C_4 \end{bmatrix}. \qquad 5.6\text{-}3$$

A comparison of (5.4-2a) and (5,6-3) defines $\underset{\sim}{\Lambda}$. The inversion of $\underset{\sim}{\Lambda}$ is rather lengthy and will not be examined here. It is sufficient to represent the elements of the inverted matrix $\underset{\sim}{A}$ by a_{ij} $(i = 1 \ldots 4,\ j = 1 \ldots 4)$. The complete expressions for a_{ij} are given in Appendix [4].

Therefore, we can write (5.6-3) as:

$$\underset{\sim}{C} = \underset{\sim 1}{A} \begin{bmatrix} p \\ q \end{bmatrix} + \underset{\sim 2}{A} \begin{bmatrix} p' \\ q' \end{bmatrix},$$

where

$$\underset{\sim 1}{A} = \begin{bmatrix} a_{11} & a_{12} \\ \vdots & \vdots \\ a_{41} & a_{42} \end{bmatrix}, \text{ and } \underset{\sim 2}{A} = \begin{bmatrix} a_{13} & a_{14} \\ \vdots & \vdots \\ a_{43} & a_{44} \end{bmatrix}. \qquad 5.6\text{-}5$$

The boundary conditions for the second layer (half-plane) are:

$$\left.\begin{aligned} \sigma_y\ (\bar{x},\ \infty) &= 0, \\ \tau_{xy}\ (\bar{x},\ \infty) &= 0, \end{aligned}\right\} \qquad 5.6\text{-}6a$$

and

$$\left.\begin{aligned} \sigma_{xy}\ (\bar{x},\ 1) &= p'\ \cos(\lambda\bar{x}), \\ \tau_{xy}\ (\bar{x},\ 1) &= q'\ \sin(\lambda\bar{x}). \end{aligned}\right\} \qquad 5.6\text{-}6b$$

By an inspection of equation (5.4-1), we observe, that for conditions (5.6-6a) to be satisfied, we require:

5.6.1) contd.

$$C_1' = C_3' = 0;$$

therefore:

$$\begin{bmatrix} p' \\ q' \end{bmatrix} = \begin{bmatrix} -\lambda^2 e^{-\alpha'} & -\lambda^2 e^{-\beta'} \\ -\lambda\alpha' e^{-\alpha'} & -\lambda\beta' e^{-\beta'} \end{bmatrix} \begin{bmatrix} C_2' \\ C_4' \end{bmatrix}, \qquad 5.6\text{-}7$$

and

$$\begin{bmatrix} C_2' \\ C_4' \end{bmatrix} = \begin{bmatrix} a_{21}' & a_{22}' \\ a_{41}' & a_{42}' \end{bmatrix} \begin{bmatrix} p' \\ q' \end{bmatrix}, \qquad 5.6\text{-}8$$

where a_{21}' ... etc. are given in Appendix [4].

Considering the displacements at the interface ($\bar{y} = 1$), we can establish the matrices $\underset{\sim}{D}$ and $\underset{\sim}{D}'$, in the following form:

$$\mathcal{D} = \begin{bmatrix} \frac{\alpha^2 \ell_{11} - \lambda \ell_{12}}{\lambda} \left[e^{\alpha}; e^{-\alpha} \right] & ; & \frac{\beta^2 \ell_{11} - \lambda \ell_{12}}{\lambda} \left[e^{\beta} ; e^{-\beta} \right] \\ \frac{\alpha^2 \ell_{12} - \lambda \ell_{22}}{\alpha} \left[e^{\alpha}; e^{-\alpha} \right] & ; & \frac{\beta^2 \ell_{12} - \lambda \ell_{22}}{\beta} \left[e^{\beta} ; e^{-\beta} \right] \end{bmatrix}, \qquad 5.6\text{-}9a$$

$$\mathcal{D}' = \begin{bmatrix} \frac{\alpha'^2 \ell_{11}' \lambda^2 \ell_{12}'}{\lambda} e^{-\alpha'} & ; & \frac{\beta'^2 \ell_{11}' - \lambda^2 \ell_{12}'}{\lambda} e^{-\beta'} \\ \frac{\lambda^2 \ell_{22}' - \alpha'^2 \ell_{12}'}{\alpha'} e^{-\alpha'} & ; & \frac{\lambda^2 \ell_{22}' - \beta'^2 \ell_{12}'}{\beta'} e^{-\beta'} \end{bmatrix}. \qquad 5.6\text{-}9b$$

It follows that since $\underset{\sim}{B} = \underset{\sim}{D}\,\underset{\sim}{A}$ (see equation (5.4-10a), the elements of $\underset{\sim}{B}$ are given by:

$$b_{mn} = \sum_{j=1}^{4} (d_{mj}\, a_{jn}) \quad , \text{for } m = 1,2;\ n = 1 \text{ ... } 4,$$

and the elements of $\underset{\sim}{B}'$ by:

$$b_{mn}' = \sum_{j=2,4} (d_{mj}'\, a_{jn}'), \text{ for } m = 1,2 \ ;\ n = 1,2,$$

5.6.1) contd.

where d_{mj} and d'_{mj} are the elements of $\underset{\sim}{D}$ and $\underset{\sim}{D}'$ respectively (see equations 5.6-9a and b).

From the partitioned $\underset{\sim}{B}$ and $\underset{\sim}{B}'$ (see equation 5.4-10b), we can determine $\underset{\sim}{F}$ through the following relation:

$$\underset{\sim}{F} = \underset{\sim}{B}_1 \left[\underset{\sim}{B}'_1 - \underset{\sim}{B}_2 \right]^{-1}.$$

The constants $\underset{\sim}{C}$ and $\underset{\sim}{C}'$ are then given by:

$$\left[\underset{\sim}{C} \; ; \; \underset{\sim}{C}' \right] = \left[\underset{\sim}{A}_o \; ; \; \underset{\sim}{A}'_o \right] \begin{bmatrix} p \\ q \end{bmatrix}, \qquad 5.6\text{-}11$$

where

$$\underset{\sim}{A}_o = \underset{\sim}{A}_1 + \underset{\sim}{A}_2 \underset{\sim}{F}, \qquad 5.6\text{-}12a$$

and

$$\underset{\sim}{A}'_o = \underset{\sim}{A}'_1 \underset{\sim}{F}. \qquad 5.6\text{-}12b$$

We rewrite equation (5.4-1b) in the following form:

$$\underset{\sim}{E}^i = \begin{bmatrix} \underset{\sim}{E}^i_x & \cos(\lambda \bar{x}) \\ \underset{\sim}{E}^i_y & \cos(\lambda \bar{x}) \\ \underset{\sim}{E}^i_{xy} & \sin(\lambda \bar{x}) \end{bmatrix}. \qquad 5.6\text{-}13$$

Then, the stresses at any point in the 2-layer half-plane are given by:

$$[\underset{\sim}{S} \; ; \; \underset{\sim}{S}'] = \begin{bmatrix} [\underset{\sim}{R}_x \; ; \; \underset{\sim}{R}'_x] \cos(\lambda \bar{x}) \\ [\underset{\sim}{R}_y \; ; \; \underset{\sim}{R}'_y] \cos(\lambda \bar{x}) \\ [\underset{\sim}{R}_{xy} \; ; \; \underset{\sim}{R}'_{xy}] \sin(\lambda \bar{x}) \end{bmatrix} \begin{bmatrix} p \\ q \end{bmatrix}, \qquad 5.6\text{-}14a$$

where

$$[\underset{\sim}{R}_j \; ; \; \underset{\sim}{R}'_j] = [\underset{\sim}{A}_o \; ; \; \underset{\sim}{A}'_o] \; [\underset{\sim}{E}_j \; ; \; \underset{\sim}{E}'_j], \qquad 5.6\text{-}14b$$

for j = x, y, xy.

5.6.2) "Smooth interface" condition.

The case of the "smooth interface" condition will

5.6.2) contd.

not be described in detail, since all the matrices required for the solution of the problem have already been given in the previous section.

For example:

$\underset{\sim}{A}_{11}$, $\underset{\sim}{A}_{21}$, $\underset{\sim}{A}'_{11}$ are the first columns of $\underset{\sim}{A}_1$, $\underset{\sim}{A}_2$, $\underset{\sim}{A}'_1$ respectively (see equations 5.6-5 and 5.6-8). Similarly, $\underset{\sim}{V}$ and $\underset{\sim}{V}'$ are the second rows of $\underset{\sim}{D}$ and $\underset{\sim}{D}'$ (see equations 5.6-9a and b).

Then

$$F = \frac{B_{11}}{B'_{11} - B_{21}}, \qquad 5.6\text{-}15$$

where

$$[B_{11}; B_{21}] = \underset{\sim}{V}[\underset{\sim}{A}_{11} ; \underset{\sim}{A}_{21}],$$

and $$B'_{11} = \underset{\sim}{V}' \underset{\sim}{A}'_{11} .$$

Finally, the stresses of any point in the 2-layer half-plane are given by:

$$[\underset{\sim}{S} ; \underset{\sim}{S}'] = \begin{bmatrix} [\underset{\sim}{R}_x ; \underset{\sim}{R}'_x] & \cos(\lambda\bar{x}) \\ [\underset{\sim}{R}_y ; \underset{\sim}{R}'_y] & \cos(\lambda\bar{x}) \\ [\underset{\sim}{R}_{xy}; \underset{\sim}{R}'_{xy}] & \sin(\lambda\bar{x}) \end{bmatrix} p_{eqv.}, \qquad 5.6\text{-}16a$$

where

$$[\underset{\sim}{R}_j ; \underset{\sim}{R}'_j] = [\underset{\sim}{A}_o; \underset{\sim}{A}'_o] [\underset{\sim}{E}_j ; \underset{\sim}{E}'_j]$$

$$\text{for } j = x, y, xy,$$

$$\underset{\sim}{A}_o = \underset{\sim}{A}_{11} + \underset{\sim}{A}_{21} F, \quad \underset{\sim}{A}'_o = \underset{\sim}{A}'_{11} F,$$

$$p_{eqv.} = p + \frac{B_{12}}{B_{11}} q, \qquad 5.6\text{-}16b$$

and $\underset{\sim}{E}_j, \underset{\sim}{E}'_j$ are defined by equation (5.6-13).

5.7) Two layer half-plane subjected to partially distributed uniform load; concentrated load.

We consider the case of an orthotropic 2-layer half-plane, which is subjected on its boundary to a partially distributed uniform normal stress of intensity ω and width '2ℓ', applied symmetrically about the Y-axis.

This type of load can be expressed in a Fourier integral form, as follows:

$$p(\bar{x}) = \frac{2\omega\ell}{\pi h} \int_0^\infty \frac{\sin(\lambda\bar{\ell})}{\lambda\bar{\ell}} \cos(\lambda\bar{x})\, d\lambda, \qquad 5.7\text{-}1$$

where $\bar{\ell} = \ell/h$.

Equation (5.7-1), represents a summation of an infinite number of sinusoidal loads, of the type:

$$\left[\frac{2\omega\ell}{\pi h} \frac{\sin(\lambda\bar{\ell})}{\lambda\bar{\ell}} d\lambda \right] \cos(\lambda\bar{x}), \qquad 5.7\text{-}2$$

which can be identified as the applied load 'p' on the layered half-plane, as given by equation 5.6-2a.

Using the representation in (5.7-1), the stresses in the layered half-plane due to a partially distributed uniform load, can be expressed in the following form:

$$\left[\sigma_x;\sigma_y;\tau_{xy}\right] = \frac{2\omega\ell}{\pi h} \int_0^\infty \frac{\sin(\lambda\bar{\ell})}{\lambda\bar{\ell}} \left[R_x\cos(\lambda\bar{x});R_y\cos(\lambda\bar{x});R_{xy}\sin(\lambda\bar{x})\right] d\lambda. \qquad 5.7\text{-}3.$$

By making use of the condition:

$$\lim_{\bar{\ell} \to 0} \frac{\sin(\lambda\bar{\ell})}{\lambda\bar{\ell}} = 1,$$

and the condition $2\omega\ell \to P$ as $\ell \to 0$, we can obtain from equation (5.7-3) the solution to the problem of an orthotropic 2-layer half-plane, which is subjected on its boundary to a normal concentrated force P/unit thickness. The stress components are

5.7) contd.

then given by:

$$\left[\sigma_x;\sigma_y;\tau_{xy}\right] = \frac{P}{\pi h}\int_0^\infty \left[R_x\cos(\lambda\bar{x});R_y\cos(\lambda\bar{x});R_{xy}\sin(\lambda\bar{x})\right]d\lambda. \quad 5.7\text{-}4$$

5.8) Numerical results.

The method of solution developed in Section 5.6 for the 2-layer half-plane, assuming perfect continuity between the layers, was employed to obtain numerical results for the stress distributions induced along the interface by a concentrated force, applied normal to the boundary of the half-plane, which is assumed to deform under plane strain conditions.

The evaluation of the stresses was accomplished in two steps:

Step 1 involved the determination of the functions R_x, R_y, R_{xy}, for a range of values of λ, where $0 \leq \lambda \leq \lambda_{max}$. λ_{max} was increased until the magnitude of R_x, R_y, R_{xy} was less than 10^{-4}.

Step 2 involved the determination of the stresses, by numerical evaluation of the integrals in equation (5.7-4), using Simpson's rule.

Numerical results are presented for the variation of normal stress σ_y along the interface, for a range of values for the elastic constants of the materials which constitute the two orthotropic layers.

The elastic constants of the materials are varied through the following ratios:

$$\frac{E_y}{E_x}, \quad \frac{E_y}{G_{xy}}, \quad \frac{E'_y}{E'_x}, \quad \frac{E'_y}{G'_{xy}}, \quad \nu_{xy}, \quad \nu'_{xy}, \quad \frac{E'_y}{E_y}$$

Because of the many variables involved, six are kept constant, while different values are assigned

5.8) contd.

to the seventh one. It is assumed that $\nu_{xy} = \nu'_{xy} = 0.25$.

5.9) Conclusions.

From the graphical representation of the results in Fig.5.3-5.7 we can make the following observations.

a) Decreasing values of E_y/E_x, reduce the magnitude of the σ_y.

b) The ratio E_y/E'_y affects the stress distribution considerably. When E_y/E'_y increases, the stresses are reduced and a "spreading out" effect is introduced.

c) Increasing values of E_y/G_{xy}, increase the magnitude of σ_y, while increasing values of E'_y/G'_{xy} reduce it.

d) The distribution of σ_y along the interface is mainly governed by the properties of the first layer. The stress σ_y is relatively insensitive to changes in E'_y/E'_x but is affected to a small degree by E'_y/G_{xy}.

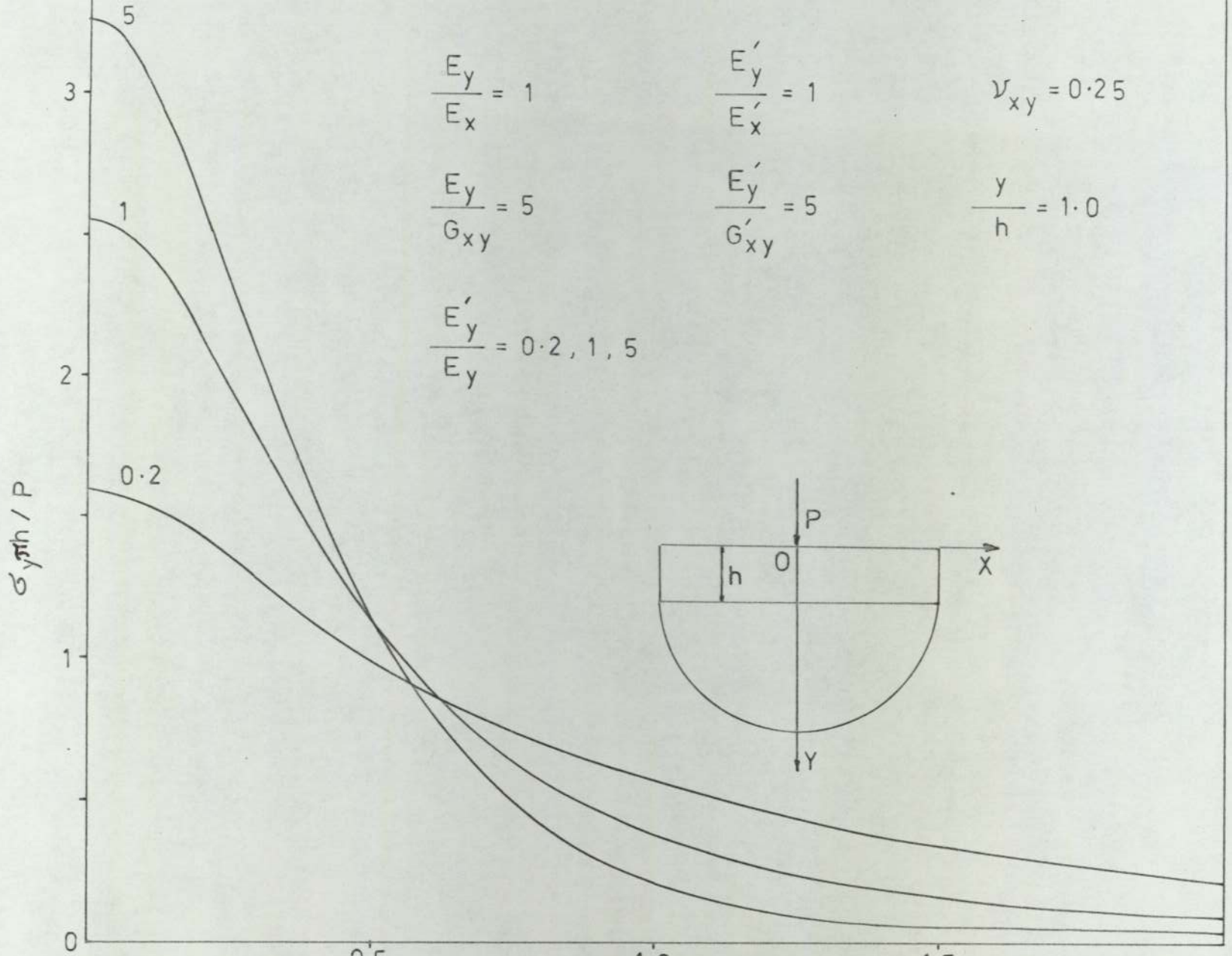

FIG. 5.3 Variation of σ_y along the interface

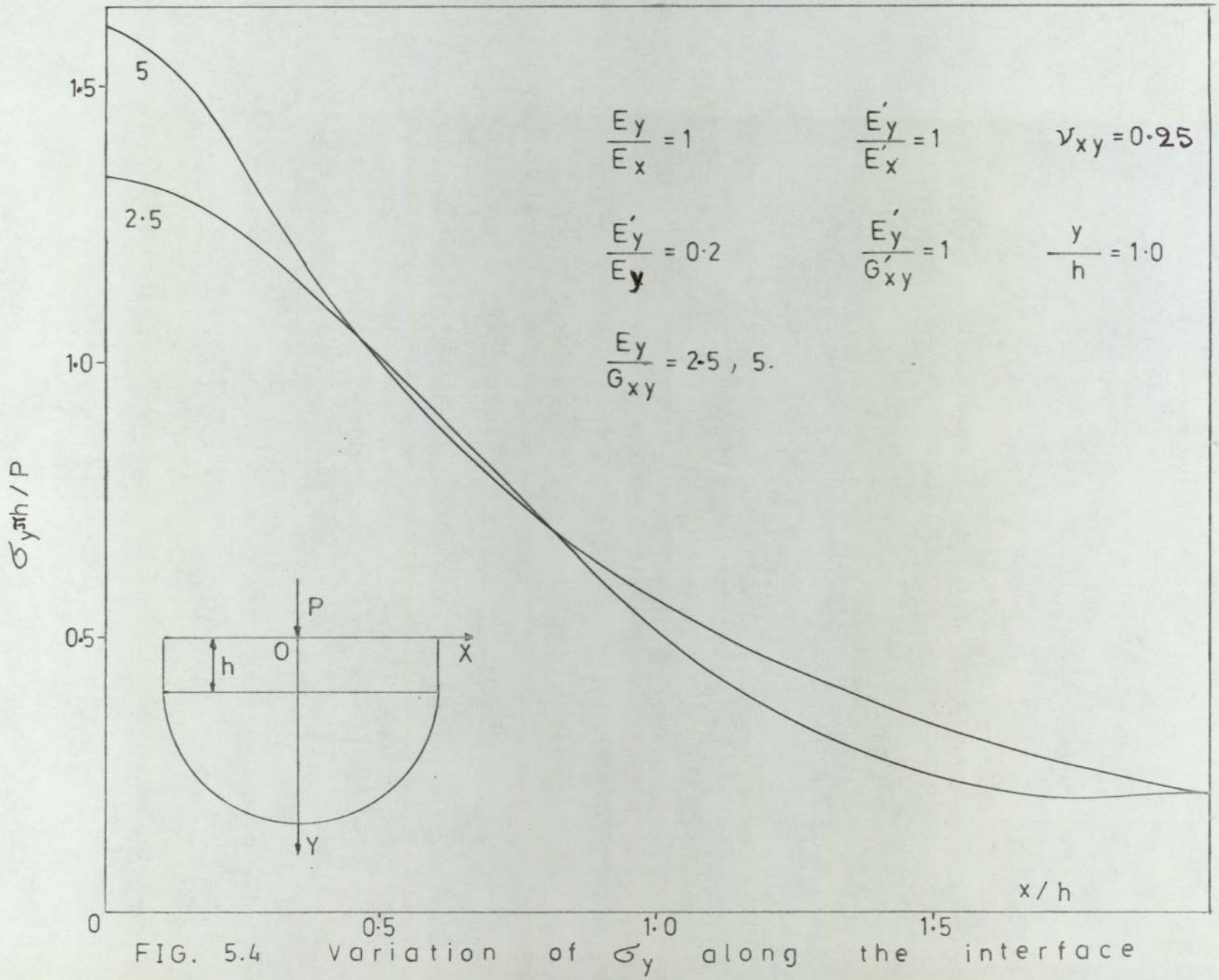

FIG. 5.4 Variation of σ_y along the interface

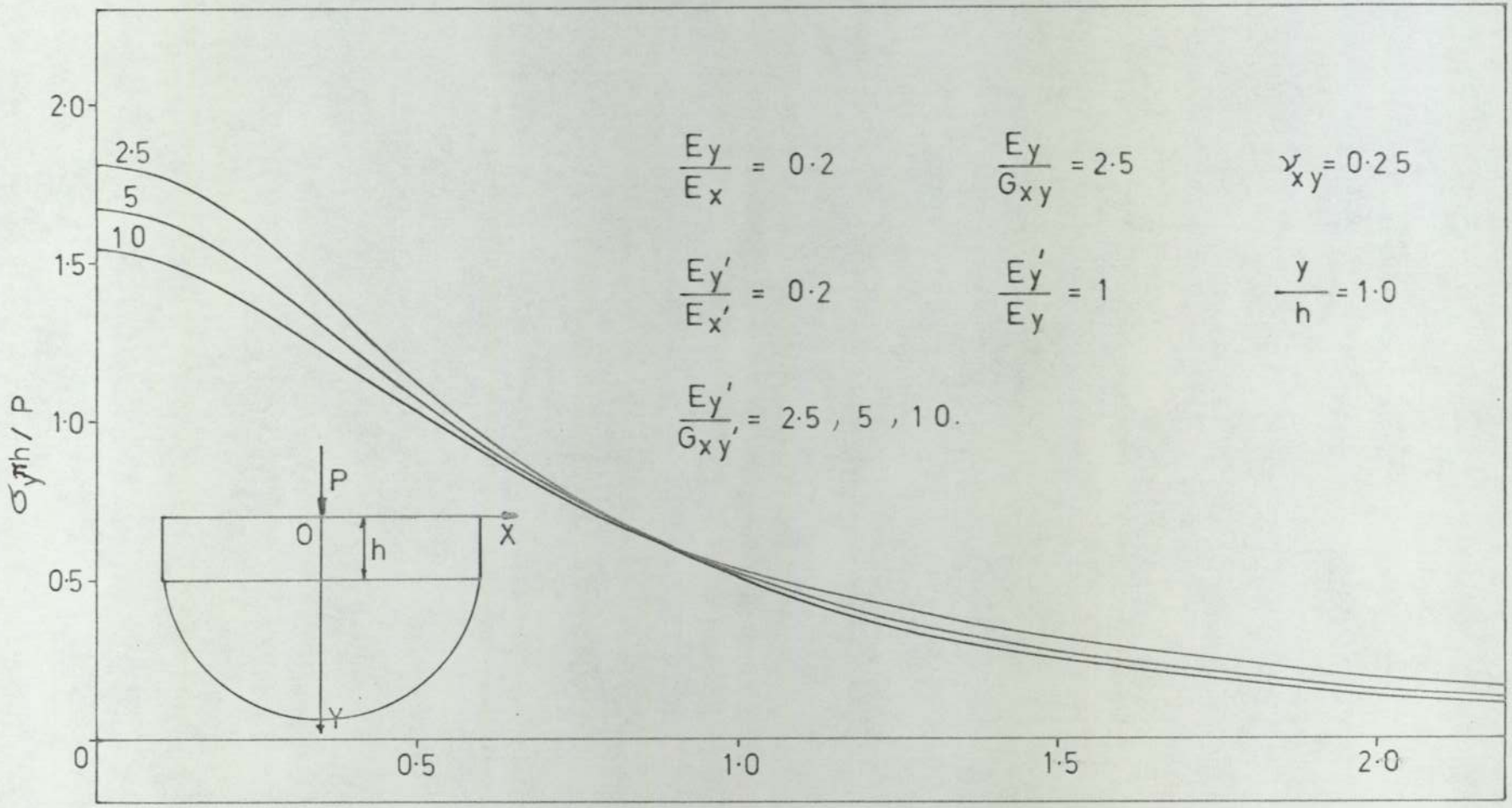

FIG. 5·5 Variation of σ_y along the interface

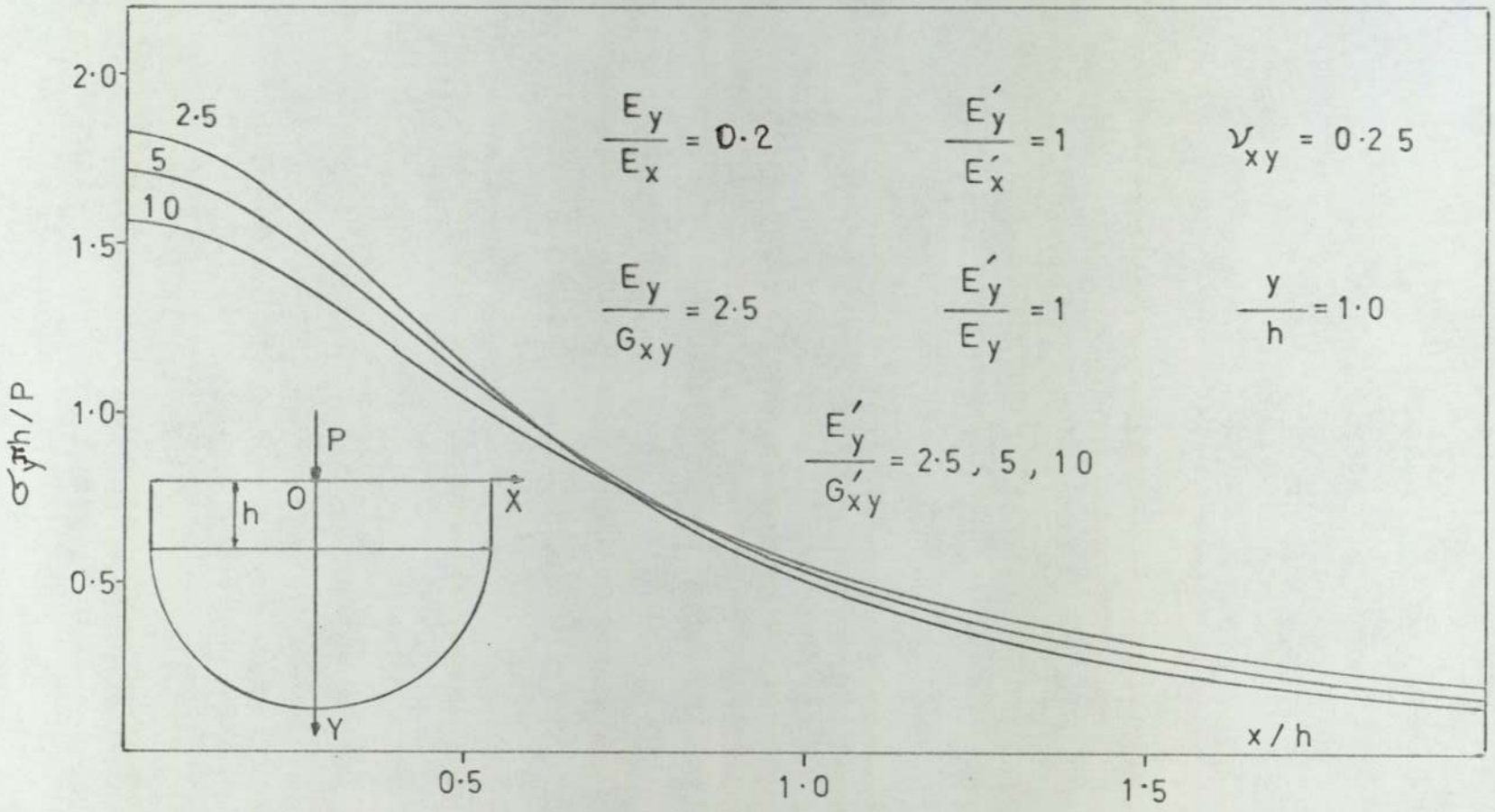

FIG. 5:6 Variation of σ_y along the interface

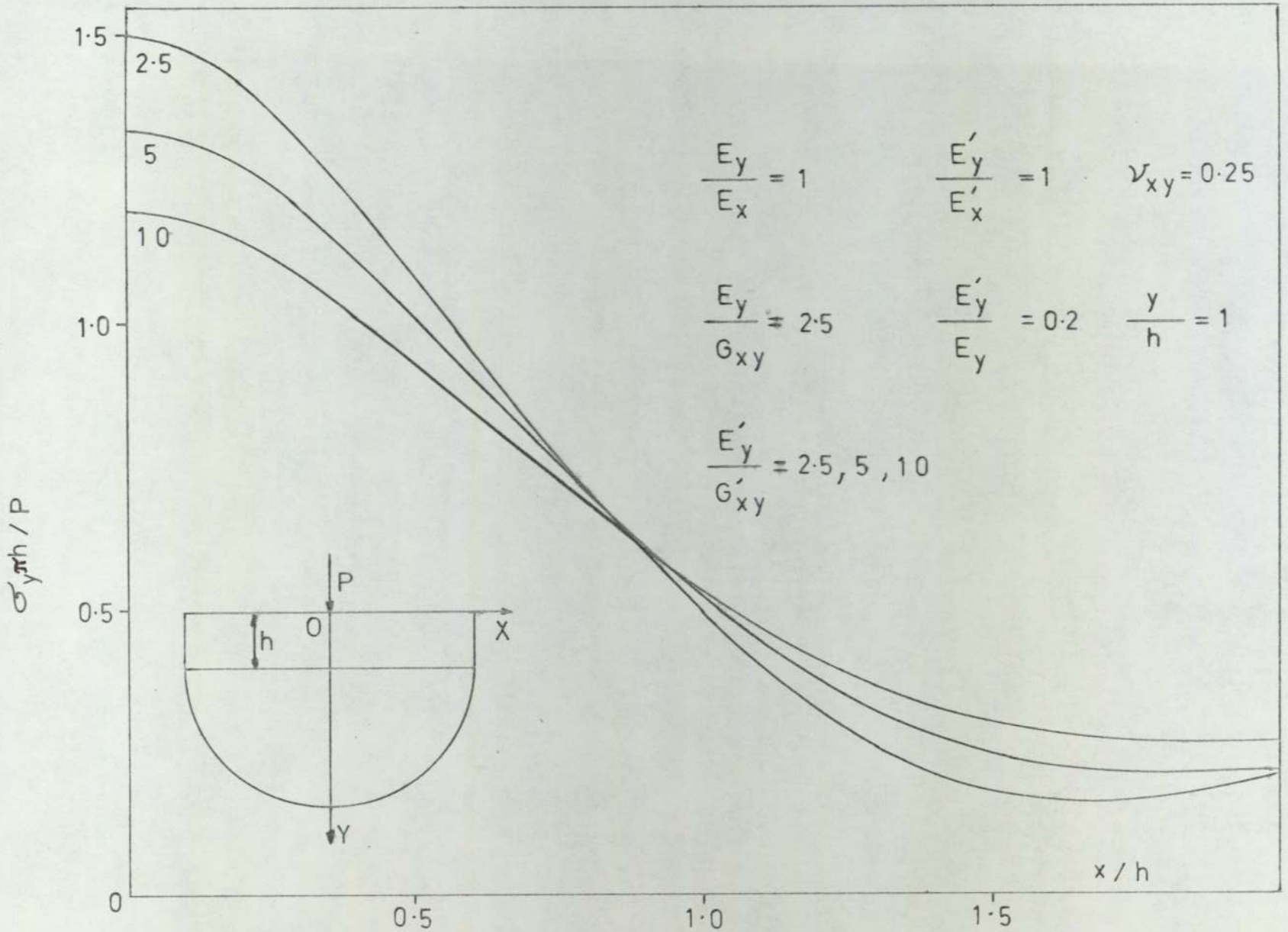

FIG. 5.7 Variation of σ_y along the interface

CHAPTER 6

ORTHOTROPIC QUARTER PLANE.

6.1) Introduction.

The elastic quarter-plane constitutes a special case of the more general class of elastic wedge problems, which have received considerable attention.

Stress distributions in isotropic elastic wedges subjected to concentrated or distributed loads acting on its sides, and/or to concentrated forces or couples acting at its apex, have been analysed by Levy (1898) and Carothers (1912). Also, integral transform techniques, such as Mellin transforms, have been discussed by Tranter (1948), Sneddon (1951), Godfrey (1955) and Sternberg and Koiter (1958), in connection with the above class of problems. The problem of an elastic quarter-plane with arbitrary loadings on the boundaries has been solved by Iyengar (1962), using a Fourier-integral approach.

Stress distributions in anisotropic elastic wedges due to various surface loadings have been analysed by Lekhnitskii (1963), Benthem (1963) and Baker (1964).

Hetenyi (1960) developed a method of solution for the isotropic quarter-plane due to either concentrated or distributed loads acting on its boundaries. Craft and Richardson (1970), employed Hetenyi's method to obtain the state of stress in an isotropic quarter-plane containing a circular inclusion.

Hetenyi's method of solution for the isotropic quarter-plane, is basically a superposition of the solutions to three half-plane problems. The half-planes are loaded on their straight boundaries in such a manner, that the resulting stress distribution satisfies the traction boundary conditions of the quarter-plane. The loadings on the half-planes can be determined by repeated superposition of known solutions for the

6.1) contd.

half-plane. Such a procedure leads to a sequence of infinite integrals of recursive pattern. Hetenyi has shown that this sequence of integrals leads to a convergent result; therefore the superposition technique may be continued to obtain the solution to the quarter-plane problem, to any required order of accuracy.

In this chapter, Hetenyi's method is employed to formulate a general method of solution to problems associated with an orthotropic elastic quarter-plane. It is assumed that the axes of orthotropy coincide with the Cartesian coordinate axes X,Y. Examples are given, in which the quarter-plane is subjected to surface or interior loadings. Numerical results are presented for the special cases, when the orthotropic material is a Boron-epoxy or a graphite-epoxy composite.

6.2) General solution.

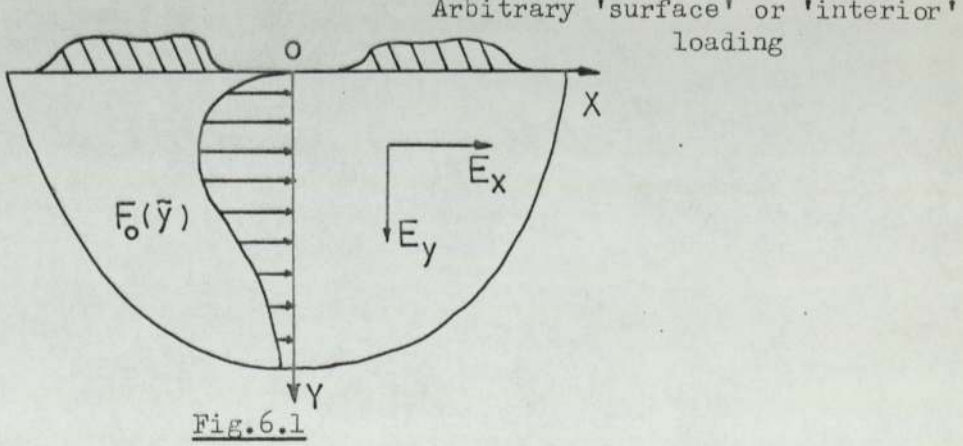

Fig.6.1

We consider an orthotropic half-plane occupying the region $-\infty < \bar{x} < +\infty$, $0 \leq \bar{y} < \infty$, (see Fig.6.1), where

$$\bar{x} = \frac{x}{a} \quad , \quad \bar{y} = \frac{y}{a} \quad , \qquad 6.2\text{-}1$$

are dimensionless coordinates and 'a' is a typical length parameter.

6.2) contd.

We assume that this half-plane is subjected to force systems (applied either at the boundary or at the interior) in such a manner that the resulting state of stress is symmetric about the Y-axis. We shall refer to this state of stress as the "basic state of stress". By virtue of the symmetry of this basic state of stress, the shear stresses are zero on the plane of symmetry. The plane X = o is therefore subjected to only a normal stress $F_o(\tilde{y})$, where $\tilde{y}$ denotes $\bar{y}$ coordinates of points on the x = o boundary (i.e. $\tilde{y} = (o,\bar{y})$). (Similar definition follows for $\tilde{x}$).

Therefore, for the basic state of stress $(\sigma_x^o, \sigma_y^o, \tau_{xy}^o)$:

$$\sigma_x^o(o,\bar{y}) = F_o(\tilde{y}) \ , \quad \tau_{xy}(o,\bar{y}) = 0. \qquad 6.2\text{-}2$$

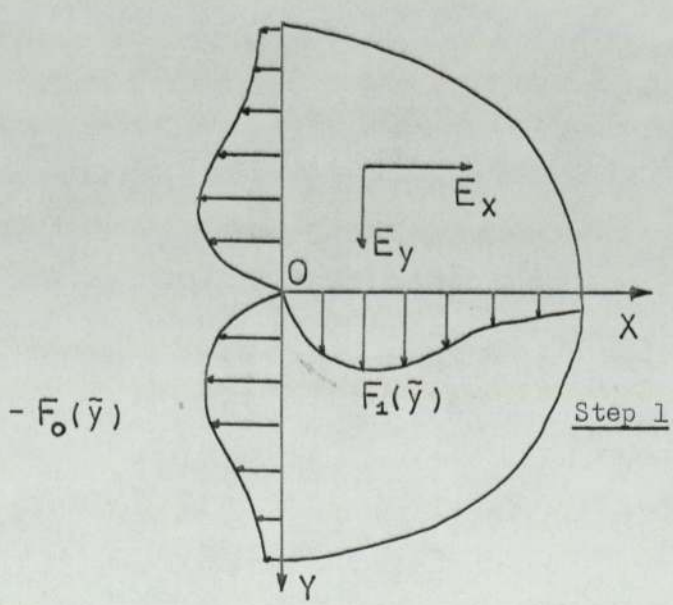

Fig.6.2

We consider now the problem of the half-plane $0 \leq \bar{x} < \infty$, $-\infty < \bar{y} < \infty$ (see Fig.6.2), which is subjected to a symmetric stress distribution $-F_o(\tilde{y})$ on its boundary X = o (step 1).

The resulting state of stress can be determined

6.2) contd.

by an integration of the stress components due to the Flamant problem (see equations 4.9-2). The resulting expressions can be written in the form:

$$\left[\sigma_x^1;\ \sigma_y^1;\ \tau_{xy}^1\right] = -\frac{k_1k_2(k_1+k_2)}{a\pi}\int_0^\infty F_o(\tilde{y})\left[J_x(\tilde{y});J_y(\tilde{y});J_{xy}(\tilde{y})\right]d\tilde{y}, \qquad 6.2\text{-}3a$$

where

$$J_x(\tilde{y}) = J_x^+(\tilde{y}) + J_x^-(\tilde{y}),$$
$$J_y(\tilde{y}) = J_y^+(\tilde{y}) + J_y^-(\tilde{y}), \qquad 6.2\text{-}3b$$
$$J_{xy}(\tilde{y}) = J_{xy}^+(\tilde{y}) + J_{xy}^-(\tilde{y}),$$

and

$$\left[J_x^{\pm}(\tilde{y});J_y^{\pm}(\tilde{y});J_{xy}^{\pm}(\tilde{y})\right] = \frac{\left[\tilde{x}^3;\ \tilde{x}(\tilde{y}\pm\bar{y})^2\ ;\ \tilde{x}^2(\tilde{y}\pm\bar{y})\right]}{\left[k_1^2\tilde{x}^2+(\tilde{y}\pm\bar{y})^2\right]\left[k_2^2\tilde{x}^2+(\tilde{y}\pm\bar{y})^2\right]} \quad . \qquad 6.2\text{-}3c$$

Thus combining the stress components derived from step 1 with those of the basic state of stress, renders the plane X = o free of normal traction, but gives rise to a non-zero normal traction $-F_1(\tilde{x})$ on the plane Y = 0, where

$$F_1(\tilde{x}) = \frac{k_1k_2(k_1+k_2)}{\pi a}\int_0^\infty \frac{F_o(\tilde{y})\,2\tilde{x}\,\tilde{y}^2\,d\tilde{y}}{(k_1^2\,\tilde{x}^2+\tilde{y}^2)(k_2^2\tilde{x}^2+\tilde{y}^2)} \quad . \qquad 6.2\text{-}4$$

(Again, by symmetry of loading $\tau_{xy}^1(\bar{x},o) = o$.).

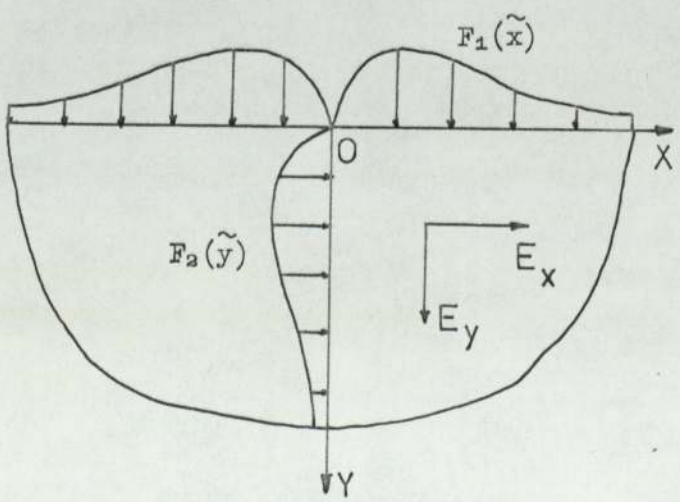

Fig.6.3

6.2) contd.

To eliminate $-F_1(\tilde{x})$, we consider the orthotropic half-plane $0 \leq \bar{y} < \infty$, $-\infty < \bar{x} < \infty$, subjected on its boundary to a symmetric stress distribution $F_1(\tilde{x})$(Fig.6.3) (step 2). Again, the stress components σ_x^2, σ_y^2, τ_{xy}^2, can be determined by an itegration of equations (4.2-4) for the concentrated force problem. We have:

$$\left[\sigma_x^2;\sigma_y^2;\tau_{xy}^2\right] = \frac{k_1+k_2}{\pi a}\int_0^\infty F_1(\tilde{x})\left[K_x(\tilde{x});K_y(\tilde{x});K_{xy}(\tilde{x})\right]d\tilde{x}, \qquad 6.2\text{-}5a$$

where
$$\begin{aligned} K_x(\tilde{x}) &= K_x^+(\tilde{x}) + K_x^-(\tilde{x}), \\ K_y(\tilde{x}) &= K_y^+(\tilde{x}) + K_y^-(\tilde{x}), \\ K_{xy}(\tilde{x}) &= K_{xy}^+(\tilde{x}) + K_{xy}^-(\tilde{x}), \end{aligned} \qquad 6.2\text{-}5b$$

and

$$\left[K_x^{\pm}(\tilde{x});K_y^{\pm}(\tilde{x});K_{xy}^{\pm}(\tilde{x})\right] = \frac{\left[(\bar{x}\pm\tilde{x})^2\bar{y};\bar{y}^3;(\bar{x}\pm\tilde{x})^2\ \bar{y}^2\right]}{\left[k_1^2(\bar{x}\pm\tilde{x})^2+\bar{y}^2\right]\left[k_2^2(\bar{x}\pm\tilde{x})^2+\bar{y}^2\right]} . \qquad 6.2\text{-}5c$$

It can be verified that the state of stress represented by (6.2-5a), eliminates the normal stress $-F_1(\tilde{x})$ on the plane $Y = 0$, but in doing so, gives rise to a normal traction $F_2(\tilde{y})$ on the plane $X = 0$,
where

$$F_2(\tilde{y}) = \frac{k_1+k_2}{\pi a}\int_0^\infty \frac{2F_1(\tilde{x})\,\tilde{x}^2\,\tilde{y}\,d\tilde{x}}{(k_1^2\tilde{x}^2+\tilde{y}^2)(k_2^2\,\tilde{x}^2+\tilde{y}^2)} . \qquad 6.2\text{-}6$$

It is now evident that the techniques outlined in steps 1 and 2 have to be repeatedly applied in order to satisfy traction boundary conditions on the planes $X = 0$ and $Y = 0$. This procedure leads to a set of integrals of recursive pattern and the combination of these individual states of stress, henceforth referred to as the "corrective state of stress" gives :

6.2) contd.

$$\left[\sigma_x^c;\sigma_y^c;\tau_{xy}^c\right] = \sum_{n=1}^{\infty} \left[\sigma_x^n;\ \sigma_y^n;\ \tau_{xy}^n\right], \qquad 6.2\text{-}7$$

which in the orthotropic quarter-plane satisfies the boundary conditions:

$$\sigma_x^c(o,\bar{y}) = -F_o(\tilde{y}),\ \sigma_x^c(\bar{x},o) = \tau_{xy}^c(\bar{x},o) = \tau_{xy}^c(o,\bar{y}) = 0. \qquad 6.2\text{-}8$$

Using equations (6.2-3a) and (6.2-5a), the relation (6.2-7) can be written in the form:

$$\left[\sigma_x^c;\ \sigma_y^c;\ \tau_{xy}^c\right] = \frac{k_1+k_2}{\pi a}\left\{ - k_1k_2 \int_o^{\infty} \left[J_x(\tilde{y});J_y(\tilde{y});J_{xy}(\tilde{y})\right] \sum_{m=o,2,4\ldots}^{\infty} F_m(\tilde{y})\, d\tilde{y} + \int_o^{\infty} \left[K_x(\tilde{x});K_y(\tilde{x});K_{xy}(\tilde{x})\right] \sum_{m=1,3,5\ldots}^{\infty} F_m(\tilde{x})\, d\tilde{x} \right\}. \qquad 6.2\text{-}9$$

The functions $F_m(\tilde{x})$ and $F_m(\tilde{y})$ are given by the recurrence relations:

$$F_{m+1}(\tilde{x}) = \frac{k_1k_2(k_1+k_2)}{\pi a} \int_o^{\infty} \frac{2F_m(\tilde{y})\tilde{x}\,\tilde{y}^2\, d\tilde{y}}{(k_1^2\tilde{x}^2+\tilde{y}^2)(k_2^2\tilde{x}^2+\tilde{y}^2)}, \qquad 6.2\text{-}10a$$

$$F_{m+1}(\tilde{y}) = \frac{k_1+k_2}{\pi a} \int_o^{\infty} \frac{2F_m(\tilde{x})\,\tilde{x}^2\,\tilde{y}\, d\tilde{x}}{(k_1^2\tilde{x}^2+\tilde{y}^2)(k_2^2\tilde{x}^2+\tilde{y}^2)}. \qquad 6.2\text{-}10b$$

The complete solution to the orthotropic quarter plane problem is obtained by combining the basic state and the corrective state of stress:

$$\left[\sigma_x;\sigma_y;\tau_{xy}\right] = \left[\sigma_x^o;\sigma_y^o;\tau_{xy}^o\right] + \left[\sigma_x^c;\sigma_y^c;\tau_{xy}^c\right]. \qquad 6.2\text{-}11$$

Therefore, a solution to any quarter-plane problem can be obtained, as long as the equivalent basic

6.2) contd.

state of stress can be fully defined $(\sigma_x^o, \sigma_y^o, \tau_{xy}^o, F_o(\tilde{y}))$.

6.3) Convergence of the method.

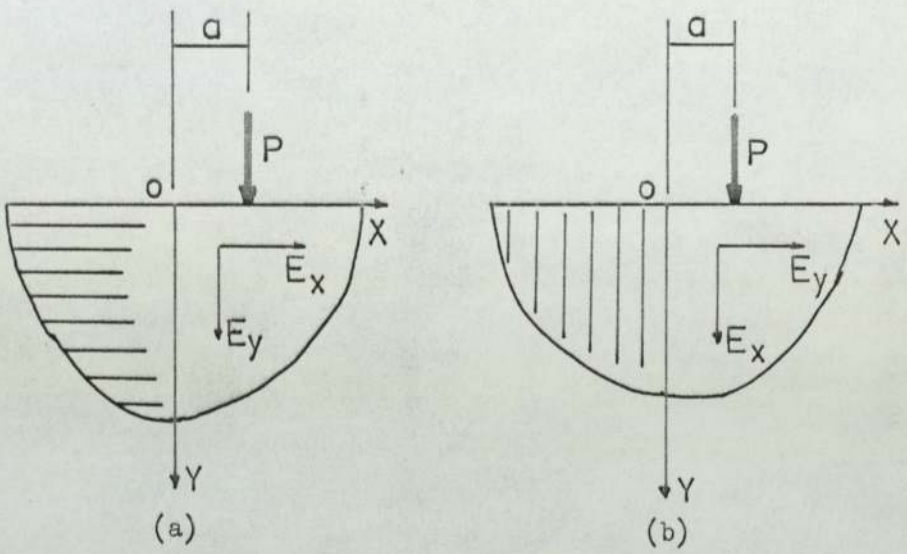

Fig.6.4

We consider the orthotropic half-plane $0 \leq \bar{y}$, $-\infty < \bar{x} < \infty$, which is subjected at its boundary to a normal concentrated force P/unit thickness at point (a,o).

By integration of the expression for σ_x (see equation 4.2-4) with respect to y between the limits 0 and ∞, we have:

$$\int_0^\infty \sigma_x \, dy = \frac{P(k_1+k_2)}{\pi} \int_0^\infty \frac{(x-a)^2 \, y \, dy}{[k_1^2(x-a)^2+y^2][k_2^2(x-a)^2+y^2)]} = \frac{P}{\pi(k_1-k_2)} \ell n \frac{k_1}{k_2} \, .$$

6.3-1

The result, which is the total resultant force in the X-direction on a plane parallel to the YZ plane is seen to be independent of the position of the load or of the location of the plane. Since any normal load on the boundary of a half-plane can be represented as a series of concentrated forces, it can be stated that:

6.3) contd.

Total lateral thrust =

Total finite normal load on boundary $\times \frac{\ell n\, k_1 - \ell n\, k_2}{\pi(k_1-k_2)}$. 6.3-2

For $k_1 = k_2 = 1$ (isotropic material), the expression $\ell n(k_1/k_2)/\pi(k_1-k_2)$ can be evaluated by means of L'Hospital's rule to give $1/\pi$, which is the result obtained by Hetenyi (1960) for isotropic materials.

Applying equation 6.3-2 to the F-functions (see equations 6.2-10a and b) we obtain:

$$\int_0^\infty F_{m+1}(\tilde{x})\, d\tilde{x} = \frac{\ell nk_1 - \ell nk_2}{\pi(k_1-k_2)}\, k_1k_2 \int_0^\infty 2F_m(\tilde{y})d\tilde{y}, \qquad 6.3\text{-}3a$$

and

$$\int_0^\infty F_{m+1}(\tilde{y})d\tilde{y} = \frac{\ell nk_1 - \ell nk_2}{\pi(k_1-k_2)} \int_0^\infty 2F_m(\tilde{x})d\tilde{x}. \qquad 6.3\text{-}3b$$

For the F-functions to be convergent, the coefficients in equations (6.3-3a and b) should satisfy the following condition:

$$\frac{2(\ell nk_1 - \ell nk_2)}{\pi(k_1-k_2)} \left[1 \; ; \; k_1k_2\right] < 1. \qquad 6.3\text{-}4$$

For various combinations of values for k_1 and k_2, inequality (6.3-4) is not satisfied. However, if we consider successive F-functions on the same plane (say the X=0 plane), we have:

$$\int_0^\infty F_{m+2}(\tilde{y})d\tilde{y} = \left[\frac{2(\ell nk_1 - \ell nk_2)}{\pi(k_1-k_2)}\right]^2 k_1k_2 \int_0^\infty F_m(\tilde{y})d\tilde{y}. \qquad 6.3\text{-}5$$

(A similar expression can be obtained for the Y=0 plane).

Then, it can be shown (see Appendix [5]), that for $k_1 > k_2 > 0$,

6.3) contd.

$$\left[\frac{2(\ell nk_1-\ell nk_2)}{\pi(k_1-k_2)}\right]^2 k_1k_2 < 1, \qquad 6.3\text{-}6$$

which guarantees the convergence of the recurrent integrals (6.2-10a and b).

It is therefore concluded that the speed of convergence depends on the orthotropic constants k_1, k_2 of the material.

6.4) Concentrated force acting normal to the boundary.

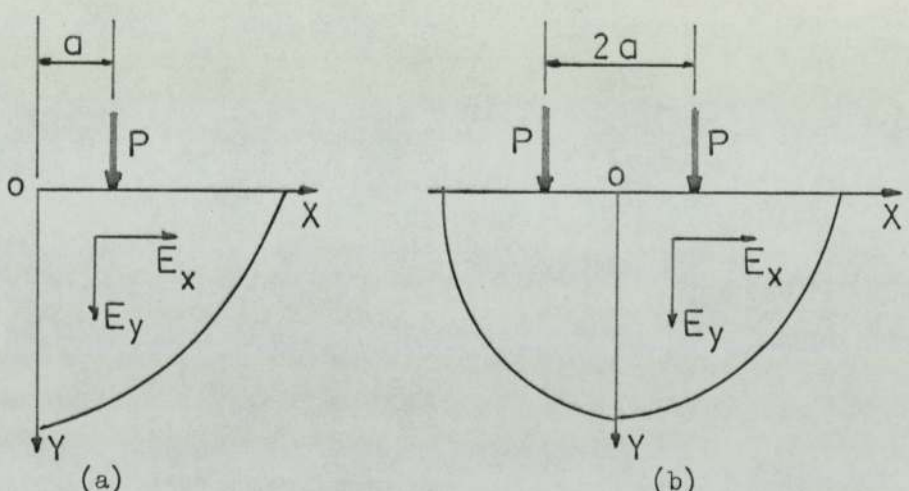

Fig.6.5

Consider an orthotropic quarter-plane $X > 0$, $Y > 0$, which is subjected to a concentrated force P/unit thickness, acting at point (a,o) and normal to the boundary (see Fig.6.5a).

The basic state of stress can be obtained by combining the results for two concentrated normal forces, acting equidistant from the origin, on the boundary of a half-plane ($Y > 0$) (see Fig.6.5b). The components of stress are then given by the following expressions (see equations 4.2-4):

$$\left[\sigma_x^o; \sigma_y^o; \tau_{xy}^o\right] = \frac{P(k_1+k_2)}{\pi a}\left[S_x; S_y; S_{xy}\right], \qquad 6.4\text{-}1a$$

where

6.4) contd.

$$\left[S_x;S_y;S_{xy}\right] = \left[S_x^+ + S_x^-;\ S_y^+ + S_y^-\ ;\ S_{xy}^+ + S_{xy}^-\right], \qquad 6.4\text{-}1b$$

and

$$\left[S_x^{\pm};\ S_y^{\pm};\ S_{xy}^{\pm}\right] = \frac{\left[(\bar{x}\pm 1)^2\bar{y};\ \bar{y}^3;\ (\bar{x}\pm 1)\bar{y}^2\right]}{\left[k_1^2(\bar{x}\pm 1)^2+\bar{y}^2\right]\left[k_2^2(\bar{x}\pm 1)^2+\bar{y}^2\right]}\ . \qquad 6.4\text{-}1c$$

The distribution of normal stress on the plane of symmetry ($X = 0$) is:

$$F_o(\tilde{y}) = \frac{2P}{\pi a}\ \frac{(k_1+k_2)\tilde{y}}{(k_1^2+\tilde{y}^2)(k_2^2+\tilde{y}^2)}\ . \qquad 6.4\text{-}2$$

6.5) Partially distributed uniform load acting normal to the boundary.

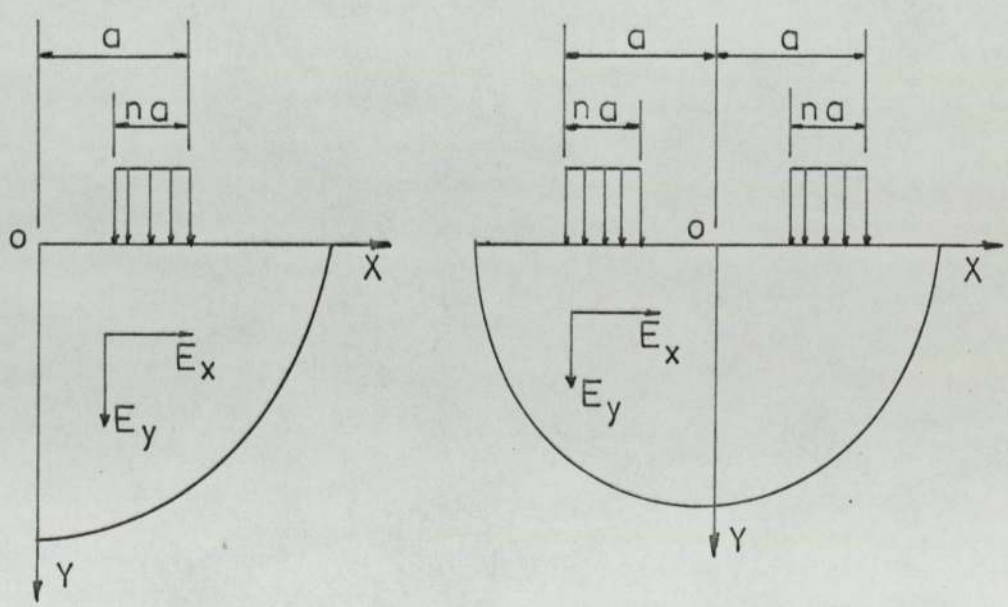

Fig.6.6

We now consider the problem of an orthotropic quarter-plane ($X > 0$, $Y > 0$), which is subjected to a unifirmly distributed stress of intensity p acting normal to the $Y = 0$ boundary. The applied load extends from $\bar{x} = (1-n)$ to $\bar{x} = 1$ (see Fig.6.6a).

The basic state of stress (see Fig.6.6b) can be obtained from the results for the uniformly distributed load solution of the half-plane problem (see Section 4.4), and it

6.5) contd.

can be expressed by the following relations:

$$\left[\sigma_x^o;\sigma_y^o;\tau_{xy}^o\right] = \frac{P}{\pi(k_1-k_2)}\left[\left(\frac{T_2}{k_2}-\frac{T_1}{k_1}\right);\ (T_1k_1-T_2k_2);\ \tfrac{1}{2}\,\ell n\left(\frac{t_1}{t_2}\right)\right], \quad 6.5\text{-}1a$$

where

$$T_i = T_i^+ + T_i^-\ ,\ t_i = t_i^+\ t_i^-\ ,\ \text{for } i = 1,2,$$

and

$$T_i^{\pm} = \mp\left\{\tan^{-1}\frac{k_i[\bar{x}\pm(1-n)]}{\bar{y}} - \tan^{-1}\frac{k_i(\bar{x}\pm 1)}{\bar{y}}\right\},$$

$$t_i^{\pm} = \frac{\bar{y}^2+k_i^2\,[\bar{x}\pm(1-n)]^2}{\bar{y}^2+k_i^2\,(\bar{x}\pm 1)^2}\ . \quad 6.5\text{-}1b$$

The distribution of normal stress on the plane of symmetry X = 0, is given by:

$$F_o(\tilde{y}) = \frac{2P}{\pi(k_1-k_2)}\left\{\frac{1}{k_2}\left[\tan^{-1}\frac{k_2(1-n)}{\bar{y}} - \tan^{-1}\frac{k_2}{\bar{y}}\right] - \right.$$

$$\left. - \frac{1}{k_1}\left[\tan^{-1}\frac{k_1(1-n)}{\bar{y}} - \tan^{-1}\frac{k_1}{\bar{y}}\right]\right\}. \quad 6.5\text{-}2$$

6.6 Concentrated force acting at the interior.

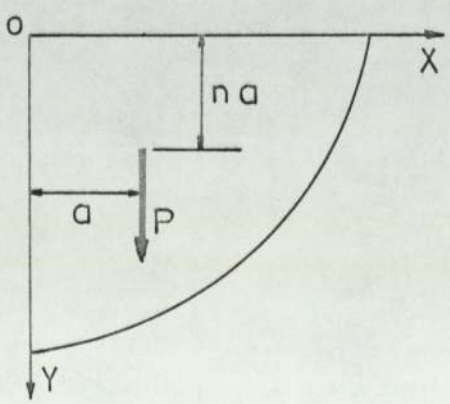

Fig.6.7

6.6) contd.

We consider the case of an orthotropic quarter-plane ($X > 0$, $Y > 0$) which is subjected to a concentrated force P/unit thickness acting at point (a,na). We shall limit our discussion on the case of the concentrated force being applied in the positive Y-direction.

The basic state of stress can be determined from the results for the interior concentrated force solution for the orthotropic half-plane (see Section 4.7).

The stress components for the basic state of stress are given by the following relations:

$$\left[\sigma_x^o;\ \sigma_y^o;\ \tau_{xy}^o\right] = \frac{P}{\pi a(k_1^2-k_2^2)} \Big\{ (\alpha_1+\alpha_3) r_1 \left[f_1;\ -f_1k_1^2;\ -k_1^2x\right]$$
$$+ \alpha_1 r_2 \left[-f_2;\ f_2k_1^2;\ k_1^2x\right]$$
$$+ (\alpha_2-\alpha_4) r_3 \left[f_1;\ f_1k_2^2;\ -k_2^2x\right]$$
$$+ \alpha_2 r_4 \left[-f_2;\ f_2k_2^2;\ k_2^2x\right]$$
$$+ \alpha_3 r_5 \left[-f_3;\ f_3k_2^2;\ k_1^2k_2^2x\right]$$
$$+ \alpha_4 r_6 \left[f_4;\ f_4k_1^2;\ -k_1^2k_2^2x\right] \Big\} \qquad 4.7\text{-}3$$

where

$$r_i = r_i^+ + r_i^- \quad , \quad \text{for } i = 1,2 \ldots 6,$$

and

$$\left.\begin{matrix} f_1 \\ f_2 \end{matrix}\right\} = \bar{y} \pm n \quad , \qquad f_3 = k_1(k_1\bar{y} + k_2n),$$
$$f_4 = k_2(k_2\bar{y} + k_1n),$$

$$r_1^{\pm} = \left[k_1^2(\bar{x}\pm 1)^2+(\bar{y}+n)^2\right]^{-1},\ r_2^{\pm} = \left[k_1^2(\bar{x}\pm 1)^2+(\bar{y}-n)^2\right]^{-1},$$

$$r_3^{\pm} = \left[k_2^2(\bar{x}\pm 1)^2+(\bar{y}+n)^2\right]^{-1},\ r_4^{\pm} = \left[k_2^2(\bar{x}\pm 1)^2+(\bar{y}-n)^2\right]^{-1},$$

$$r_5^{\pm} = \left[k_1^2k_2^2(\bar{x}\pm 1)^2+(k_2n+k_1\bar{y})^2\right]^{-1},\ r_6^{\pm} = \left[k_1^2k_2^2(\bar{x}\pm 1)^2+(k_1n+k_2\bar{y})^2\right]^{-1}.$$

α_i (for $i = 1 \ldots 4$) are defined by equation (4.7-4).

6.6) contd.

The normal stress distribution on the plane X = 0, is:

$$F_o(\tilde{y}) = \frac{2P}{\pi a(k_1^2-k_2^2)} \left\{ (\bar{y}+n) \left[\frac{(\alpha_1+\alpha_3)}{k_1^2+(\bar{y}+n)^2} + \frac{(\alpha_2-\alpha_4)}{k_2^2+(\bar{y}+n)^2} \right] - \right.$$

$$-(\bar{y}-n) \left[\frac{\alpha_1}{k_1^2+(\bar{y}-n)^2} + \frac{\alpha_2}{k_2^2+(\bar{y}-n)^2} \right] -$$

$$- \frac{\alpha_3 k_1 (k_2 n+k_1 \bar{y})}{[k_1^2 k_2^2+(k_2 n+k_1 \bar{y})^2]} +$$

$$\left. + \frac{\alpha_4 k_2 (k_1 n+k_2 \bar{y})}{[k_1^2 k_2^2+(k_1 n+k_2 \bar{y})^2]} \right\} \qquad 6.6\text{-}2$$

6.7) Evaluation of the stresses.

Numerical values for the stresses induced in an orthotropic quarter-plane by an arbitrary loading system, can be obtained in the following five steps:

Step 1: The basic state of stress $(\sigma_x^o, \sigma_y^o, \tau_{xy}^o)$ and $F_o(\tilde{y})$ are evaluated for the particular loading system.

Step 2: The $F_m(\tilde{x})$ and $F_m(\tilde{y})$ functions are determined by numerical evaluation of the integrals (equations 6.2-10a and b), in the logarithmic scale, using Simpson's rule.

Step 3: The boundary stresses applied on the two overlapping half-planes are then calculated by summation of the applied stresses for each reversal of loading:

$$\sigma_x(o,\bar{y}) = \sum_{m = o,2,4\ldots}^{\infty} F_m(\tilde{y}),$$

$$\sigma_y(\bar{x},o) = \sum_{m = 1,3,5\ldots}^{\infty} F_m(\tilde{x}). \qquad 6.7\text{-}1$$

6.7) contd.

Step 4: The corrective state of stress $(\sigma_x^c, \sigma_y^c, \tau_{xy}^c)$ in the quarter-plane is calculated by combining the stresses induced in the respective half-planes by the boundary stresses(6.7-1). In order to evaluate σ_x^c, σ_y^c, τ_{xy}^c, the boundary stresses (on the half-planes) are represented as a series of uniformly distributed loads of finite but variable width. It is found that this particular uniform load representation of the boundary stresses leads to a better convergence of results when evaluating the stress components in the vicinity of the boundaries of the quarter-plane.

Step 5: The basic state of stress is combined with the corrective state of stress to yield the complete solution to the orthotropic quarter-plane problem.

6.8) Numerical results.

In order to obtain numerical results for the state of stress in an orthotropic quarter-plane due to various loading systems, two main computer programs were written.

The first program computes the boundary stresses on the two overlapping half-planes, for a given initial stress distribution $F_o(\tilde{y})$ on the plane of symmetry X = 0.

The accuracy of the numerical integrations involved, depends mainly on the following parameters:

i) the upper limit of the integration, and

ii) the number of slices used for the application of Simpson's rule.

Both parameters are increased during the first integration for the evaluation of $F_1(\tilde{x})$ until $F_1(\tilde{x})$ is accurate to at least 5 decimals and $F_1(\tilde{x})$ at the upper limit is less than 0.005% of $F_1(\tilde{x})_{max.}$.

For the orthotropic materials considered,namely,

6.8) contd.

unidirectional graphite-epoxy and boron-epoxy composites, it was found that an upper limit of $\bar{x},\bar{y}$ = 150 and 120 slices produced results that satisfied the above requirements.

The reversal of loading is carried out until the boundary stresses are accurate to at least 5 decimals. It was found that for the materials considered, this order of accuracy was attained in 30 reversals of loading.

The second of the computer programs written, computes the corrective stresses in the quarter-plane. In this program, the boundary stresses are treated as a series of uniformly distributed loads of finite but variable width (see Fig.6.8).

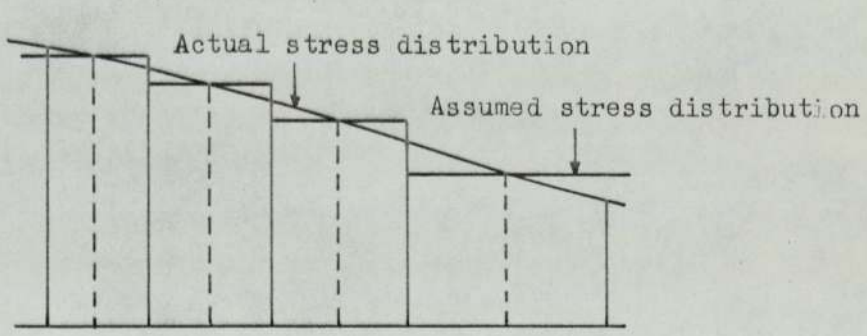

Fig.6.8

Attempts to treat the boundary stresses as a series of concentrated forces, resulted in high stresses in the vicinity of the boundaries to a depth of $\bar{x},\bar{y}$ = 0.5. For $\bar{x},\bar{y} > 1.5$, the two solutions gave the same resultsto at least 3 decimal places.

Finally, a separate program was written for each type of loading considered, to compute the stresses for the basic state of stress and combine them with the stresses of the corrective state of stress.

6.8) contd.

Numerical results are presented for two types of loading:

i) A concentrated force acting normal to the boundary of the quarter-plane, at point (a,o).

ii) A concentrated force acting at the interior of the quarter-plane, at point (a,a), in the positive Y-direction.

The properties of the materials considered are listed in Table 6.1 (Saha et al. 1972). It is assumed that the X-axis of the quarter-plane coincides with the direction of the fibres (i.e. high modulus axis).

The stress distributions, induced in the quarter-plane by the two types of load, are shown in Fig.6.9-6.20. The results are presented as a variation of stress $[\sigma_x;\sigma_y;\tau_{xy}]a/p$ with $\bar{x}$ for different values of $\bar{y}$.

Type of material	l_{11}	l_{22}	l_{12}	l_{44}	k_1	k_2	η
Boron Epoxy	3.624×10^{-3}	36.247×10^{-3}	-0.906×10^{-3}	96.665×10^{-3}	1.6055	0.1969	-0.25
Graphite Epoxy	3.624×10^{-3}	90.62×10^{-3}	-0.906×10^{-3}	181.257×10^{-3}	1.3998	0.1428	-0.25

[All dimensional quantities are in mm^2/kN]

TABLE 6.1

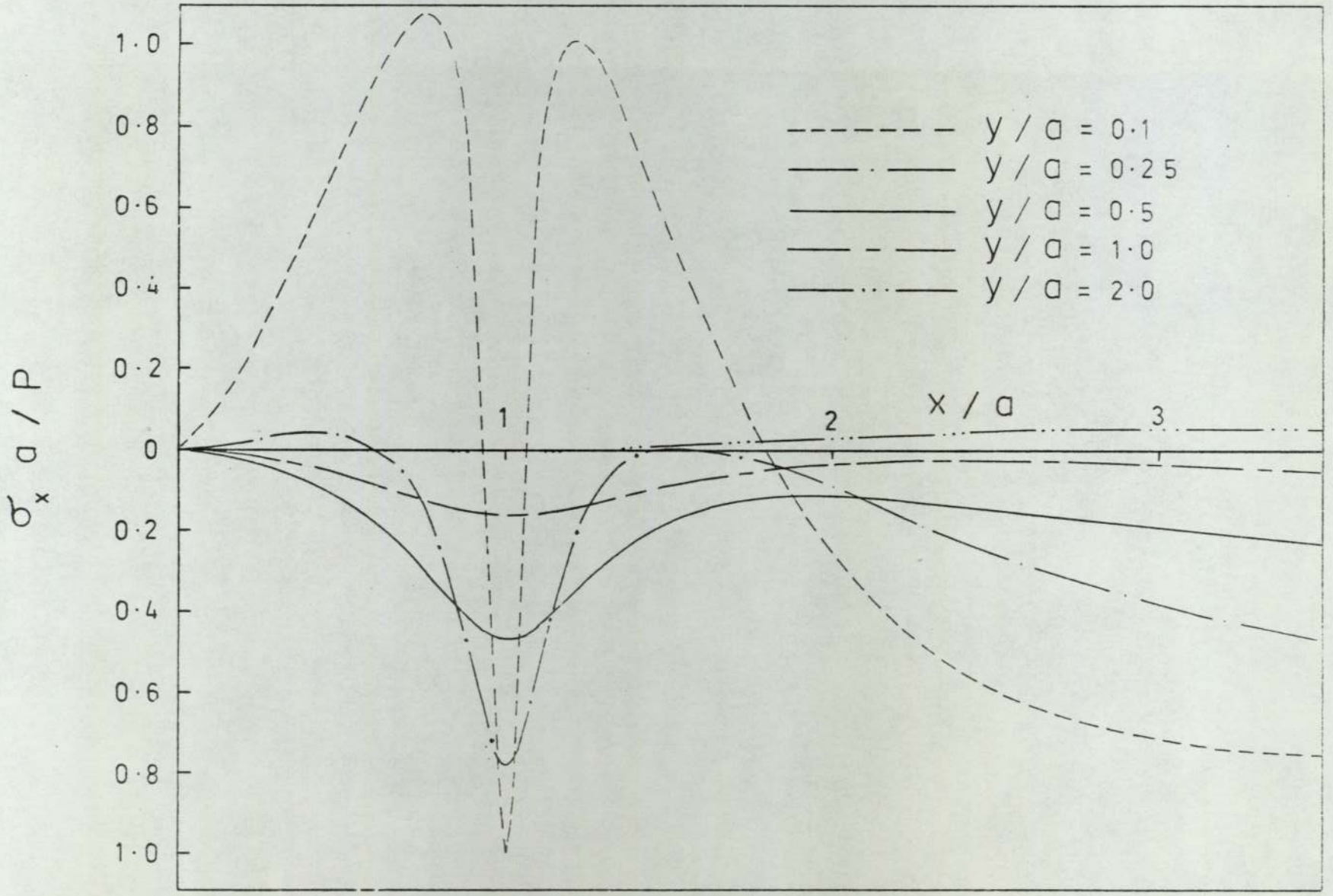

Fig. 6.9 Surface force – Variation of σ_x with x/a - Graphite - epoxy composite

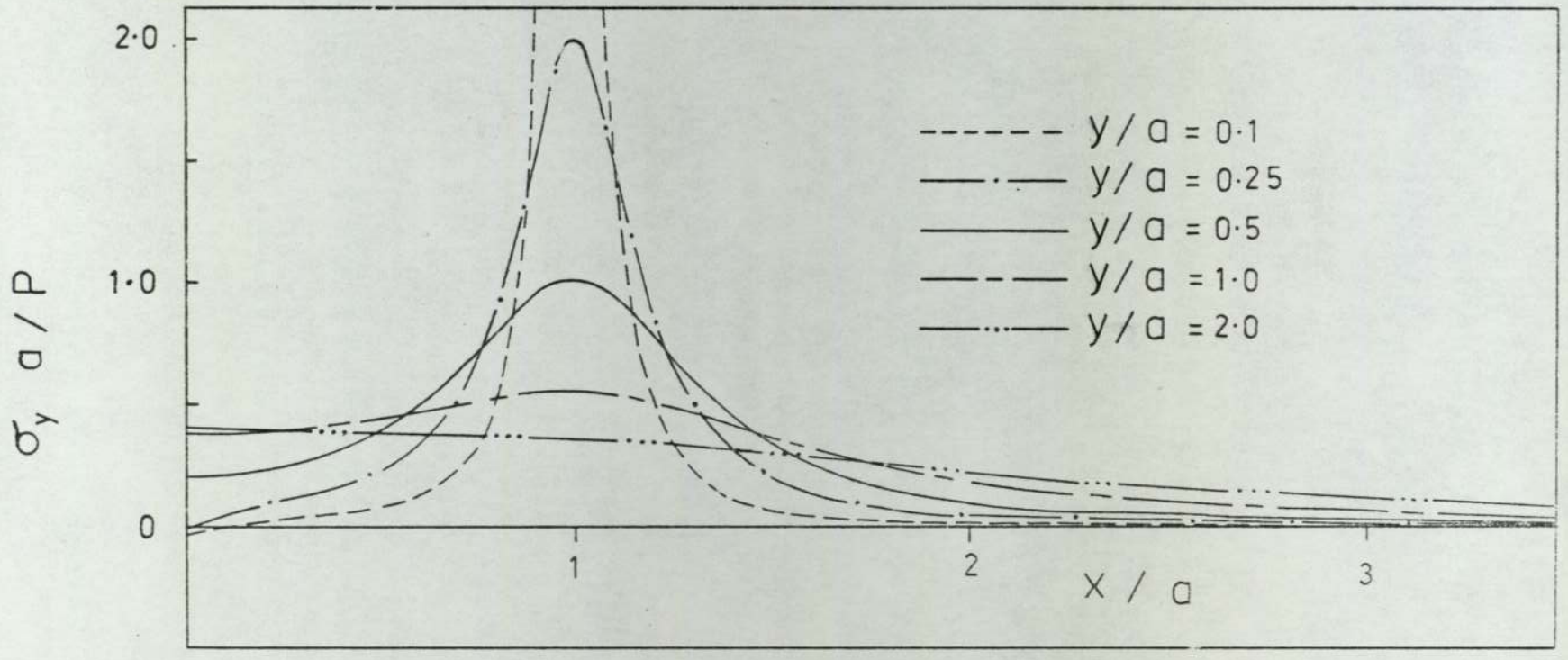

Fig 6.10 Surface force – Variation of σ_y with x/a – Graphite – epoxy composite

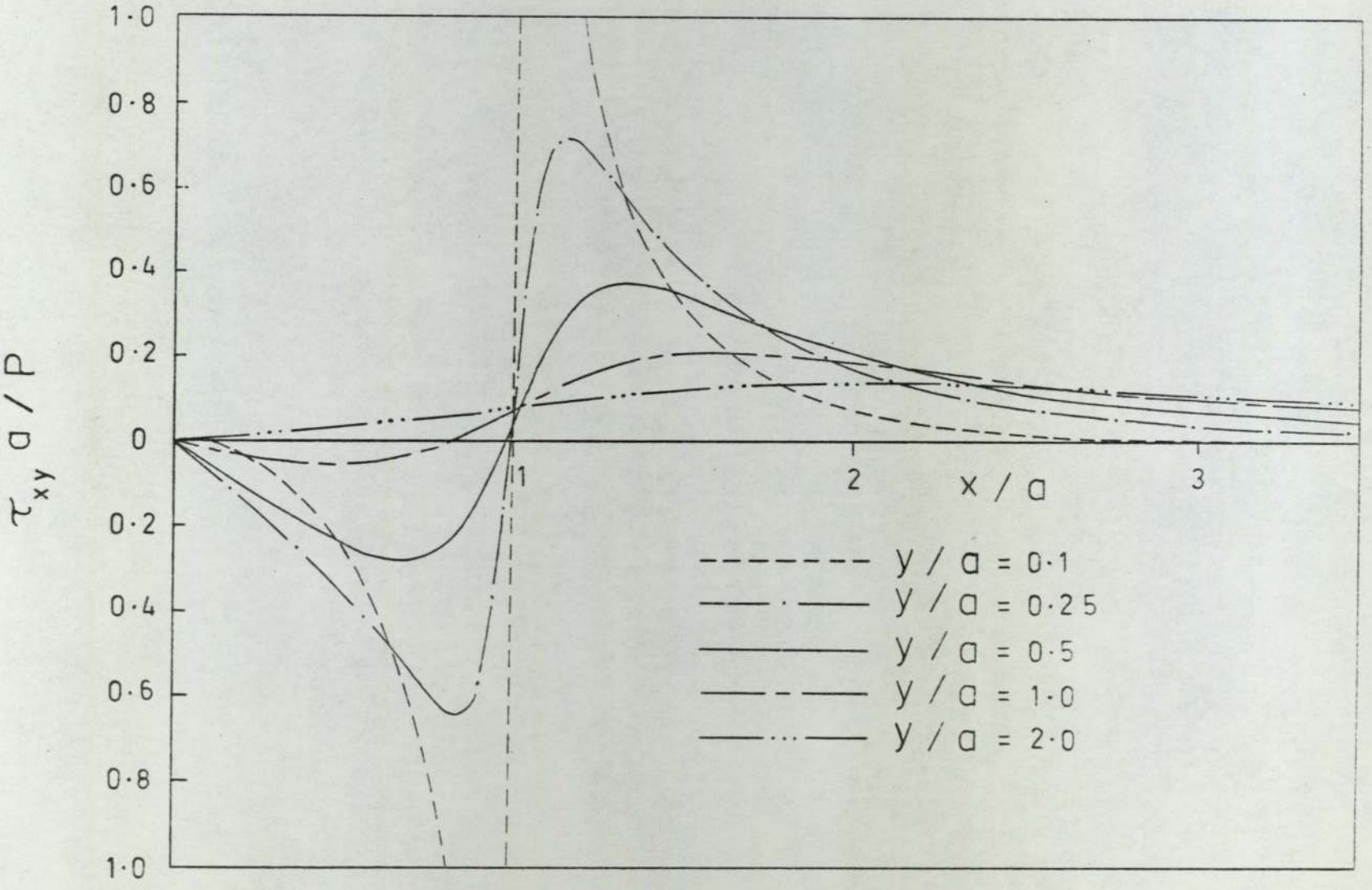

Fig. 6.11 Surface force — Variation of τ_{xy} with x/a — graphite-epoxy composite

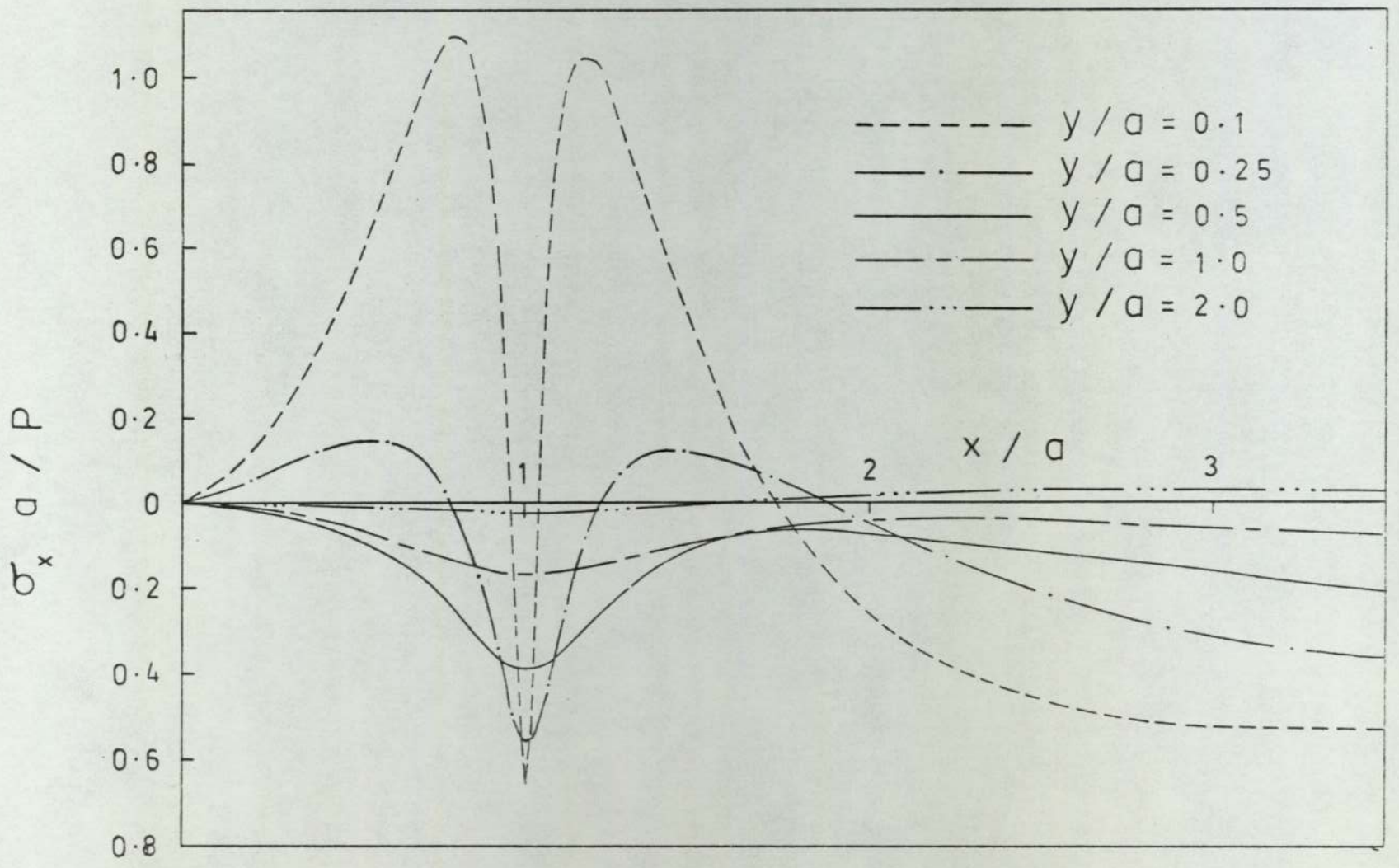

Fig. 6.12 Surface force – Variation of σ_x with x/a – Boron - epoxy composite

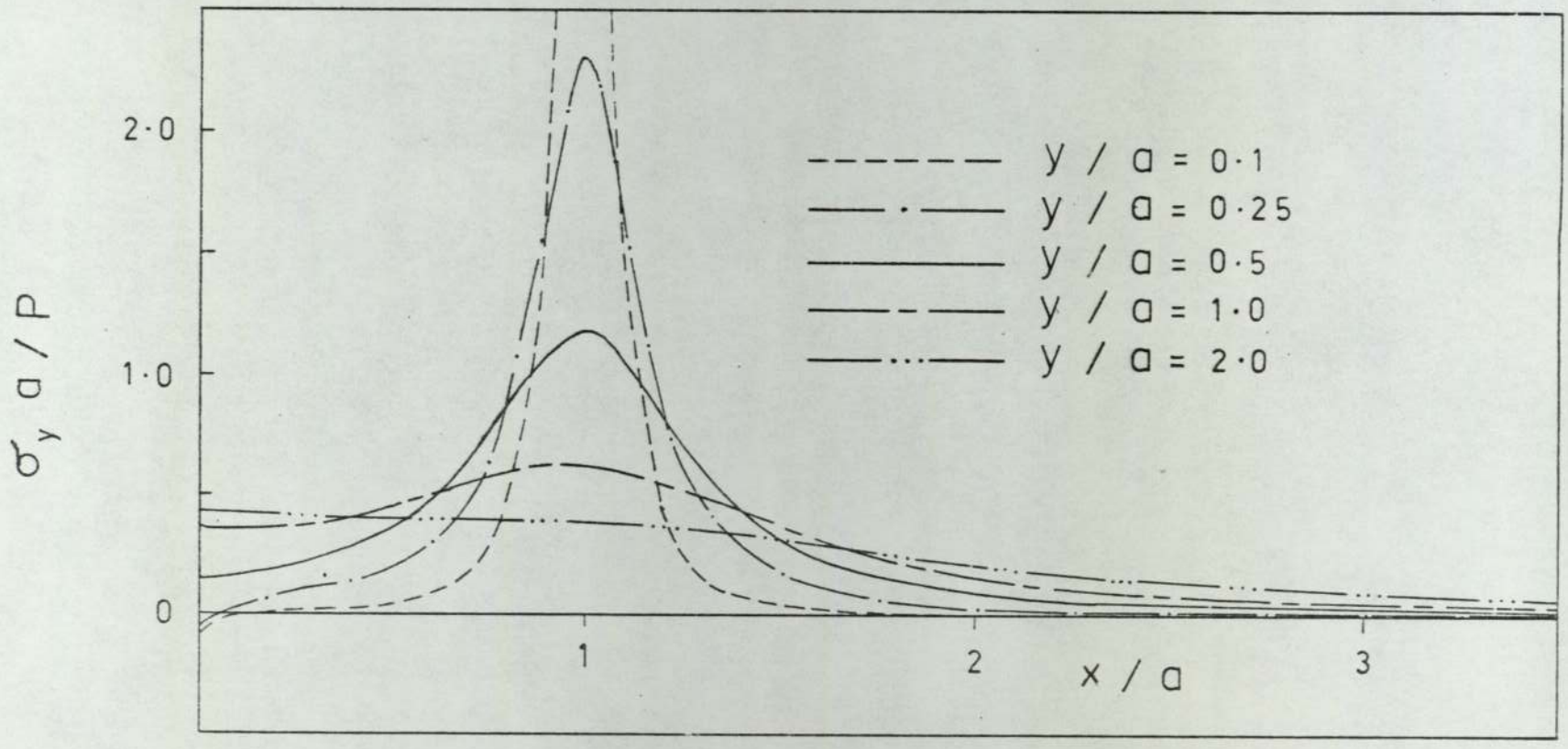

Fig. 6.13 Surface force - Variation of σ_y with x/a - Boron - epoxy composite

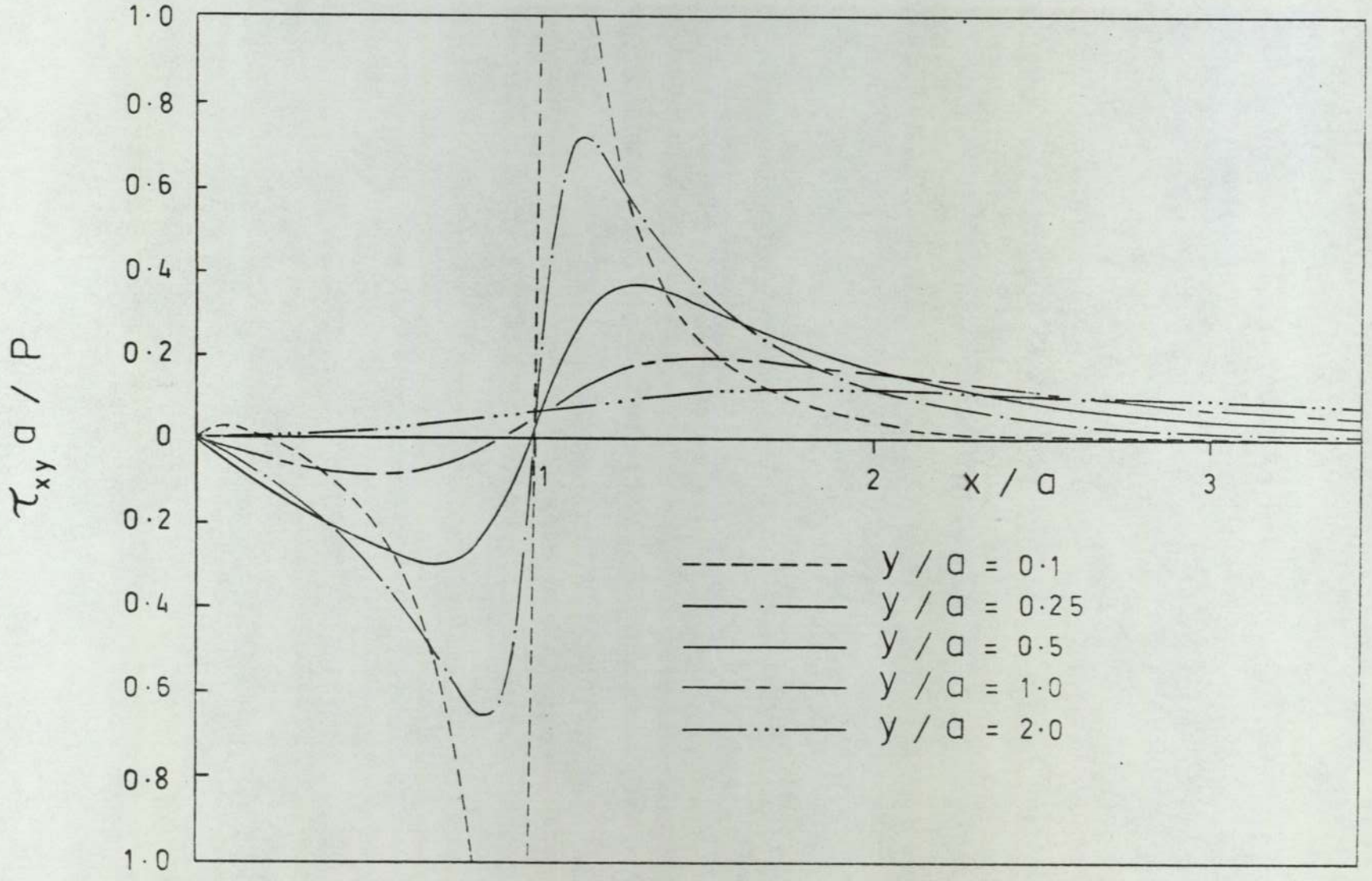

Fig. 6.14 Surface force – Variation of τ_{xy} with X/a – Boron - epoxy composite

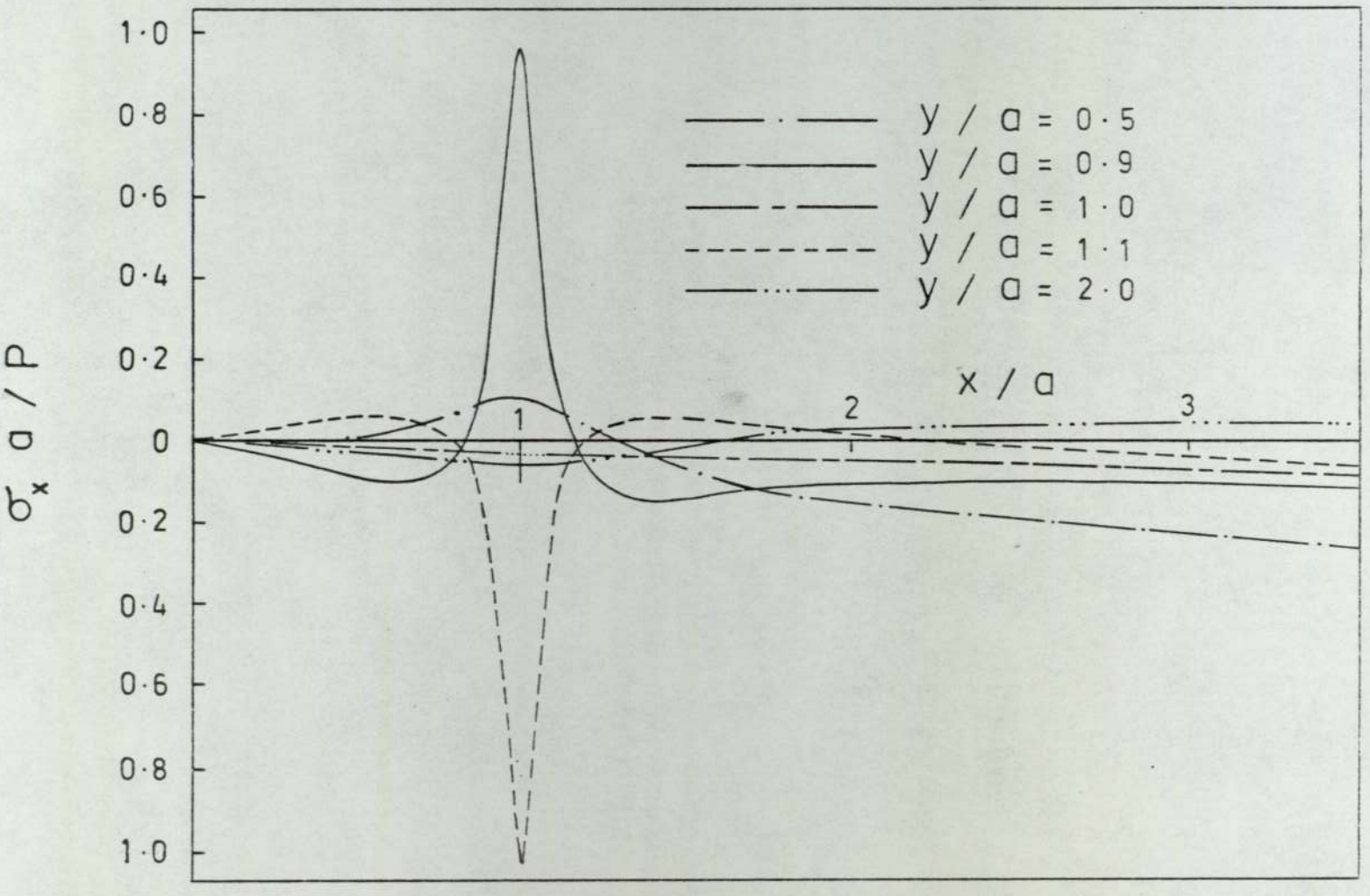

Fig 6.15 Interior force — Variation of σ_x with x/a — graphite - epoxy composite

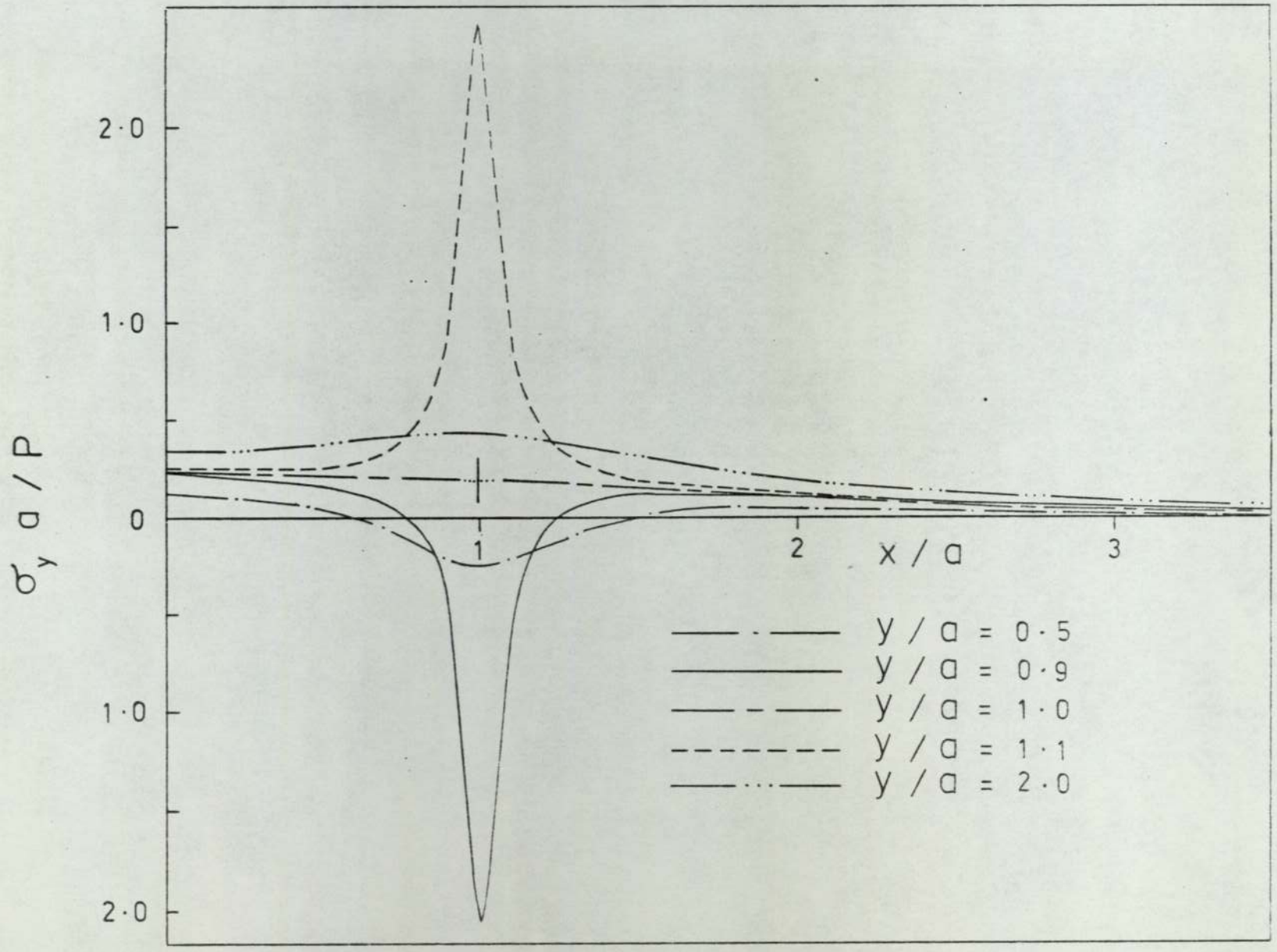

Fig. 6.16 Interior force — Variation of σ_y with x/a — graphite - epoxy composite

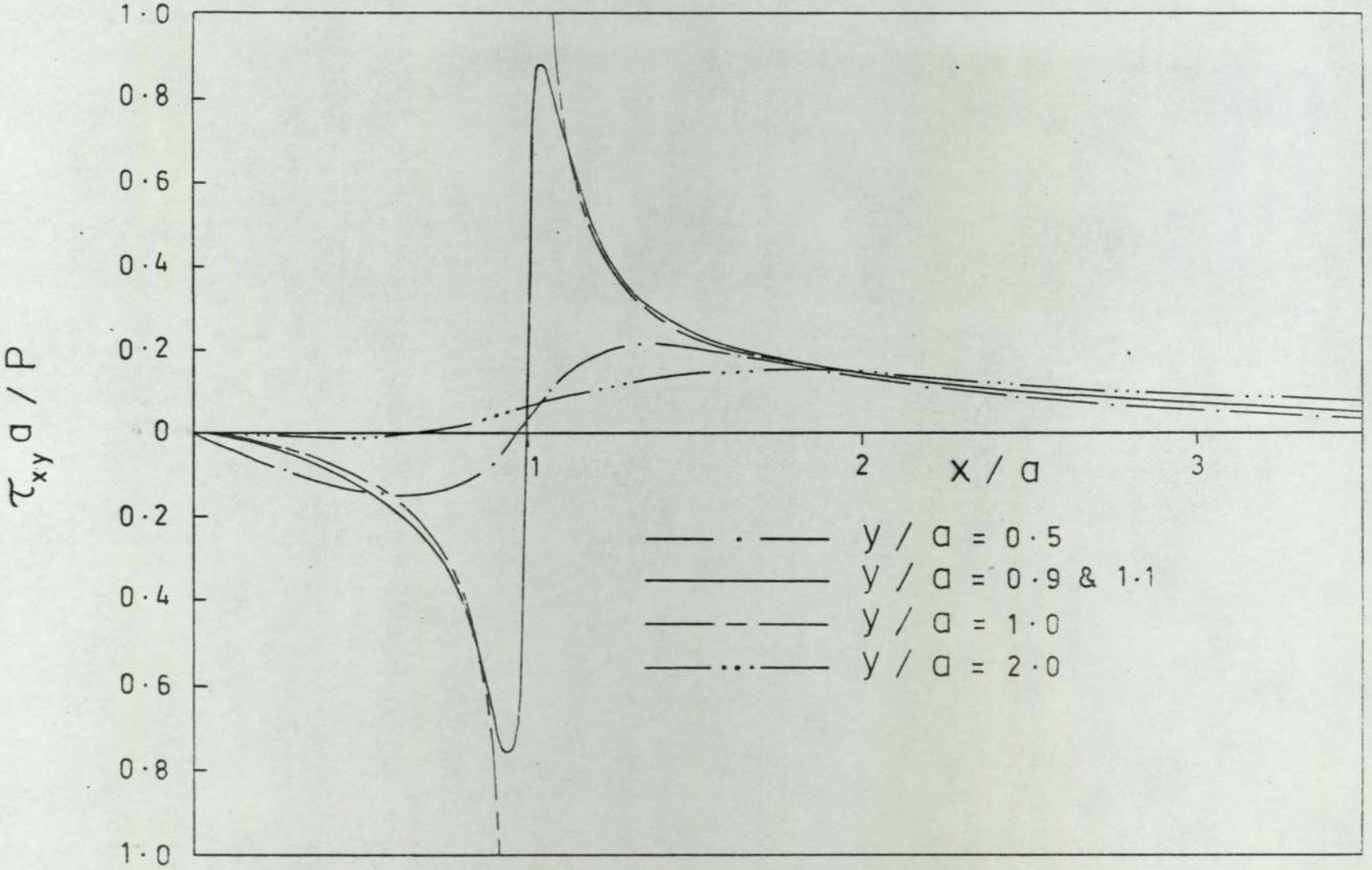

Fig. 6.17 Interior force - Variation of τ_{xy} with x/a - Graphite - epoxy composite

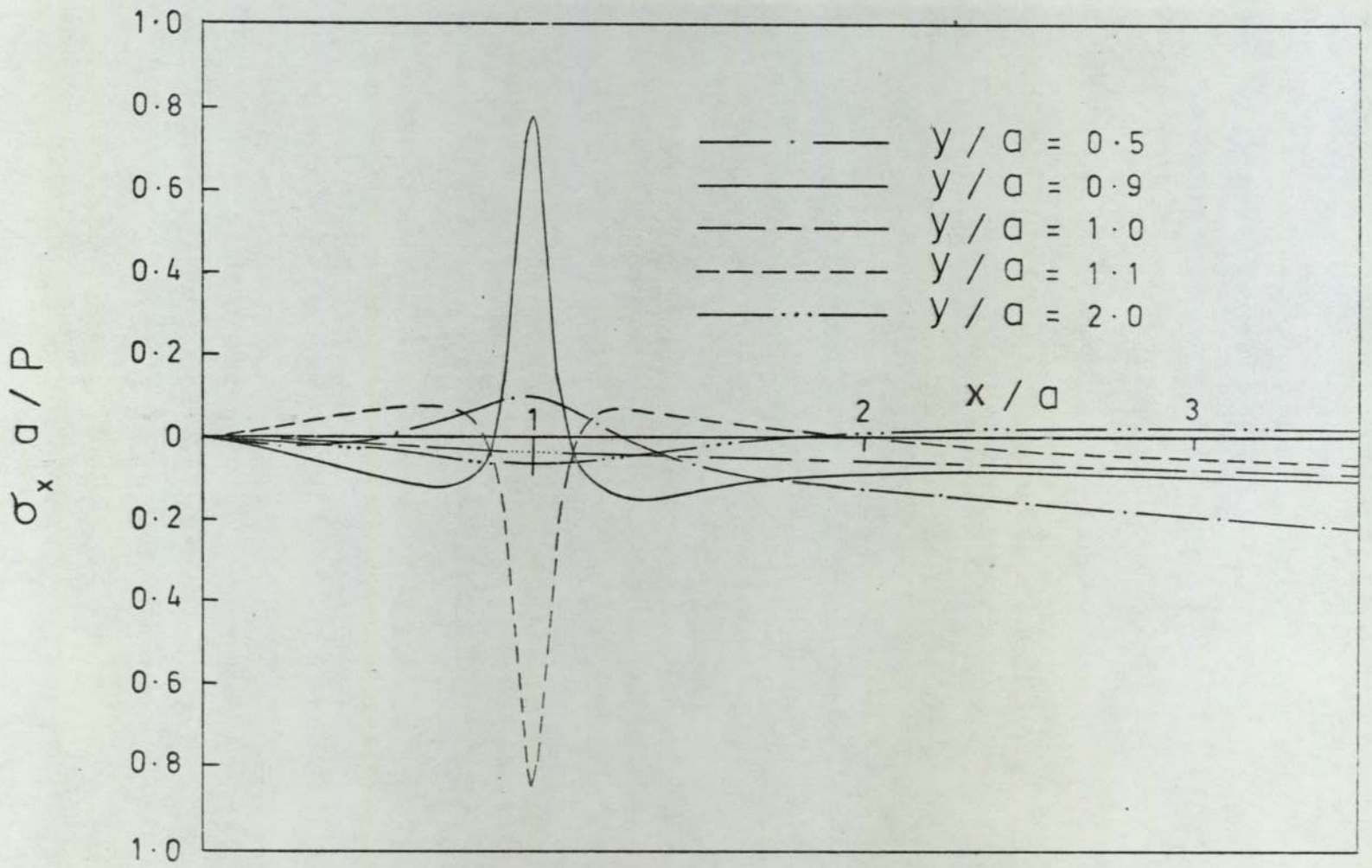

Fig. 6.18 Interior force - Variation of σ_x with x/a Boron – epoxy composite

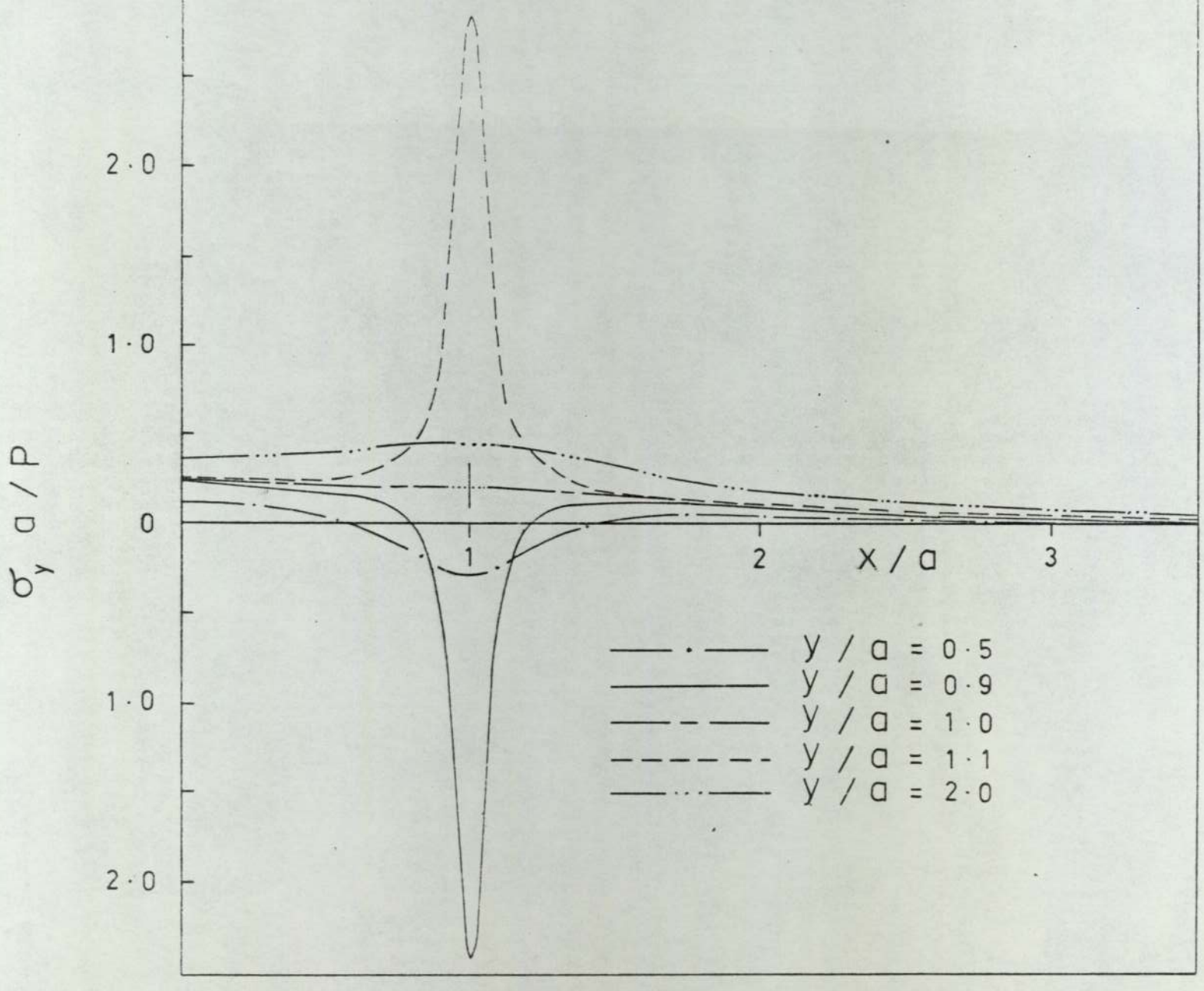

Fig. 6.19. Interior force – Variation of σ_y with X/a – Boron - epoxy composite

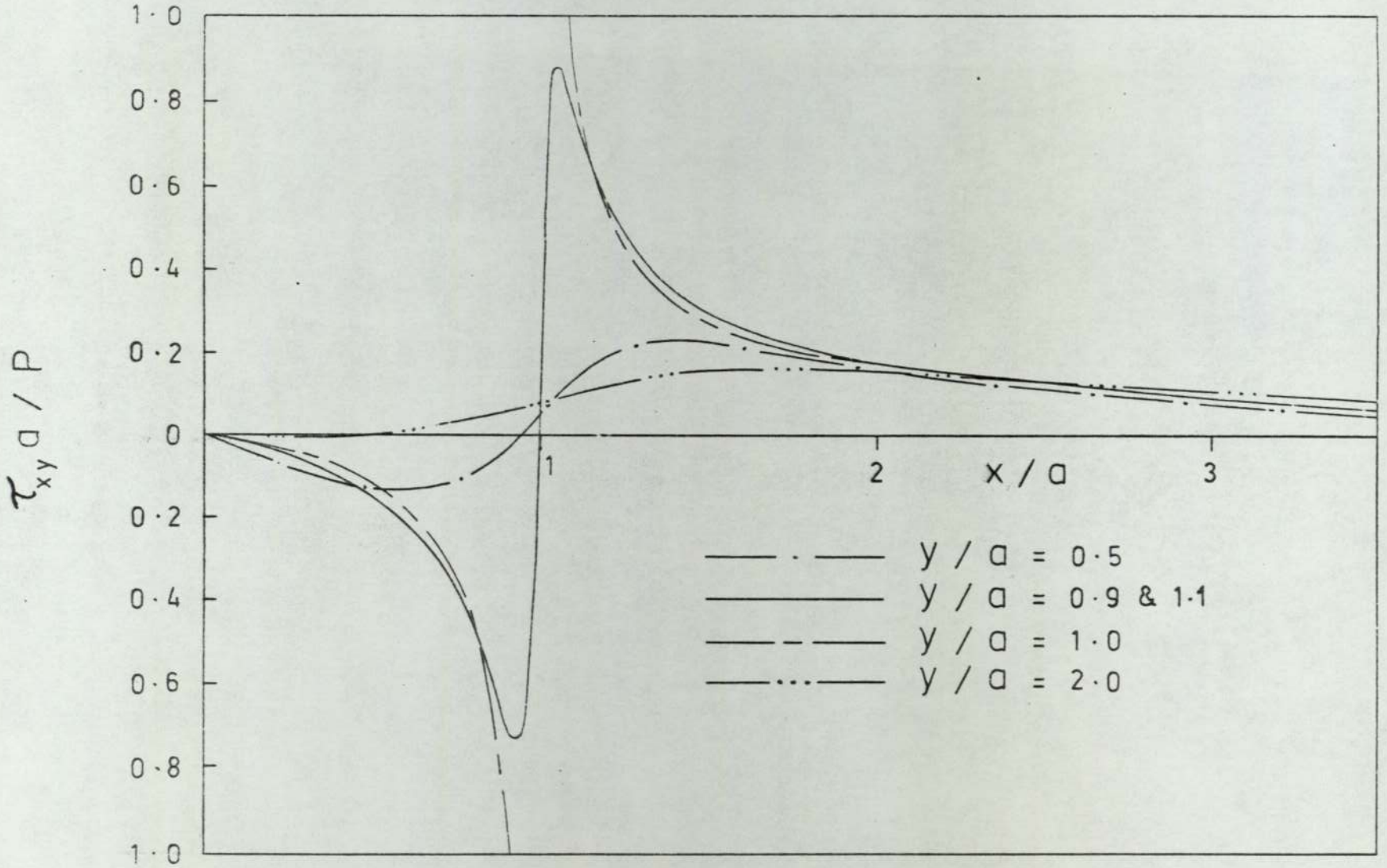

Fig. 6.20 Interior force — Variation of τ_{xy} with X/a — Boron - epoxy composite

6.9) Conclusions.

From the graphical results developed for the two composite materials (boron-epoxy and graphite-epoxy) (Fig.6.9-6.20), the following observations can be made.

1) The stresses σ_y and τ_{xy} diminish rapidly as $\bar{x}$ increases and become relatively insignificant for $\bar{x} > 4$. Similar behaviour is observed for $\bar{y} > 4$.

2) The stress σ_x diminishes very slowly, particulary for $\bar{y} < 0.5$. For example, $\sigma_x a/P$ at the point $\bar{x} = 50$, $\bar{y} = 0.1$, for graphite-epoxy composite under surface load, is 20% of its value at point $\bar{x} = 4$, $\bar{y} = 0.1$. On the other hand, σ_x diminishes rapidly with $\bar{y}$ and for $\bar{y} > 3$ it becomes relatively insignificant.

3) Comparing the results for the two orthotropic materials, we observe that as the ratio E_y/E_x increases (in this case for E_x = constant) σ_y increases, while σ_x decreases. τ_{xy} is practically unaffected by the change in E_y/E_y.

6.10) Suggestions and recommendations.

The analysis of the quarter-plane presented in the previous sections of this chapter can be employed in a number of problems encounted in engineering practice. For example, the quarter-plane loaded by a concentrated force at its interior, represents the situation which can occur in the vicinity of a metal connector in timber or fibre reinforced structural elements. In the special case when the concentrated force migrates to the boundary of the quarter-plane, we have a condition that may be encounted at the support of a structural element. Similar conditions may arise in Geotechnical and Foundation engineering (e.g. continuous footings near large excavations or embankments,

6.10) contd.

anchorage of suspension cables in bridges, etc.) where the loadings are better approximated by uniformly distributed or parabolic loads either at the boundary or at the interior of the quarter plane.

The analysis of the quarter plane was presented in a general form, so that it is possible to obtain the state of stress for oblique loads, concentrated couples, or finite distributed loads.

Further investigation can be made into the effects of transporting the internal concentrated force to various positions in the quarter-plane.

The analysis presented in this chapter is valid for orthotropic materials with their axes of orthotropy coinciding with the reference coordinate axes. However, a similar method of solution can be employed for the case in which the orthotropic axes are inclined at an angle to the coordinate axes. Assuming that the corresponding basic state of stress can be fully defined, the plane $X = 0$ is not a plane of symmetry and consequently shear stresses as well as normal stresses will develop along its surface. Therefore, each reversal of load should include a reversal of both normal and shear stresses.

CHAPTER 7

ORTHOTROPIC INFINITE STRIP.

7.1) Introduction

7.1.1) Definitions.

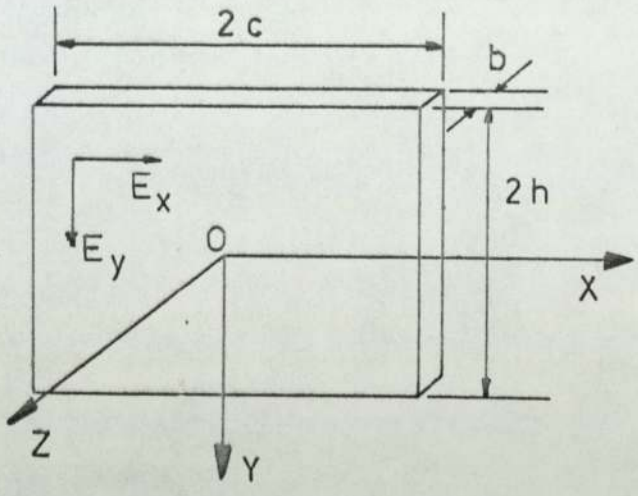

Fig.7.1

We consider a rectangular plate of length '2c', width '2h' and thickness 'b', with its sides parallel to the Cartesian coordinate axes X,Y,Z (see Fig.7.1). The centre of the plate is assumed to coincide with the origin of the coordinate axes O.

The plate, which is assumed to be in a state of plane stress (with $b << h$), may be subjected to load systems acting on its boundaries or at the interior.

We distinguish between the following cases:

a) The length (2c) of the plate is comparable with its width (2h). In such cases, the plate is referred to as a "deep beam" or simply as "plate".

b) The length (2c) of the plate is much greater than its width (2h), but 'c' is finite. Plates of this type are usually referred to as "beams".

c) In the third case, the plate is assumed to be of infinite length, and then it is usually referred to as "infinite beam" or "infinite strip".

7.1.1) contd.

We shall limit our discussion on problems associated with the infinite strip. In particular, the strip is assumed to be composed of an orthotropic elastic material, with the axes of orthotropy coinciding with the Cartesian coordinate axes X,Y,Z. The half width (h) of the strip is considered as the characteristic length of the problem, and, the dimensionless coordinates $\bar{x}$, $\bar{y}$, are defined by:

$$\bar{x} = \frac{x}{h}, \quad \bar{y} = \frac{y}{h}. \qquad 7.1\text{-}1$$

7.1.2) Historical background.

The first analytical and detailed work on the problem of determining the stresses and displacements in an isotropic elastic rectangular plate, loaded along its sides by any system of tractions, was presented by Filon (1903). Filon's analysis was based on Fourier series representation of the boundary loads, and, on the assumption that the normal and shear stress distributions over the terminal sections ($x = \pm c$), could be replaced by total resultant forces and moments. This technique produced accurate results, only if the length of the plate was large compared with its width, in which case, according to Saint-Venant's principle the assumption was justified.

Howland (1929), employed Filon's method to develop a solution to the problem of a concentrated force acting at the interior of the strip and in either of the coordinate directions. The strip was regarded as of infinite length, so that Fourier integrals were used instead of Fourier series. A similar method was used by Girkmann (1943).

Biot (1935), employed the elastic beam theory to

7.1.2) contd.

develop expressions for the stresses in a soil layer, resting on a "slippery rigid bed" or on a "rough rigid bed", and subjected on its boundary to a concentrated normal force. He also produced numerical results for the normal stress distribution along the inferface between the layer and the rigid bed.

Green (1939), employed Howland's method to investigate problems related to the orthotropic infinite strip. In particular, he considered the case of an infinite strip subjected to either a longitudinal or a transverse concentrated force, acting at any point of the strip. Green's work was limited to the derivation of the equations for the stresses and no numerical results were given.

Conway (1955c) presented numerical results for the stresses induced in an orthotropic infinite strip by two equal and opposite concentrated forces, acting centrally and parallel to its long sides.

Hashin (1967), investigated stress and displacement distributions in an anisotropic beam, under any polynomial loading applied on its long sides and for given force and moment resultants on the terminal sections ($x = \pm c$).

Gerrard (1967), considered the problem of an anisotropic infinite strip resting on a smooth rigid bed and subjected on its boundary to a partially distributed uniform normal load. He obtained a limited number of solutions, indicating the effect of anisotropy on the stress distribution beneath the strip. Since Gerrard's work was mainly on soil and rock mechanics, the infinite strip was assumed to be in a state of plane strain.

Finally, Yu (1973) obtained a solution for the

7.1.2) contd.

bending, shearing and normal stresses in an orthotropic beam, subjected to a transverse concentrated force, acting at the boundary y = -h. Numerical results were presented for two orthotropic materials, namely three layered plywood and pine wood.

7.1.3) Scope of investigation.

The work on the orthotropic infinite strip, deals with the following problems.

1) An investigation into the effects of orthotropy on the stress distributions in an infinite strip, which is subjected on its boundaries y = $\pm$ h, to symmetric, equal and opposite concentrated or distributed loads.

2) The development of a method of solution to the problem of an infinite strip which is subjected to an arbitrary self-equilibrating load system, acting either at the boundaries or at the interior of the strip. The work described in this section, is not meant to be in any way original; the basic purpose of the investigation is to illustrate an alternative method for the analysis of infinite strip problems. This method is based on the superposition of known solutions to infinite-plane and half-plane problems, such that the resulting stress field satisfies the boundary conditions of the infinite strip.

7.2) Orthotropic infinite strip subjected to symmetric boundary loads.

7.2.1) Sinusoidal loads.

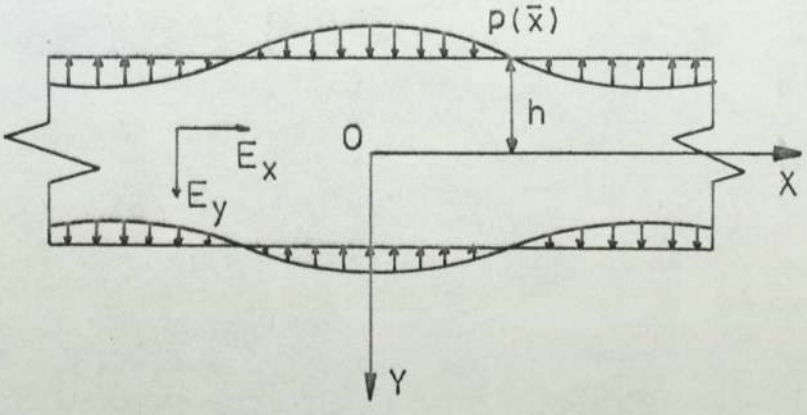

Fig.7.2

We consider the case of an orthotropic infinite strip subjected on its boundaries $y = \pm h$ to a normal stress distribution $p(x)$, where

$$p(x) = p \cos(\lambda^* x), \qquad 7.2\text{-}1a$$

and λ^* is a constant.

$$\text{Let } \lambda^* = \frac{\lambda}{h}. \qquad 7.2\text{-}1b$$

Then, equation (7.2-1a) can be written in the form:

$$p(\bar{x}) = p \cos(\lambda \bar{x}), \qquad 7.2\text{-}2$$

where $\bar{x} = x/h$ (see equation 7.1-1).

The assumed stress function is:

$$\Phi = (C_1 e^{\alpha\bar{y}} + C_2 e^{-\alpha\bar{y}} + C_3 e^{\beta\bar{y}} + C_4 e^{-\beta\bar{y}}) \cos(\lambda \bar{x}), \qquad 7.2\text{-}3$$

where

$\alpha = \frac{\lambda}{k_1}$, $\beta = \frac{\lambda}{k_2}$ and $C_1 \ldots C_4$ are constants that can be determined by the boundary conditions (see Section 5.3).

Expressions for the stress components can be obtained by substituting (7.2-3) in (2.6-1). These stress components can be written in the following form:

7.2.1) contd.

$$\sigma_x = \lambda^2 \left[\frac{C_1}{k_1^2} e^{\alpha\bar{y}} + \frac{C_2}{k_1^2} e^{-\alpha\bar{y}} + \frac{C_3}{k_2^2} e^{\beta\bar{y}} + \frac{C_4}{k_2^2} e^{-\beta\bar{y}} \right] \cos(\lambda \bar{x}),$$

$$\sigma_y = -\lambda^2 \left[C_1 e^{\alpha\bar{y}} + C_2 e^{-\alpha\bar{y}} + C_3 e^{\beta\bar{y}} + C_4 e^{-\beta\bar{y}} \right] \cos(\lambda \bar{x}), \qquad 7.2\text{-}4$$

$$\tau_{xy} = \lambda^2 \left[\frac{C_1}{k_1} e^{\alpha\bar{y}} - \frac{C_2}{k_1} e^{-\alpha\bar{y}} + \frac{C_3}{k_2} e^{\beta\bar{y}} - \frac{C_4}{k_2} e^{-\beta\bar{y}} \right] \sin(\lambda \bar{x}).$$

The boundary conditions for the infinite strip problem are:

a) $\sigma_y(\bar{x}, -1) = p \cos(\lambda \bar{x})$,

b) $\tau_{xy}(\bar{x}, -1) = 0$, 7.2-5

c) $\sigma_y(\bar{x}, 1) = p \cos(\lambda \bar{x})$,

d) $\tau_{xy}(\bar{x}, 1) = 0$.

By substitution of equations (7.2-4) into (7.2-5), we obtain a system of our simultaneous equations, which we can then solve, to obtain expressions for the constants $C_1 \ldots C_4$, in the following form:

$$C_1 = C_2 = A_1 \frac{p}{\lambda^2},$$

$$C_3 = C_4 = A_2 \frac{p}{\lambda^2}, \qquad 7.2\text{-}6a$$

where

$$A_1 = k_1(e^{\beta} - e^{-\beta})/\Delta,$$

$$A_2 = -k_2(e^{\alpha} - e^{-\alpha})/\Delta, \qquad 7.2\text{-}6b$$

and

$$\Delta = k_2(e^{\alpha} - e^{-\alpha})(e^{\beta} + e^{-\beta}) - k_1(e^{\alpha} + e^{-\alpha})(e^{\beta} - e^{-\beta}).$$

The stresses at any point in the infinite strip, can then be obtained by substitution of equation (7.2-6) into (7.2-4):

$$\sigma_x = p R_x \cos(\lambda \bar{x}),$$

$$\sigma_y = p R_y \cos(\lambda \bar{x}), \qquad 7.2\text{-}7a$$

$$\tau_{xy} = p R_{xy} \sin(\lambda \bar{x}),$$

7.2.1) contd.

where

$$R_x = \frac{A_1}{k_1^2}\left(e^{\alpha\bar{y}} + e^{-\alpha\bar{y}}\right) + \frac{A_2}{k_2^2}\left(e^{\beta\bar{y}} + e^{-\beta\bar{y}}\right),$$

$$R_y = -A_1\left(e^{\alpha\bar{y}} + e^{-\alpha\bar{y}}\right) - A_2\left(e^{\beta\bar{y}} + e^{-\beta\bar{y}}\right), \qquad 7.2\text{-}7b$$

$$R_{xy} = \frac{A_1}{k_1}\left(e^{\alpha\bar{y}} - e^{-\alpha\bar{y}}\right) + \frac{A_2}{k_2}\left(e^{\beta\bar{y}} - e^{-\beta\bar{y}}\right).$$

7.2.2) Partially distributed uniform load; concentrated load.

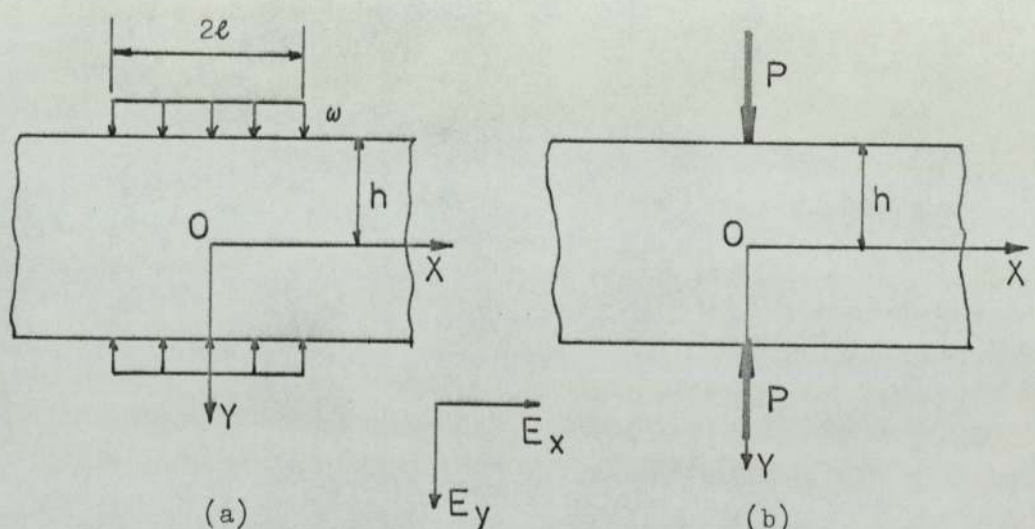

Fig.7.3

We consider the case of an orthotropic infinite strip, which is subjected on its boundaries $y = \pm h$, to a partially distributed normal stress of intensity ω and width '2ℓ', applied symmetrically about the Y-axis (see Fig.7.3a).

This type of load can be expressed as a Fourier integral, in the following form:

$$p(\bar{x}) = \frac{2\omega\ell}{\pi h}\int_0^\infty \frac{\sin(\lambda\,\bar{\ell})}{\lambda\,\bar{\ell}}\cos(\lambda\,\bar{x})\,d\lambda, \qquad 7.2\text{-}8$$

where $\bar{\ell} = \ell/h$.

Equation (7.2-8) represents a summation of an infinite number of sinusoidal loads, of the type:

7.2.2) contd.

$$\left[\frac{2\omega\ell}{\pi h} \frac{\sin(\lambda \bar{\ell})}{\lambda \bar{\ell}} \, d\lambda \right] \cos(\lambda \bar{x}). \qquad 7.2\text{-}9$$

We can then identify this sinusoidal load, as that applied on the infinite strip; namely $p(\bar{x})$ as given by equation (7.2-2).

Using the representation in (7.2-8), the stresses in the infinite strip due to a partially distributed uniform load, can be expressed in the following form:

$$\sigma_x = \frac{2\omega\ell}{\pi h} \int_0^\infty R_x \frac{\sin(\lambda \bar{\ell})}{\lambda \bar{\ell}} \cos(\lambda \bar{x}) \, d\lambda,$$

$$\sigma_y = \frac{2\omega\ell}{\pi h} \int_0^\infty R_y \frac{\sin(\lambda \bar{\ell})}{\lambda \bar{\ell}} \cos(\lambda \bar{x}) \, d\lambda, \qquad 7.2\text{-}10$$

$$\tau_{xy} = \frac{2\omega\ell}{\pi h} \int_0^\infty R_{xy} \frac{\sin(\lambda \bar{\ell})}{\lambda \bar{\ell}} \sin(\lambda \bar{x}) \, d\lambda.$$

By making use of the condition:

$$\underset{\bar{\ell} \to 0}{\text{limit}} \frac{\sin(\lambda \bar{\ell})}{\lambda \bar{\ell}} = 1,$$

and the condition $2\omega\ell \to P$ as $\ell \to 0$, we can obtain from equation (7.2-10), the solution to the problem of an infinite strip which is subjected on its boundaries $\bar{y} = \pm 1$ to equal normal concentrated forces P/unit thickness. The stress components are then given by:

$$\sigma_x = \frac{P}{\pi h} \int_0^\infty R_x \cos(\lambda \bar{x}) d\lambda,$$

$$\sigma_y = \frac{P}{\pi h} \int_0^\infty R_y \cos(\lambda \bar{x}) d\lambda, \qquad 7.2\text{-}11$$

$$\tau_{xy} = \frac{P}{\pi h} \int_0^\infty R_{xy} \sin(\lambda \bar{x}) d\lambda$$

7.2.3) Numerical Results.

The expressions for the stress components in an infinite orthotropic strip, due to symmetric , partially distributed uniform loads (equation 7.2-10), or due to symmetric concentrated forces (equation 7.2-11), are functions of the orthotropic constants of the material k_1 and k_2. In the case of the uniform load, the stresses are also functions of the half-width of the load 'ℓ'.

The orthotropic constants k_1 and k_2, which are functions of the constants ℓ_{ij} (see equation 2.6-4), can be expressed in terms of the following ratios:

$$\frac{\ell_{12}}{\ell_{22}} , \quad \frac{\ell_{66}}{\ell_{22}} , \quad \frac{\ell_{11}}{\ell_{22}} .$$

Therefore, the effects of orthotropy on the stress distribution in an infinite strip can be investigated by varying the values of the three ratios, which in the case of plane stress reduce to:

$$\nu_{xy} , \quad \frac{E_y}{G_{xy}} , \quad \frac{E_y}{E_x} .$$

For the purpose of the numerical computations, we assume $\nu_{xy} = 0.25$. This value of ν_{xy} is frequently encountered, particularly in connection with fibre-reinforced composites (Saha et al.(1972), Al-Khayatt (1974)). We then assign a value to one of the ratios, say E_y/E_x, while varying the other (E_y/G_{xy}). The process can be repeated for various values of E_y/E_x.

It must be pointed out, that owing to the symmetry condition $\nu_{xy} E_y = \nu_{yx} E_x$, and the condition (see equation 2.4-4b)

$$\left|\nu_{yx}\right| < \sqrt{\frac{E_y}{E_x}} , \qquad 7.2\text{-}12$$

for $\nu_{xy} = 0.25$, the upper limit of the ratio E_y/E_x is 16.

7.2.3) contd.

In addition, for k_1 and k_2 to be real and positive (see Section 2.6)

$$\frac{E_y}{G_{xy}} > 2\left[\sqrt{\frac{E_y}{E_x}} + \nu_{xy}\frac{E_y}{E_x}\right]. \qquad 7.2\text{-}13$$

1) Infinite strip subjected to concentrated forces.

The stresses induced in an infinite strip by equal, concentrated forces acting normal to the boundaries $\bar{y} = \pm 1$ (see Fig.7.3b), were obtained from equation (7.2-12) by numerical evaluation of the integrals, using Simpson's rule. The number of slices used and the upper limit of the integration procedure were varied, so that the results obtained were accurate to at least three decimal places (on average 2,000 slices were used and an upper limit of 24).

The results for the stresses (e.g. σ_x $\pi h/P$) are presented in a graphical form (see Fig.7.4-7.11) as a variation of stress with $\bar{x}$ or $\bar{y}$, for various values of E_y/G_{xy}, when: a) $E_y/E_x = 1$, and, b) $E_y/E_x = 0.05$, c) $E_y/E_x = 5$.

In addition, the variation of σ_y and σ_x at point (0,0) with E_y/E_x and E_y/G_{xy}, is presented in Fig.7.12 and 7.13.

2) Infinite strip subjected to partially distributed uniform load.

The stresses induced in an infinite strip by the above type of loading (see also Fig.7.3a), were obtained by numerical evaluation of the integrals in equation (7.2-10), using Simpson's rule. The stresses were determined for points along the X-axis when $\bar{\ell} = 1$ and $\bar{\ell} = 0.5$, for various values of E_y/G_{xy} and E_y/E_x, and are shown in Fig.7.14-7.21.

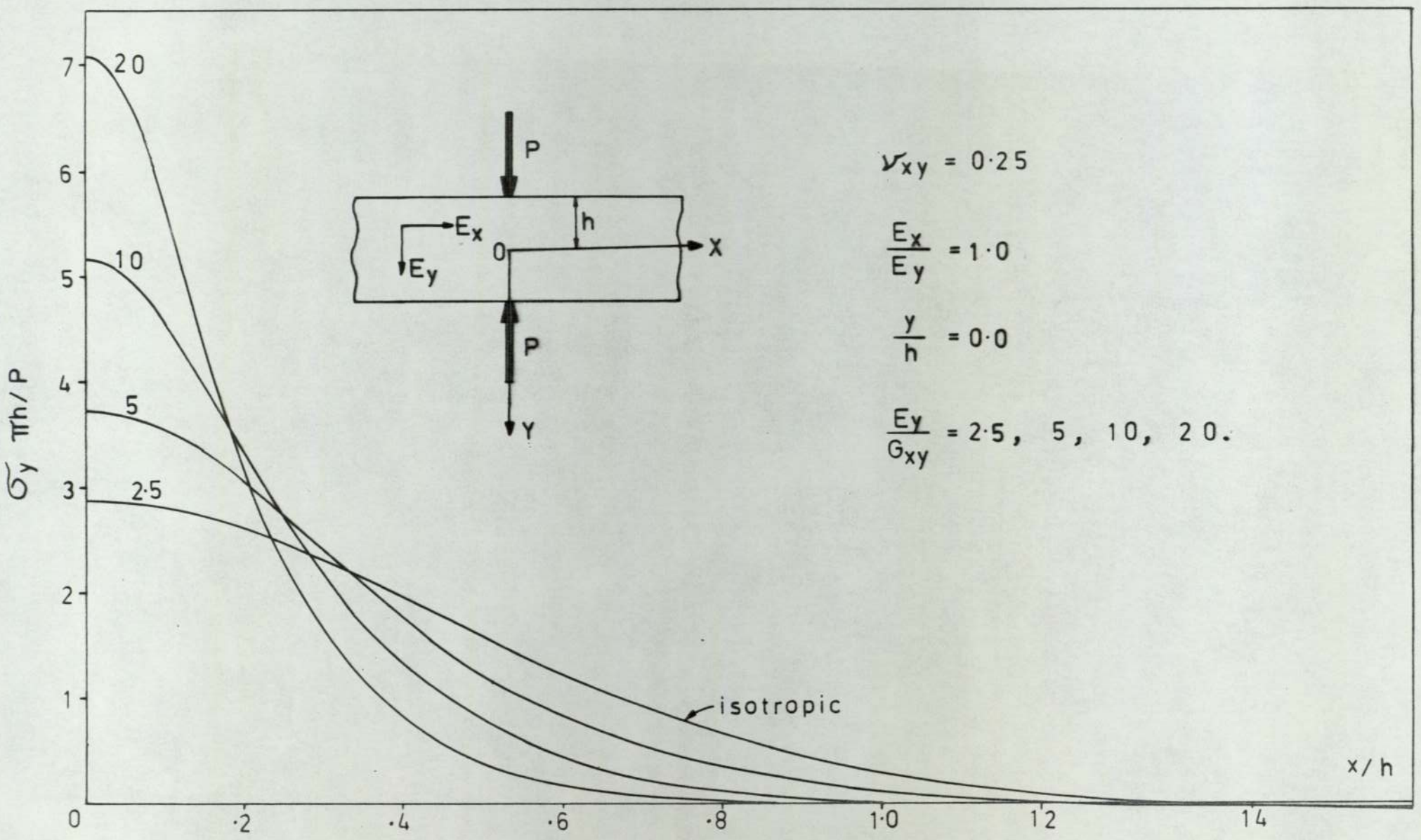

FIG· 7·4 Variation of σ_y with x/h along the X–axis; E_y/E_x = 1·0

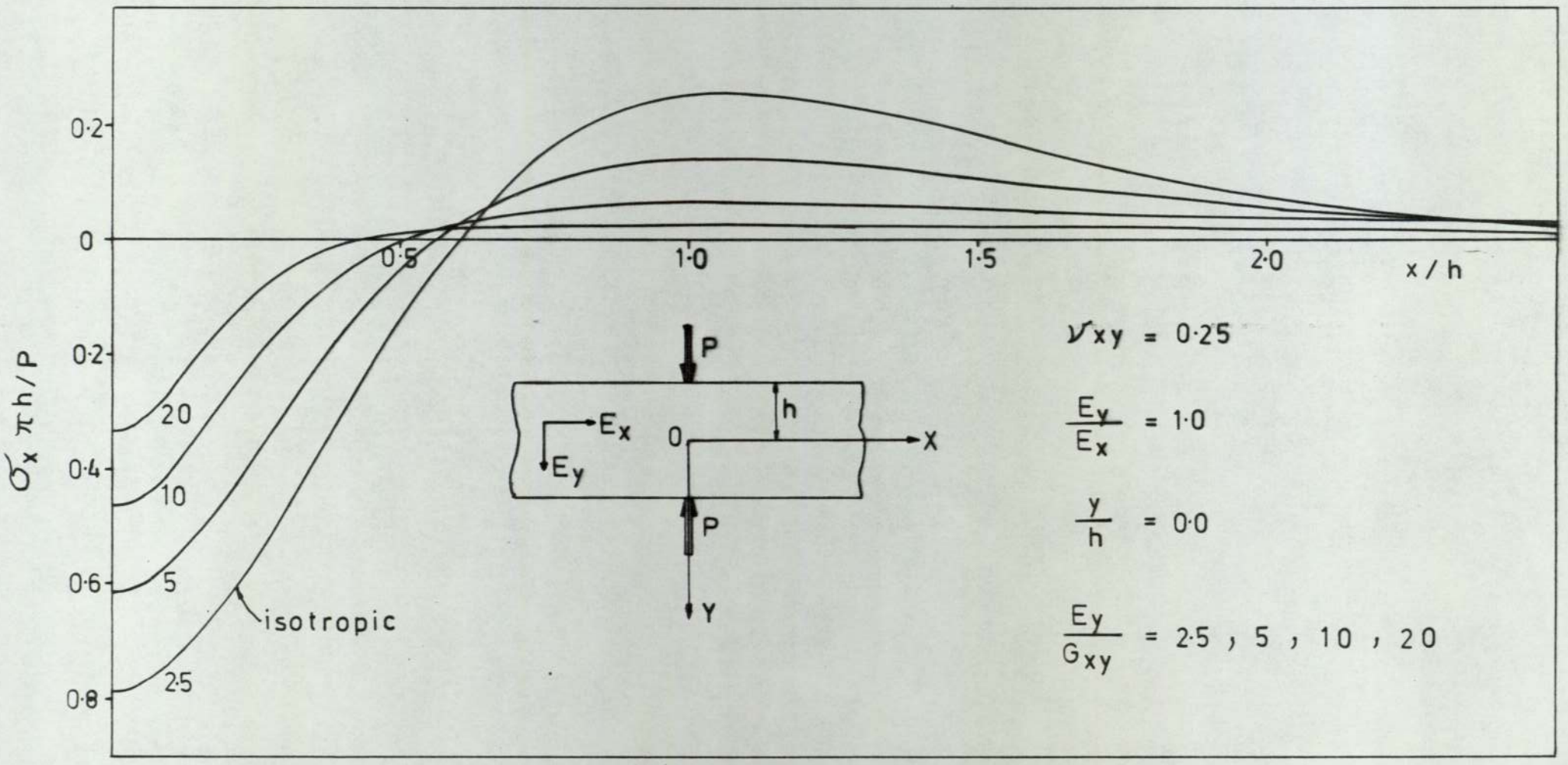

FIG. 7.5 Variation of σ_x with x/h along the x-axis $\frac{E_y}{G_{xy}} = 1$

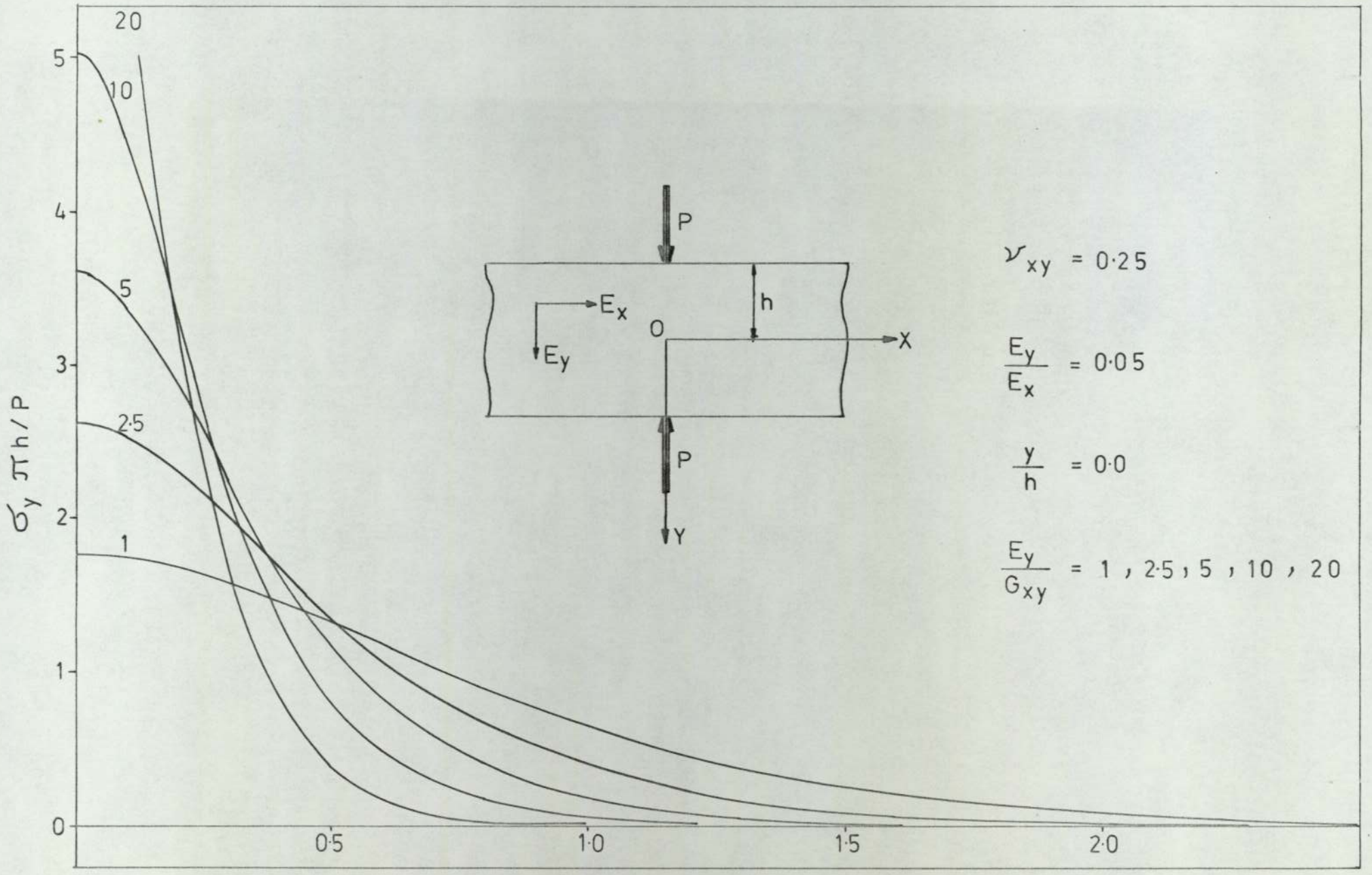

FIG· 7·6 Variation of σ_y with x/h along the x–axis ; $\frac{E_y}{E_x} = 0{\cdot}05$

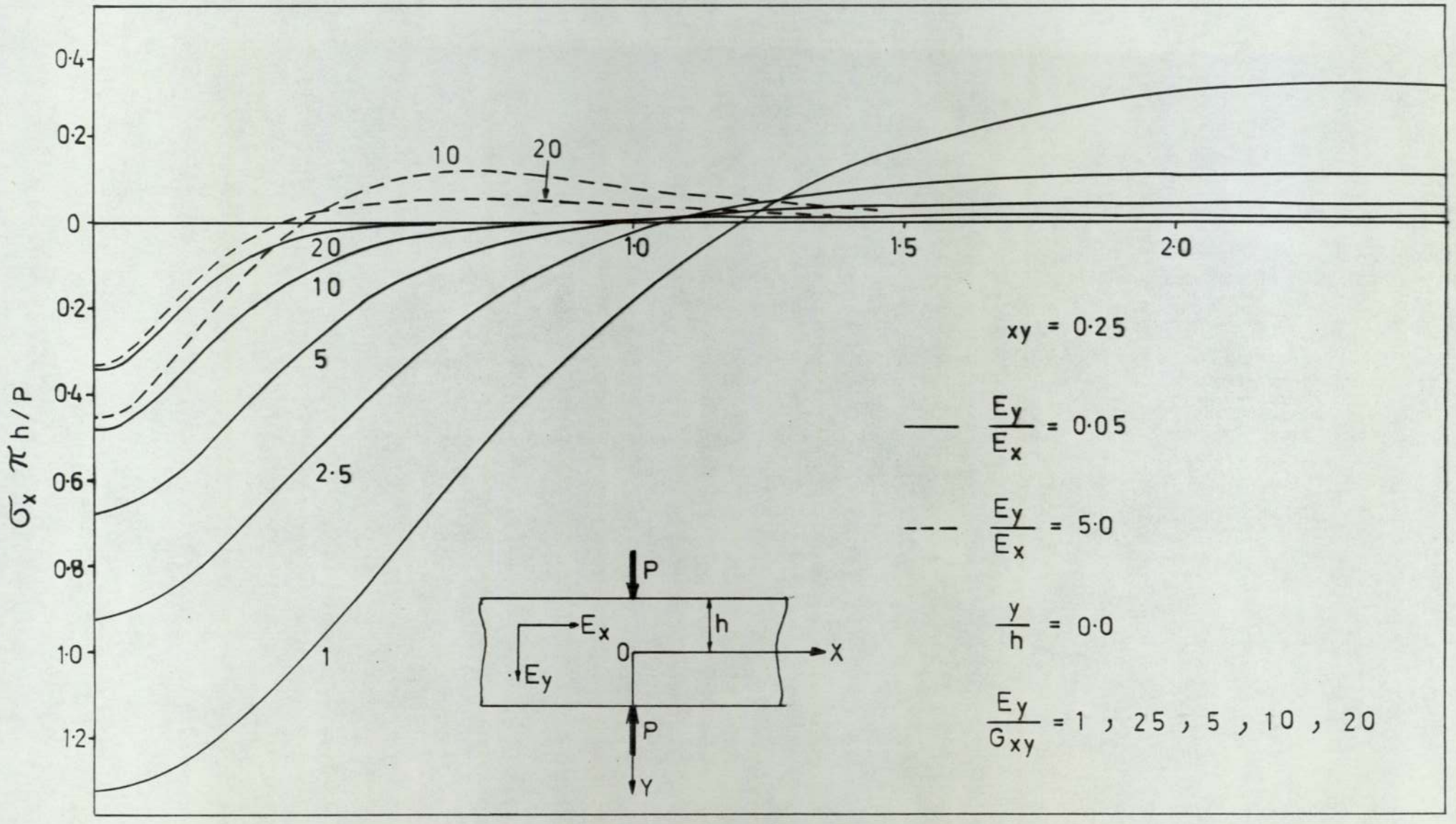

FIG· 7·7 Variation of σ_x with x/h along the x axis E_y/E_x = 0·05 & 5·0

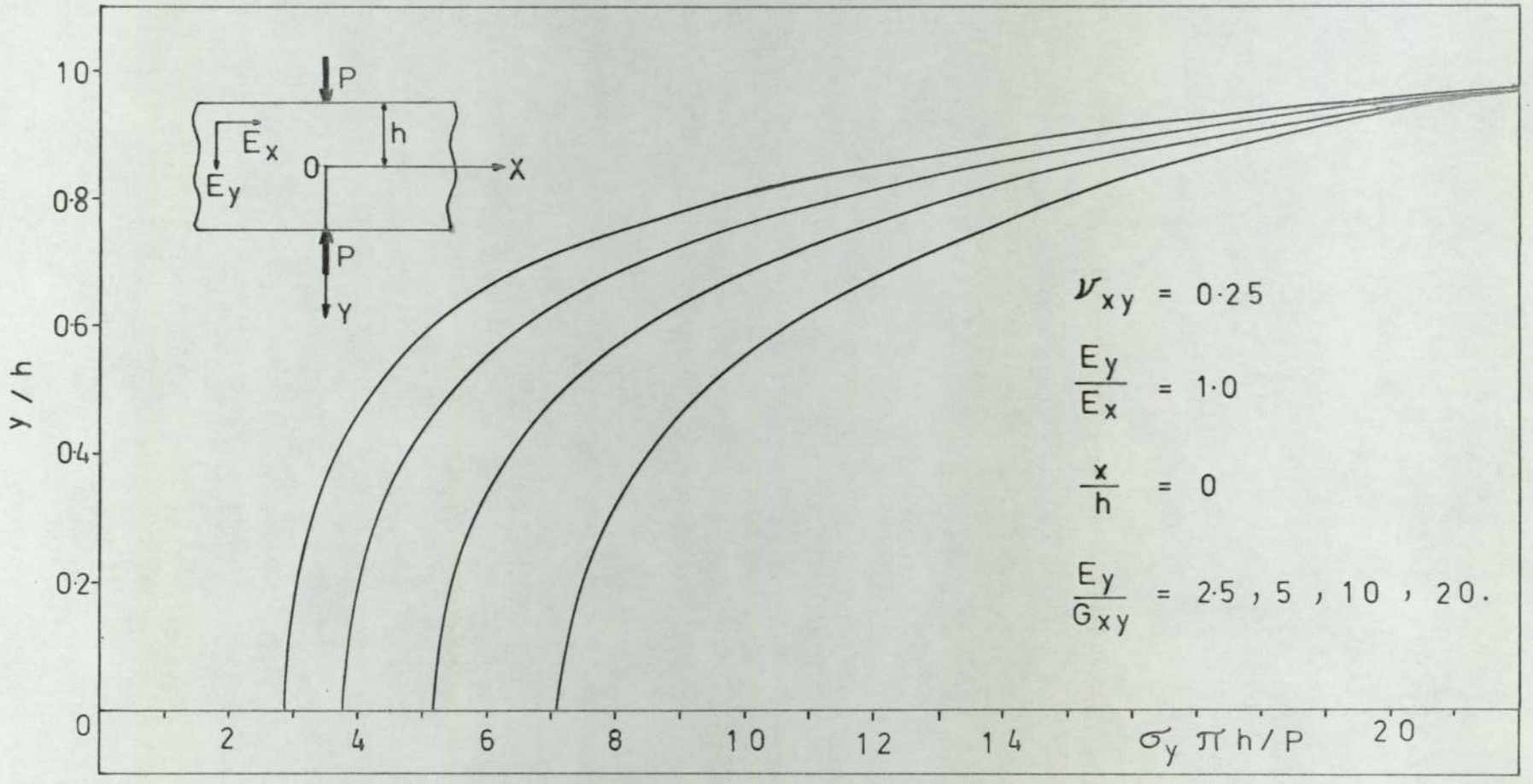

FIG. 7·8 Variation of σ_y with y/h along the Y–axis

$E_y / E_x = 1$

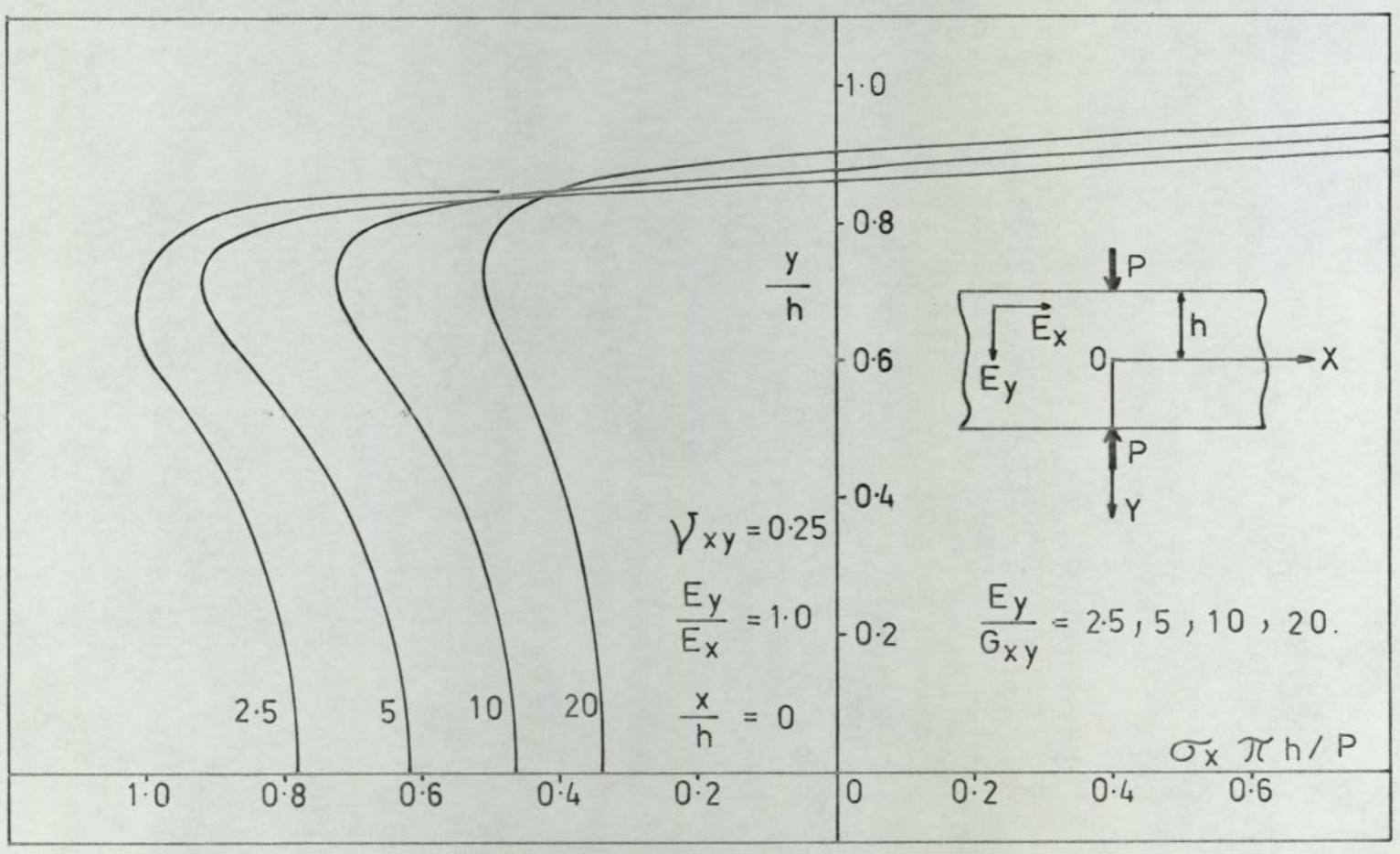

FIG. 7.9 Variation of σ_x with y/h along the Y–axis

$E_y / E_x = 1$

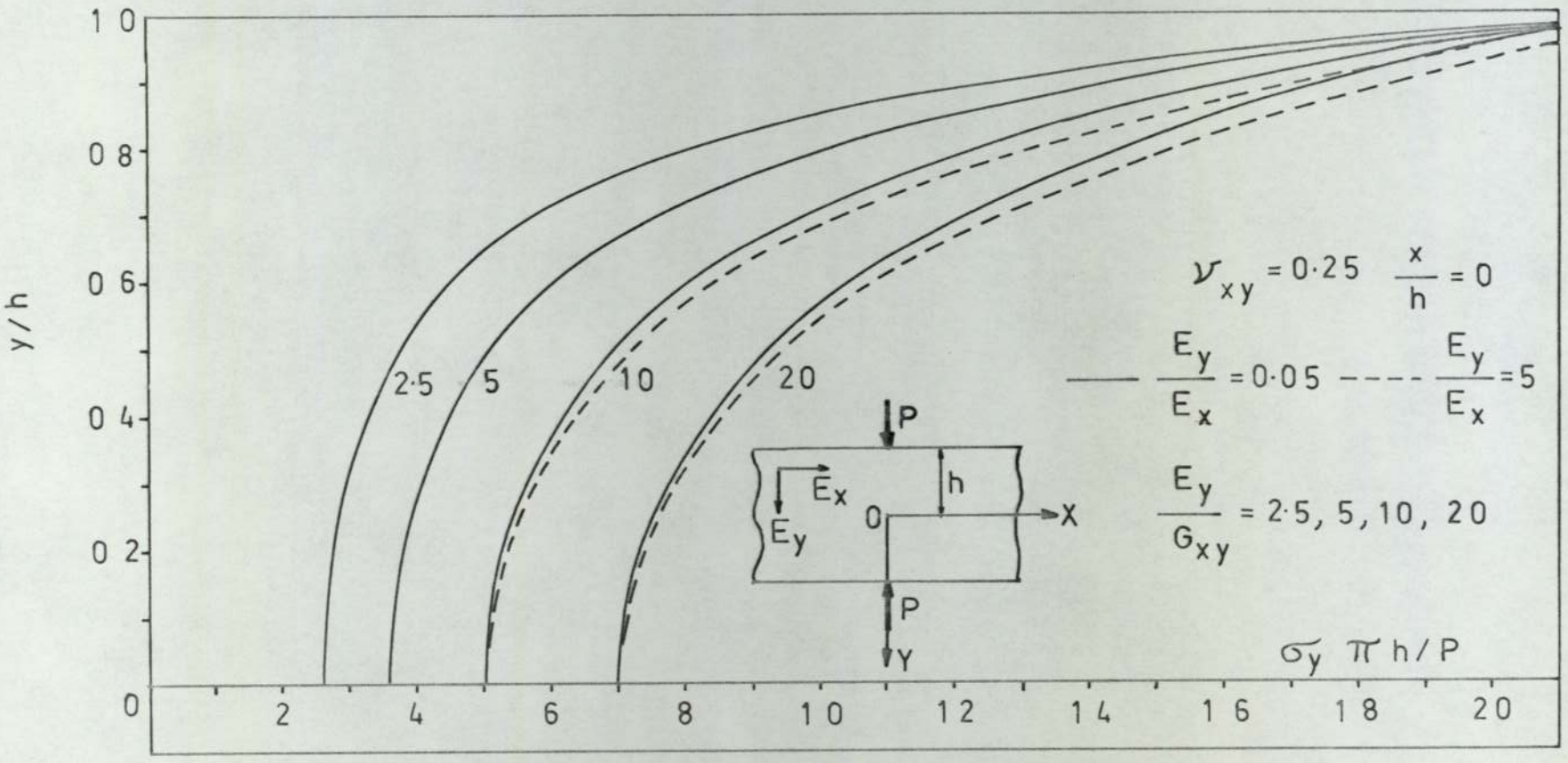

FIG. 7.10 Variation of σ_y with y/h along the Y-axis

$E_y / E_x = 0{\cdot}05, 5$

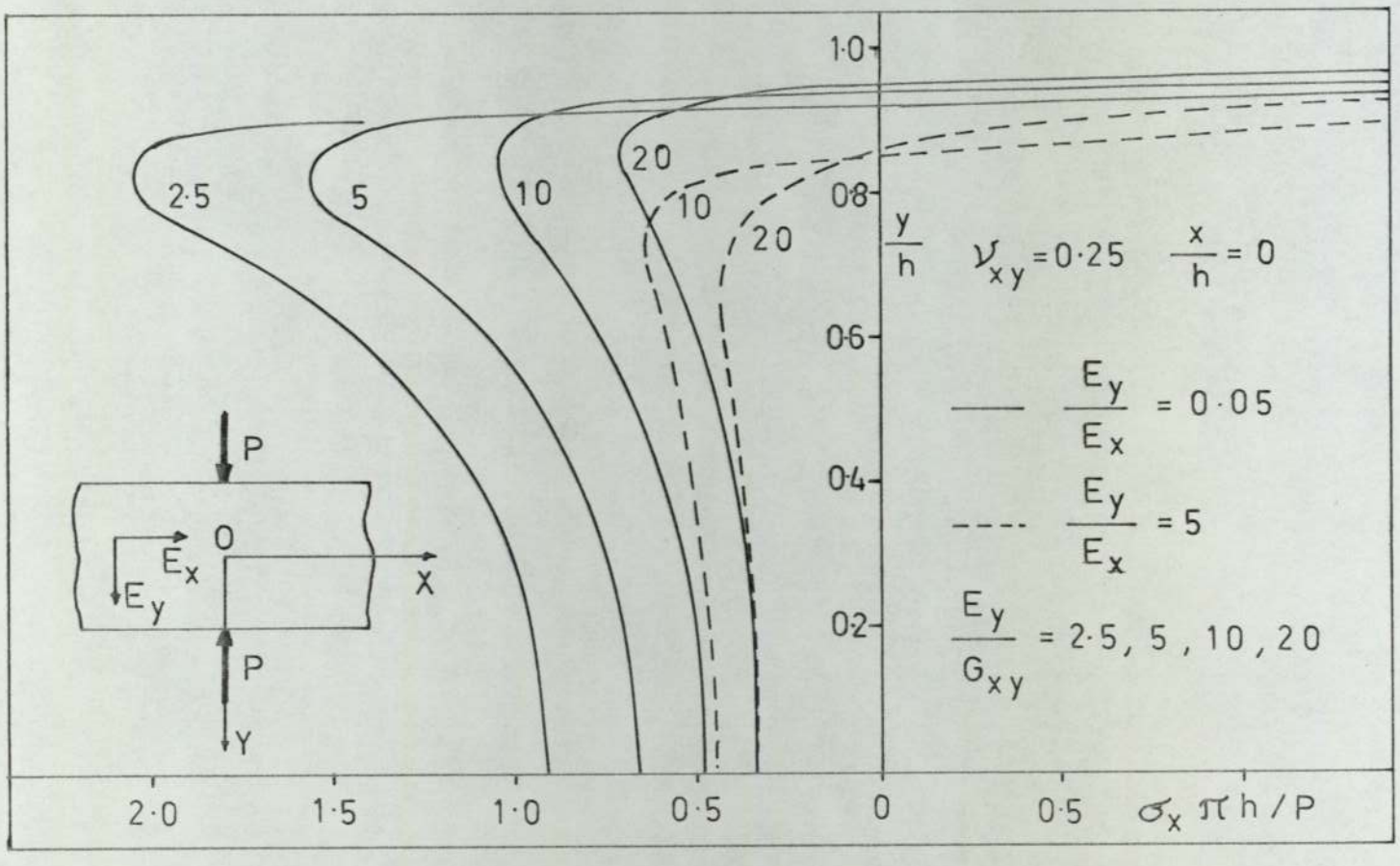

FIG. 7.11 Variation of σ_x with y/h along the Y-axis

$E_y / E_x = 0·05, 5$

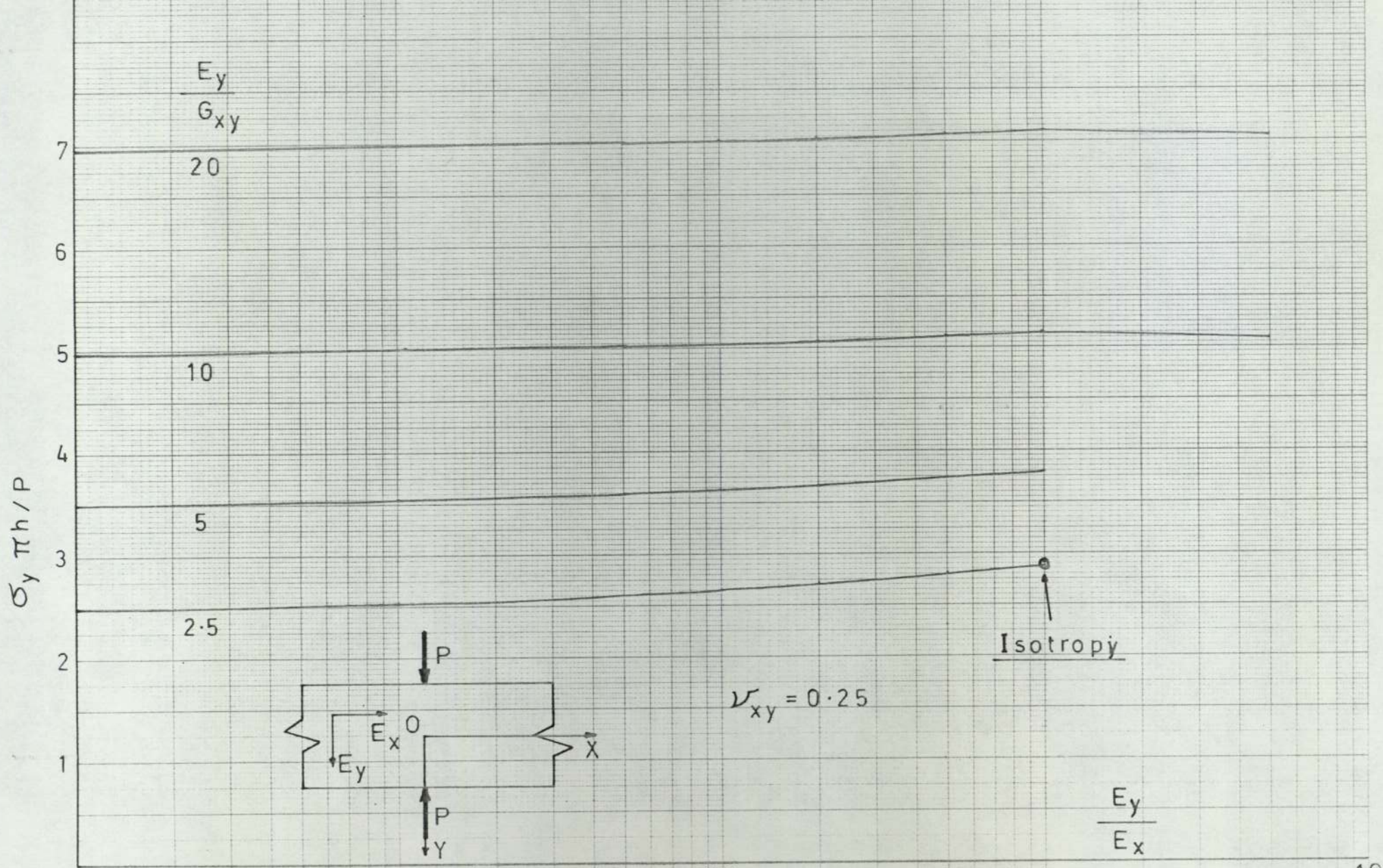

FIG. 7.12 Variation of σ_y at point (0,0) with E_y / E_x

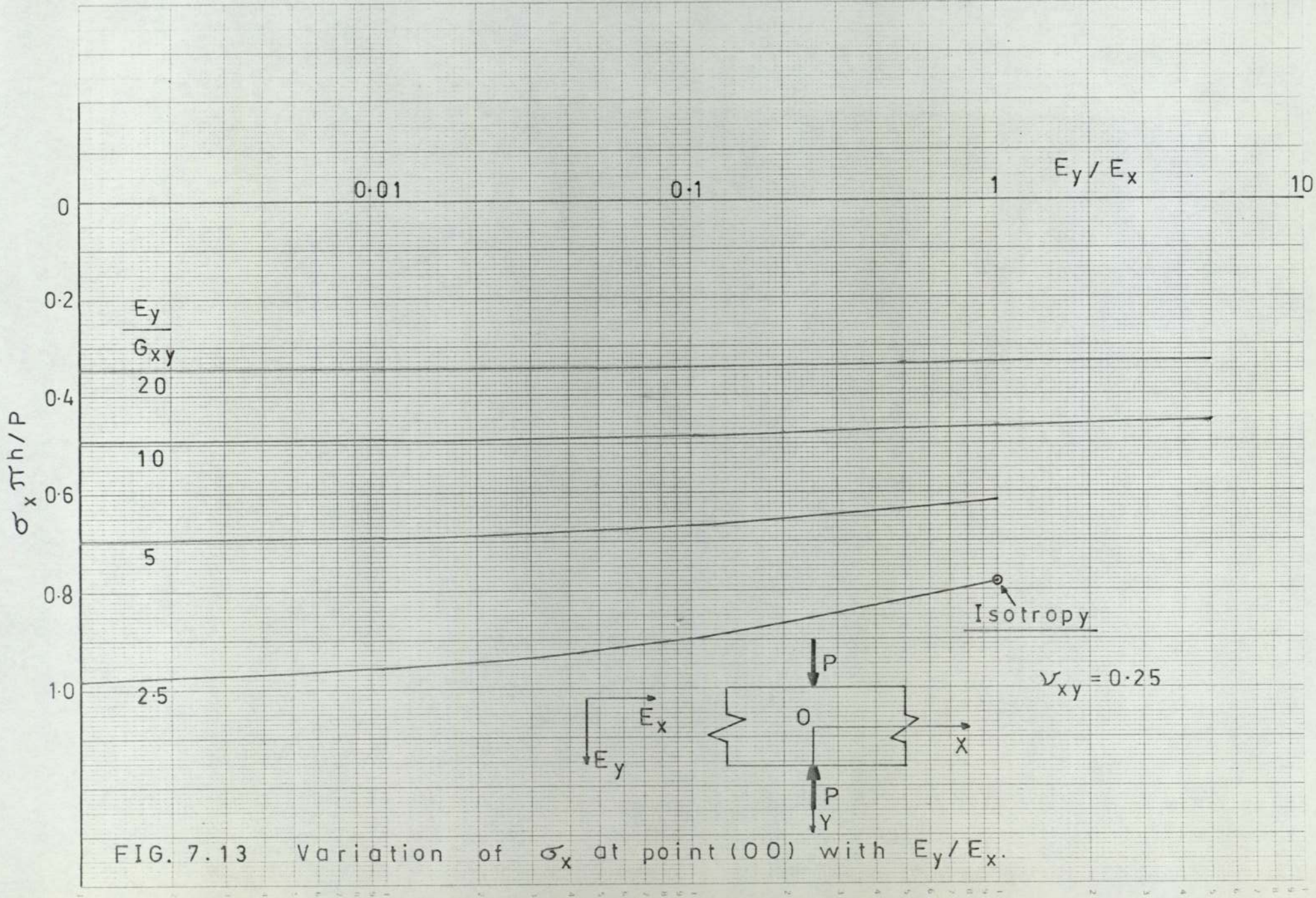

FIG. 7.13 Variation of σ_x at point (00) with E_y / E_x.

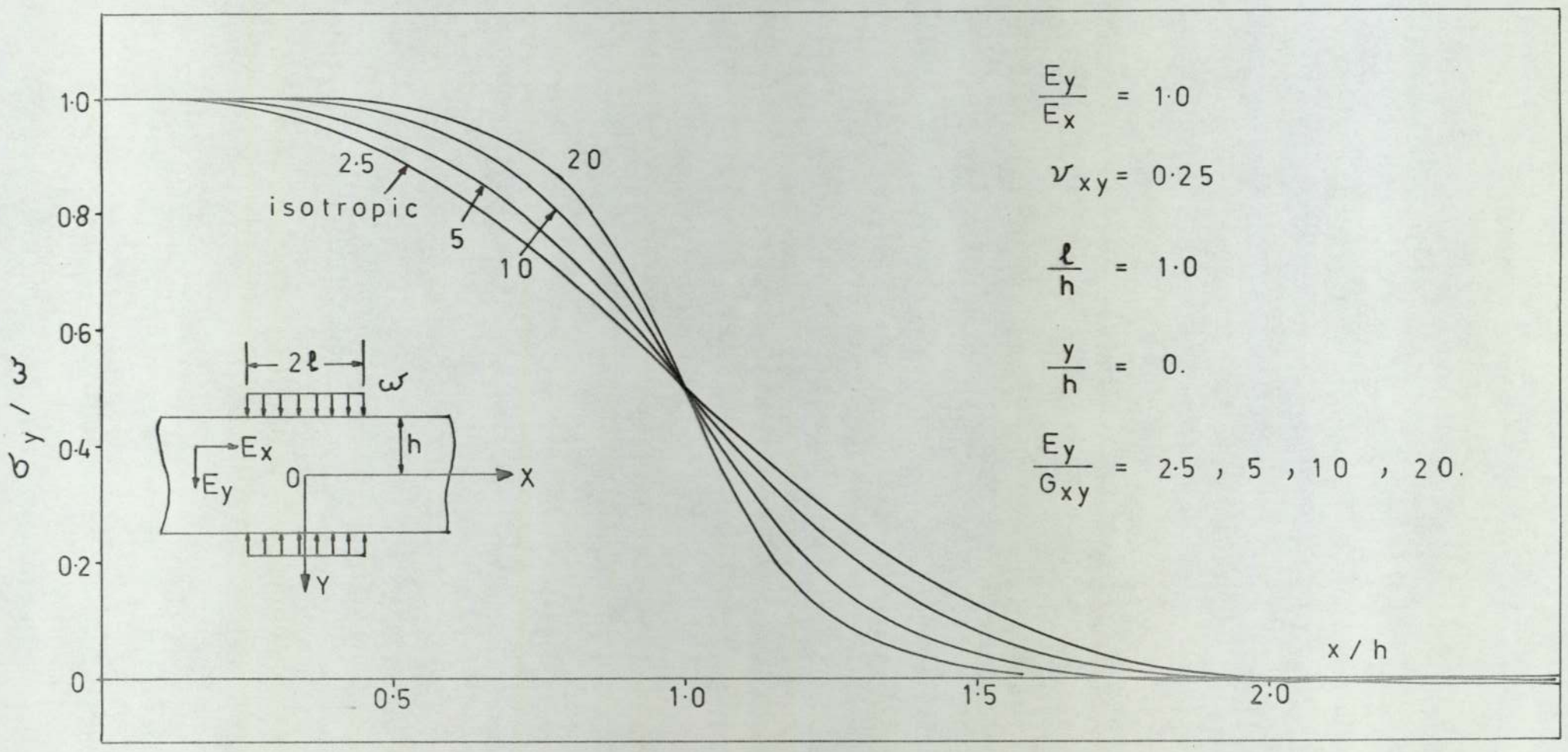

FIG· 7·14 Variation of σ_y with x/h along the x—axis; $E_y / E_x = 1·0$

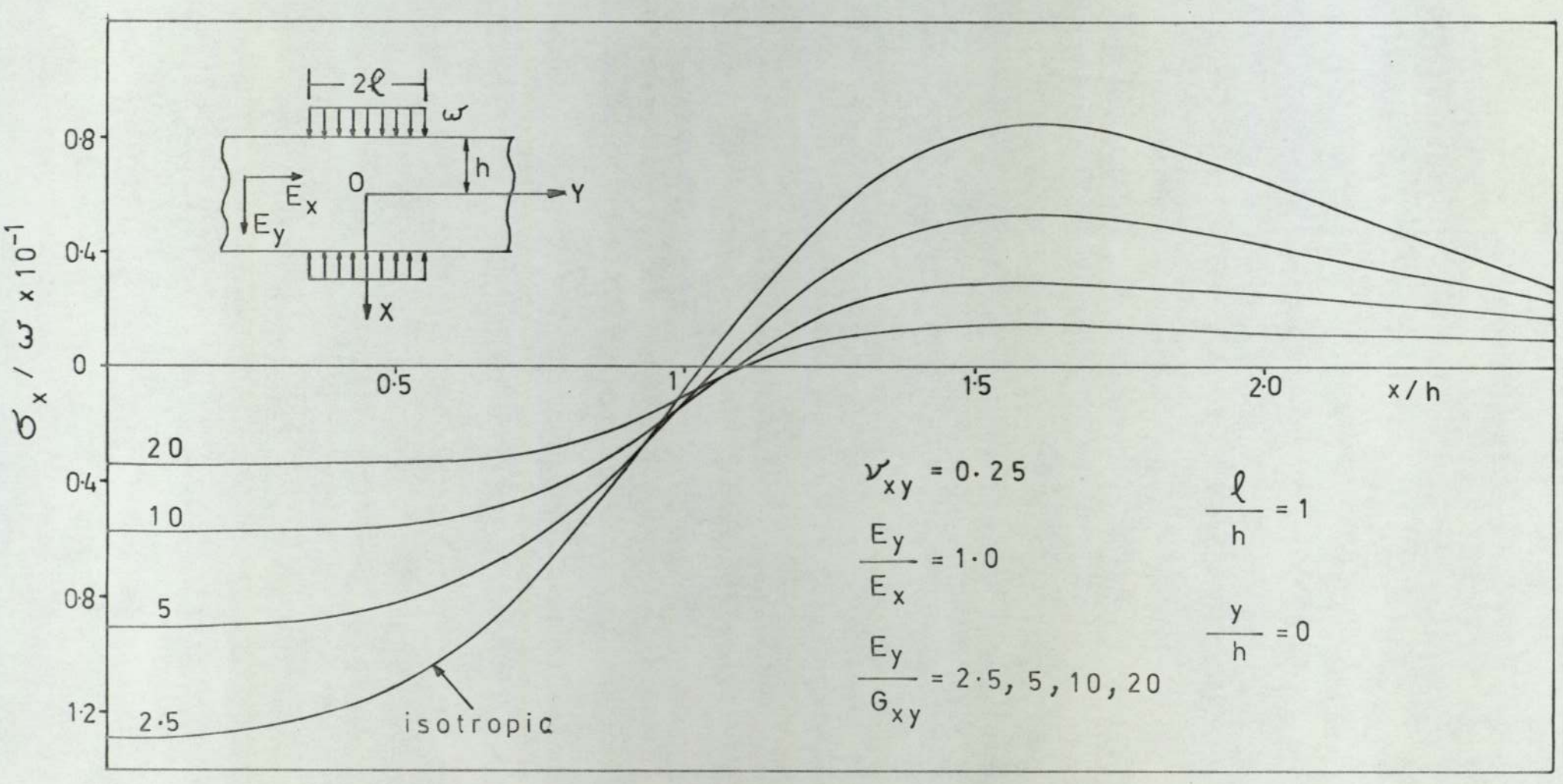

FIG. 7·15 Variation of σ_x with x/h along the X-axis $E_y / E_x = 1$

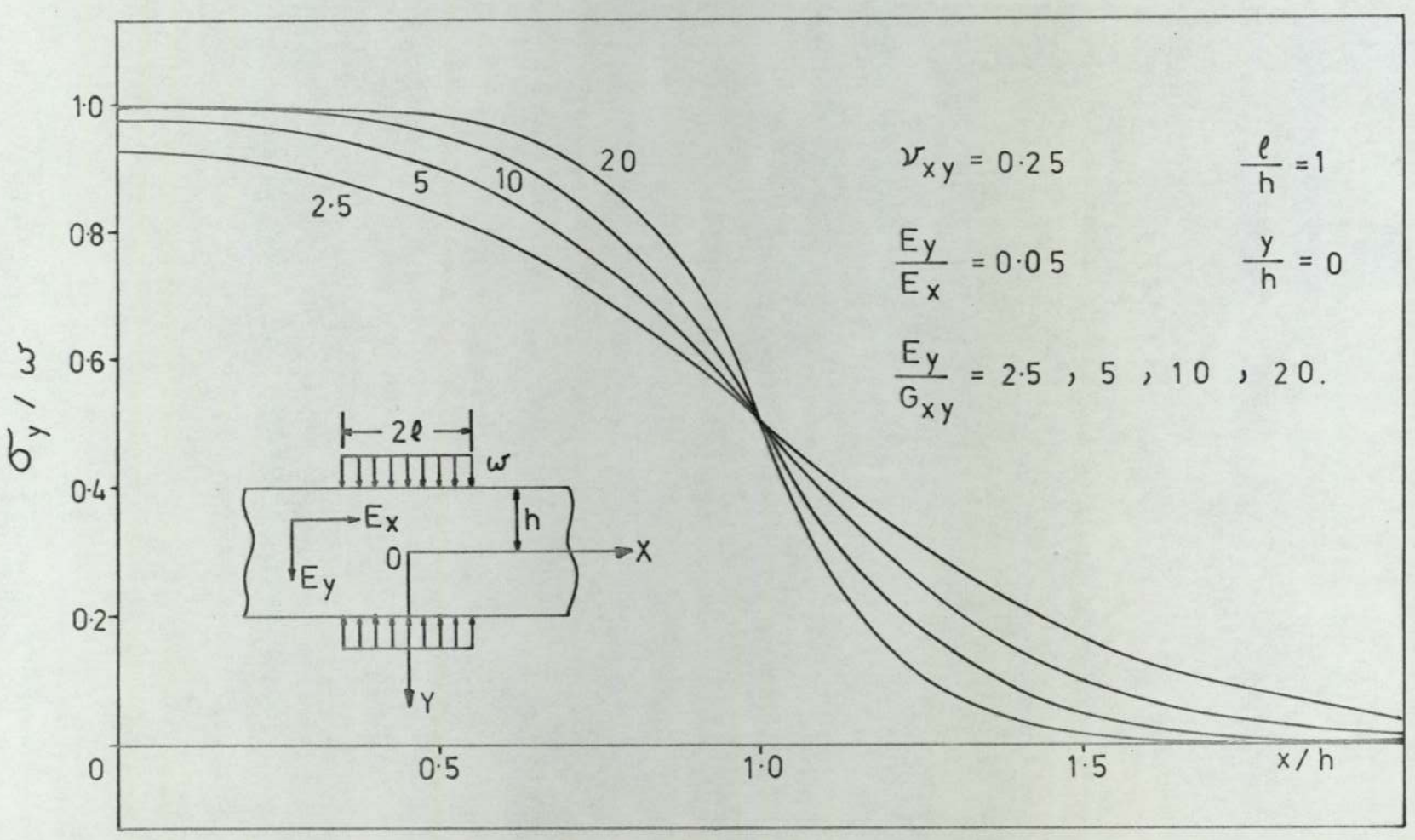

FIG. 7.16 Variation of σ_y with x/h along the X–axis

$E_y / E_x = 0{\cdot}05$

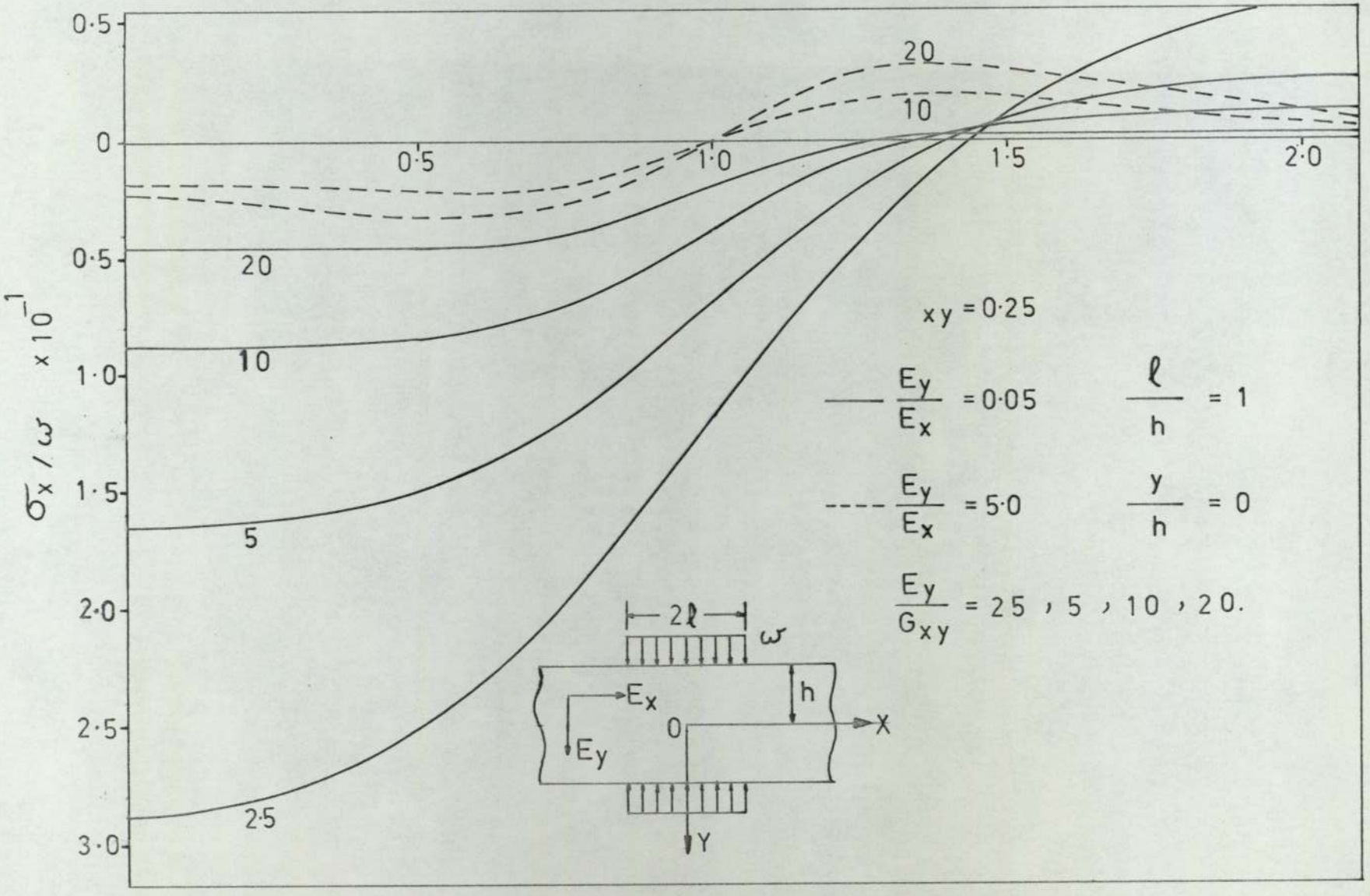

FIG· 7.17 Variation of $\bar{\sigma}$ with x/h along the x axis

$E_y / E_x = 0·05$

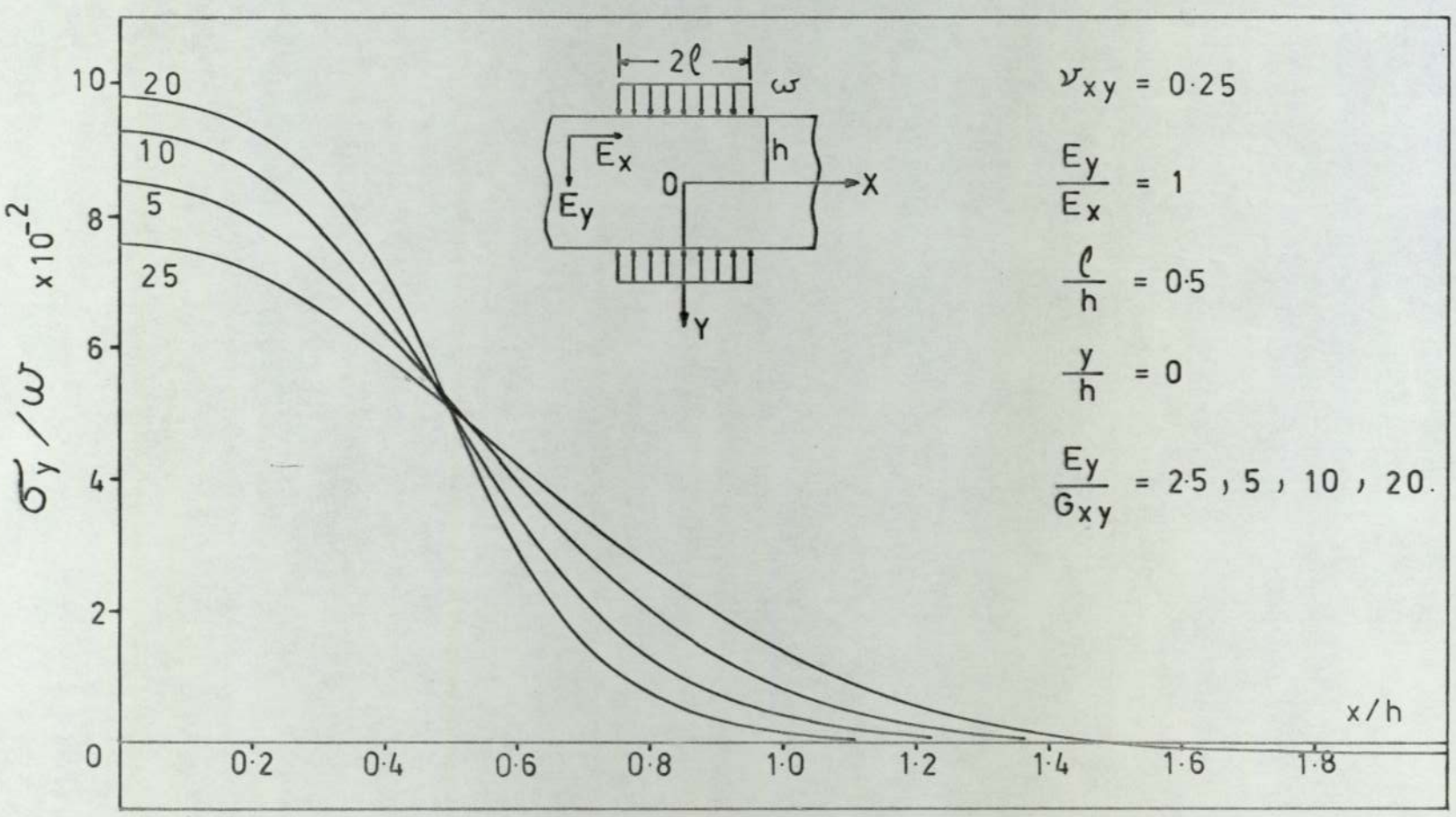

FIG. 7.18 Variation of σ_y with x/h along the X–axis

$E_y / E_x = 1{\cdot}0$

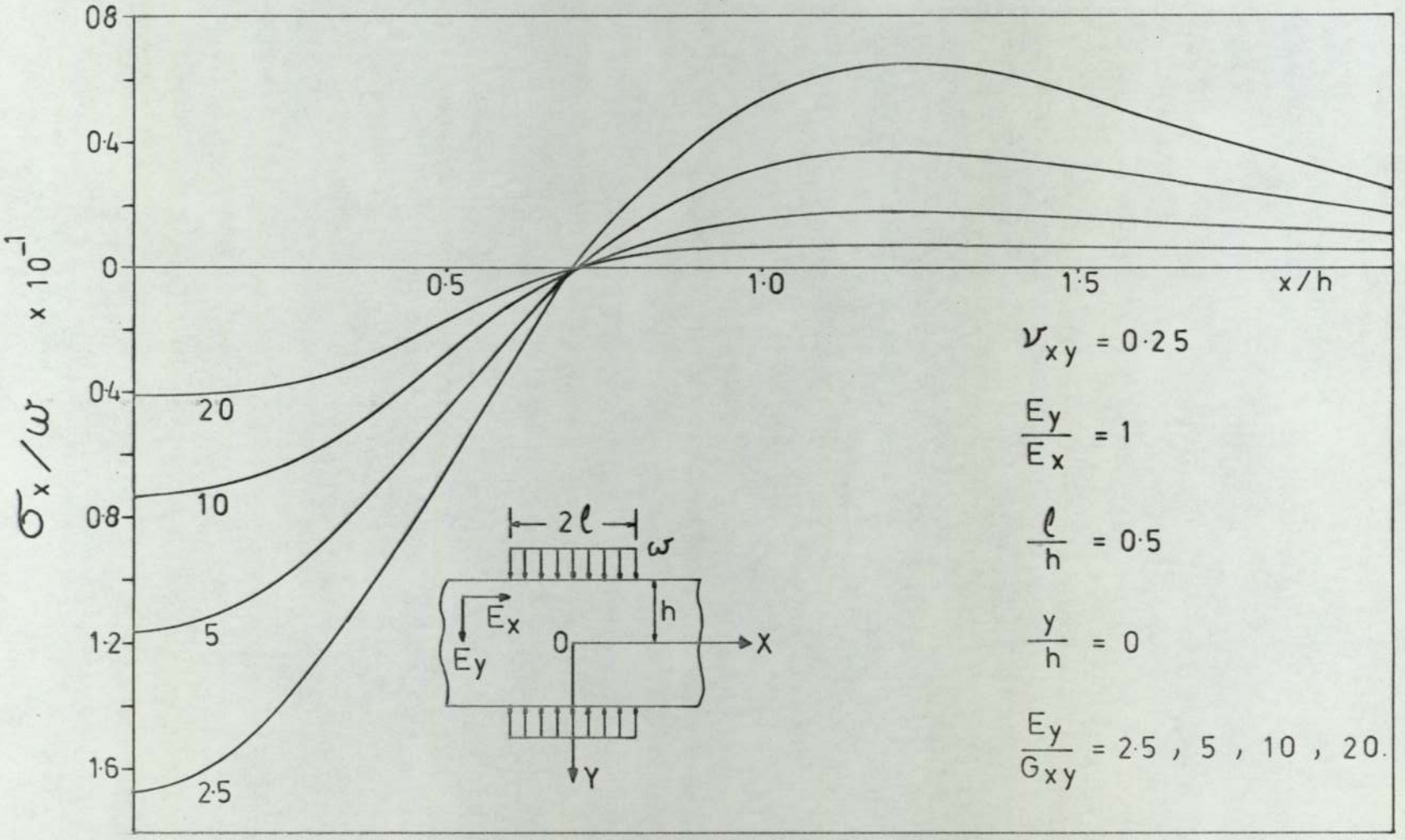

FIG. 7.19 Variation of σ_x with x/h along the X-axis

$E_y/E_x = 1$

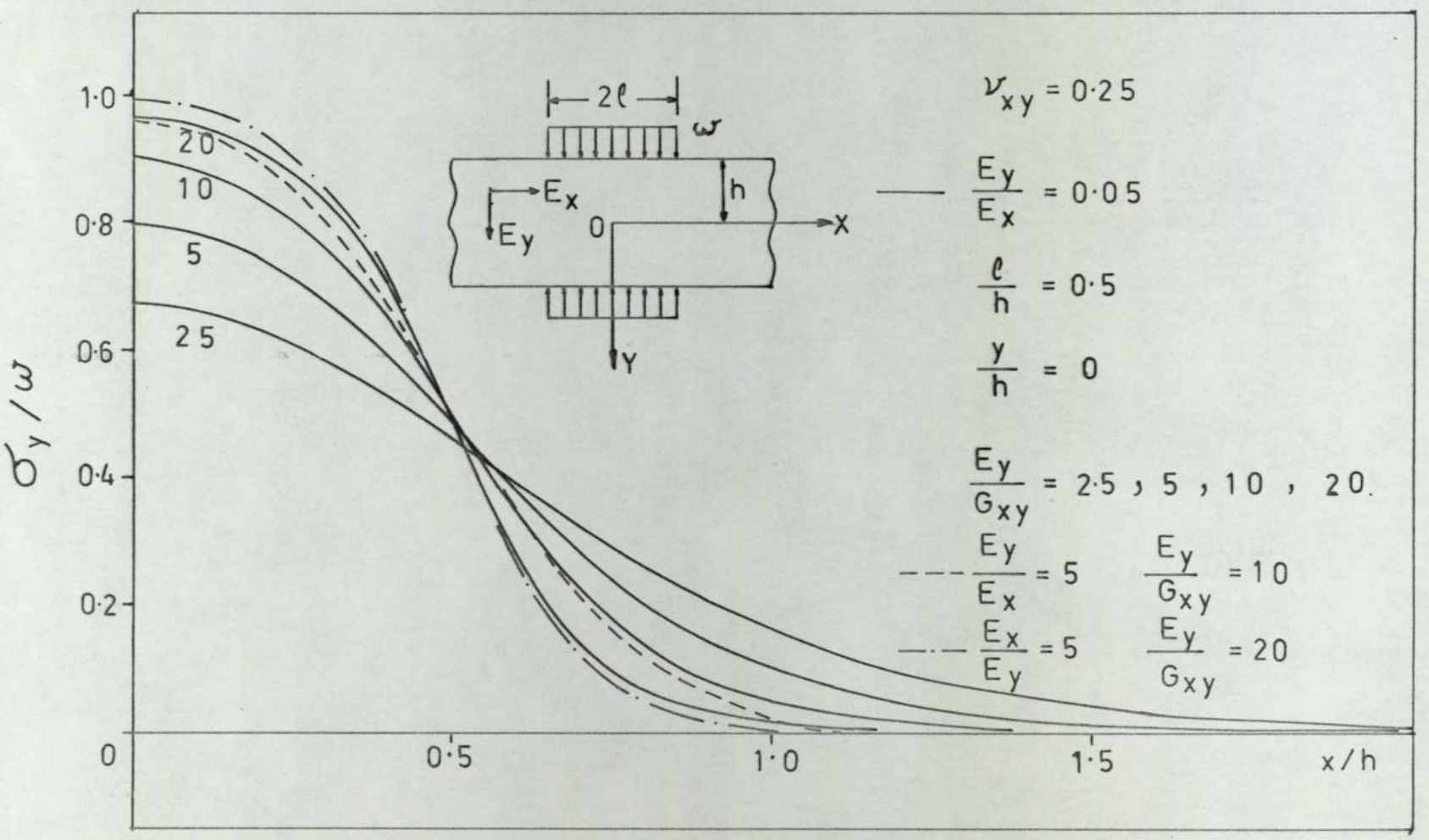

FIG. 7.20 Variation of σ_y with x/h along the X-axis
$E_y / E_x = 0{\cdot}05$ & 5

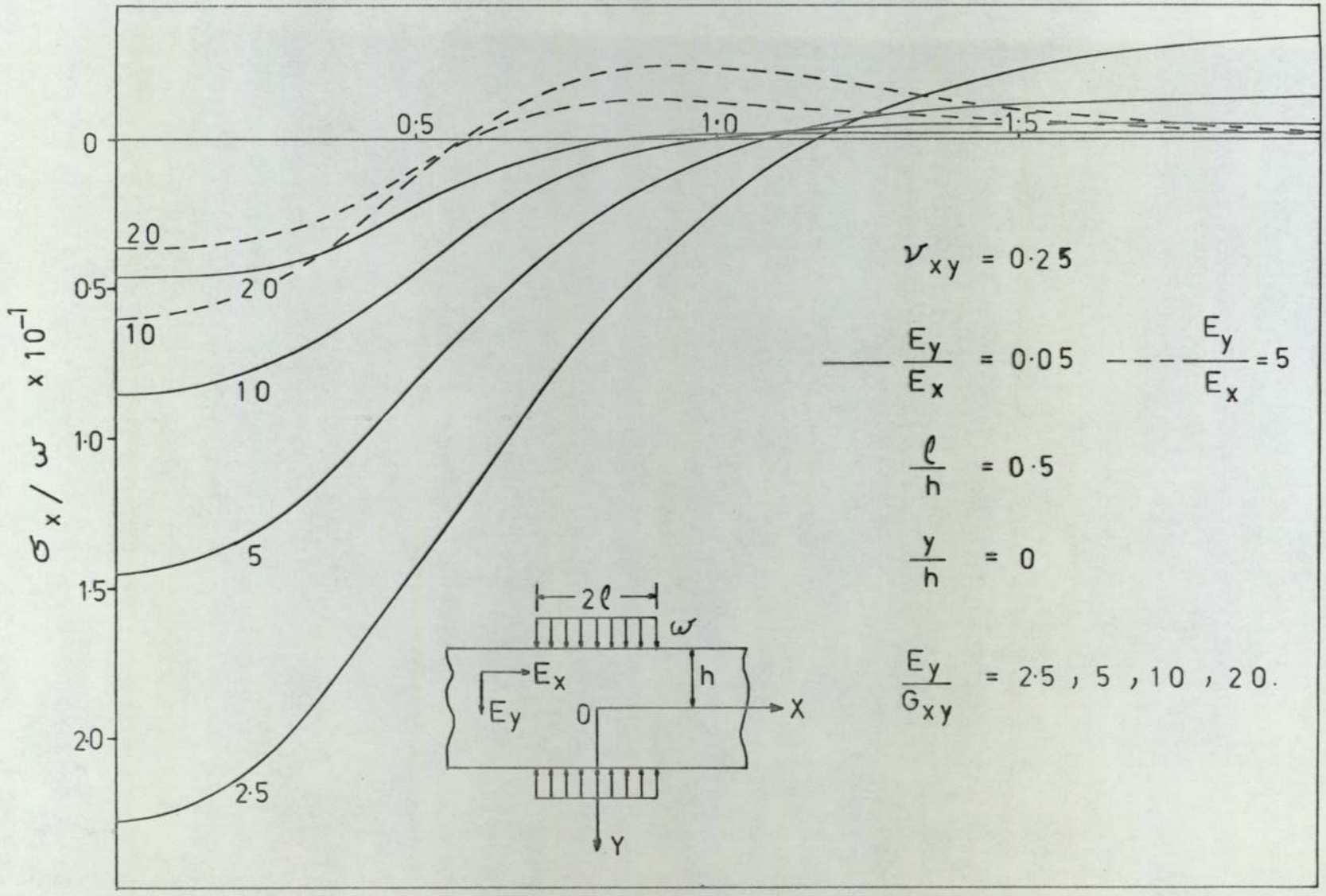

FIG. 7.21 Variation of σ_x with x/h along the X–axis

$E_y / E_x = 0.05, 5$

7.2.4) Conclusions.

From the graphical representation of the results in Fig.7.4-7.21, we can make the following observations:

1) Concentrated force.

The stress σ_y, on the X-axis, diminishes very rapidly with increasing $\bar{x}$ and becomes relatively insignificant for $\bar{x} > 2.5$. The distribution of σ_y is greatly affected by changes in E_y/G_{xy}, but is relatively insensitive to changes in E_y/E_x. In the case of an isotropic material, the distribution of σ_y is in agreement with Biot's (1935) results.

The distribution of σ_x along the X-axis (see Fig.7.5 and 7.7), indicates that if $E_y/E_x \approx 1$, stresses of high magnitude are encountered only for $\bar{x} < 2.5$. If $E_y/E_x << 1$, σ_x does not diminish rapidly with increasing $\bar{x}$. The effect becomes more prominent for small values of E_y/G_{xy}. It can be concluded that the distribution of σ_x along the X-axis, is affected by the magnitude of both ratios E_y/E_x and E_y/G_{xy}.

The maximum stresses (σ_x and σ_y) along the X-axis, are encountered at the origin (0,0). The magnitude of these stresses is mainly governed by the ratio E_y/G_{xy} (see Fig.7.12 and 7.13) and for $E_y/G_{xy} \geq 10$, the stresses may be assumed to be independent of E_y/E_x. If $E_y/G_{xy} < 10$, the magnitude of the stresses is affected by the ratio E_y/E_x, particularly if $E_y/E_x > 0.1$.

The stress distribution (σ_x and σ_y) along the Y-axis, follows the general pattern, with σ_y mainly governed by the magnitude of the ratio E_y/G_{xy}, while σ_x is governed by both ratios E_y/G_{xy} and E_y/E_x.

7.2.4) contd.

2) Uniformly distributed load.

The distribution of σ_y along the X-axis (Fig. 7.14, 7.16, 7.18, 7.20), indicates that, in general, for $\ell/h \leq 1$, σ_y diminishes rapidly with x/h and becomes relatively insignificant for $x/h > 2$. This distribution is mainly governed by the ratio E_y/G_{xy}. Only if $E_y/G_{xy} < 5$, the effects of E_y/E_x become significant.

If $\ell/h = 1$ and $E_y/E_x = 1$, σ_y at the point (0,0) is always equal to the applied pressure, irrespective of the magnitude of E_y/G_{xy}.

The distribution of σ_x along the X-axis is greatly affected by E_y/E_x with σ_x increasing for decreasing values of E_y/E_x. Similar behaviour is observed for decreasing values of E_y/G_{xy}.

7.3) Orthotropic infinite strip subjected to arbitrary loads.

7.3.1) Formulation of the problem.

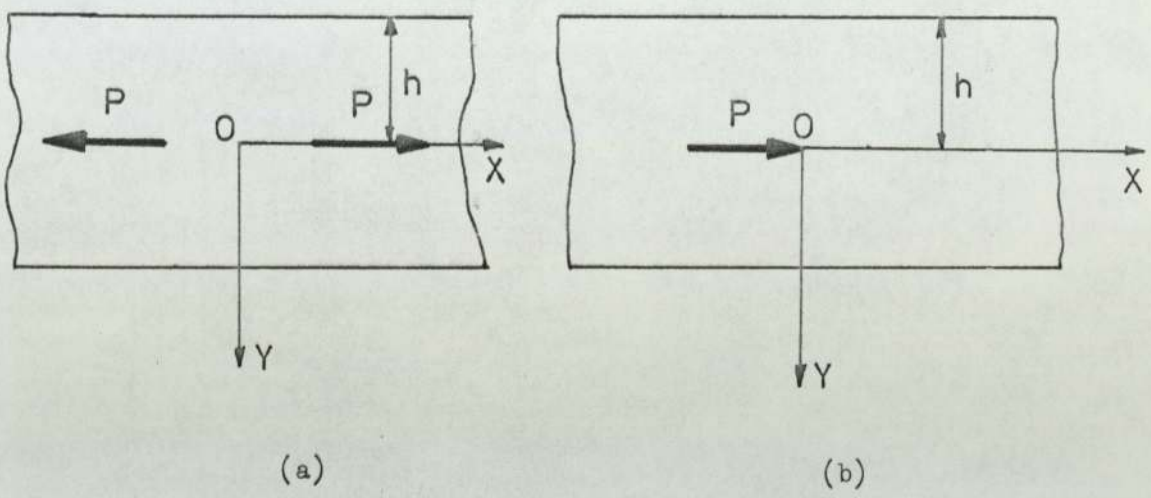

(a) (b)

Fig.7.22

We consider the case of an orthotropic infinite strip, which is subjected to arbitrary load systems, acting on its boundaries or at the interior.

We distinguish between the following two cases:

a) The applied load system is self-equilibrating, so that the stresses diminish with increasing $\bar{x}$ and they tend to zero as $\bar{x} \to \pm \infty$. In addition the resultant moment of the load system about any point of the strip is zero. Such a case of loading is shown in Fig.7.22a.

b) The applied load system is not self-equilibrating, in which case non-zero stresses exist at all points of the strip, even at $x = \pm \infty$. Such a case of loading is shown in Fig.7.22b.

We shall limit our discussion on the former case, that of a self-equilibrating load system.

7.3.2) Method of solution.

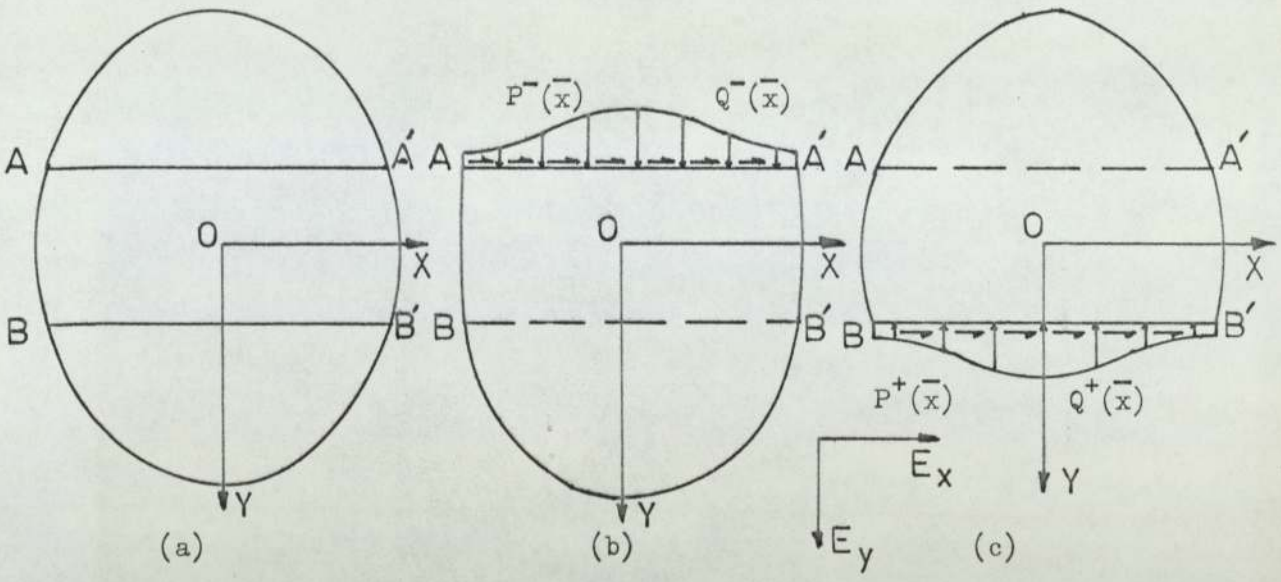

Fig.7.23

A superposition technique is adopted for the purpose of accomplishing the infinite strip solution. This technique involves the superposition of known solutions to the following three problems.

a) The orthotropic strip is assumed to occupy the region AA'B'B of an infinite plane (see Fig.7.23a), where AA' and BB' are parallel to the X-axis of the plane and at distance $\bar{y} = \pm 1$ respectively. The resulting stress field will be referred to as the basic state of stress and the stress components will be denoted by $\overset{o}{\sigma}_x$, $\overset{o}{\sigma}_y$, $\overset{o}{\tau}_{xy}$.

b) The second problem is an orthotrpic half-plane, occupying the region $-\infty < \bar{x} < \infty$, $-1 \leq \bar{y} < \infty$ which is subjected on its boundary to normal and shear stress distributing $P^-(\bar{x})$ and $Q^-(\bar{x})$ respectively (see Fig.7.23 b).

c) The third problem is an orthotropic half-plane, occupying the region $-\infty < \bar{x} < \infty$, $-\infty < \bar{y} \leq 1$ which is subjected on its boundary to normal and shear stress distributions $P^+(\bar{x})$ and $Q^+(\bar{x})$ respectively (see Fig.7.23c).

The resulting stress field from the combination of

7.3.2) contd.

the two half-plane solutions, will be referred to as the corrective state of stress and the stress components will be denoted by σ_x^c, σ_y^c, τ_{xy}^c.

The problem then involves the determination of the functions $P^{\pm}(\bar{x})$ and $Q^{\pm}(\bar{x})$, so that after superposition of the three systems (a), (b), (c), the resulting stress field satisfies the boundary conditions of the infinite strip.

The proposed method for the evaluation of the functions $P^{\pm}(\bar{x})$ and $Q^{\pm}(\bar{x})$, is an extension of the superposition method used by Hetènyi (1960) in the analysis of the isotropic quarter-plane. It involves the successive elimination of the stresses on surfaces AA' and BB', by superposing solutions to suitably loaded half-planes. We shall describe this method in detail in Section 7.3.4.

7.3.3) Basic state of stress.

We assume that the basic state of stress can be uniquely determined from the theory of the infinite plane and that the stress components are given by:

$$\left[\sigma_x^o ; \sigma_y^o ; \tau_{xy}^o \right] = \frac{\psi}{y} \left[S_x^o ; S_y^o ; S_{xy}^o \right], \qquad 7.3\text{-}1$$

where ψ is a load parameter.

Furthermore, the normal and shear stress distributions on surfaces AA' and BB' (i.e. $\bar{y} = \pm 1$), due to the basic state of stress, are denoted by $F^{\pm}(\bar{x})$ and $G^{\pm}(\bar{x})$, where

$$\left[F^-(\bar{x}) ; G^-(\bar{x}) \right] = \frac{\psi}{h} \left[S_y^o ; S_{xy}^o \right]_{\bar{x},\bar{y} = -1},$$

$$\left[F^+(\bar{x}) ; G^+(\bar{x}) \right] = \frac{\psi}{h} \left[S_y^o ; S_{xy}^o \right]_{\bar{x},\bar{y} = +1}. \qquad 7.3\text{-}2$$

7.3.4) Corrective state of stress.

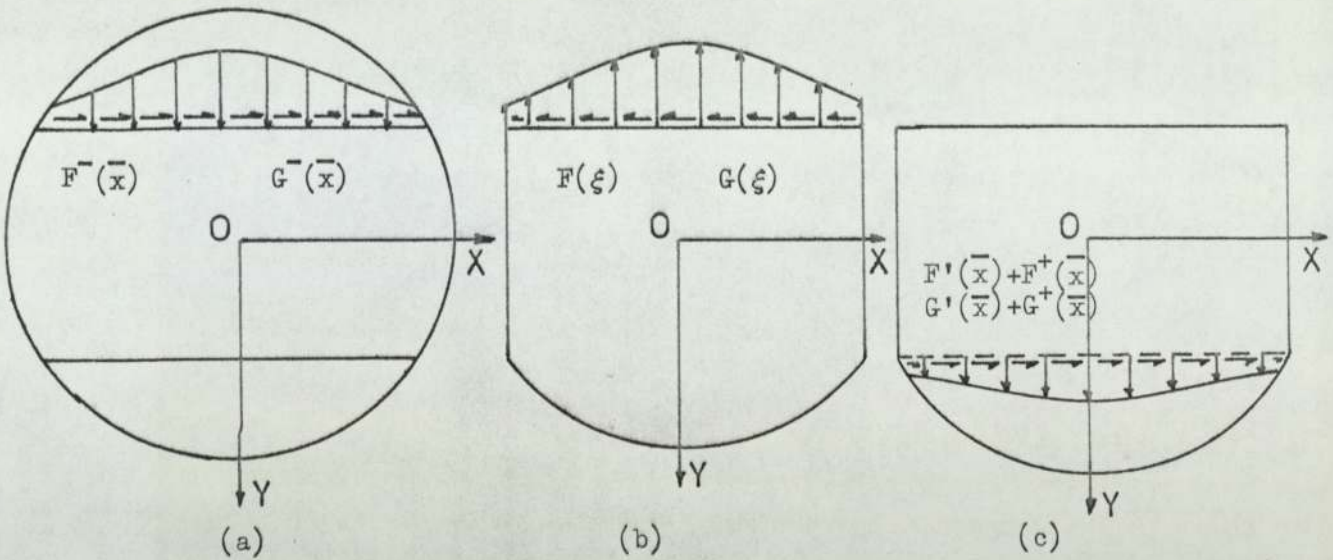

Fig.7.24

Step 1. In order to eliminate the stresses ($F^-(\bar{x})$ and $G^-(\bar{x})$) on the surface AA' of the infinite plane due to the basic state of stress (see Fig.7.24a), we consider a half-plane ($-1 \leq \bar{y} < \infty$) which is subjected on its boundary to normal and shear stress distributions $F(\xi)$ and $G(\xi)$ respectively, where

$$F(\xi) = - F^-(\bar{x}),$$
$$G(\xi) = - G^-(\bar{x}). \qquad 7.3\text{-}3$$

(see Fig.7.24b).

Then, the combination of the solution to the half-plane problem together with the solution to the infinite plane, renders the surface AA' free of traction, but in doing so, gives rise to normal and shear stresses $F'(\bar{x})$, $G'(\bar{x})$ respectively on surface BB'($\bar{y} = +1$), where

7.3.4) contd.

$$F'(\bar{x}) = (k_1+k_2)\left\{ \int_{-\infty}^{\infty} \frac{8F(\xi)d\xi}{D(\xi)} + k_1k_2 \int_{-\infty}^{\infty} \frac{4G(\xi)(\bar{x}-\xi)d\xi}{D(\xi)} \right\}, \qquad 7.3\text{-}4a$$

$$G'(\bar{x}) = (k_1+k_2)\left\{ \int_{-\infty}^{\infty} \frac{4F(\xi)(\bar{x}-\xi)d\xi}{D(\xi)} + k_1k_2 \int_{-\infty}^{\infty} \frac{2G(\xi)(\bar{x}-\xi)^2 d\xi}{D(\xi)} \right\},$$

(see equations 4.2-4 and 4.3-3)

and

$$D(\xi) = \left[k_1^2(\bar{x}-\xi)^2 + 4\right]\left[k_2^2(\bar{x}-\xi)^2 + 4\right]. \qquad 7.3\text{-}4b$$

Therefore, the problem reduces to a half-plane $-1 \leq \bar{y} < \infty$, $-\infty < \bar{x} < \infty$, with a traction free boundary (see Fig.7.24c), and with total stresses on the surface BB' given by:

Normal stresses : $F'(\bar{x}) + F^+(\bar{x})$, $G'(\bar{x}) + G'(\bar{x})$. 7.3-5

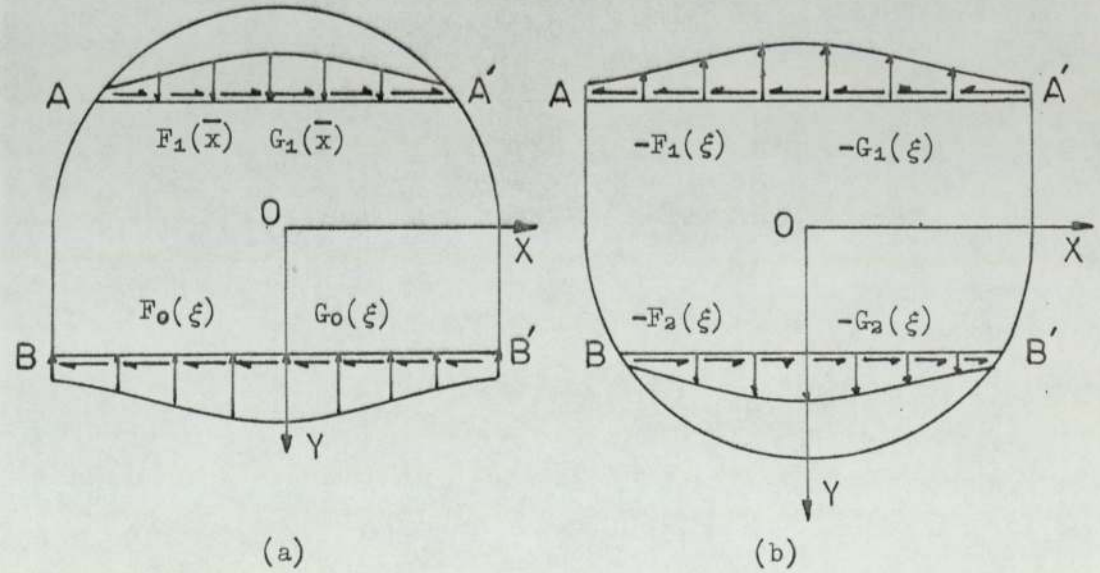

Fig.7.25.

Step 2. In order to eliminate the stresses on the surface BB' ($\bar{y} = 1$) of the half-plane (see Fig.7.24c), we superpose the solution to a half-plane ($-\infty < \bar{x} < \infty$, $-\infty < \bar{y} \leq 1$), which is subjected along its boundary to normal and shear stress

7.3.4) contd.

distributions $F_o(\xi)$ and $G_o(\xi)$ respectively (see Fig.7.25a), where

$$F_o(\xi) = -\left[F'(\bar{x}) + F^+(\bar{x})\right],$$
$$G_o(\xi) = -\left[G'(\bar{x}) + G^+(\bar{x})\right]. \qquad 7.3\text{-}6$$

The combination will render the surface BB' free of traction, but will give rise to normal and shear stresses $F_1(\bar{x})$, $G_1(\bar{x})$ respectively, on surface AA', where

$$F_1(\bar{x}) = (k_1+k_2)\left\{\int_{-\infty}^{\infty}\frac{8F_o(\xi)d\xi}{D(\xi)} - k_1k_2\int_{-\infty}^{\infty}\frac{4G_o(\xi)(\bar{x}-\xi)d\xi}{D(\xi)}\right\},$$
$$7.3\text{-}7$$
$$G_1(\bar{x}) = (k_1+k_2)\left\{-\int_{-\infty}^{\infty}\frac{4F_o(\xi)(\bar{x}-\xi)d\xi}{D(\xi)} + k_1k_2\int_{-\infty}^{\infty}\frac{2G_o(\xi)(\bar{x}-\xi)^2d\xi}{D(\xi)}\right\}.$$

Step 3. In order to eliminate the stresses $F_1(\bar{x})$ and $G_1(\bar{x})$ from the surface AA' (see Fig.7.25a), we superpose the solution to a half-plane ($-\infty < \bar{x} < \infty$, $-1 \leq \bar{y} < \infty$), which is subjected along its boundary to normal and shear stress distributions $-F_1(\xi)$ and $-G_1(\xi)$ respectively (see Fig.7.25b). This will give rise to stresses $-F_2(\bar{x})$ and $-G_2(\bar{x})$ on the surface BB', where

$$F_2(\bar{x}) = (k_1+k_2)\left\{\int_{-\infty}^{\infty}\frac{8F_1(\xi)d\xi}{D(\xi)} + k_1k_2\int_{-\infty}^{\infty}\frac{4G_1(\xi)(\bar{x}-\xi)d\xi}{D(\xi)}\right\},$$
$$7.3\text{-}8$$
$$G_2(\bar{x}) = (k_1+k_2)\left\{\int_{-\infty}^{\infty}\frac{4F_1(\xi)(\bar{x}-\xi)d\xi}{D(\xi)} + k_1k_2\int_{-\infty}^{\infty}\frac{2G_1(\xi)(\bar{x}-\xi)^2d\xi}{D(\xi)}\right\}.$$

It is now evident that the techniques outlined in Steps 2 and 3 have to be repeatedly applied in order to satisfy traction boundary conditions on the surfaces AA' and BB'. After an infinite number of reversals, the total loads

7.3.4) contd.

applied on AA' and BB' are:

a) On AA' ($\bar{y} = -1$)

$$P^-(\bar{x}) = -F^-(\bar{x}) - \sum_{m = 1,3,5\ldots}^{\infty} F_m(\bar{x}),$$

$$Q^-(\bar{x}) = -G^-(\bar{x}) - \sum_{m = 1,3,5\ldots}^{\infty} G_m(\bar{x}), \qquad 7.3\text{-}9a$$

b) On BB' ($\bar{y} = 1$)

$$P^+(\bar{x}) = \sum_{m = 0,2,4\ldots}^{\infty} F_m(\bar{x}),$$

$$Q^+(\bar{x}) = \sum_{m = 0,2,4\ldots}^{\infty} G_m(\bar{x}), \qquad 7.3\text{-}9b$$

where

$$F_{m+1}(\bar{x}) = (k_1+k_2)\left\{ \int_{-\infty}^{\infty} \frac{8F_m(\xi)d\xi}{D(\xi)} + k_1k_2\Omega \int_{-\infty}^{\infty} \frac{4G_m(\xi)(\bar{x}-\xi)d\xi}{D(\xi)} \right\},$$

$$G_{m+1}(\bar{x}) = (k_1+k_2)\left\{ \Omega \int_{-\infty}^{\infty} \frac{4F_m(\xi)(\bar{x}-\xi)d\xi}{D(\xi)} + k_1k_2 \int_{-\infty}^{\infty} \frac{2G_m(\xi)(\bar{x}-\xi)^2 d\xi}{D(\xi)} \right\}. \qquad 7.3\text{-}10$$

where $\Omega = -(-1)^m$.

The stress components for the corrective state of stress are then given by:

$$\left[\sigma_x^c \; ; \; \sigma_y^c \; ; \; \tau_{xy}^c\right] = \frac{\psi}{h}(k_1+k_2)\left\{ \right.$$

$$\int_{-\infty}^{\infty} \frac{P^-(\xi)}{D^+(\xi)} \left[(\bar{x}-\xi)(1+\bar{y}) \; ; \; (1+\bar{y})^3 \; ; \; (\bar{x}-\xi)(1+\bar{y})^2 \right] d\xi$$

$$+k_1k_2 \int_{-\infty}^{\infty} \frac{Q^-(\xi)}{D^+(\xi)} \left[(\bar{x}-\xi)^3 \; ; \; (\bar{x}-\xi)^3(1+\bar{y})^2 \; ; \; (\bar{x}-\xi)^2(1+\bar{y}) \right] d\xi$$

7.3.4) contd.

$$+\int_{-\infty}^{\infty} \frac{P^{+}(\xi)}{D^{-}(\xi)} \left[(\bar{x}-\xi)(1-\bar{y}) \quad ; \quad (1-\bar{y})^{3} \; ; -(\bar{x}-\xi)(1-\bar{y})^{2} \right] d\xi$$

$$+k_1 k_2 \int_{-\infty}^{\infty} \frac{Q^{+}(\xi)}{D^{-}(\xi)} \left[-(\bar{x}-\xi)^{3} \quad ; \; -(\bar{x}-\xi)(1-\bar{y})^{2} \; ; (\bar{x}-\xi)^{2}(1-\bar{y} \right] d\xi \Bigg\},$$

7.3-11a

where

$$D^{\pm}(\xi) = \left[k_1^{2}(\bar{x}-\xi)^{2}+(1\pm\bar{y})^{2} \right] \left[k_2^{2}(\bar{x}-\xi)^{2}+(1\pm\bar{y})^{2} \right]. \qquad 7.3\text{-}11b$$

The total stresses at any point of the infinite strip due to the applied arbitrary load can be obtained by a summation of the corresponding stress components due to the basic and the corrective states of stress:

$$\left[\sigma_x \; ; \; \sigma_y \; ; \; \tau_{xy} \right] = \frac{\psi}{h} \left\{ \left[\sigma_x^{o} \; ; \; \sigma_y^{o} \; ; \; \tau_{xy}^{o} \right] + \left[\sigma_x^{c} \; ; \; \sigma_y^{c} \; ; \; \tau_{xy}^{c} \right] \right\}. \qquad 7.3\text{-}12$$

7.3.5) Numerical results.

The method of solution developed in the previous sections, was employed to obtain numerical results for the stresses which are induced in an infinite orthotropic strip by the following self-equilibrating loading systems:

a) Two equal and opposite concentrated forces, acting in the X-direction at points $\bar{x} = \pm 0.2$, $\bar{y} = 0$ (see Fig.7.26a).

b) Two equal and opposite concentrated forces, acting in the Y-direction at points $\bar{x} = 0$, $\bar{y} = \pm 0.5$ (see Fig.7.26b).

The evaluation of the stresses was accomplished in two steps.

Step 1, involved the determination of the functions $F_m(\bar{x})$, $G_m(\bar{x})$, by numerical evaluation of the integrals in equation 7.3-10, using Simpson's rule. The numerical integration was carried out on a logarithmic scale, using 268 slices between the limits -40 and +40. Due to the geometrical and loading symmetry of the problems considered, the function $P^{\pm}(\bar{x})$ and $Q^{\pm}(\bar{x})$ should satisfy the following conditions:

$$P^{+}(\bar{x}) = P^{-}(\bar{x}) \text{ and } Q^{+}(\bar{x}) = -Q^{-}(\bar{x}). \qquad 7.3\text{-}13$$

This condition was used as a criterion for the number of load reversals to be carried out. It was found, that with 9 reversal of load, $P^{+}(\bar{x})$ was equal to $P^{-}(\bar{x})$ to within an accuracy of $\pm$ 0.2%, and, $|Q^{+}(\bar{x})|$ was equal to $|Q^{-}(\bar{x})|$ to within an accuracy of 0.1%. At $\bar{x} = \pm 40$, the magnitude of $P^{\pm}(\bar{x})$ was 0.4% of its maximum value at $\bar{x} = 0$, whereas $Q^{\pm}(\bar{x})$ was 5% of its maximum value at $\bar{x} \approx \pm 0.38$.

Step 2, involved the evaluation of the stresses

7.3.5) contd.

at various points of the infinite strip, due to the corrective and the basic states of stress.

With regard to the corrective state of stress, the boundary loads $\overset{\pm}{P}(\bar{x})$ and $\overset{\pm}{Q}(\bar{x})$ were considered as a series of partially distributed uniform loads of variable width, instead of as a series of concentrated forces. This resulted in a better representation of the boundary loads and facilitated accurate evaluation of the stresses at points near the boundaries $\bar{y} = \pm 1$ of the infinite strip.

With regard to the basic state of stress, the stress components were determined using the theory of the infinite orthotropic plane (see Section 3.3).

7.3.6) Presentation of results.

In both problems considered, the infinite strip is assumed to consist of an orthotropic elastic material, which has the following hypothetical properties:

$$\frac{E_y}{E_x} = 0.05, \quad \frac{E_y}{G_{xy}} = 2.5, \quad \nu_{xy} = 0.25,$$

and

$$k_1 = 1.5667 \quad , \quad k_2 = 0.1427.$$

Numerical results are presented for the distributions of stress (σ_x, σ_y, τ_{xy}), on cross sections at various distances from the origin of the coordinate axes and are shown in Fig.7.27-7.32. Due to the symmetry of the stress distribution in the two problems, only the first quadrant is considered.

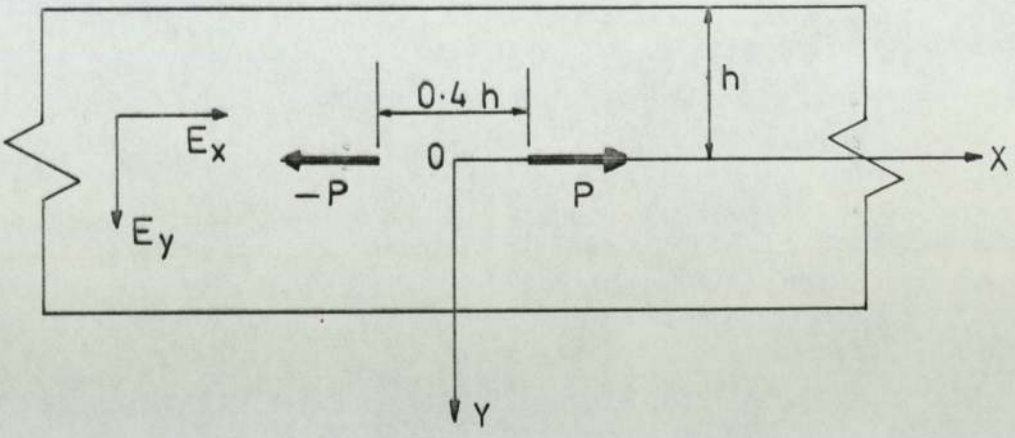

FIG· 7·26a Infinite strip; longitudinal loads.

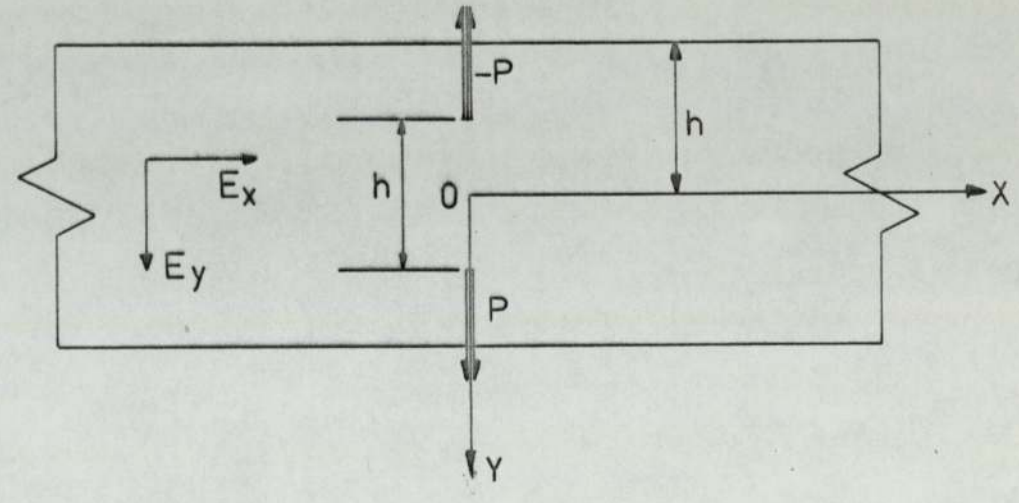

FIG· 7·26b Infinite strip; transverse loads.

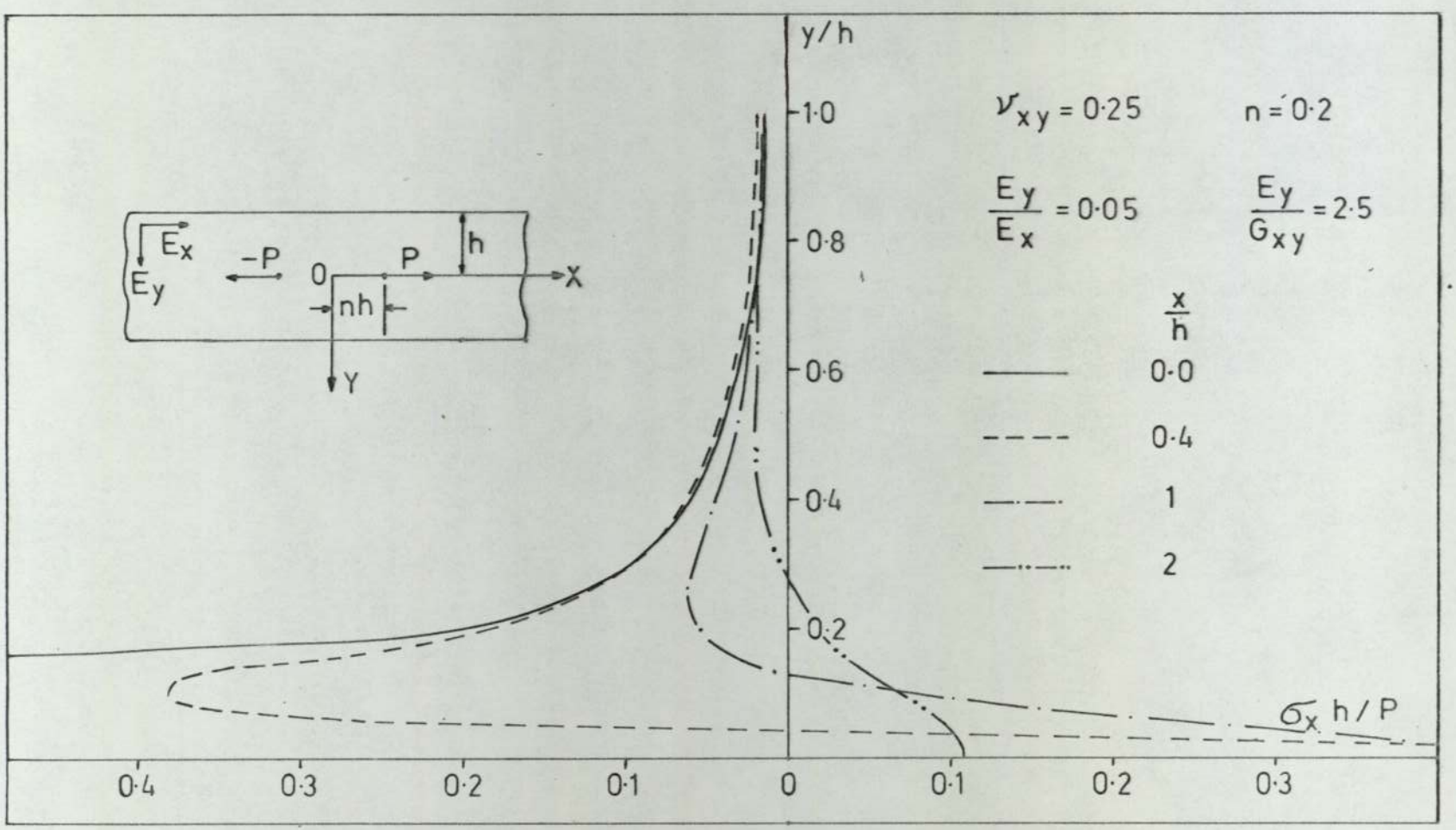

FIG. 7.27 Variation of σ_x with y/h —Longitudinal load

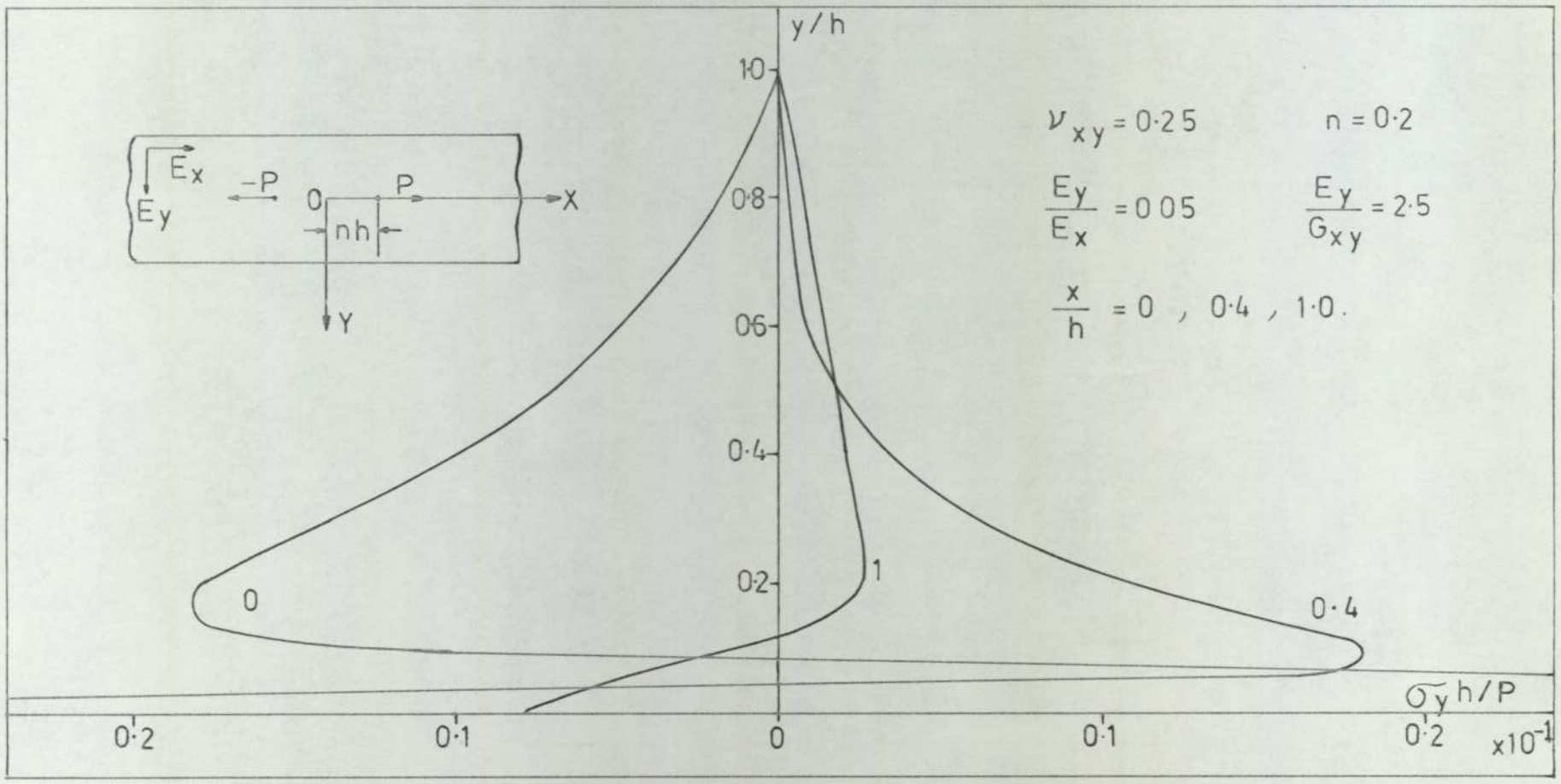

FIG. 7.28 Variation of σ_y with y/h —Longitudinal load

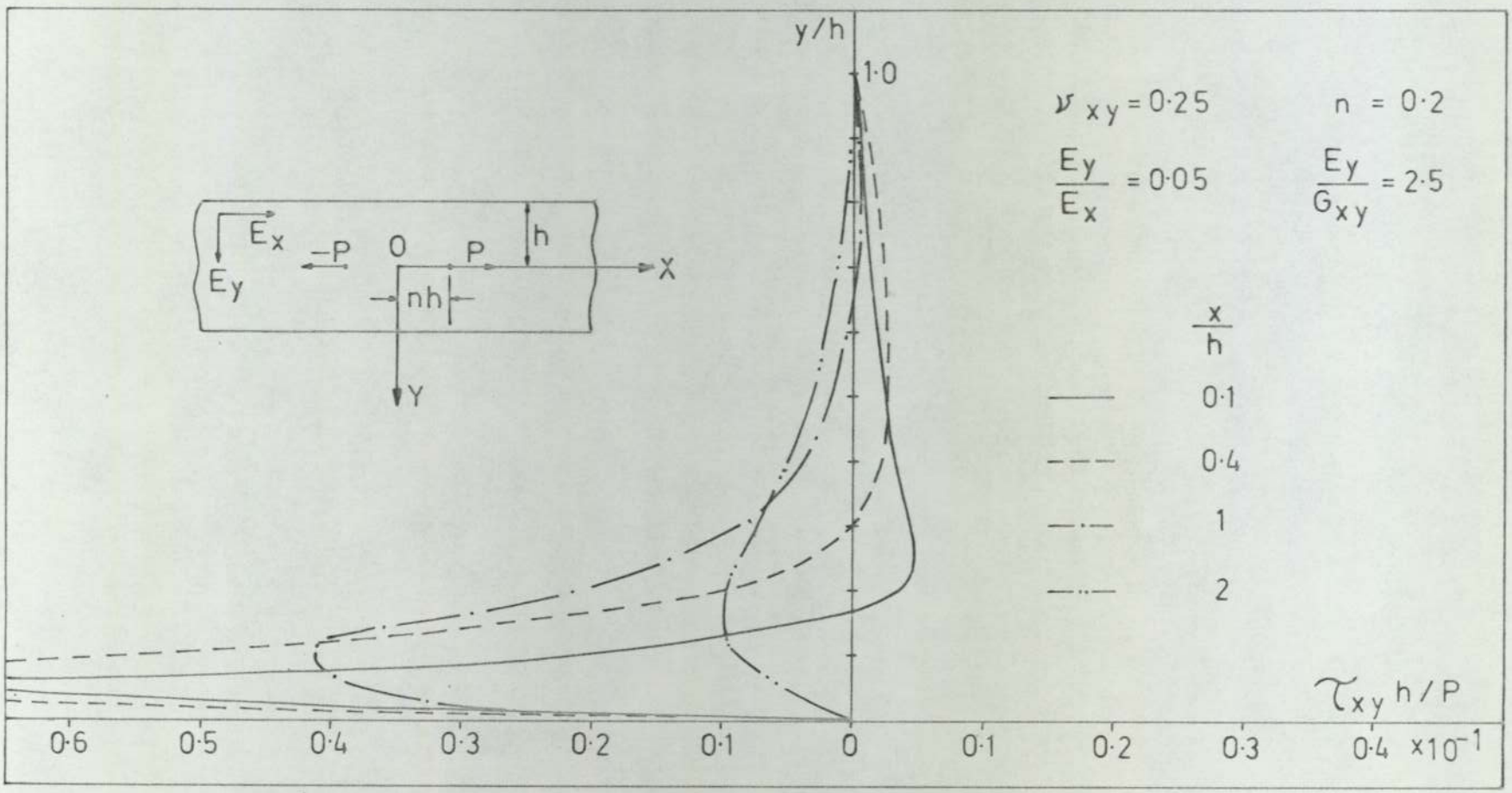

FIG. 7.29 Variation of τ_{xy} with y/h — Longitudinal load

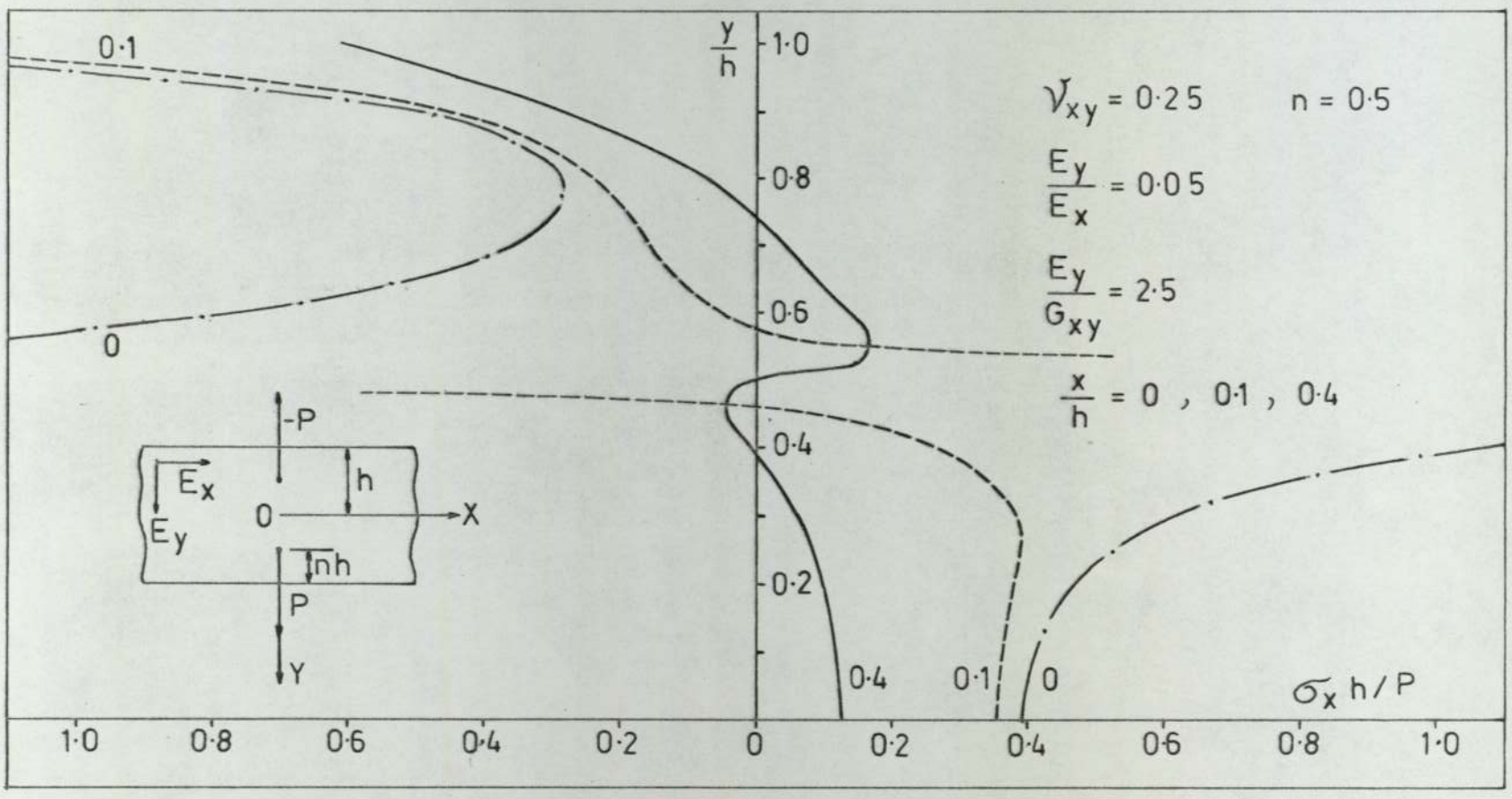

FIG. 7.30 Variation of σ_x with y/h — Transverse load

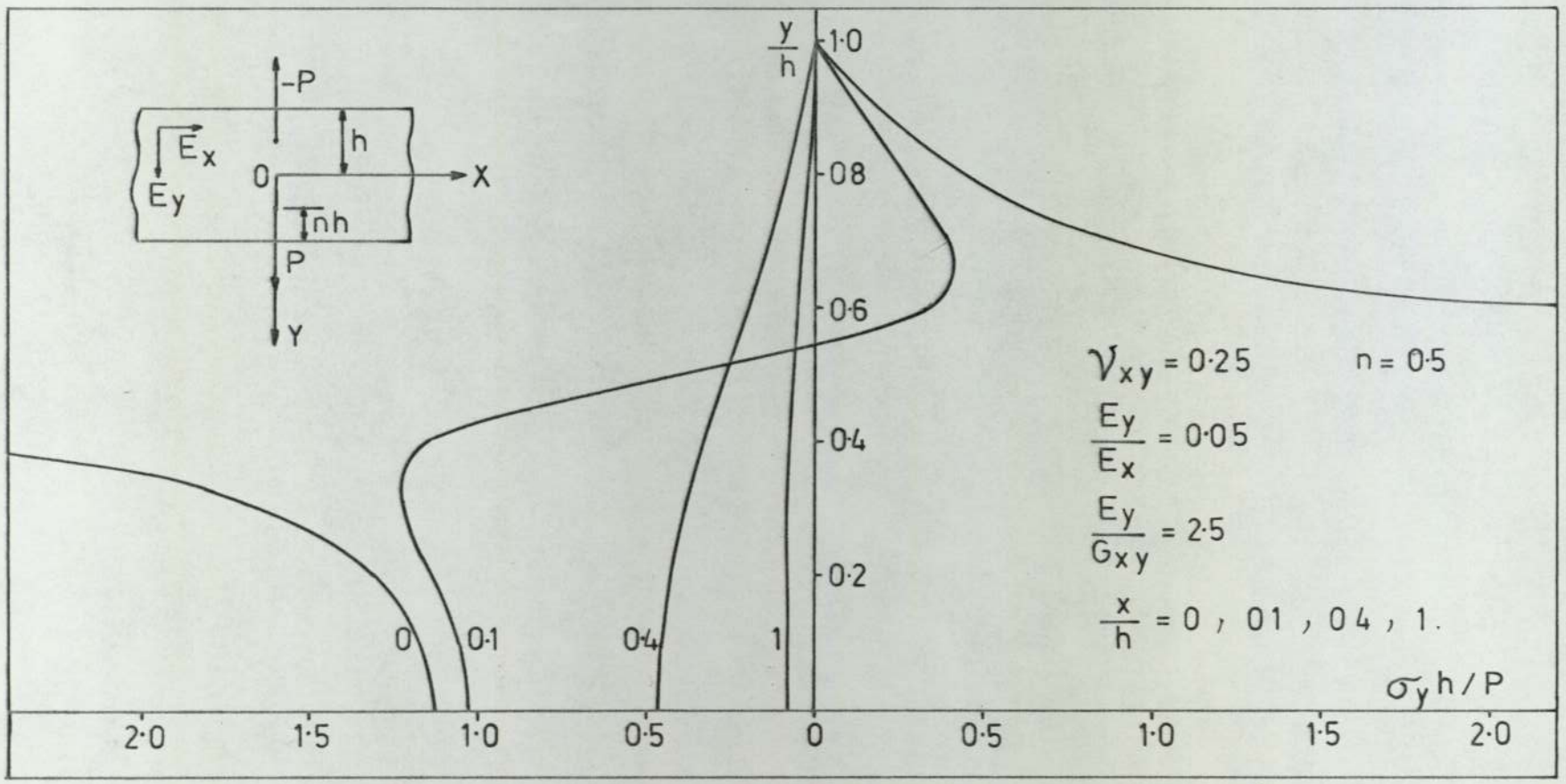

FIG· 7·31 Variation of σ_y with y/h — Transverse load.

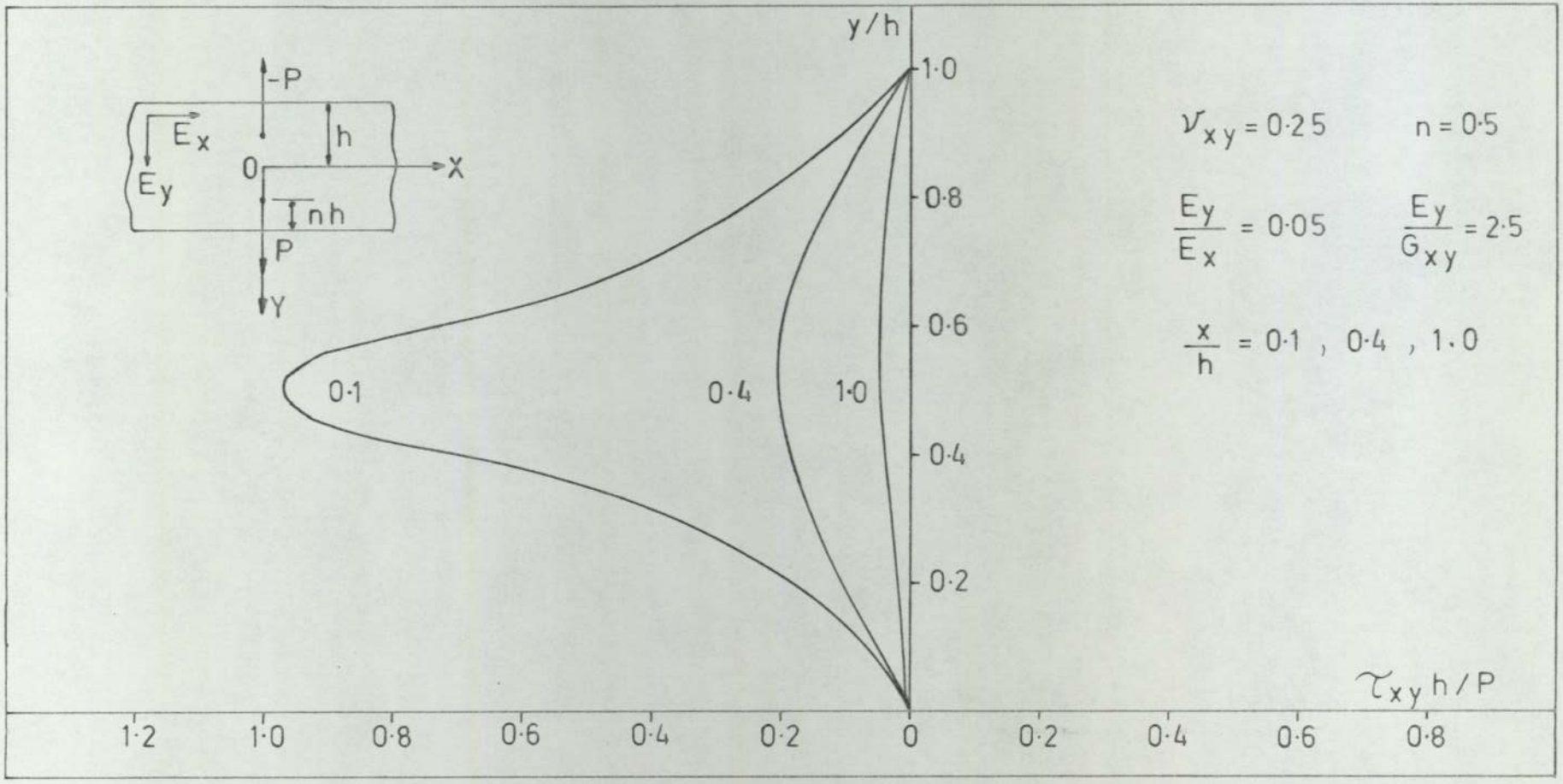

FIG 7.32 Variation of τ_{xy} with y/h — Transverse load

7.3.7) Conclusions.

From the graphical representation of the results in Fig.7.27-7.32, we can make the following observations:

1) Longitudinal loads.

The distribution of σ_x over the width of the infinite strip, indicates that regardless of the position of the cross section on which the stress is determined, σ_x is of significant magnitude only for $y/h < 0.5$ (see Fig.7.27). Along the longitudinal axis of the strip, σ_x diminishes very slowly, thus indicating that in orthotropic strips, the effects of self-equilibrating localized loads are not restricted in the vicinity of the loads.

The variation of τ_{xy} with y/h, (see Fig.7.29) indicates that maximum shear stresses are encountered for $0 < y/h < 0.2$.

2) Transverse loads.

σ_x diminishes slowly with x/h, and attains high values of points near the boundaries of the infinite strip. σ_y decreases rapidly with x/h, and for $x/h > 1$ it is relatively insignificant.

CHAPTER 8

HALF-PLANE WITH IRREGULAR BOUNDARY.

8.1) Introduction.

The elastic analysis of the half-plane with a straight boundary, provides a convenient method for the determination of stresses or displacements in materials, whose boundaries can be approximated to those of the half-plane. Nevertheless, in many cases the boundary surface of the material cannot be approximated to the straight boundary of a half-plane. Such cases arise when the boundary is irregular and the size of the irregularities is large compared with the other length parameters of the problem (e.g. width of applied load).

Such cases are frequently encountered in Civil Engineering practice, in connection with soil mechanics and foundation engineering problems. Embankments of rivers or motorways, large excavations, coastal works, abutments of bridges and earth dams, present a variety of problems that fall into this category (see Fig.8.1).

It is the usual practice to treat such problems with "finite element" or "finite difference" techniques. These techniques, when applied without refinement, fail to give satisfactory results in the vicinity of re-entrant corners, or highly localized loads, where the accurate determination of the stresses is important. It is believed therefore, that an analytical solution to this type of problem would offer the advantage of accurate evaluation of the stresses or displacements, at any point of the material.

Such an analytical solution is developed, for the particular case of a half-plane with a "stepped" boundary (AO*OC), as shown in Fig.8.2

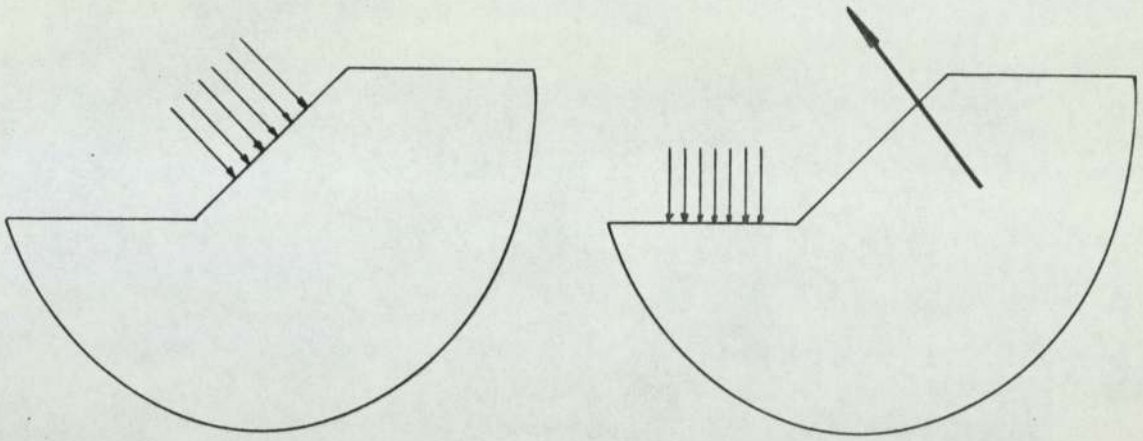

a) Abutments of bridges

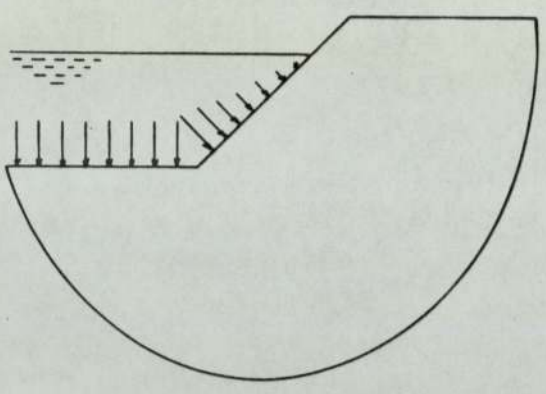

b) Dams

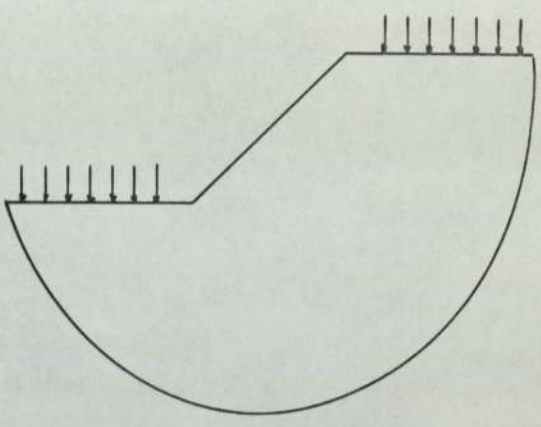

c) Motorways

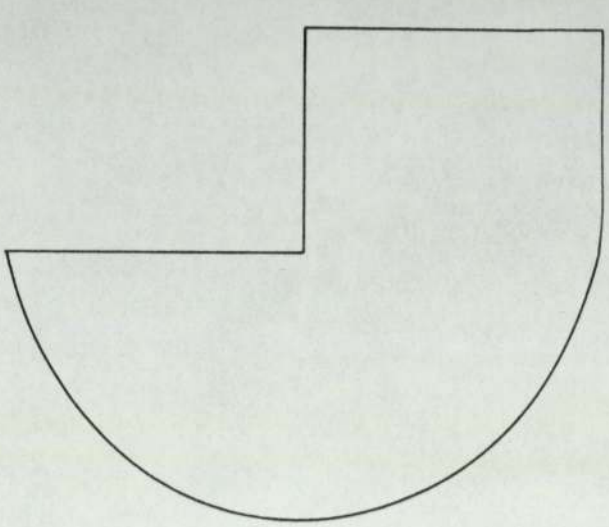

d) Excavations; self-weight

FIG. 8.1

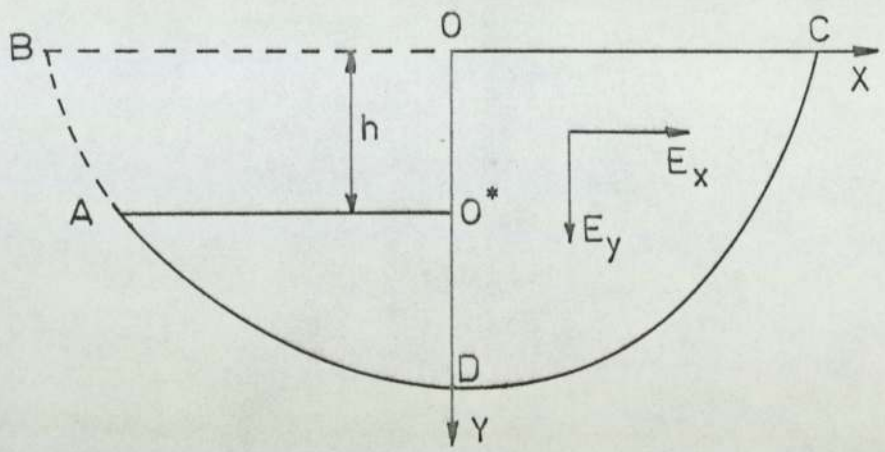

Fig.8.2

The inclined part of the boundary (OO*) is assumed to coincide with the Y-axis, while O*A is parallel to the X-axis. The Cartesian coordinates are expressed in a dimensionless form $\bar{x},\bar{y}$, where

$$\bar{x} = \frac{x}{h}\,, \quad \bar{y} = \frac{y}{h}\,, \qquad 8.1\text{-}1$$

and 'h' is the height of the "step".

The solution is developed for an arbitrary load, acting either on the boundary or at the interior of the "stepped" half-plane.

8.2) Method of solution.

The proposed method of solution for an orthotropic "stepped" half-plane, is a method of superposition of two half-plane solutions, such that the resulting stress field satisfies the traction boundary conditions of the "stepped" half-plane.

First, the "stepped" half-plane is assumed to occupy the region AO*OCD of an orthotropic half-plane (see Fig.8.3b). The state of stress in the "complete" half-plane will be referred to as the basic state of stress and the stress

8.2) contd.

components will be denoted by $\overset{o}{\sigma}_x$, $\overset{o}{\sigma}_y$, $\overset{o}{\tau}_{xy}$. The basic state of stress can be determined using the theory of the orthotropic half-plane and the corresponding equations for the particular type of loading (see Chapter 4).

We then consider an orthotropic half-plane ($-\infty < \bar{x} < \infty$, $0 \leq \bar{y} < \infty$) which is subjected on the $\bar{x} = 0$ plane (for $0 \leq \bar{y} \leq 1$) to a normal stress $\bar{F}(\bar{y})$ and a shear stress $\bar{G}(\bar{y})$, and on the $\bar{y} = 1$ plane (for $-\infty < \bar{x} \leq 0$) to a normal stress $\bar{P}(\bar{x})$ and a shear stress $\bar{Q}(\bar{x})$ (see Fig.8.3c). The state of stress induced in the orthotropic half-plane by the above loading system, will be referred to as the corrective state of stress and the stress components will be denoted by σ_x^c, σ_y^c, τ_{xy}^c. The corrective state of stress can be determined by considering the applied stresses (given by the functions $\bar{F}$, $\bar{G}$, $\bar{P}$ and $\bar{Q}$) as a series of closely spaced concentrated forces applied at the interior of the half-plane. The stress components can then be obtained by integration of equations (4.7-3) and (4.8-1) between the appropriate limits.

The functions $\bar{F}$, $\bar{G}$, $\bar{P}$ and $\bar{Q}$ can be evaluated, using the superposition technique developed by Hetènyi(1960) for the solution of the isotropic elastic quarter-plane. In relation to the "stepped" half-plane this procedure consists of successive reversals of the stresses on the planes 00* and 0*A (see Fig.8.3a), which lead to a convergent result. The functions $\bar{F}$, $\bar{G}$, $\bar{P}$ and $\bar{Q}$, can then be obtained by a summation of the stresses applied on each plane (00* or 0*A) by the reversal procedure. We shall describe this procedure in detail in Section 8.5.

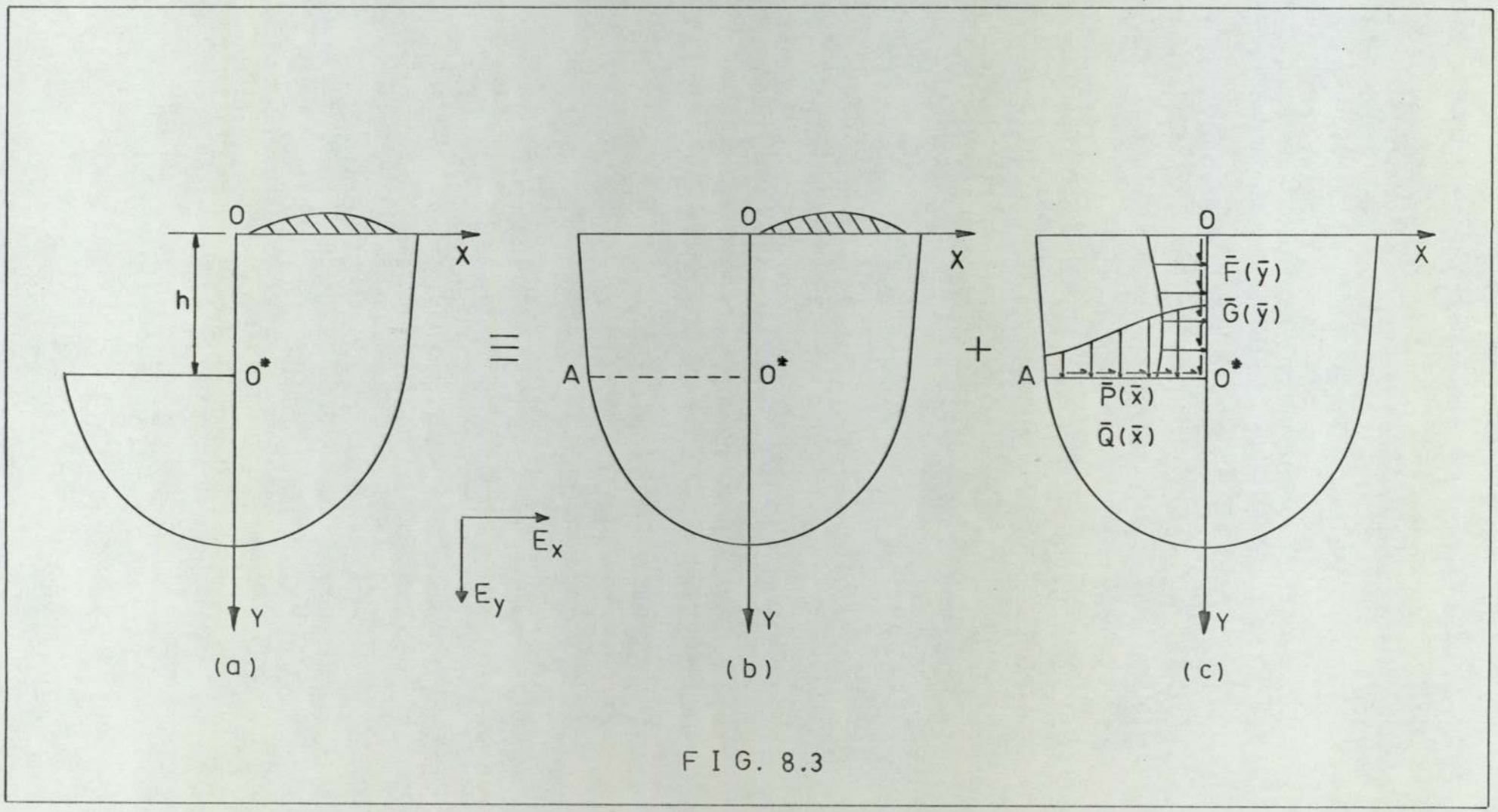

FIG. 8.3

8.3) Basic equations.

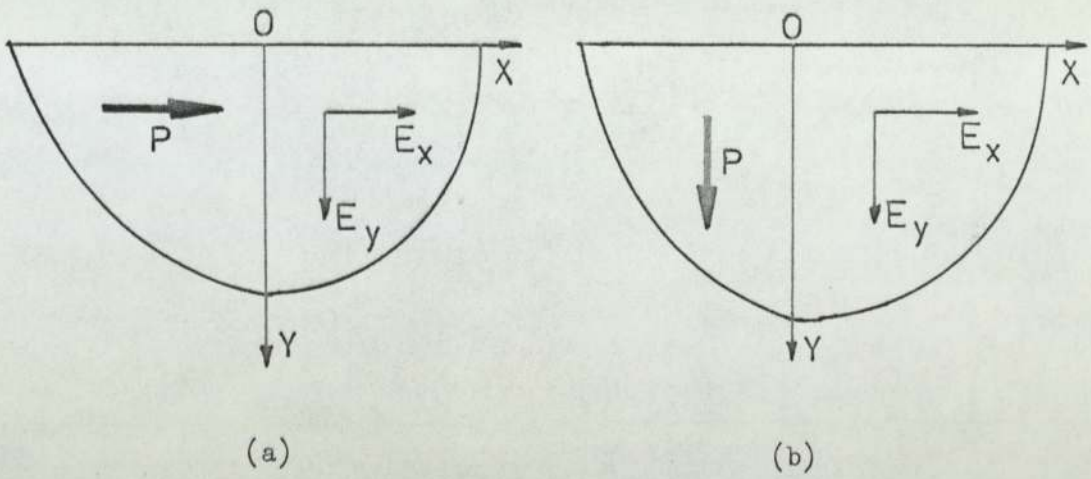

Fig.8.4

The solution to the problem of an orthotropic half-plane which is subjected at its interior to a concentrated force acting in either coordinate direction, has been presented in sections 4.7 and 4.8. Since some changes in the notation are necessary, equations (4.7-3) and (4.8-1) are reproduced in the following paragraphs.

It is assumed that the concentrated force P/unit thickness is applied at point $(\bar{x}_o, \bar{y}_o)$, as shown in Fig.8.4a and b.

8.3.1) Concentrated force acting in the X-direction.

The state of stress in the orthotropic half-plane is given by:

$$\left[\sigma_x;\ \sigma_y;\tau_{xy}\right] = \frac{P}{h}\ \left[J^x_{xx};\ J^x_{yy};\ J^x_{xy}\ \right], \qquad 8.3\text{-}1a$$

where

8.3.1) contd.

$$\left[J^{x}_{xx};\ J^{x}_{yy};\ J^{x}_{xy}\right] = \frac{k_1 k_2}{\pi(k_1^2-k_2^2)} \Bigg\{$$

$$(\alpha_2-\alpha_4)\, r_1 \left[-f_o \ ;\ k_1^2 f_o \ ;\ -f_1 \right]$$

$$+\ \alpha_2 r_2 \left[f_o \ ;\ -k_1^2 f_o \ ;\ f_2 \right]$$

$$+\ (\alpha_1+\alpha_3) r_3 \left[-f_o \ ;\ k_2^2 f_o \ ;\ -f_1 \right]$$

$$+\ \alpha_1 r_4 \left[f_o \ ;\ -k_2^2 f_o \ ;\ f_2 \right]$$

$$+\ \alpha_4 r_5 \left[-k_1^2 f_o \ ;\ k_1^2 k_2^2 f_o \ ;\ -f_3 \right]$$

$$+\ \alpha_3 r_6 \left[k_2^2 f_o \ ;\ -k_1^2 k_2^2 f_o \ ;\ f_4 \right] \Bigg\}, \qquad 8.3\text{-}1b$$

and $f_o = \bar{x} - x_o$,

$$\left.\begin{matrix} f_1 \\ f_2 \end{matrix}\right\} = \bar{y} \pm \bar{y}_o \quad , \quad \left.\begin{matrix} f_3 \\ f_4 \end{matrix}\right\} = k_1 k_2 \bar{y}_o + \left\{\begin{matrix} k_1^2\, \bar{y} \\ k_2^2\, \bar{y} \end{matrix}\right. ,$$

$$\left.\begin{matrix} r_1 \\ r_2 \end{matrix}\right\} = \left[k_1^2 f_o^2 + (\bar{y} \pm \bar{y}_o)^2\right]^{-1}, \quad \left.\begin{matrix} r_3 \\ r_4 \end{matrix}\right\} = \left[k_2^2 f_o^2 + (\bar{y} \pm \bar{y}_o)^2\right]^{-1},$$

$$r_5 = \left[(k_1 k_2 f_o)^2 + (k_1 \bar{y} + k_2 \bar{y}_o)^2\right]^{-1}, \quad r_6 = \left[(k_1 k_2 f_o)^2 + (k_2 \bar{y} + k_1 \bar{y}_o)^2\right]^{-1}.$$

8.3-1c

The constants $\alpha_1 \ldots \alpha_4$, are as defined by the equation (4.74).

8.3.2) Concentrated force acting in the Y-direction.

The state of stress in the orthotropic half-plane is given by:

$$\left[\sigma_x;\sigma_y;\tau_{xy}\right] = \frac{P}{h} \left[J^{y}_{xx};\ J^{y}_{yy};\ J^{y}_{xy}\right], \qquad 8.3\text{-}2a$$

where

8.3.2) contd.

$$\left[J^{y}_{xx};\ J^{y}_{yy};\ J^{y}_{xy} \right] = \frac{1}{\pi(k_1^2-k_2^2)} \Big\{$$

$$(\alpha_1+\alpha_3)\, r_1 \quad \left[f_1 ;\ -k_1^2 f_1 ;\ -k_1^2 f_o \right]$$

$$+\ \alpha_1\, r_2 \quad \left[-f_2 ;\ k_1^2 f_2 ;\ k_1^2 f_o \right]$$

$$+\ (\alpha_2-\alpha_4)\, r_3 \quad \left[f_1 ;\ -k_2^2 f_1 ;\ -k_2^2 f_o \right]$$

$$+\ \alpha_2\, r_4 \quad \left[-f_2 ;\ k_2^2 f_2 ;\ k_2^2 f_o \right]$$

$$+\ \alpha_3\, r_5 \quad \left[-f_3 ;\ k_2^2 f_3 ;\ k_1^2 k_2^2 f_o \right]$$

$$+\ \alpha_4\, r_6 \quad \left[f_4 ;\ -k_1^2 f_4 ;\ -k_1^2 k_2^2 f_o \right] \Big\}.$$

8.3-2b

8.3.3) Notation.

With regard to the corrective state of stress, a concentrated force P, applied at the interior of the half-plane in the X-direction, is interpreted as a force which can act normal to the plane 00* or tangential to the plane 0*A. Similarly, a concentrated force applied in the Y-direction, can act normal to the plane 0*A or tangential to the plane 00*.

In all the above cases, it is necessary to determine the stresses which are induced on the planes 00* and 0*A by the corresponding concentrated force. For that purpose, we shall adopt the notation $J^{ij}_{k\ell}$ to denote the expressions J^{x}_{xx}, J^{y}_{yy}, J^{y}_{xy} etc. (see equations 8.3-1b and 8.3-2b) when applied to points on the planes 00* and 0*A, where

8.3.3) contd.

i : denotes the direction in which the concentrated force is applied,

j : denotes the direction of the normal to the plane on which the force is applied,

k : denotes the direction in which the stress is determined, and,

ℓ : denotes the direction of the normal to the plane on which the stress is determined.

For example, J^{xy}_{xx} denotes the expression for the evaluation of the normal stress at a point $(0,\bar{y})$ on the plane 00*, due to a concentrated force applied at a point $(\bar{x}_o,1)$ and acting tangential to the plane 0*A. We can then write $J^{xy}_{xx}(\bar{x}_o,\bar{y})$

In general, we have:

$$J^{iy}_{k\ell}(\bar{x}_o,\bar{y}) \equiv \left[J^{i}_{k\ell}(\bar{x}_o,\bar{y})\right]_{\bar{y}_o=1,\ \bar{x}=0},$$

and 8.3-3

$$J^{ix}_{k\ell}(\bar{x},\bar{y}_o) \equiv \left[J^{i}_{k\ell}(\bar{x},\bar{y}_o)\right]_{\bar{x}_o=0,\ \bar{y}=1}.$$

8,4) Basic state of stress.

We assume that the basic state of stress can be uniquely determined from the theory of the half-plane, and that the stress components are given by:

$$\left[\overset{o}{\sigma}_x;\ \overset{o}{\sigma}_y;\ \overset{o}{\tau}_{xy}\right] = \frac{\psi}{h}\left[\overset{o}{S}_x;\ \overset{o}{S}_y;\ \overset{o}{S}_{xy}\right], \qquad 8.4\text{-}1$$

where ψ is a load parameter.

8.4) contd.

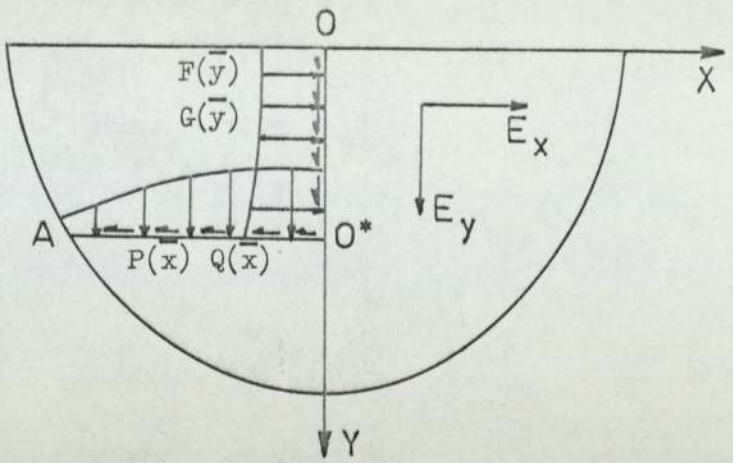

Fig.8.5

Let $F(\bar{y})$ and $G(\bar{y})$ denote the normal and shear stress distribution respectively, induced on the plane OO* by the basic state of stress. Similarly, let $P(\bar{x})$ and $Q(\bar{x})$ denote the normal and shear stress distribution respectively on the plane O*A (see Fig.8.5).

Then

$$\left[F(\bar{y});\ G(\bar{y})\right] = \frac{\psi}{h}\left[S_s^{\circ};\ S_{xy}^{\circ}\right]_{\bar{y},\bar{x}\,=\,0},$$

and 8.4-2

$$\left[P(\bar{x});Q(\bar{x})\right] = \frac{\psi}{h}\left[S_y^{\circ};\ -S_{xy}^{\circ}\right]_{\bar{x},\bar{y}\,=\,1.}.$$

8.5) Corrective state of stress.

8.5.1) Determination of the functions $\bar{F},\bar{G},\bar{P},\bar{Q}$.

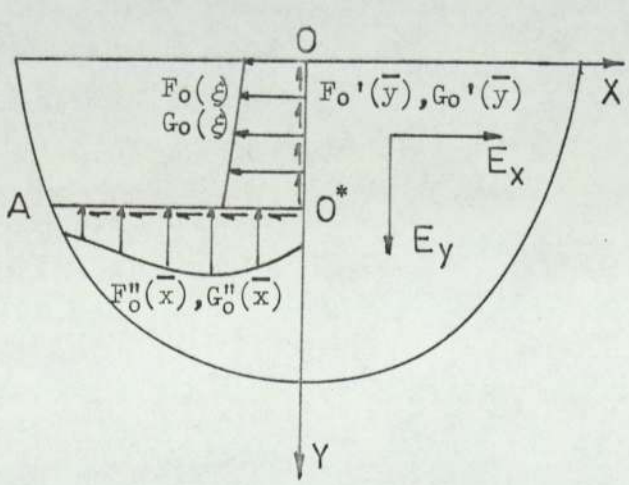

Fig.8.6

8.5.1) contd.

In order to successively reduce the stresses on the planes 00* and 0*A, we proceed by considering the plane 00* first.

Step 1. Consider an orthotropic half-plane $-\infty < \bar{x} < \infty$, $0 \leq \bar{y} < \infty$, which is subjected to a normal stress distribution $F_o(\xi)$ and shear stress distribution $G_o(\xi)$, along the $\bar{x} = 0$ plane, for $0 \leq \bar{y} \leq 1$ (i.e. the plane 00* in Fig.8.6). We define $F_o(\xi)$ and $G_o(\xi)$ as follows:

$$F_o(\xi) = - F(\bar{y}) \ , \ G_o(\xi) = - G(\bar{y}) \qquad 8.5\text{-}1$$

This system of stresses will in general give rise to normal and shear stresses on both planes 00* and 0*A. These stresses can be written in the following form:

a) Normal stress on 00*

$$F_o'(\bar{y}) = \int_0^1 F_o(\xi) J_{xx}^{xx}(\xi) d\xi + \int_0^1 G_o(\xi) J_{xx}^{yx}(\xi) d\xi. \qquad 8.5\text{-}2a$$

b) Shear stress on 00*

$$G_o'(\bar{y}) = \int_0^1 F_o(\xi) J_{yx}^{xx}(\xi) d\xi + \int_0^1 G_o(\xi) J_{yx}^{yx}(\xi) d\xi. \qquad 8.5\text{-}2a$$

c) Normal stress on 0*A,

$$F_o''(\bar{x}) = \int_0^1 F_o(\xi) J_{yy}^{xx}(\xi) d\xi + \int_0^1 G_o(\xi) J_{yy}^{yx}(\xi) d\xi. \qquad 8.5\text{-}2c$$

d) Shear stress on 0*A,

$$G_o''(\bar{x}) = \int_0^1 F_o(\xi) J_{xy}^{xx}(\xi) d\xi + \int_0^1 G_o(\xi) J_{xy}^{yx}(\xi) d\xi. \qquad 9.5\text{-}2d$$

The prime ('), e.g. $F_o'(\bar{y})$, denotes stress distributions on the plane where the load is applied; in this case 00*. The double-prime (") e.g. $F_o''(\bar{x})$, denotes stress

8.5.1) contd.

distributions induded by the load, on the other plane considered; in this case O*A.

Combining the stress system given by equation (8.5-2), with the basic state of stress, the total normal and shear stress distributions on the plane OO* are given by:

$$\begin{aligned} &\text{Normal stress :} && -F_o(\bar{y}) + F_o'(\bar{y}), \\ &\text{Shear stress :} && -G_o(\bar{y}) + G_o'(\bar{y}), \end{aligned} \qquad 8.5\text{-}3a$$

and on the plane O*A, are given by:

$$\begin{aligned} &\text{Normal stress :} && P(\bar{x}) + F_o''(\bar{x}), \\ &\text{Shear stress :} && Q(\bar{x}) + G_o''(\bar{x}). \end{aligned} \qquad 8.5\text{-}3b$$

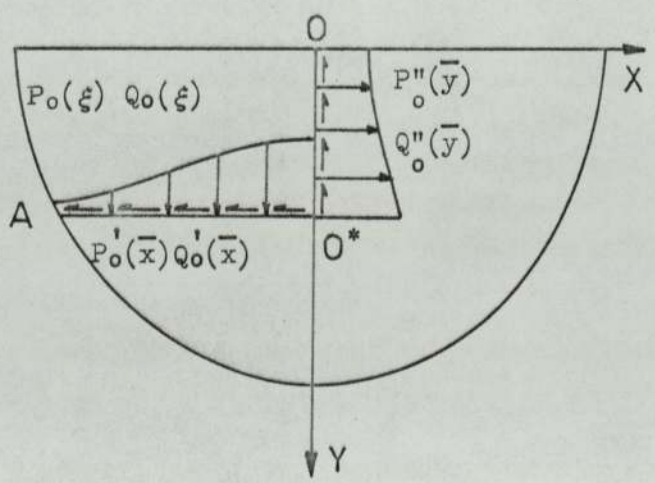

Fig.8.7

Step 2. In orer to reduce the stresses on the plane O*A (equation 8.5-3b), we consider an orthotropic half-plane, $-\infty < \bar{x} < \infty$, $0 \leq \bar{y} < \infty$, which is subjected along the $\bar{y} = 1$ plane, for $-\infty < \bar{x} \leq 0$, (see Fig.8.7) to a normal stress distribution $P_o(\xi)$, and, a shear stress distribution $Q_o(\xi)$. We define $P_o(\xi)$ and $Q_o(\xi)$ as follows:

8.5.1) contd.

$$P_o(\xi) = -\left[P(\bar{x}) + F_o''(\bar{x}) \right],$$
$$Q_o(\xi) = -\left[Q(\bar{x}) + G_o''(\bar{x}) \right]. \qquad 8.5\text{-}4$$

The application of $P_o(\xi)$ and $Q_o(\xi)$ on the plane O*A, will give rise to normal and shear stresses on both planes OO* and O*A, given by the following expressions:

$$\left[P_o'(\bar{x});\ Q_o'(\bar{x}) \right] = \int_{-\infty}^{o} P_o(\xi) \left[J_{yy}^{yy}(\xi);\ J_{xy}^{yy}(\xi) \right] d\xi$$
$$+ \int_{-\infty}^{o} Q_o(\xi) \left[J_{yy}^{xy}(\xi);\ J_{xy}^{xy}(\xi) \right] d\xi , \qquad 8.5\text{-}5a$$

and

$$\left[P_o''(\bar{y});\ Q_o''(\bar{y}) \right] = \int_{-\infty}^{o} P_o(\xi) \left[J_{xx}^{yy}(\xi);\ J_{yx}^{yy}(\xi) \right] d\xi$$
$$+ \int_{-\infty}^{o} Q_o(\xi) \left[J_{xx}^{xy}(\xi);\ J_{yx}^{xy}(\xi) \right] d\xi . \qquad 8.5\text{-}5b$$

The combination of the stresses given by the equations(8.5-3) and (8.5-5), will result in a total normal and shear stress distribution on the plane OO*, given by

Normal stress : $-F_o(\bar{y}) + F_o'(\bar{y}) + P_o''(\bar{y})$,
Shear stress : $-G_o(\bar{y}) + G_o'(\bar{y}) + Q_o''(\bar{y})$, $\qquad 8.5\text{-}6a$

and on the plane O*A, given by:

Normal stress : $-P_o(\bar{x}) + P_o'(\bar{x})$,
Shear stress : $-Q_o(\bar{x}) + Q_o'(\bar{x})$. $\qquad 8.5\text{-}6b$

8.5.1) contd.

Step 3. The stresses on the plane 00*, given by equation (8.5-6a), can be reduced by superposing the solution to an orthotropic half-plane ($-\infty < \bar{x} < \infty$, $0 \leq \bar{y} < \infty$), which is subjected along its 00* plane, to normal and shear stresses $F_1(\xi)$ and $G_1(\xi)$ respectively, where

$$F_1(\xi) = -\left[-F_o(\bar{y}) + F_o'(\bar{y}) + P_o''(\bar{y})\right],$$
$$G_1(\xi) = -\left[-G_o(\bar{y}) + G_o'(\bar{y}) + Q_o''(\bar{y})\right]. \qquad 8.5\text{-}7$$

This loading system, will induce stresses $(F_1'(\bar{y}), G_1'(\bar{y}), F_1''(\bar{x}), G_1''(\bar{x}))$ on both planes 00* and 0*A. These stresses can be evaluated using equation (8.5-2), by replacing $F_o(\xi)$ by $F_1(\xi)$ and $G_o(\xi)$ by $G_1(\xi)$.

Then, the total stresses on the plane 00*, are:

$$\text{Normal stress} : -F_1(\bar{y}) + F_1'(\bar{y}),$$
$$\text{Shear stress} : -G_1(\bar{y}) + G_1'(\bar{y}), \qquad 8.5\text{-}8a$$

and on the plane 0*A, are

$$\text{Normal stress} : -P_o(\bar{x}) + P_o'(\bar{x}) + F_1''(\bar{x}),$$
$$\text{Shear stress} : -Q_o(\bar{x}) + Q_o'(\bar{x}) + G_1''(\bar{x}). \qquad 8.5\text{-}8b$$

Step 4. The stresses on the plane 0*A, given by equation (8.5-8b) can be reduced by applying equal and opposite stresses $P_1(\xi)$, $Q_1(\xi)$ along the plane 0*A of an orthotropic half-plane ($-\infty < \bar{x} < \infty$, $0 \leq \bar{y} < \infty$), and superposing the two solutions.

The functions $P_1(\xi)$ and $Q_1(\xi)$, are given by:

$$P_1(\xi) = -\left[-P_o(\bar{x}) + P_o'(\bar{x}) + F_1''(\bar{x})\right],$$
$$Q_1(\xi) = -\left[-Q_o(\bar{x}) + Q_o'(\bar{x}) + G_1''(\bar{x})\right]. \qquad 8.5\text{-}9$$

The resulting stress distributions on the planes 00* and 0*A, by the superposition of the two solutions, are given by:

8.5.1) contd.

On the plane 0*A:

$$\text{Normal stress: } -P_1(\bar{x}) + P_1'(\bar{x}),$$
$$\text{Shear stress: } -Q_1(\bar{x}) + Q_1'(\bar{x}). \qquad 8.5\text{-}10a$$

On the plane 00*:

$$\text{Normal stress: } -F_1(\bar{y}) + F_1'(\bar{y}) + P_1''(\bar{y}),$$
$$\text{Shear stress: } -G_1(\bar{y}) + G_1'(\bar{y}) + Q_1''(\bar{y}), \qquad 8.5\text{-}10b$$

where $P_1'(\bar{x})$, $Q_1'(\bar{x})$, $P_1''(\bar{x})$ and $Q_1''(\bar{x})$, can be evaluated, using equation (8.5-5) and by replacing $P_0(\xi)$ and $Q_0(\xi)$ by $P_1(\xi)$ and $Q_1(\xi)$ respectively.

It is now evident that the techniques outlined in Steps 3 and 4 have to be repeatedly applied, in order to satisfy traction boundary conditions on the planes 00* and 0*A. The functions $F_m(\xi)$, $G_m(\xi)$, $P_m(\xi)$ and $Q_m(\xi)$, are then given by the recurrence relations:

$$F_{m+1}(\xi) = -\left[-F_m(\bar{y}) + F_m'(\bar{y}) + P_m''(\bar{y})\right],$$
$$G_{m+1}(\xi) = -\left[-G_m(\bar{y}) + G_m'(\bar{y}) + Q_m''(\bar{y})\right], \qquad 8.5\text{-}11$$
$$P_{m+1}(\xi) = -\left[-P_m(\bar{x}) + P_m'(\bar{x}) + F_{m+1}''(\bar{x})\right],$$
$$Q_{m+1}(\xi) = -\left[-Q_m(\bar{x}) + Q_m'(\bar{x}) + G_{m+1}''(\bar{x})\right],$$

where

$$\left[F_m'(\bar{y});\ G_m'(\bar{y});\ F_m''(\bar{x});\ G_m''(\bar{x})\right] =$$
$$\int_0^1 F_m(\xi)\left[J_{xx}^{xx}(\xi);\ J_{yx}^{xx}(\xi);\ J_{yy}^{xx}(\xi);\ J_{xy}^{xx}(\xi)\right]d\xi$$
$$+\int_0^1 G_m(\xi)\left[J_{xx}^{yx}(\xi);\ J_{yx}^{yx}(\xi);\ J_{yy}^{yx}(\xi);\ J_{xy}^{yx}(\xi)\right]d\xi, \qquad 8.5\text{-}12$$

8.5.1) contd.

and

$$\left[P_m'(\bar{x});\ Q_m'(\bar{x});\ P_m''(\bar{y});\ Q_m''(\bar{y})\ \right] =$$

$$\int_{-\infty}^{o} P_m(\xi)\ \left[J_{yy}^{yy}(\xi);\ J_{xy}^{yy}(\xi);\ J_{xx}^{yy}(\xi);\ J_{yx}^{yy}(\xi)\ \right] d\xi$$

$$+\int_{-\infty}^{o} Q_m(\xi)\ \left[J_{yy}^{xy}(\xi);\ J_{xy}^{xy}(\xi);\ J_{xx}^{xy}(\xi);\ J_{yx}^{xy}(\xi)\ \right] d\xi. \qquad 8.5\text{-}13$$

When the functions $F_m(\xi)$, $G_m(\xi)$, $P_m(\xi)$ and $Q_m(\xi)$ are evaluated(from equation 8.5-11), we can then obtain $\bar{F}(\xi)$, $\bar{G}(\xi)$, $\bar{P}(\xi)$, $\bar{Q}(\xi)$, by a summation of the stresses applied on each plane 00* and 0*A, by every reversal of load.

Then,

$$\bar{F}(\xi) = \sum_{m=o}^{\infty} F_m(\xi),$$

$$\bar{G}(\xi) = \sum_{m=o}^{\infty} G_m(\xi), \qquad 8.5\text{-}14$$

$$\bar{P}(\xi) = \sum_{m=o}^{\infty} P_m(\xi),$$

$$\bar{Q}(\xi) = \sum_{m=o}^{\infty} Q_m(\xi).$$

8.5.2) Determination of the stresses.

The corrective state of stress induced in the orthotropic half-plane by $\overline{F},\overline{G},\overline{P},\overline{Q}$ can be determined by using equations (8.3-12) and (8.3-2a). The stress components are then given by:

$$\left[\sigma_x^c\ ;\ \sigma_y^c\ ;\ \tau_{xy}^c\right] = \int_0^1 \overline{F}(\xi)\left[J_{xx}^x;\ J_{yy}^x;\ J_{xy}^x\right]d\xi$$

$$+ \int_0^1 \overline{G}(\xi)\left[J_{xx}^y;\ J_{yy}^y;\ J_{xy}^y\right]d\xi$$

$$+ \int_{-\infty}^0 \overline{P}(\xi)\left[J_{xx}^y;\ J_{yy}^y;\ J_{xy}^y\right]d\xi$$

$$+ \int_{-\infty}^0 \overline{Q}(\xi)\left[J_{xx}^x;\ J_{yy}^x;\ J_{xy}^x\right]d\xi. \qquad 8.5\text{-}15$$

8.6) Conclusions and recommendations.

The method of solution developed for the "stepped" half-plane, was based on successive reversals of stresses on the planes 00* and 0*A, located at the interior of the half-plane (see Fig.8.5). In each reversal, the stresses were only partially eliminated from the planes, since the induced stresses were in general not equal and opposite to the original ones. Under these conditions, the speed of convergence of the method would be relatively slow. Nevertheless, certain steps can be taken to improve the speed of convergence. For example, in order to reduce the normal stress $F_m(\bar{x})$ on the plane 00*, we apply an equal and opposite normal stress $F_m(\xi)$. Then, the induced normal stress on the same plane is $-F_m(\bar{x})/2$. It is then obvious, that if $F_m(\xi)$ is of magnitude $-2F_m(\bar{x})$, the normal stresses on the plane 00* will be completely eliminated.

Similar techniques can be used, in the reversal of the shear stresses on the plane 00*.

The method of solution presented in the previous sections, was developed for the particular case of a "stepped" half-plane, i.e. the part 00* of the boundary was assumed to be at right angles to the rest of the boundary of the half-plane. However, the solution can be extended to cases when the part 00* is inclined at an angle $\neq 90°$. Then, the applied loads F_m, G_m, P_m, Q_m will be functions of $\bar{x}$ and $\bar{y}$.

CHAPTER 9

EXPERIMENTAL INVESTIGATION.

9.1) Introduction.

In the previous chapters (Chapter 3 - Chapter 8), analytical or numerical solutions were developed for a number of problems under "plane deformation" conditions, employing the theory of linear orthotropic elasticity outlined in Chapter 2. Whether these solutions can predict accurately stress or strain distributions in real orthotropic materials, was the object of the experimental work undertaken.

Two types of tests were carried out, namely:

1) Plane strain tests, and
2) Plane stress tests.

In both cases, stress or strain distributions were investigated in a "half-plane" and in a "quarter-plane", which were subjected to the following loading systems:

1) Plane strain tests (boundary loads).
   a) Concentrated normal force,
   b) partially distributed uniform normal stress,
   c) parabolic normal stress, applied through a rigid block.
2) Plane stress tests (interior loads).
   a) Concentrated force applied in either of the coordinate directions.

The problems were so chosen as to cover a variety of cases, ranging from an analytical solution (half-plane; concentrated force at the boundary) to a numerical solution (quarter-plane; concentrated force at the interior).

The choice of materials and testing techniques for each test category was influenced by the following factors:

1) Plane strain tests.
   i) Plane strain conditions can be simulated in the laboratory by considering a body of very large thickness (loaded uniformly over its thickness), so

9.1) contd.

1) contd.

i) contd.

that the end-effects are negligible on the centre-line where its behaviour is investigated. With this technique, observation of deformations is limited to the boundaries of the body and therefore stress or strain fields cannot be determined at the interior.

Alternatively, a body of relatively small thickness (in the form of a plate) can be enclosed between two rigid, smooth blocks held a small fixed distance apart. In this way, the conditions of zero displacement (in the direction normal to the plane of the plate), of zero shear stress (on the sides of the plate) and of continuity of direct stress (between the plate and the blocks), necessary for plane strain deformation are ensured. Since tensile stresses cannot be transmitted between the body and the rigid blocks, the number of problems that can be investigated by this method is limited, unless, if precautions are taken to ensure that tensile stresses do not develop (e.g. by precompressing the body).

Of these two methods, the latter was adopted, because it facilitates observation of displacements at the interior of a body.

ii) To enable the measurement of displacement fields within the elastic medium by optical methods, one of the rigid smooth blocks was constructed from a pane of glass.

iii) The accuracy of optical methods in measuring displacements is limited by the resolving power of the optical instrument used. Therefore, if displacements of points

9.1) contd.

1) contd.

iii) contd.

are to be measured with a certain degree of accuracy, and if large loads are to be avoided (for reasons of stability, handling, safety etc.), the elastic modulii of the material to be tested must be low. In view of the requirements it was decided to perform the plane strain tests with a rubber-like material.

iv) The orthotropic properties were induced in the rubber-like material by constructing it in the form of a laminate. This laminate was composed of alternating layers of hard and soft isotropic rubber-like materials which were glued together. The overall behaviour of the composite in the direction normal to the layers was then predominantly governed by the soft rubber, while in the direction parallel to the layers the behaviour was governed by the hard rubber.

2) Plane stress tests.

i) The plane stress condition is assumed to exist in a body which is composed of a thin plate or sheet-like element (i.e. the longitudinal dimensions are very large compared with its thickness).

ii) Fibre-reinforced plastics can be moulded in plates of small thickness, which exhibit orthotropic elastic behaviour depending on the type and orientation of the fibre reinforcement. The properties of the orthotropic plates can be varied by using different type and/or percentages of reinforcing material.

For the reasons just mentioned and in view

9.1) contd.

2) contd.

ii) contd.

of the wide applications of fibre-reinforced composites, it was decided to perform the plane stress tests using an E-glass-reinforced polyester resin.

iii) Strain fields in fibre-reinforced plates can be observed with electric strain gauges located at salient positions.

9.2) Plane strain tests.

9.2.1) Constituent materials.

The following materials were used in the construction of a rubber block for the plane strain tests:

a) "Soft rubber". Shotblast, 70% natural rubber. Shore hardness 40-45%.

b) "Hard rubber". Vinyl, (Trade name: Velbex). Shore hardness 80%.

c) Adhesive. Dunlop rubber adhesive S738.

(The above materials were supplied by:
Rubber and Plastics Industries Ltd. The two types of rubber were supplied in strips 3.5m × 150mm × 3mm).

The elastic constants of the two types of rubber (denoted by E_h, ν_h for hard rubber and E_s and ν_s for soft rubber) were determined from tension and compression tests. From these results, the modulii of rigidity G_h and G_s were predicted from the relation (for isotropic bodies) $G = E/2(1+\nu)$

1) Determination of E in tension.

Specimens for the tension tests were cut from the 3mm thick strips with a Dumbell specimen cutter (Type A,B.S.903, pt.A16). These were subjected to static loads. Elongations were measured using a travelling microscope and the

9.2.1) contd.

1) contd.

corresponding strains were plotted against the average stress computed for the initial cross section of the specimen. (The fact that no area correction was incorporated in the calculations introduced an error in the slope of the curve. Assuming $\nu = 0.5$, and for a strain of 4% the error is of the order of 3%).

Six tests were carried out with each type of rubber; a typical set of curves is shown in Fig.9.10. Both types of rubber were tested for strains up to 10% and were found to behave linearly elastic. The Young's modulii were directly calculated from the slope of the curves, giving the following average values from six tests:

$$E_h = 7.5 \text{ N/mm}^2, \quad E_s = 3.2 \text{ N/mm}^2$$

(see also Table 9.1).

2) Determination of E and ν in compression.

The elastic constants (E_h, E_s, ν_h, ν_s) in compression, were determined by subjecting rectangular rubber blocks to compressive loads at a constant rate of strain (0.1524 mm/min). The blocks were built up from 3 mm thick rectangular pieces of soft or hard rubber, glued together with rubber adhesive. The blocks were then machined to the required size (45 × 45 × 27 mm).

During testing, the applied compressive loads were measured with a calibrated proving ring, while the displacements in the two principal directions were measured with mechanical dial gauges (see Plate 9.1). (To ensure uniform deformation of the rubber blocks, the end-plates of the compressive machine were lubricated with silicone grease).

9.2.1) contd.

2) contd.

In analysing the results, the strains in the two principal directions were plotted against the applied load and from the ratio of the slopes of the curves, Poisson's ratio of the material was determined. The value of Poisson's ratio was later employed to effect an area correction for the stress-strain curve used for the determination of the Young's modulus.

Four tests were carried out with each type of rubber and the following average results were obtained.

$$E_h = 7.2 \text{ N/mm}^2 \quad , \quad \nu_h = 0.48,$$

$$E_s = 2.9 \text{ N/mm}^2 \quad , \quad \nu_s = 0.48$$

(see also Table 9.1).

A typical set of curves is shown in Fig.9.2. Both types of rubber were tested for strains ranging from 0-7% and they exhibited linearly elastic characteristics during both loading and unloading paths.

The values of Young's modulii in compression were found to be less than the corresponding ones in tension. The difference may be attributed, partly to different elastic behaviour of rubber in tension and compression and partly to the thin layers of adhesive present between the rubber layers. The presence of a second soft material (7.5% by volume) would also effect the value of Poisson's ratio (0.48 compared with 0.495-0.499 which is a usual value for solid rubber).

From the two values of Young's modulii that were determined experimentally in tension and compression for each type of rubber, those in compression were adopted in the subsequent analysis since the effects

9.2.1) contd.

2) contd.

of the adhesive layers were included in the final result.

3) Determination of G.

The modulus of rigidity for each type of rubber was predicted from the corresponding values of E and ν in compression, and the following results were obtained:

$$G_h = 2.44 \text{ N/mm}^2 \quad , \quad G_s = 1.01 \text{ N/mm}^2$$

(see also Table 9.1).

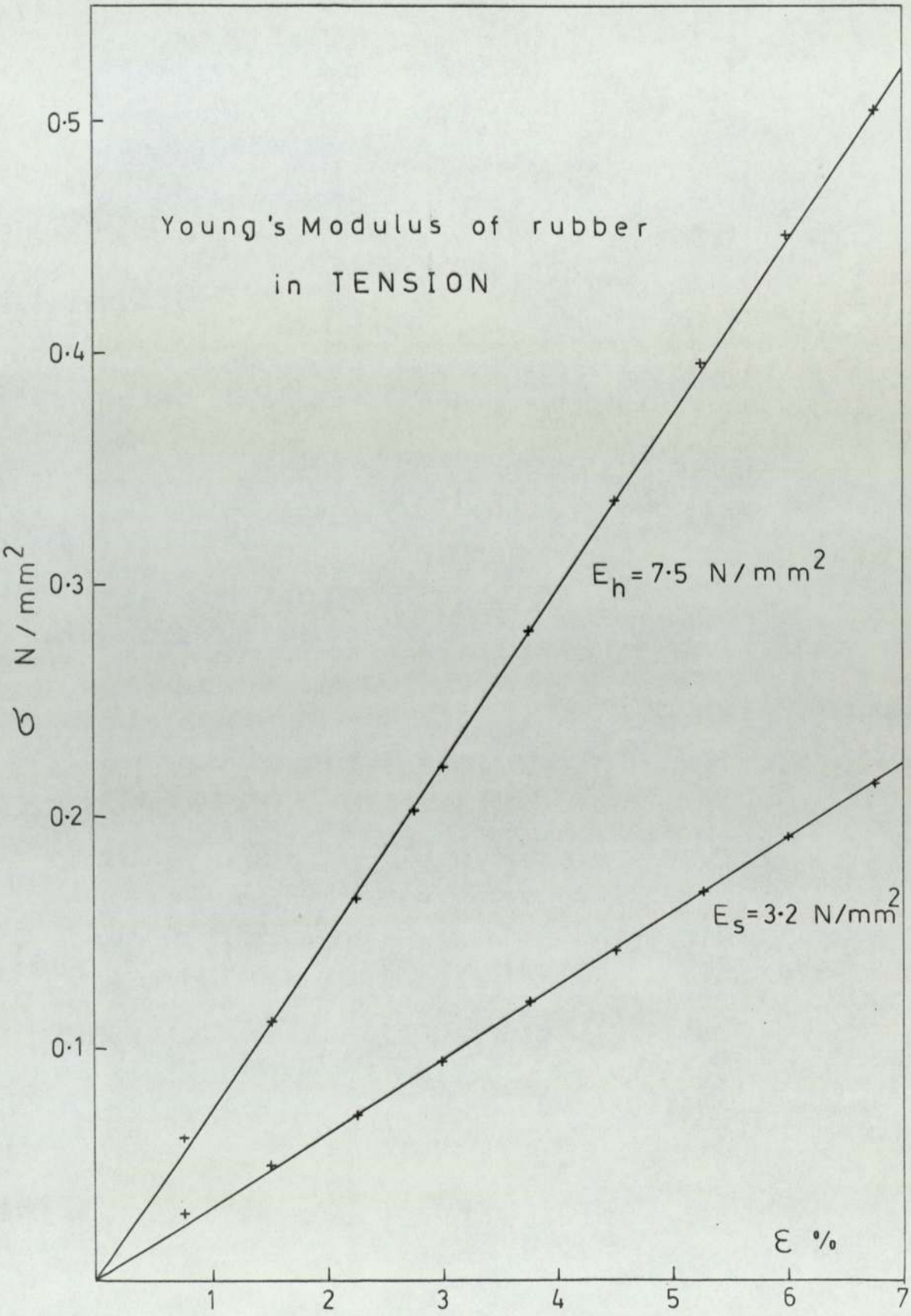

FIG. 9·1a Stress vs strain - Hard & soft rubber

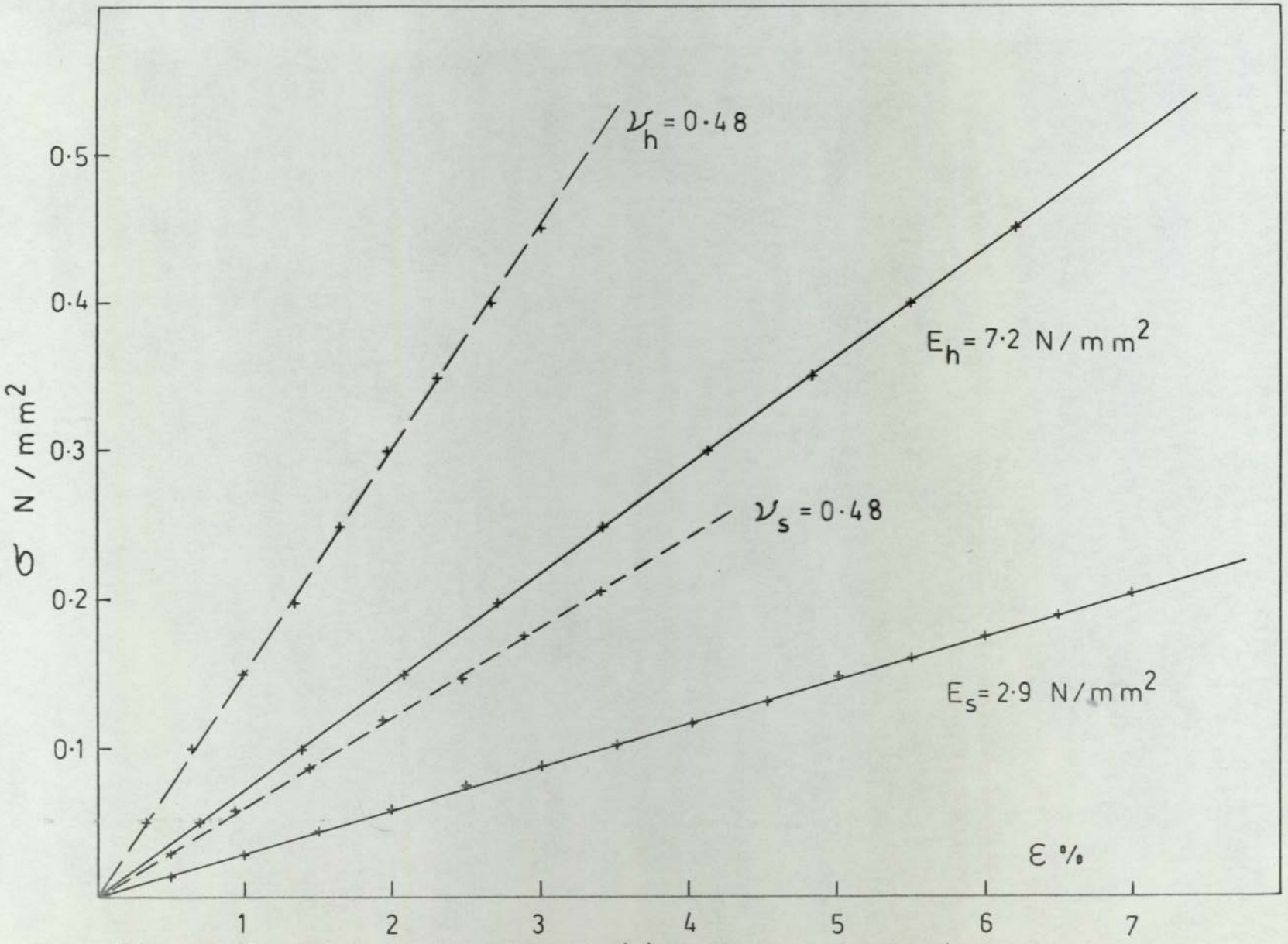

FIG. 9·1b Stress vs strain - Rubber in compression

TABLE 9.1

Type of rubber	TENSION			COMPRESSION				G N/mm^2
	Number of tests	E N/mm^2	S.D.	Number of tests	E N/mm^2	S.D.	ν	
HARD	6	7·5	0·11	4	7·2	0·1	0·48	2·44
SOFT	6	3·2	0·08	4	2·9	0·06	0·48	1·01

Properties of constituent rubber layers

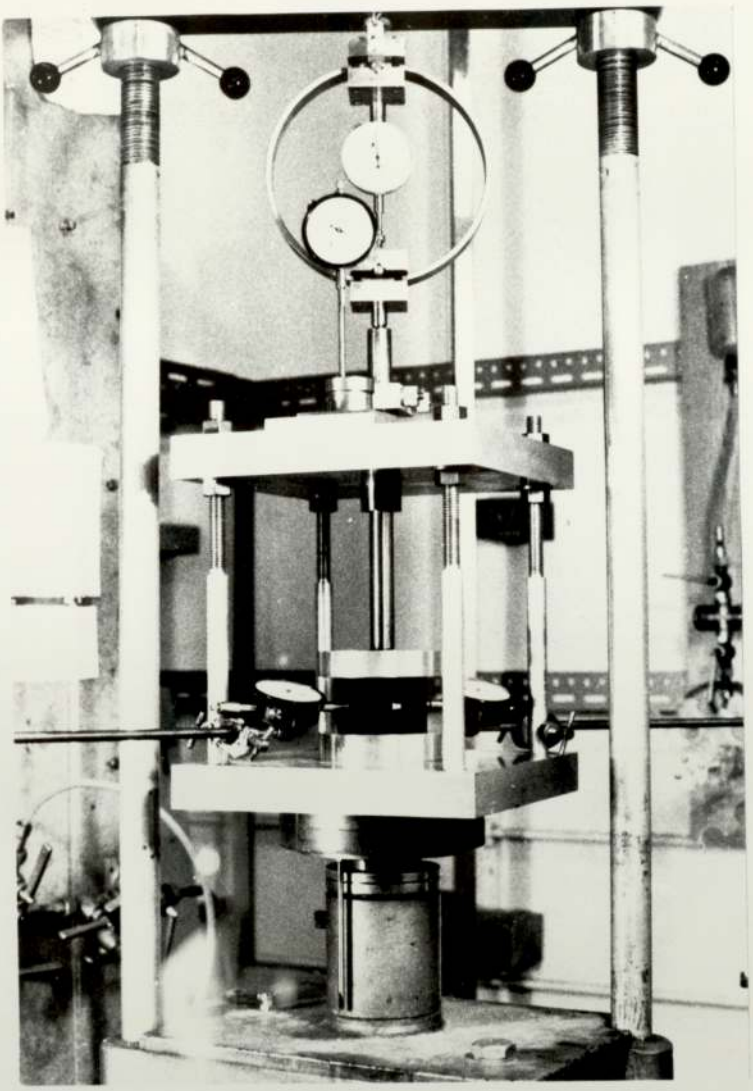

PLATE 9.1 Compression apparatus

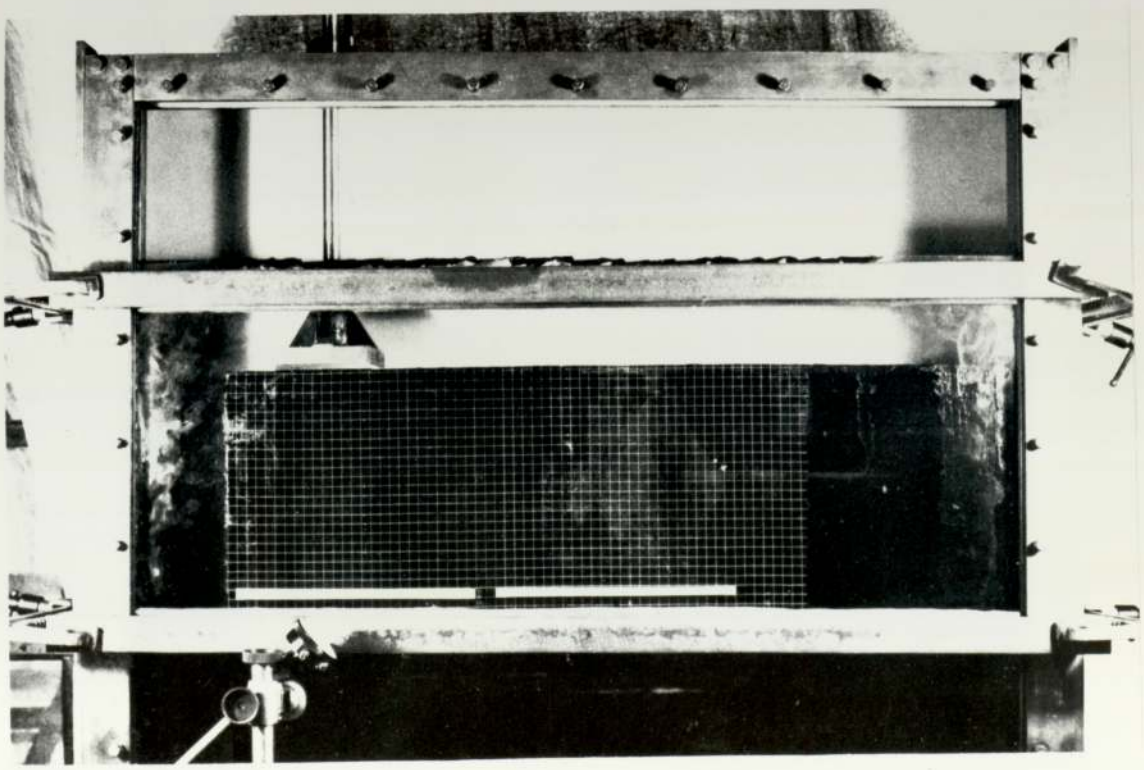

PLATE 9.2 Grid system on rubber block

9.2.2) Orthotropic material.

9.2.2.1) Manufacture of rubber block.

The manufacture of a rubber block for the tests under plane strain conditions, was accomplished in the following steps:

1) The supplied rubber strips (3.5m × 150 mm × 3 mm) were cut into 820 mm long pieces, cleaned with tricloroethylene and neutralized with ammonia.

2) The "basic unit" for the construction of the rubber block consisted of 5 strips of hard rubber and 5 strips of soft rubber glued together in alternating sequence with rubber adhesive. These "basic units" were later glued together in pairs and the process was repeated until the required thickness was attained. This technique of building up the block in steps was followed, so as to avoid excessive loads on the lower layers of the block and undue straining of the soft rubber at the early stages when the adhesive was still in liquid form.

In the final form the block consisted of 83 layers of hard rubber and 82 layers of soft rubber, and had the following dimensions:

Height: 535 mm; width: 820 mm; thickness: ≈ 150 mm.

3) The large surfaces of the rubber block were machined with abrasive paper to remove any irregularities and were then covered with approximately 0.5 mm of Latex (trade name: Revoltex) to obtain a smooth flat surface.

4) A grid, 10 mm square, was drawn on one of the large surfaces of the block with white rubber paint. (see Plate 9.2).

9.2.2.2) Prediction of elastic constants.

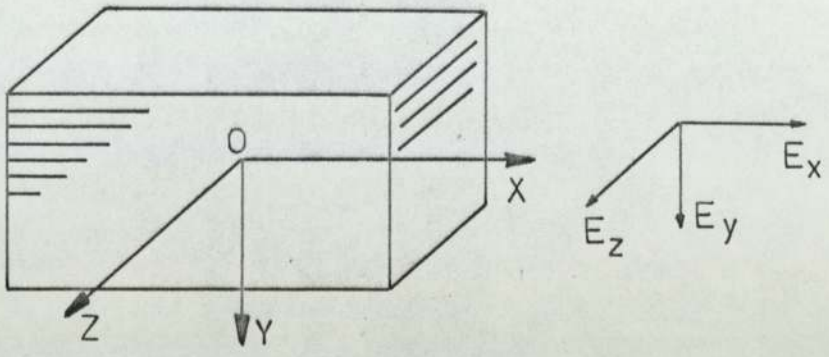

Fig.9.3

The notation for the elastic constants of the rubber block is as follows:

E_x : Young's modulus in the direction parallel to the layers.

E_y : Young's modulus in the direction normal to the layers (see Fig.9.3).

Since the material is transversely isotropic, we have $E_x = E_z$.

Employing the mechanics of materials approach (see Section 2.10) and since the volume fractions of hard and soft rubbers are approximately the same, we have:

$$E_x = \frac{E_h+E_s}{2} = 5.05 \text{ N/mm}^2 , \quad \nu_{xy} = \frac{\nu_h+\nu_s}{2} = 0.48,$$

$$E_y = \frac{2E_hE_s}{E_h+E_s} = 4.13 \text{ N/mm}^2 , \quad \nu_{yx} = \nu_{xy}\frac{E_y}{E_x} = 0.39,$$

$$G_{xy} = \frac{2G_hG_s}{G_h+G_s} = 1.43 \text{ N/mm}^2 \text{ (see also Table 9.2a)}$$

9.2.2.3) Experimental determination of elastic constants.

Four of the five elastic constants required for the complete description of elastic behaviour of the transversely isotropic rubber block were determined experimentally

9.2.2.3) contd.

while the fifth one (modulus of rigidity G_{xy}) was obtained by the 'law of mixtures' from the elastic properties of the constituent materials (equation 2.10-8).

Specially manufactured rubber samples (45 × 45 × 27 mm), identical to the large rubber block, were subjected to compressive loads at a constant rate of strain (0.1524 mm/min) along one of the principal directions. The Young's modulii (E_x, E_y) and the Poisson's ratios (ν_{xy}, ν_{yx}, ν_{xz}) were determined through a procedure, identical to that outlined in section 9.2.1/2.

The results of the tests are listed in Table 9.2a. The elastic compliances ℓ_{ij} and the orthotropic constants k_1 and k_2 of the material are listed in Table 9.2b.

Comparing the experimental results with the theoretical predictions (see Section 9.2.2.2) we observe that the theory overestimated E_x by 7.5%, E_y by 5.5%, and underestimated ν_{yx} by 5%.

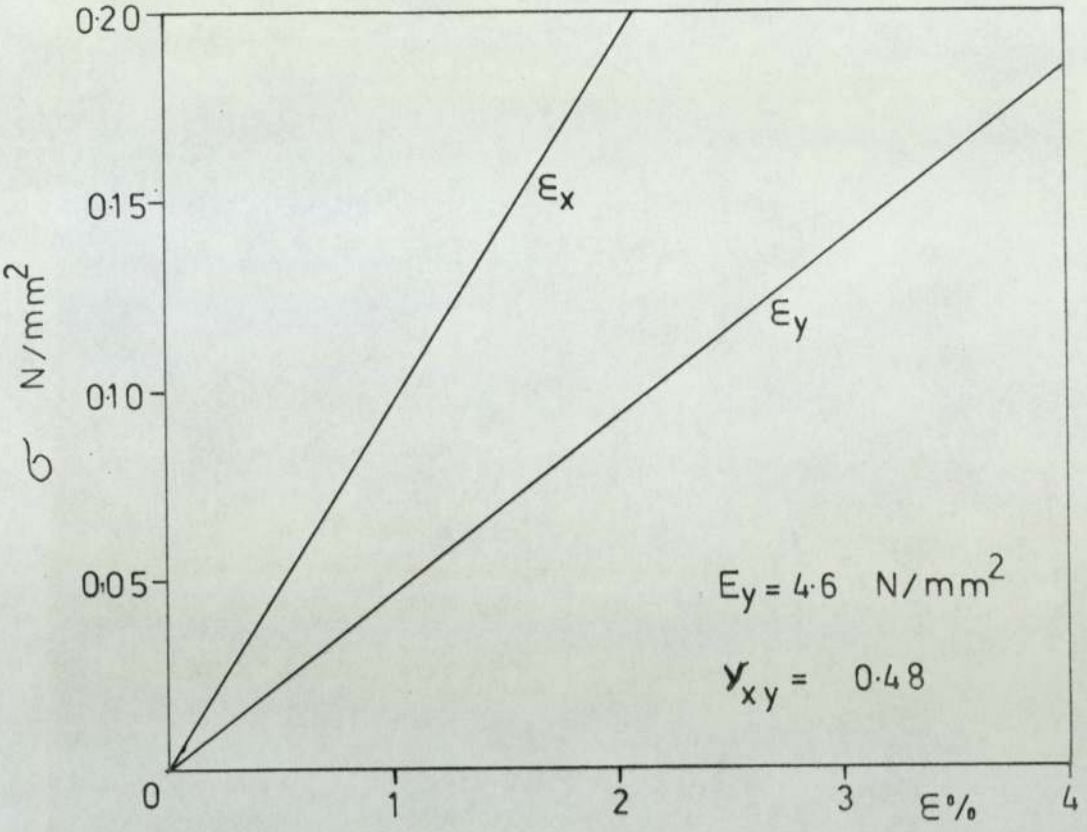

FIG.9.2a Stress vs strain
Laminated rubber — E_y

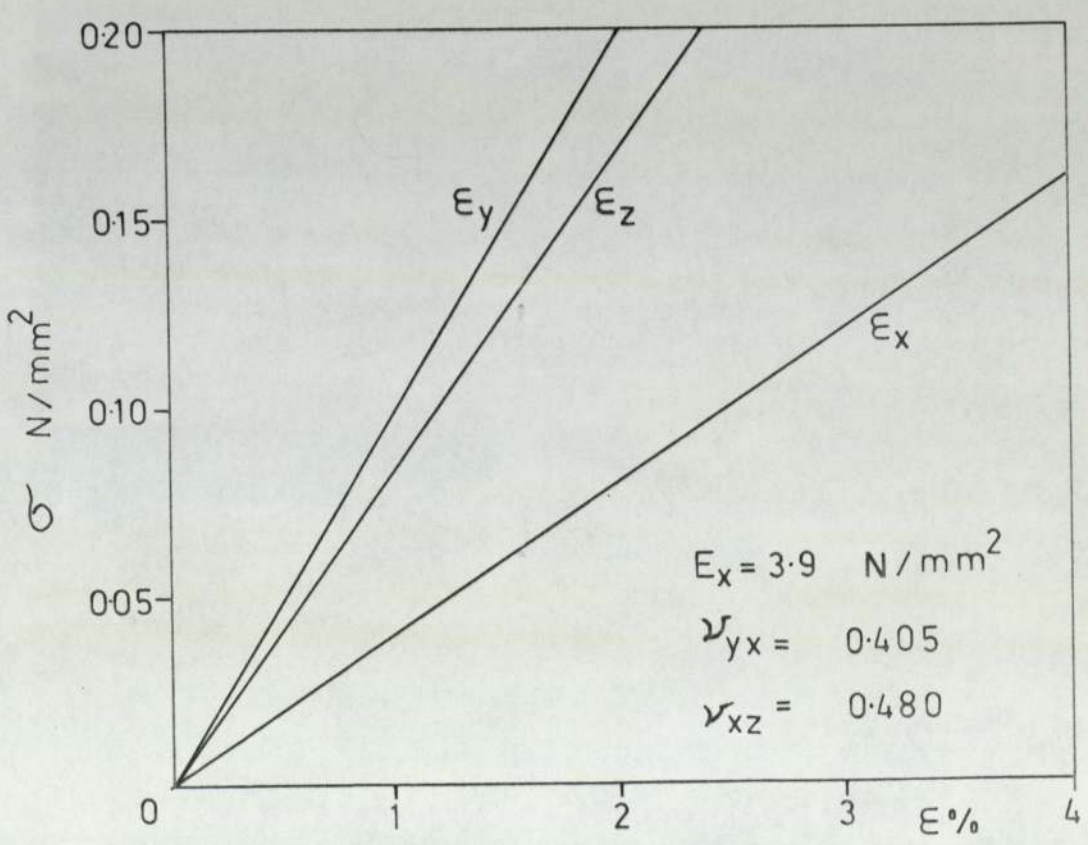

FIG.9.2b Stress vs strain
Laminated rubber — E_x

TABLE 9.2 a

	Theory	Tests	No of tests	S. D.
E_x	5·05	4·60	8	±0·06
E_y	4·14	3·90	11	±0·1
ν_{xy}	0·48	0·48	4	—
ν_{yx}	0·40	0·41	11	±0·01
ν_{xz}	0·48	0·48	4	±0·01
G_{xy}	1·43	1·30	—	—

All dimensional quantities in N/mm^2

TABLE 9.2 b

ℓ_{11}	ℓ_{12}	ℓ_{22}	ℓ_{66}	k_1	k_2
0·1673	-0·1544	0·2277	0·7692	1·332	0·676

All dimensional quantities in mm^2/N

9.2.3) Apparatus.

The apparatus for the plane strain tests consisted of a steel container (tank) to accommodate the rubber block, a 20 mm thick glass plate (1.09 × 0.855 m) and a set of loading devices capable of applying the concentrated force, the uniformly distributed stress and the "rigid punch" type of load.

1) Steel tank.

The tank was constructed out of 10 mm thick mild steel plates. Drawings of the tank and its dimensions are shown in Fig.9.4 (see also Plates 9.3a and 9.3b).

The front face of the tank consisted of a rectangular frame containing a groove 30 mm. wide and 30 mm. deep. The upper part of the frame could be dismantled so that the glass-plate could be slid into its position.

The rear plate of the tank was stiffened with four 25.4 × 25.4 mm^2 steel bars and the interior surface was covered with a layer of formica to improve its frictionless characteristics.

2) Loading devices.

As was mentioned previously, three types of loads were considered.

The loads were applied on to the material through a cylinder (20 mm in diameter and 150 mm long) for the concentrated force problem, and through a rigid plate (100 × 150 × 20 mm) for the rigid punch problem (see Plate 9.4a). In both cases a T-beam lever (4:1 ratio) was used for the application of loads (see Plates 9.3a and 9.3b).

The uniformly distributed load was applied through a specially designed pressure cell (see Fig.9.5 and

9.2.3) contd.

2) contd.

Plate 9.4b). The cell was made out of brass and it could be used with air, water or oil, but air was chosen as the pressurising medium.

A membrane, through which the pressure would be transmitted on to the material, was moulded to fit exactly the interior of the cell.

The vertical sides of the cell were made into sharp edges, so that the loaded area could be determined more accurately. In addition, two of the vertical sides were made of two separate plates P1 and P2 (see Fig.9.5). The inner plate P1 was part of the basic cell, while the outer one P2 was capable of sliding over P1 and follow the deformation of the material and the expansion of the membrane. That enabled a constant width of the applied pressure to be maintained at all stages of loading.

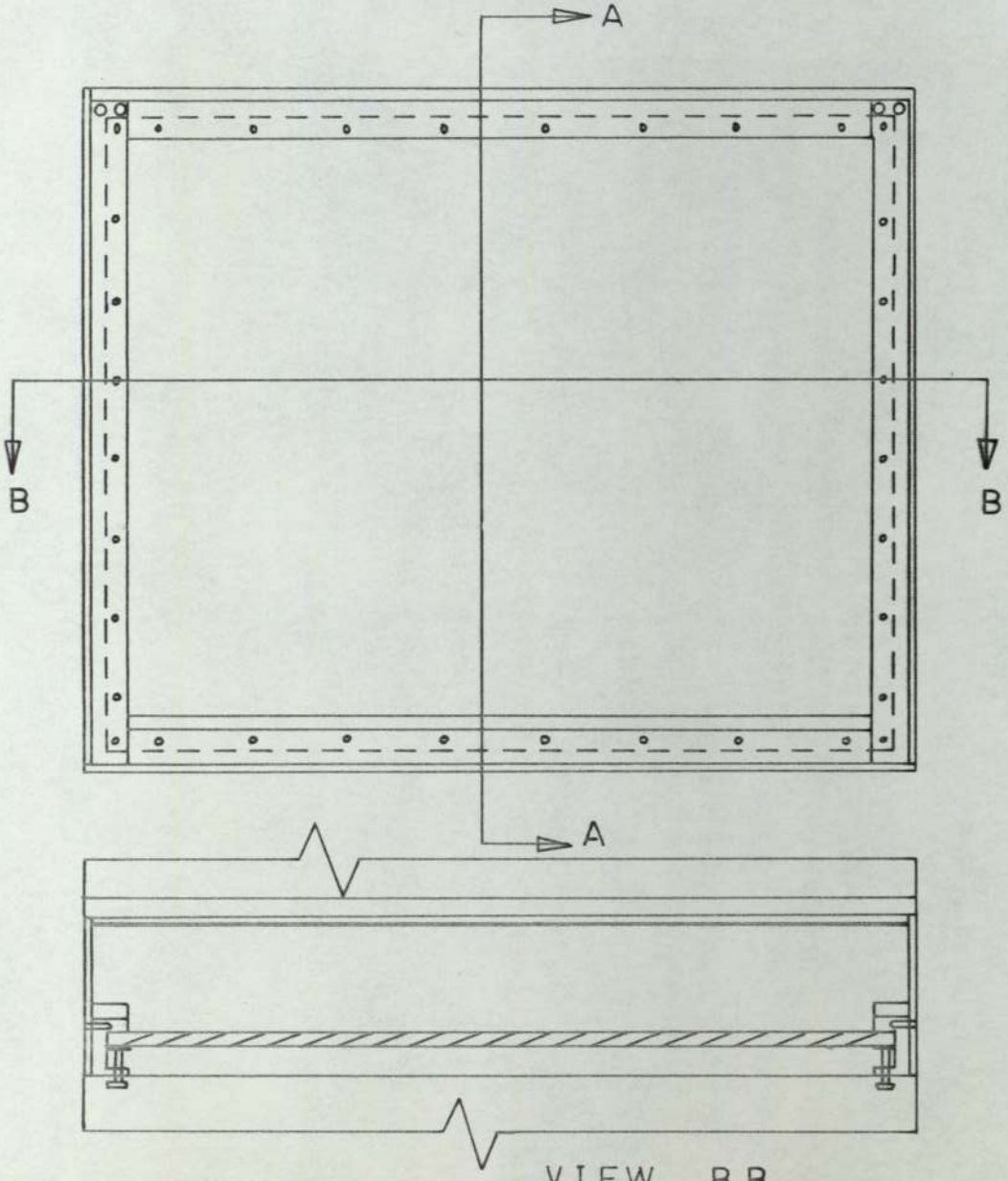

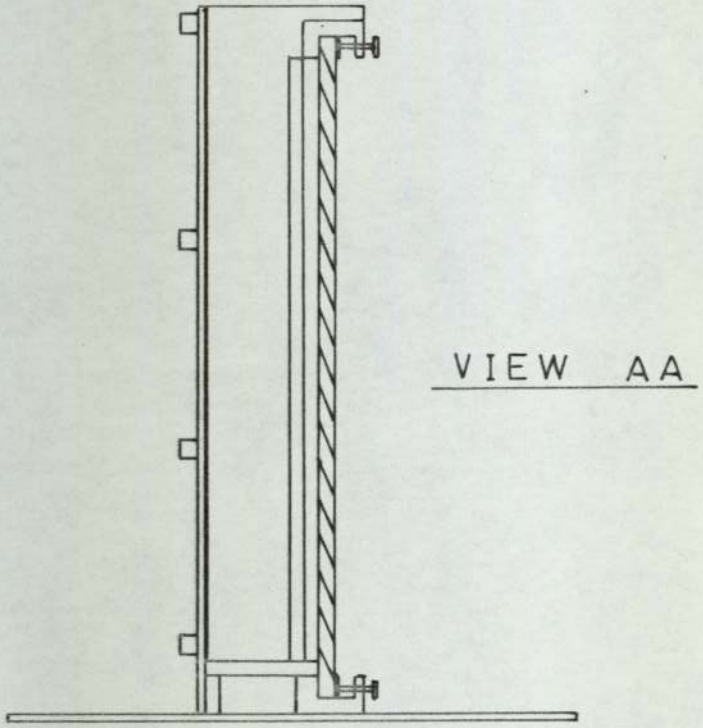

SCALE 1:10

FIG. 9.4 Steel tank

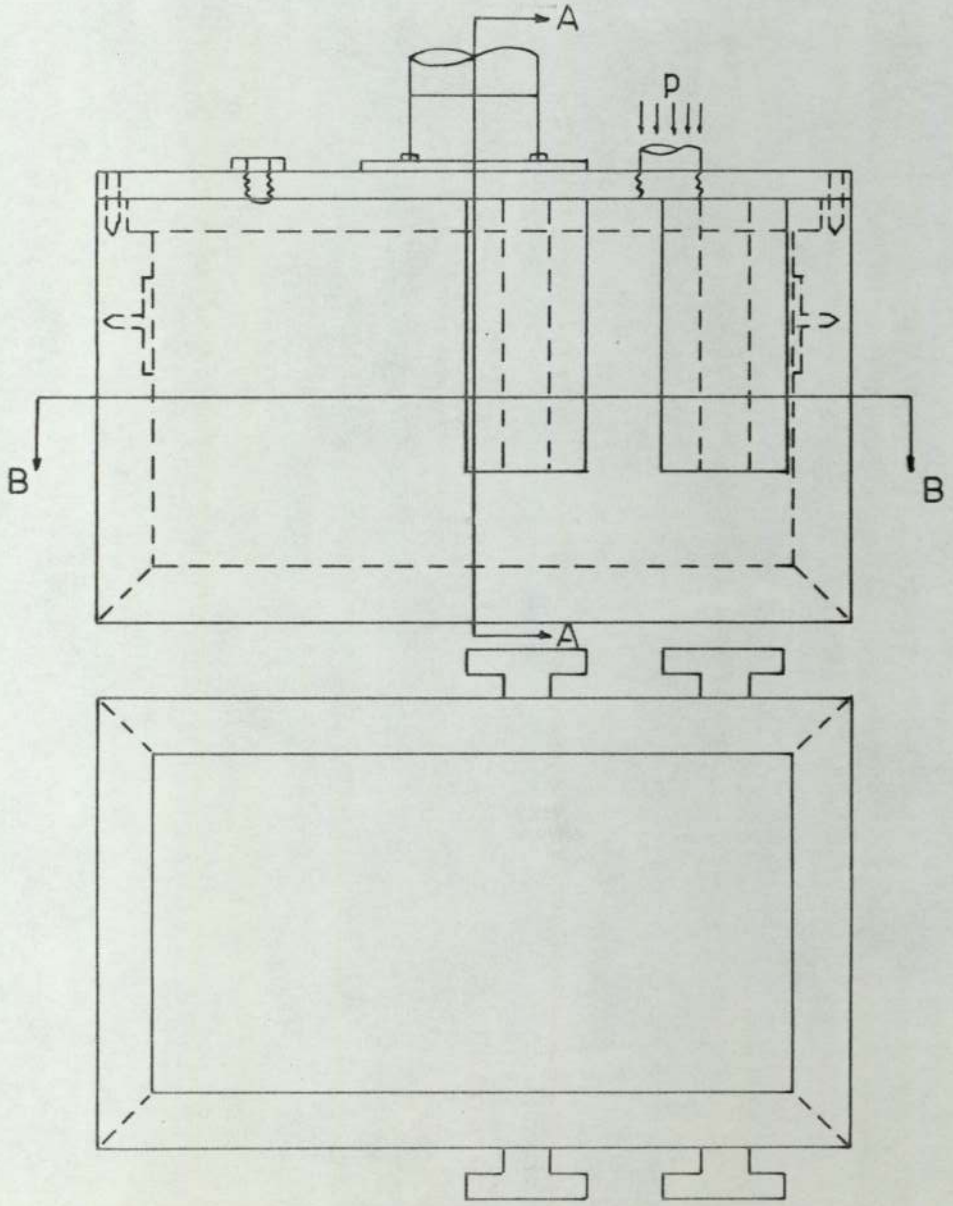

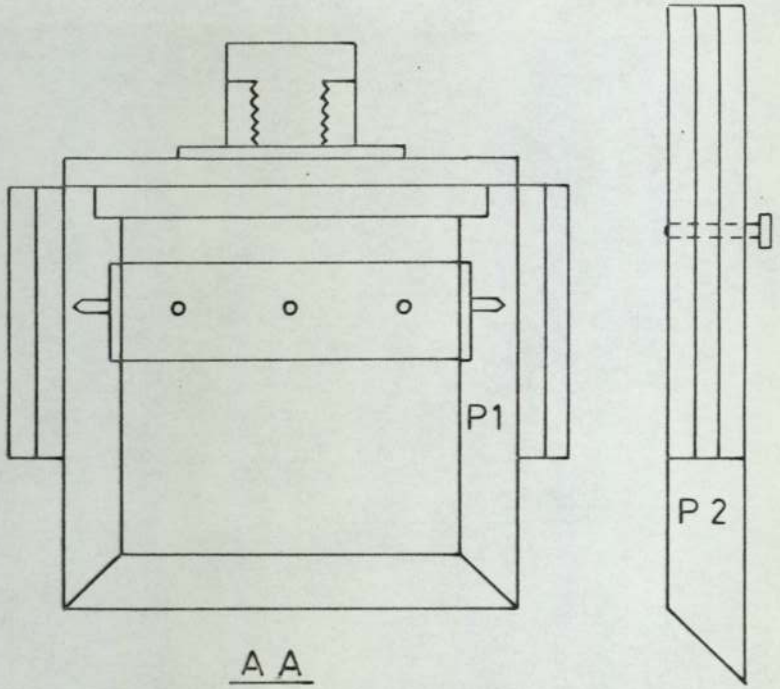

FIG. 9.5

PRESSURE CELL

Scale 2:3

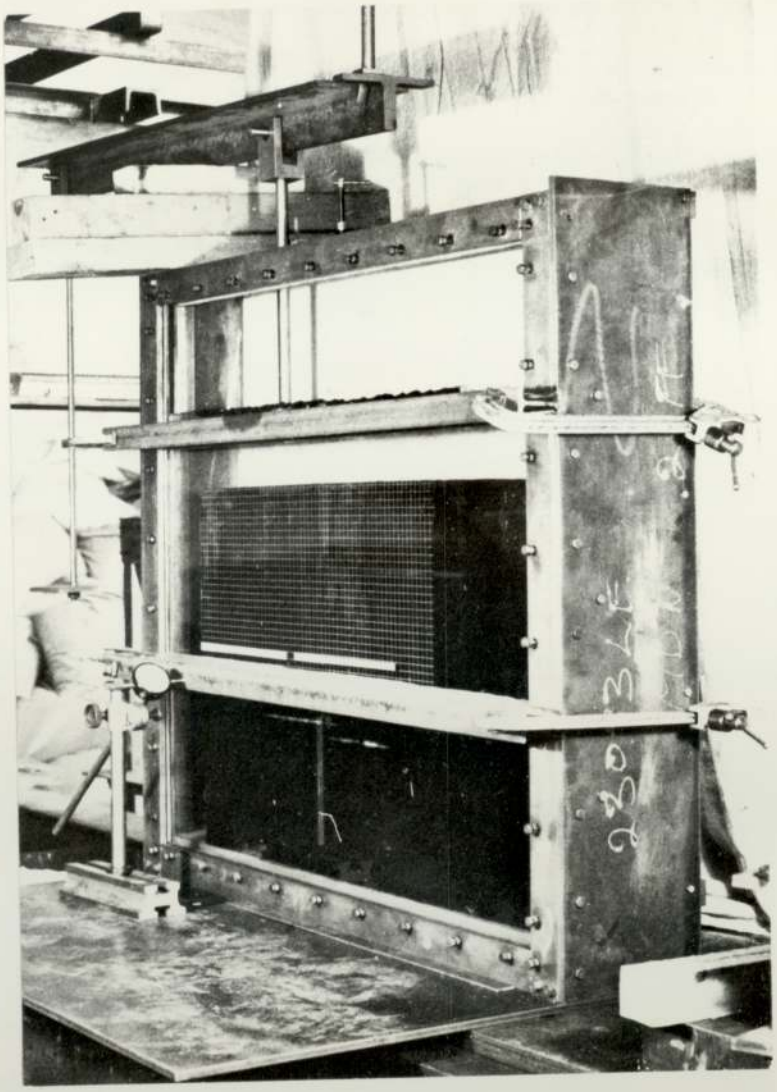

PLATE 9.3a Steel tank

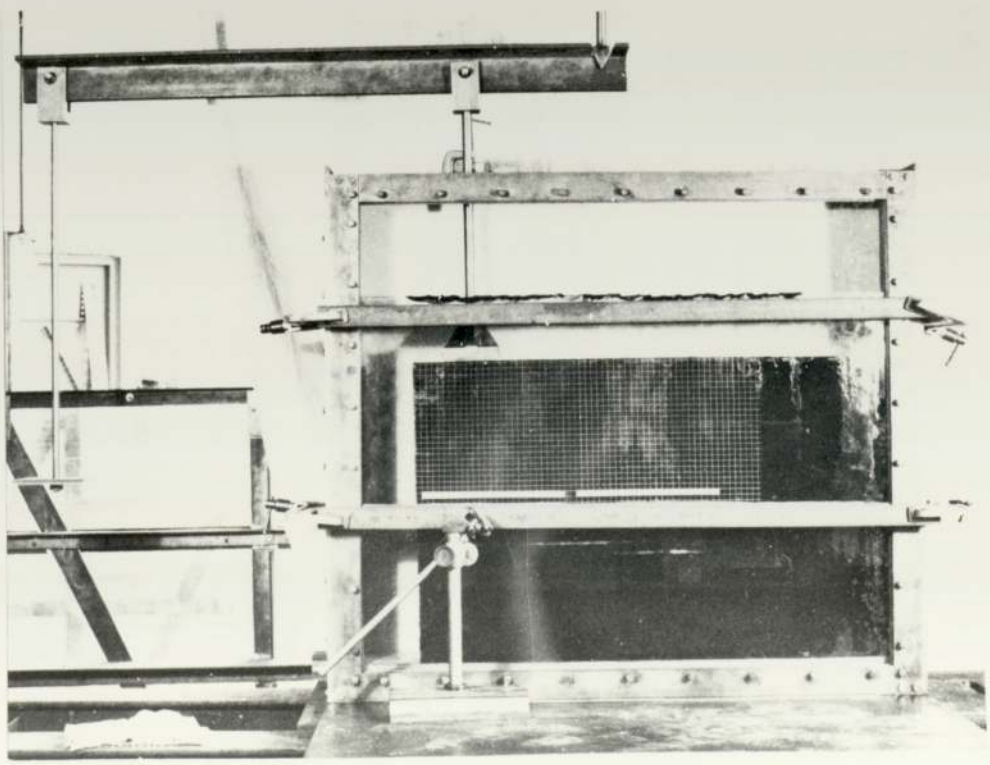

PLATE 9.3b Steel tank and 4:1 lever.

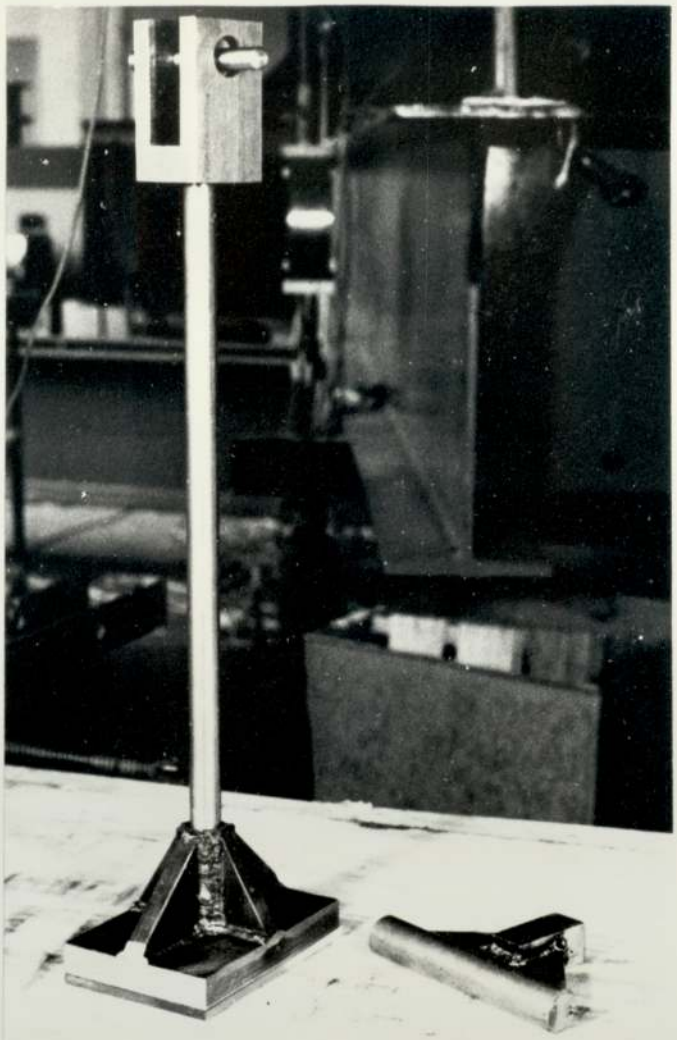

PLATE 9.4a Loading devices

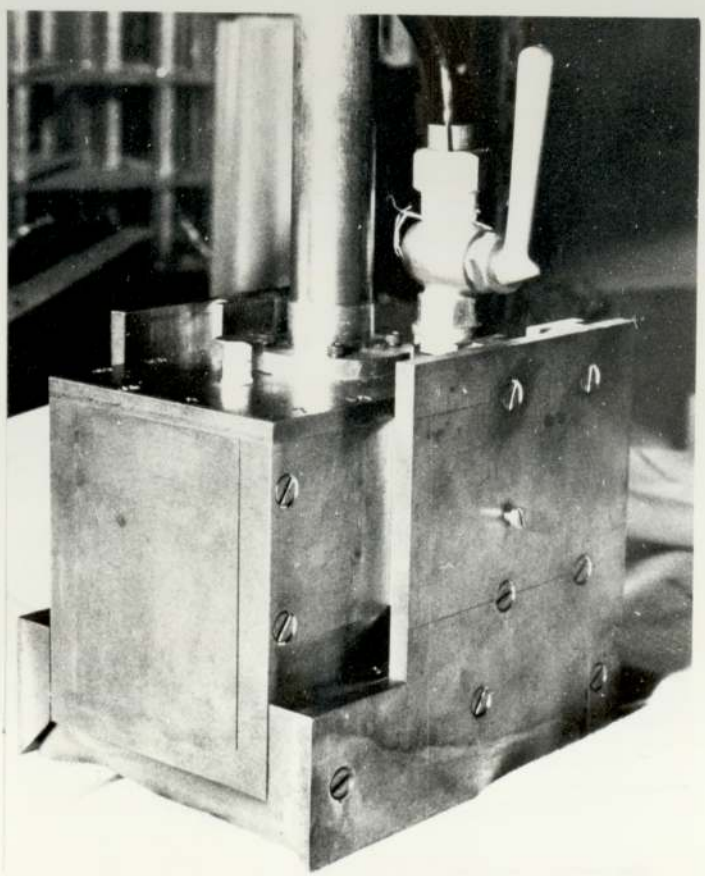

PLATE 9.4b Pressure cell.

9.2.4) Method of testing.

The surfaces of the rubber block and the internal surfaces of the steel tank were lubricated with silicon grease to minimize the friction between the rubber and the glass and metal surfaces. The block was then placed in the steel tank and the glass plate was slid into position and secured with the fixing screws. Two I-beams (38.1 × 76.2 mm) were placed at the front of the steel tank (see Plates 9.3a and 9.3b) to reduce the lateral deflection of the glass plate during loading.

The actual testing under any of the three loading systems was accomplished in the following steps:

1) The appropriate loading device was fixed into position (at the centre of the rubber block for "half-plane" problems or near a corner for "quarter-plane" problems), and the thickness of the rubber block was measured with a large micrometer.
2) Two dial gauges were positioned, one at the front and one at the rear of the steel tank to record any lateral deformations and the initial readings were taken.
3) A camera (Hassleblad 500C) was fixed 500 mm from the steel tank, opposite the region of application of loading, and an initial photograph of the grid was taken (see Plate 9.5).
4) The load was then applied in steps and for each step a photograph of the deforming grid was taken and the readings of the dial gauges were recorded.

The load increments, the maximum attainable loads and the maximum strains in the Z and Y directions, for each type of load, are shown in Table 9.3.

Photographs of the deformed grid under the various types of load are shown in Plates 9.6-9.11

9.2.4) contd.

4) contd.

TABLE 9.3

Problem	Loading Condition	Load increment	Maximum Load	Maximum ε_z	Maximum ε_y
Half plane	C.L.	20.4 kg.	300 kg	0.0009	0.1169
	R.P.	32 kg	415 kg	0.0012	0.0155
	U.D.L.	34.5 kN/m^2	242 kN/m^2	0.0018	0.0155
Quarter plane	C.L.	20.4 kg.	320 kg	0.0010	0.1082
	R.P.	32 kg	392 kg	0.0011	0.0229
	U.D.L.	34.5 kN/m^2	172.5 kN/m^2	0.0017	0.0275

where

C.L. : Concentrated load

R.P. : Rigid punch.

U.D.L. : Uniformly distributed load.

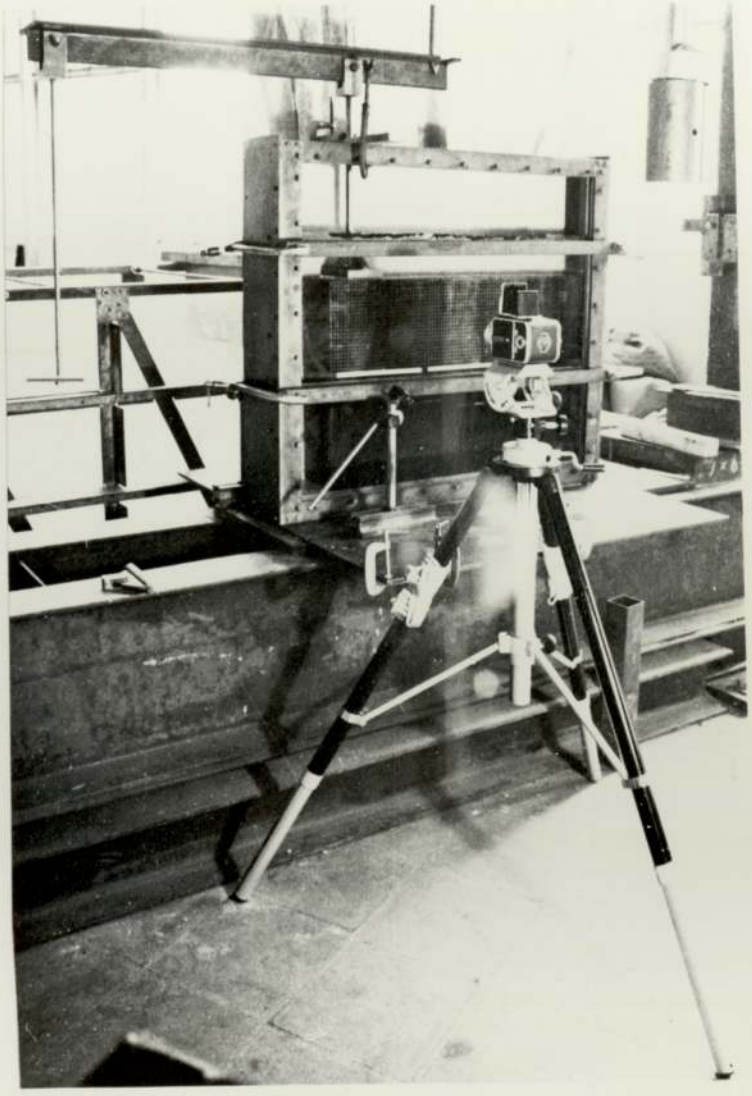

PLATE 9.5 Apparatus for plane strain tests.

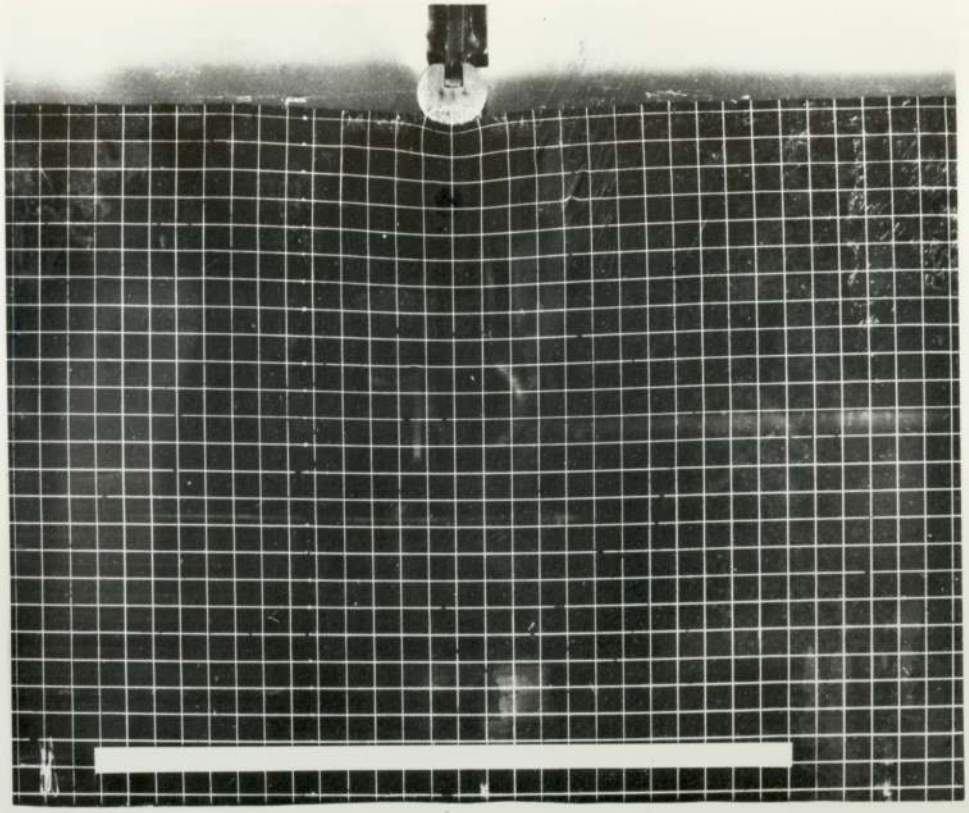

PLATE 9.6 Half-plane; concentrated force

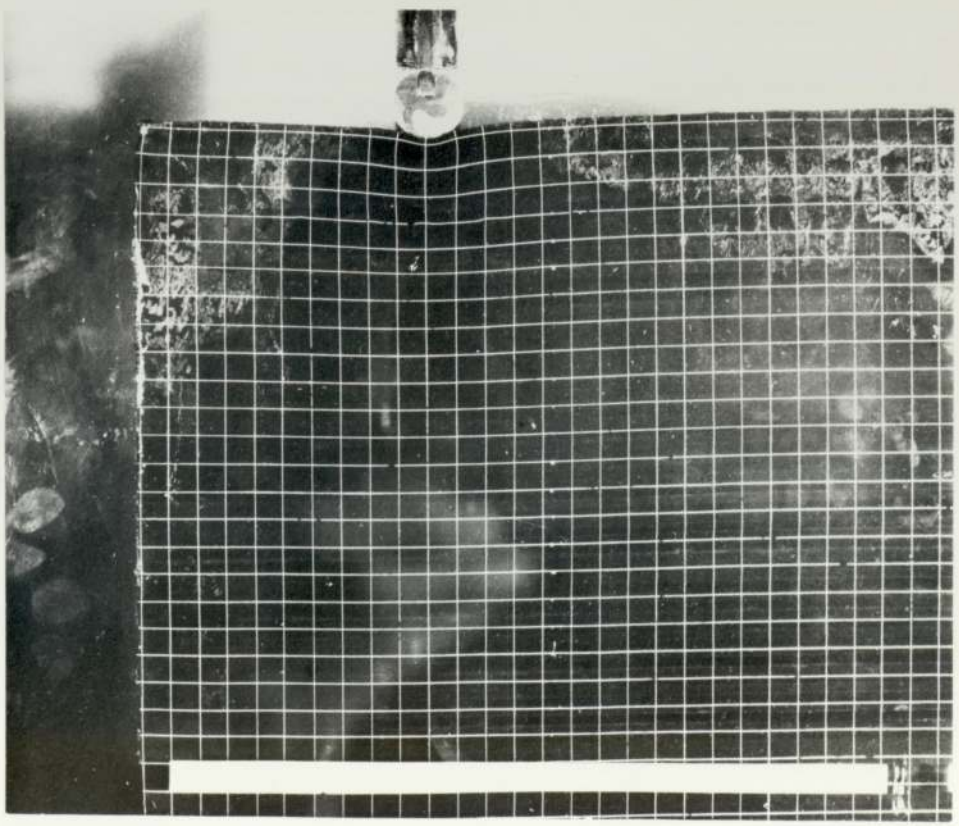

PLATE 9.7 Quarter-plane; concentrated force.

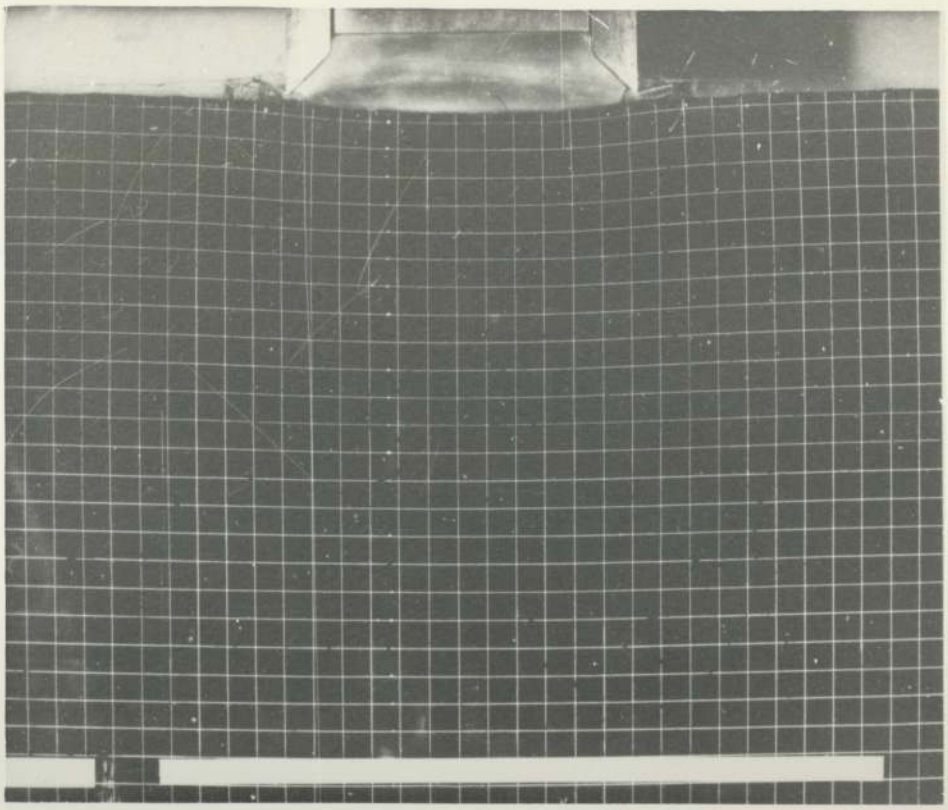

PLATE 9.8 Half-plane; uniformly distributed load.

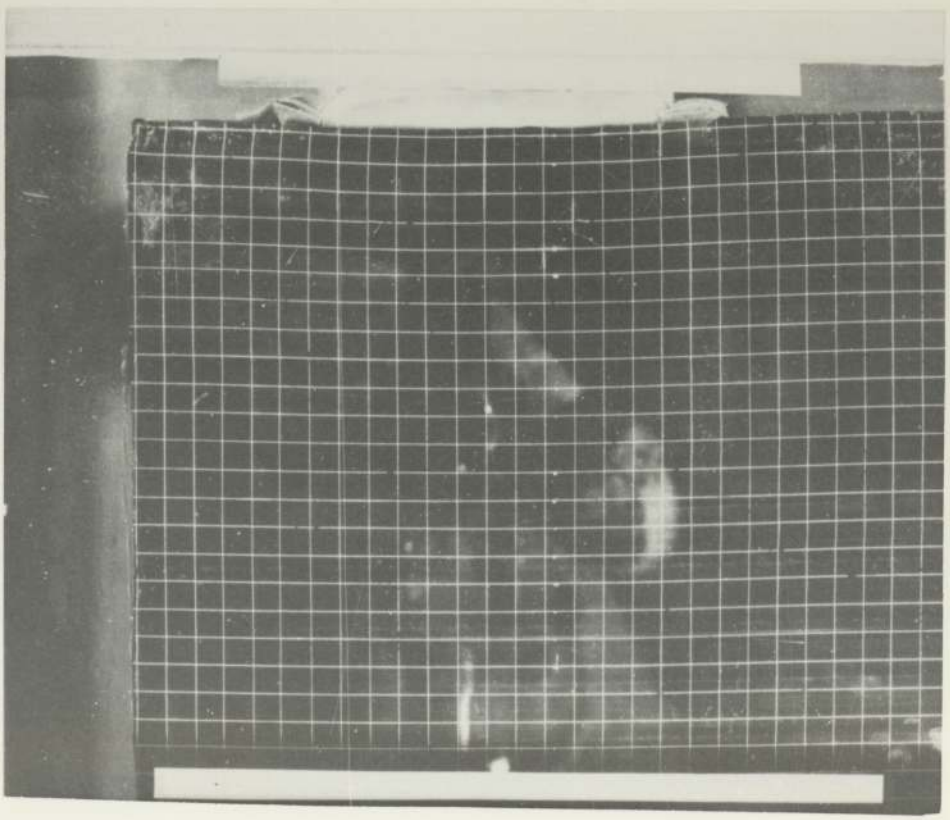

PLATE 9.9 Quarter-plane; uniformly distributed load.

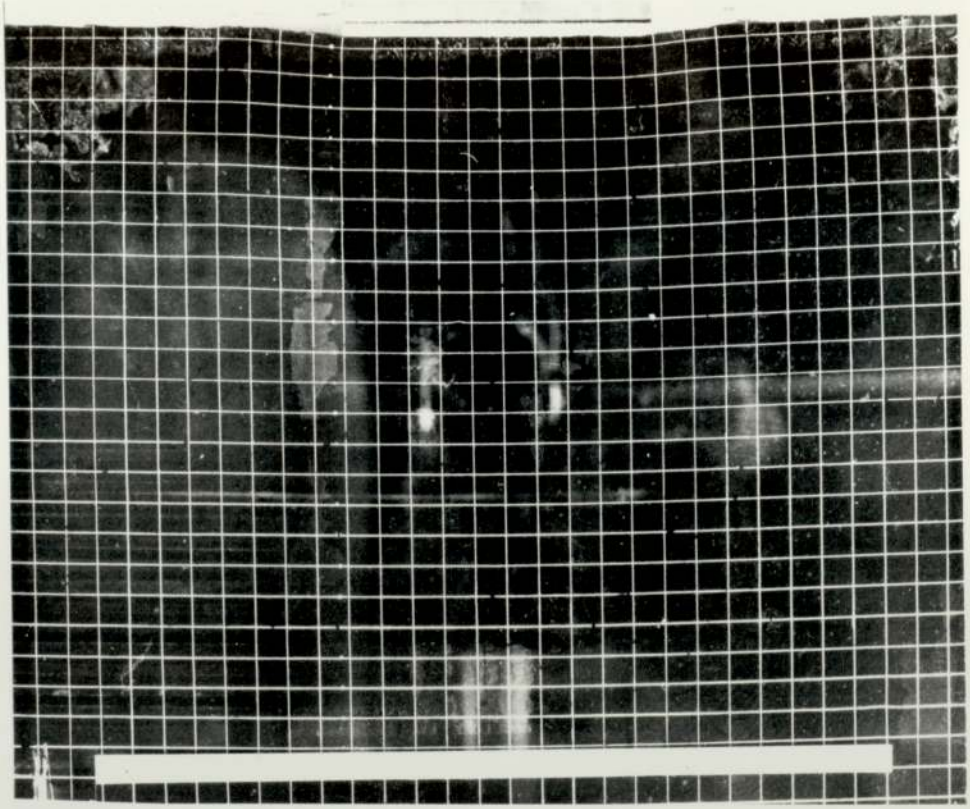

PLATE 9.10 Half-plane; rigid punch.

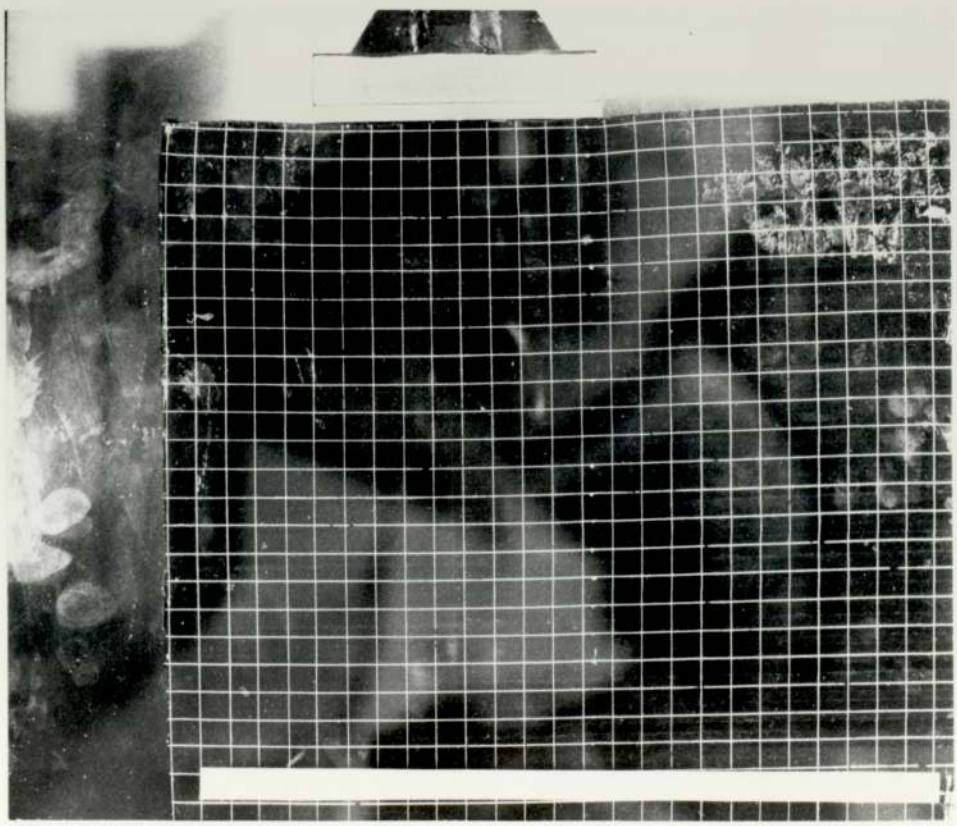

PLATE 9.11 Quarter-plane; rigid punch.

9.2.5) Analysis of test results.

9.2.5.1) Method of analysis.

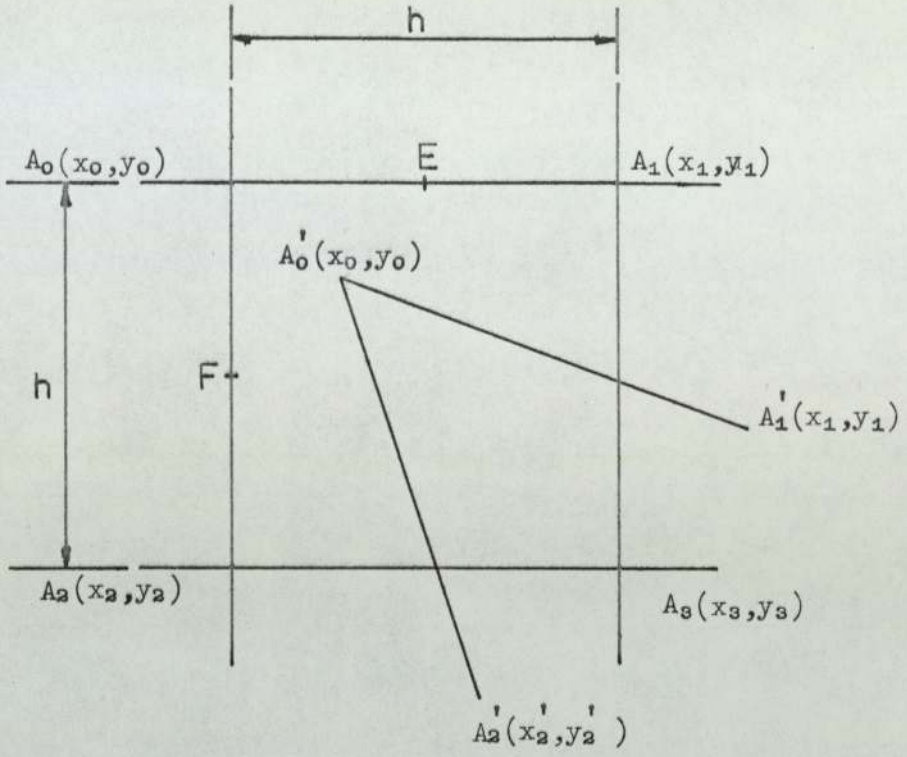

Fig.9.6

In each test, the strains induced in the material by the loading system were determined from the deformation of the grid which was drawn on the material (see Section 9.2.2.1).

Let A_0, A_1, A_2, A_3, be the points (nodes) at the corners of an element of the grid when the rubber block is in its unloaded state and A_0', A_1', A_2', A_3' the respective points after the application of the first load increment (see Fig.9.6).

The length of sides of the element 'h' is assumed to be sufficiently small, so that the variation of displacement between the points A_0' and A_1', or A_0' and A_2' can be assumed linear.

Then, the strain ε_x at point E (the mid-point

9.2.5.1) contd.

of A_0A_1) is given by:

$$\varepsilon_x(x,y) = \frac{(x_1'-x_0')-(x_1-x_0)}{(x_1-x_0)} \quad , \qquad 9.2.5\text{-}1$$

where

$$x = \frac{x_0+x_1}{2} \quad , \quad y = \frac{y_0+y_1}{2} \quad .$$

Similarly, the strain ε_y at point F (the mid-point of A_0A_2) is given by:

$$\varepsilon_y(x,y) = \frac{(y_2'-y_0')-(y_2-y_0)}{(y_2-y_0)} \quad , \qquad 9.2.5\text{-}2$$

where

$$x = \frac{x_0+x_2}{2} \quad , \quad y = \frac{y_0+y_2}{2} \quad .$$

Using such a procedure, it was possible to determine the strains at a number of points on the grid system.

The coordinates of the nodes, for each load increment, were determined from the corresponding photograph of the grid, using a "Universal Wild Plotter". From the results, the lengths of the sides of each element were calculated and plotted against the applied load. Then, the ratios of strain/load were determined from the slope of the curves.

9.2.5.2) Accuracy and errors.

All the tests under plane strain conditions involved the measurement of loads (either the total load or the pressure) and the measurement of lengths. The accuracy of the results was influenced by the accuracy with which the loads and displacements were measured.

In addition, the conditions under which the

9.2.5.2) contd.

tests were carried out should satisfy the assumptions made by the relevant theory. Any discrepancies would affect the results by introducing errors. In many cases the errors could not be eliminated but only minimized, and then it became necessary to consider their effects on the final results.

We concentrate first on the accuracy involved in the various measurements.

a) Measurement of loads.

Total loads presented no problem, since they were static loads applied on to the material through a 4:1 lever. The experimental set up ensured that friction at the pivots or supports would be minimal, and, compared with loads varying from 20 kg to 300 kg could be assumed to be negligible. Pressure was measured with a Budenberg oil pressure gauge to an accuracy of $\pm$ 0.00172 N/mm^2.

b) Measurement of lengths.

The Universal Wild Plotter that was used for measuring the dimensions of the grid elements, was accurate to 0.01 mm. With the camera positioned at 520 mm from the grid, an area of 240 x 240 mm^2 was imprinted on 25.4 x 25.4 mm^2 of film. For approximately 4:1 enlargements, 10 mm on the grid were equivalent to 4.6 mm on the prints. It follows then, that stains over an average length of 4.6 mm could be measured to an accuracy of $\pm$ 0.22%.

9.2.5.2) contd.

The main sources of error encounted in the plane strain tests are discussed in the following paragraphs.

1) Refraction in the glass plate.

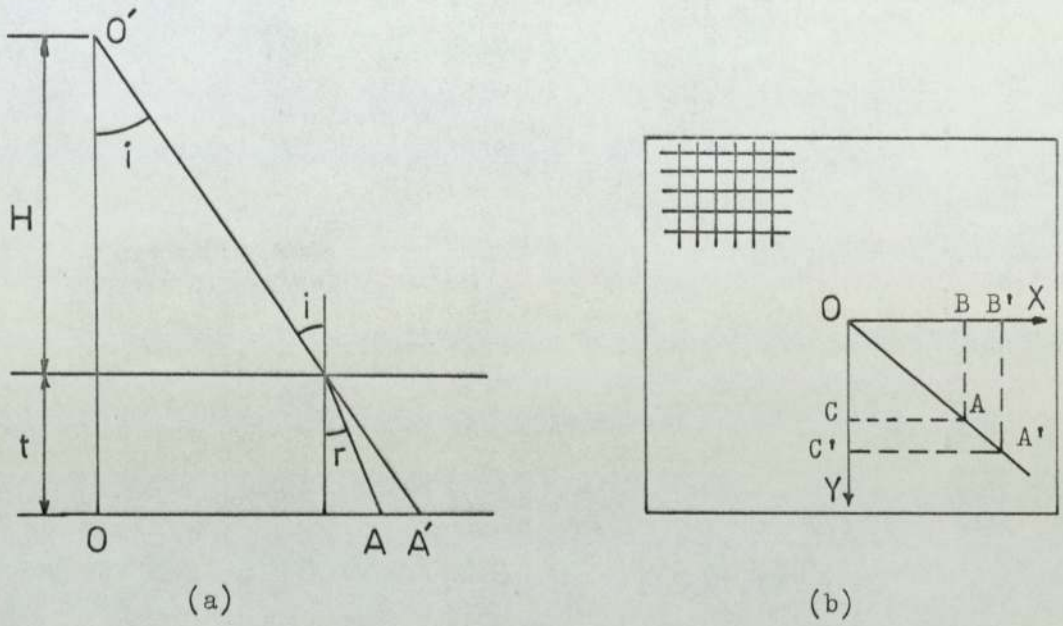

(a) (b)

Fig.9.7

Due to defraction of light in the 20 mm thick glass plate at the front of the steel tank, the nodes of the grid appeared to be in a different position than they actually were (see Fig.9.7a) and therefore the image of the grid imprinted on the film of the camera was distorted.

Consider point A in Fig.9.7a and b. A, which is assumed to represent a node of the grid, would appear to be in position A' on the line OA, where O is the projection of the centre of the camera on to the plane of the grid. The apparent displacement AA' of point A, is a function of distance OA, the refractive index (μ) and the thickness of the glass (t), and, the distance of the camera from the glass-plate (H).

For small angles of incidence (i) (see Fig.9.7a), when

9.2.5.2) contd.

1) contd.

$$\mu = \frac{\sin i}{\sin r} \approx \frac{\tan i}{\tan r}, \qquad 9.2.5\text{-}3$$

where r is the angle of refraction,

AA' is given by the following relation:

$$AA' = OA \left[\frac{t(\mu-1)}{H\mu + t}\right]. \qquad 9.2.5\text{-}4$$

Therefore, AA' is maximum for points near the corners of the grid, where OA is maximum.

AA' can be analysed into its components BB' and CC' along the X and Y axes, so that the apparent displacements of point A relative to the coordinate axes X,Y can be found.

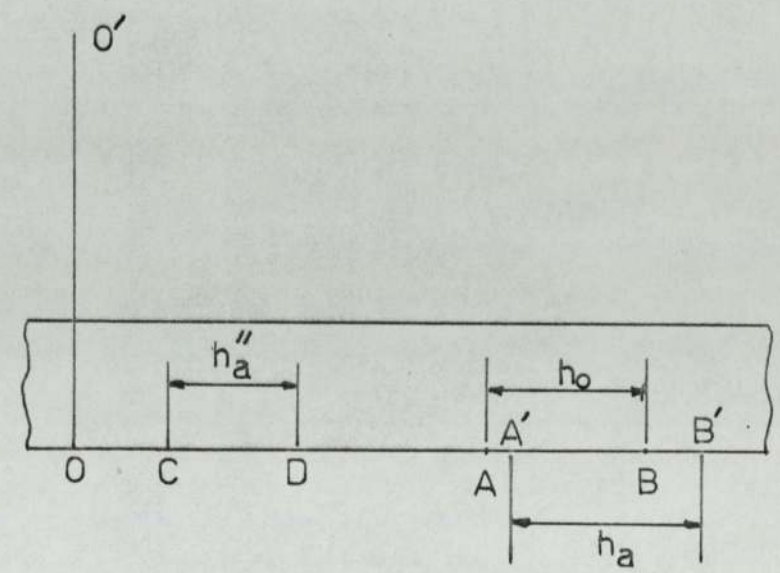

Fig.9.8

We now refer to Fig.9.8. Let A and B be two adjacent nodes of the grid, distance h_o apart, in the initial unloaded state. Due to refraction, they would appear as points A' and B' respectively, distance h_a apart. After the application of a load increment, h_o changes to h_o'. Then, according to the convention that compressive strains are assumed positive:

9.2.5.2) contd.

1) contd.

$$\varepsilon = \frac{h_o - h_o'}{h_o} \qquad 9.2.5\text{-}5$$

At this stage we have to distinguish between the following two cases:

a) h_o' remains in the vicinity of h_o, and its apparent length is h_a'. Then,

$$\varepsilon_a = \frac{h_a - h_a'}{h_a} . \qquad 9.2.5\text{-}6$$

The difference between ε and ε_a is the error introduced by the refraction in the glass plate and increases as distance OB (Fig.9.8) gets bigger. For maximum OB (OB $\approx$ 120 mm) and for a maximum strain ε = 10% over a length of 10 mm, the error is of the order of 0.0001%. Errors of this magnitude are insignificant and therefore corrections were not necessary.

b) h_o' undergoes a rigid body movement to points C-D (see Fig.9.8). This occurs to grid elements in the vicinity of the applied loads. Then, for an apparent length h_a'', the strain is given by:

$$\varepsilon_a' = \frac{h_a - h_a''}{h_a} . \qquad 9.2.5\text{-}7$$

For a maximum rigid body displacement of 15 mm, and for a strain ε = 10% over a distance of 10 mm, the error introduced is of the order of 0.1%. Therefore, for rigid body displacements of more than 5 mm, a correction was incorporated in the results.

9.2.5.2) contd.

2) Deformation of the grid.

The displacements of the nodes of the grid were determined relative to a fixed pair of axes. The origin and the orientation of these axes were established on each print, from two characteristic marks that had been made on the glass-plate (the uppermost corners of the white tape; see plate 9.2). The axes of the plotter were made to coincide with the coordinate axes of the print. The marker of the plotter was then brought over a node of the grid and its coordinates were determined.

In measurements like this, errors frequently occur in the process of placing the marker over the nodes (usually classified as a human error). Errors of this type were accounted for, by plotting the lengths of adjacent grid elements against the applied load on the same graph (see Fig.9.9). The errors were then determined by visual inspection of the curves. In addition, the slope of each curve was determined by a 'least square' technique.

3) Displacement in the Z-direction.

As discussed in Section 9.2.4, some deformation of the material was observed in the Z-direction, i.e. the direction along which the displacements are assumed to be zero, for plane strain conditions to exist.

The maximum observed strains ε_z, at a point near the point of application of the loads (for both concentrated and distributed loadings) are shown in Table 9.3.

Strains of this magnitude (0.1%-0.2%), compared

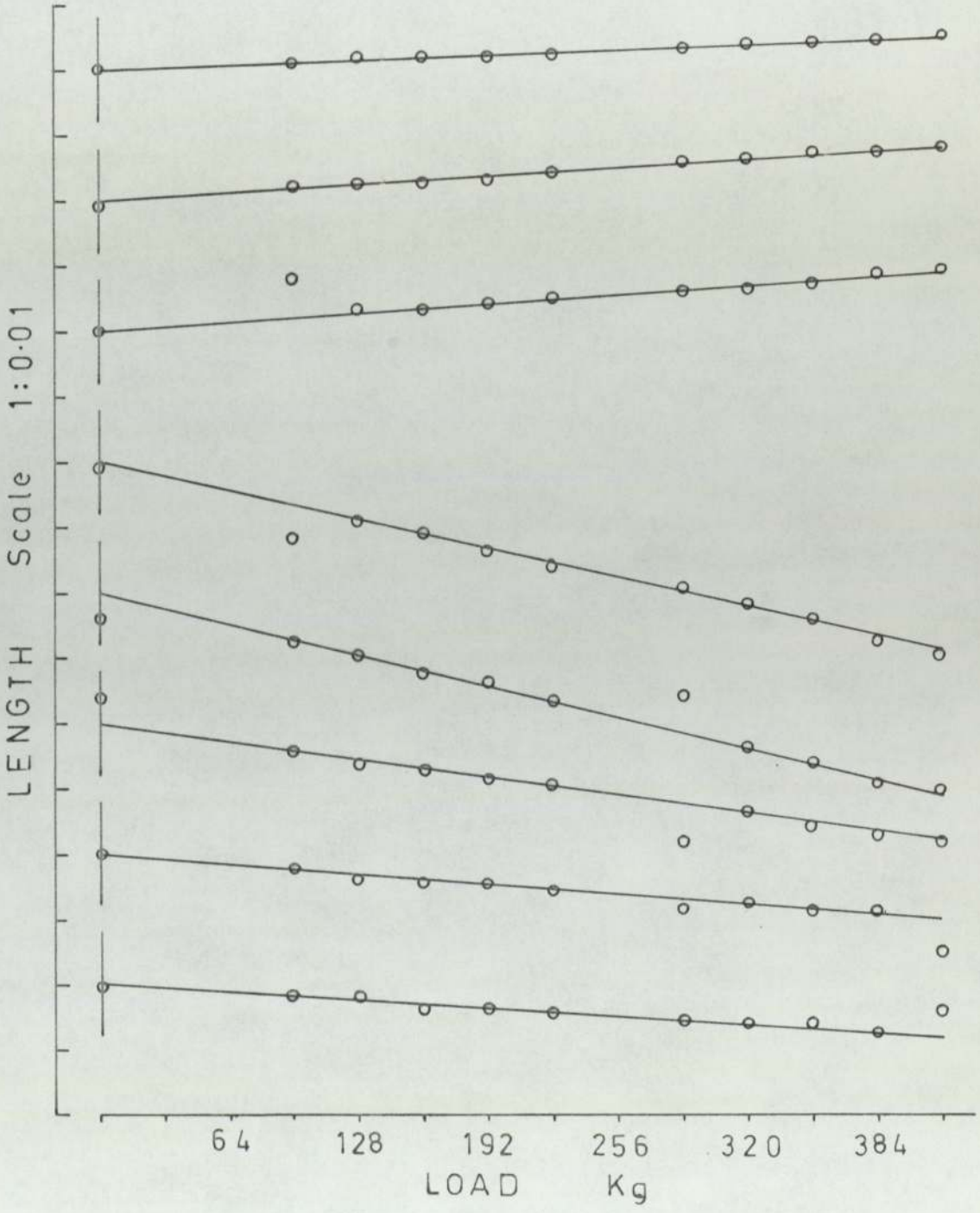

FIG. 9·9

9.2.5.2) contd.

3) contd.

with the corresponding strains in the X or Y directions, which are of the order of 2%-10% can be assumed to be negligible.

4) Shear stresses at the boundaries.

In order to ensure minimum friction at the interfaces between the material and the sides of the tank, all surfaces were lubricated with silicone-grease. The interface between the loading devices and the material was also lubricated to minimize frictional effects.

9.2.6) Presentation of results.

The series of tests that was carried out under plane strain conditions, had as an objective, the experimental determination of strain fields induced in a half-plane or a quarter-plane by the action of externally applied loading systems and a comparison of the results with the strain fields predicted by the relevant theory.

For all the tests, the results are presented as a variation of the strains ε_x/load and ε_y/load, with the dimensionless $\bar{x}$ and $\bar{y}$ coordinates, where $\bar{x}$ and $\bar{y}$ are defined in terms of a characteristic length parameter of the problem. The dimensional quantities (i.e. strain/load), are expressed in units of mm^2/N or N^{-1}.

9.2.6.1) Half-plane/quarter-plane; concentrated force.

Experimental investigation of concentrated force problems, present a difficulty due to the singular behaviour at the point of application of the force and the high stresses associated with it. Rubber-like materials, when subjected to high stresses do not exhibit linearly elastic characteristics and as a consequence the "concentrated force" had to be applied on an area wide enough, so that the stresses in the vicinity of the load should not exceed the linear elastic limit.

Therefore, it was decided to apply the "concentrated force" through a steel cylinder 20 mm. in diameter. The distribution of contact stress was assumed to be uniform and its magnitude was given by the applied load (per unit thickness) over the average length of contact (2ℓ). The length of contact for each loading stage, was measured from the corresponding photograph, and its average value was found to be 12.5 mm, for both the "half-plane" and "quarter-plane" problems.

The results from the test of the "half-plane" problem are shown in Fig.9.10 and 9.11. The half-width of the average contact area (ℓ) was taken as the characteristic length of the problem.

Referring to Fig.9.10, which shows the variation of ε_x with x/ℓ, we observe that there is good correlation between the experimental results and the theoretical curves. Similar correlation is observed in the variation of ε_y with x/ℓ (Fig.9.11), but for

9.2.6.1) contd.

$\bar{x} < 3$ and $\bar{y} < 9$, that is in the vicinity of the applied load, the experimental results deviate considerably from the theoretical curves. In most cases, the observed values of the strain are less than the theoretically predicted ones, thus indicating that the effective length of contact was larger than the assumed average of 12.5 mm.

We now refer to the case in which the concentrated force is applied normal to the boundary of a quarter plane, at distance a = 100 mm. from its apex. In this case 'a' is assumed to be the characteristic length of the problem. The variation of ε_x and ε_y with $\bar{x}$ and $\bar{y}$ is shown in Fig.9.16 and 9.17 respectively.

The theoretical curves were obtained using equations (6.4-1 and 6.2-11). The process of load reversal was carried out 20 times, using 120 slices in the application of Simpson's rule for the numerical evaluation of the integrals (see equations 6.2.9 and 6.2.10). The upper limit of the integrals was taken as 50.

9.2.6.2) Half-plane/quarter-plane; partially distributed uniform load.

In both cases (half-plane and quarter-plane) the half-width of the uniformly distributed load (ℓ = 60 mm) was assumed to be the characteristic length of the problem. The results from the tests are shown in Fig.9.12, 9.13 for the half-plane problem and in Fig.9.18, 9.19 for the quarter-plane one. The load in the ratio strain/load, is the applied pressure 'p', and for consistency in the units it must be given in N/mm^2.

The theoretical curves for the quarter-plane

9.2.6.2) contd.

problem were obtained through equations (2.5-1) and (2.5-2), with 20 reversals of load. 120 slices were used for the numerical evaluation of the integrals with an upper limit of 50.

9.2.6.3) Half-plane/quarter-plane; rigid punch.

In both cases, the half-width of the rigid plate ℓ = 50 mm, was taken as the characteristic length.

The theoretical determination of the stress (and strain) components in a half-plane (or quarter-plane) due to a rigid punch type of load, presented some difficulty for the following reasons:

a) The stresses for the half-plane problem (and for the basic state of stress in the quarter-plane problem) were determined by numerical integraion (see Section 4.6) and therefore were not exact.

b) The pressure under the rigid plate becomes infinite when $x = \pm \ell$ (i.e. $\bar{x} = \pm 1$).

In order to overcome the problems due to the singularity at points $\bar{x} = \pm 1$, it was decided to adopt the following procedure:

The applied pressure was treated as a series of uniform load elements of finite width. The spacing of the elements (and their width), was done on a logarithmic scale, such that the magnitude of the pressure for each load element was given by:

$$p(\bar{x}) = \frac{P}{\pi \sqrt{1 - \bar{x}^2}} \quad ,$$

where $\bar{x} = 1 - \zeta$, for $-\infty < \ell n\, \zeta \leq 0$.

9.2.6.3) contd.

In this way, it was possible to consider load elements as close to $x = \pm 1$ as necessary.

It was found that the best correlation between theory and experiment for the half-plane problem, was obtained for a minimum $\zeta = -2.5$, and a spacing of the elements based on $d\zeta = 0.1$ (i.e. 25 elements). The results for the half-plane problem are shown in Fig.9.14 and 9.15.

The same values for minimum ζ and $d\zeta$ were used for the solution to the quarter-plane problem. The load reversing process was carried out 20 times, with 120 slices and an upper limit of 50. The theoretical curves and the experimental results are shown in Fig.9.20 and 9.21.

In both cases (half-plane and quarter-plane), the strains are presented as a ratio of strain/load, where 'load' is the total concentrated force applied on the rigid plate. For consistency in the units, the force must be given in Newtons (N).

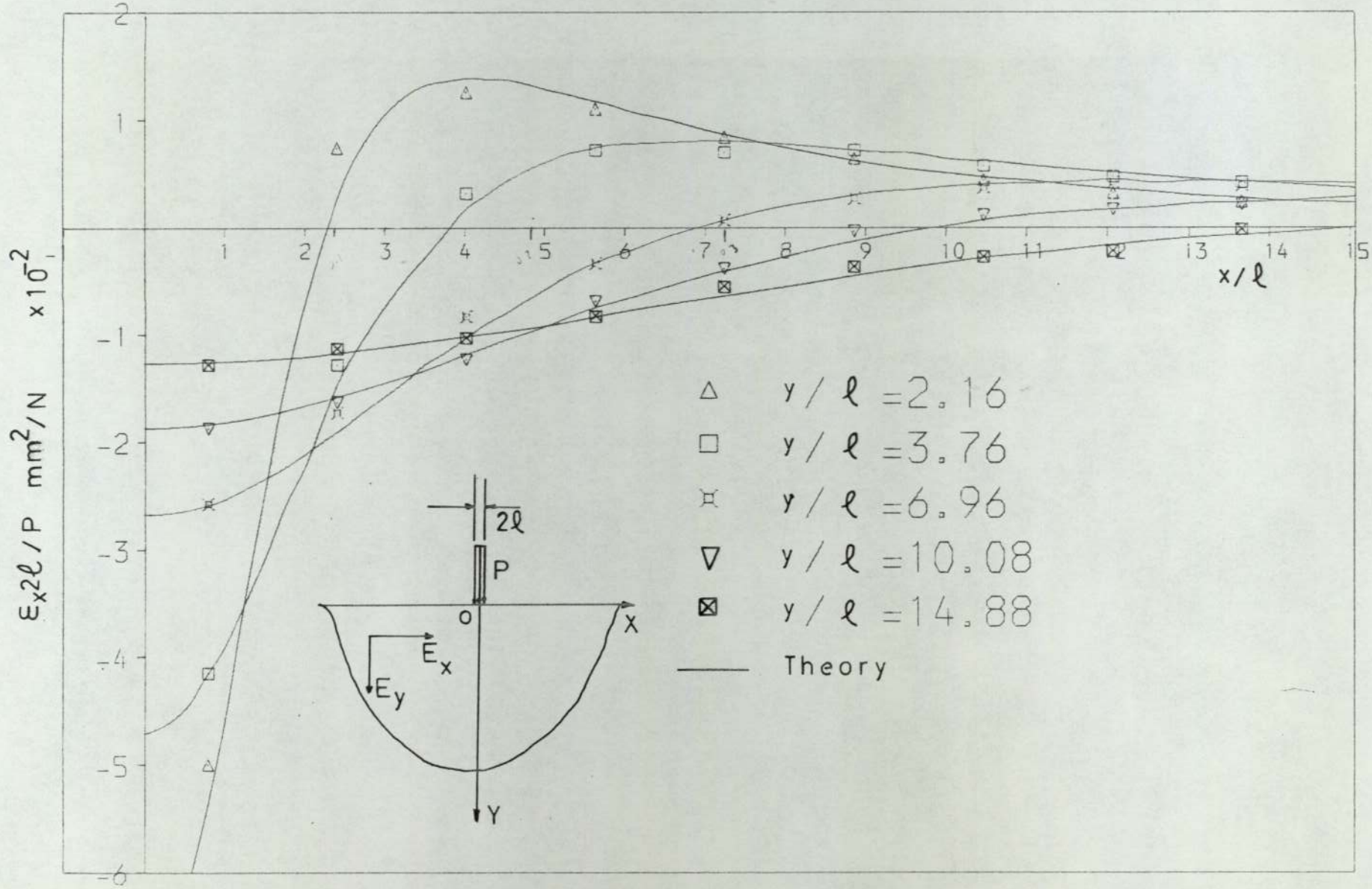

FIG. 9.10 HALF PLANE - CONCENTRATED LOAD - $\varepsilon_x 2\ell/P$ vs x/ℓ

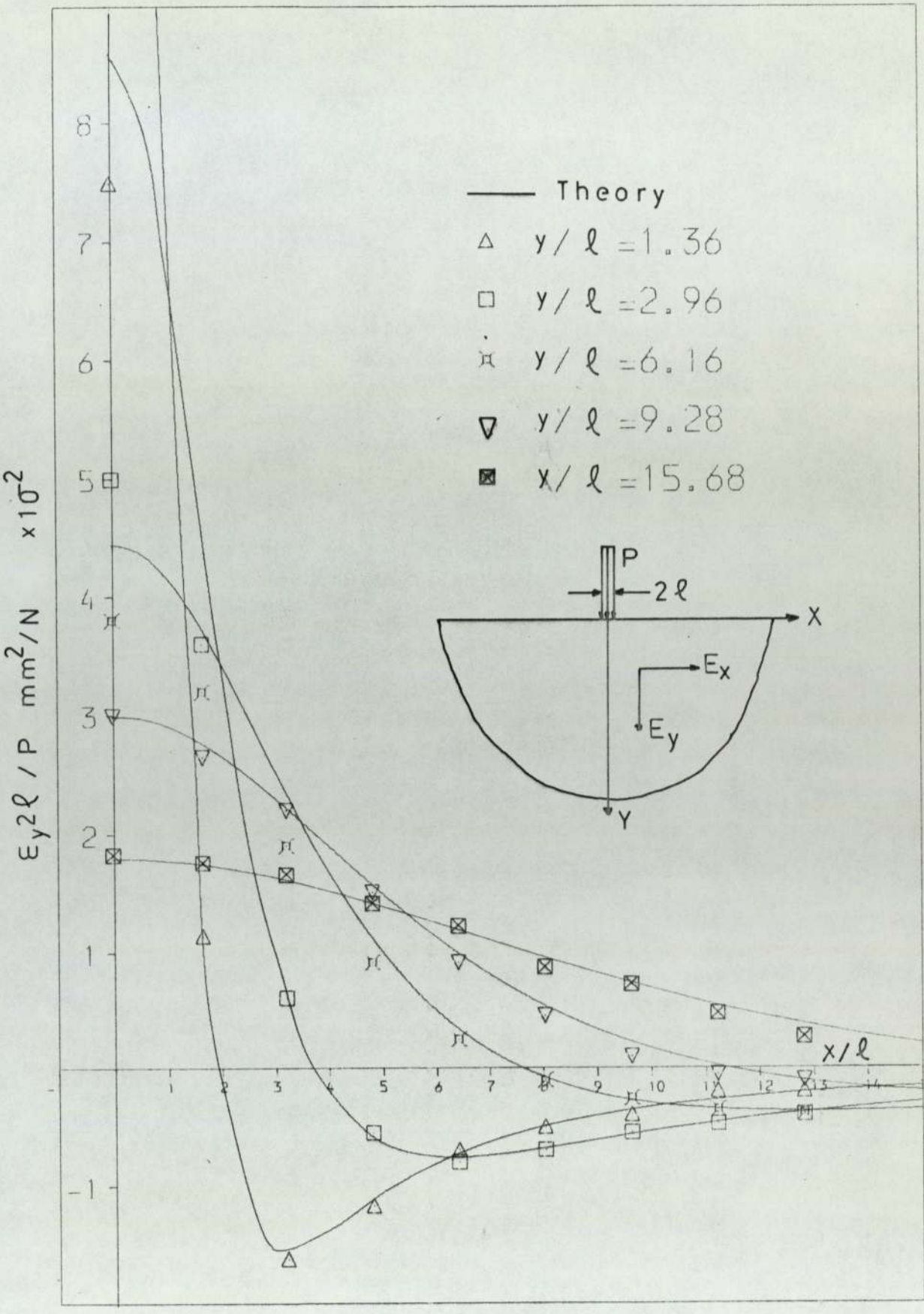

FIG.9.11 HALF PLANE - CONCENTRATED LOAD - $\varepsilon_y 2\ell/P$ vs x/ℓ

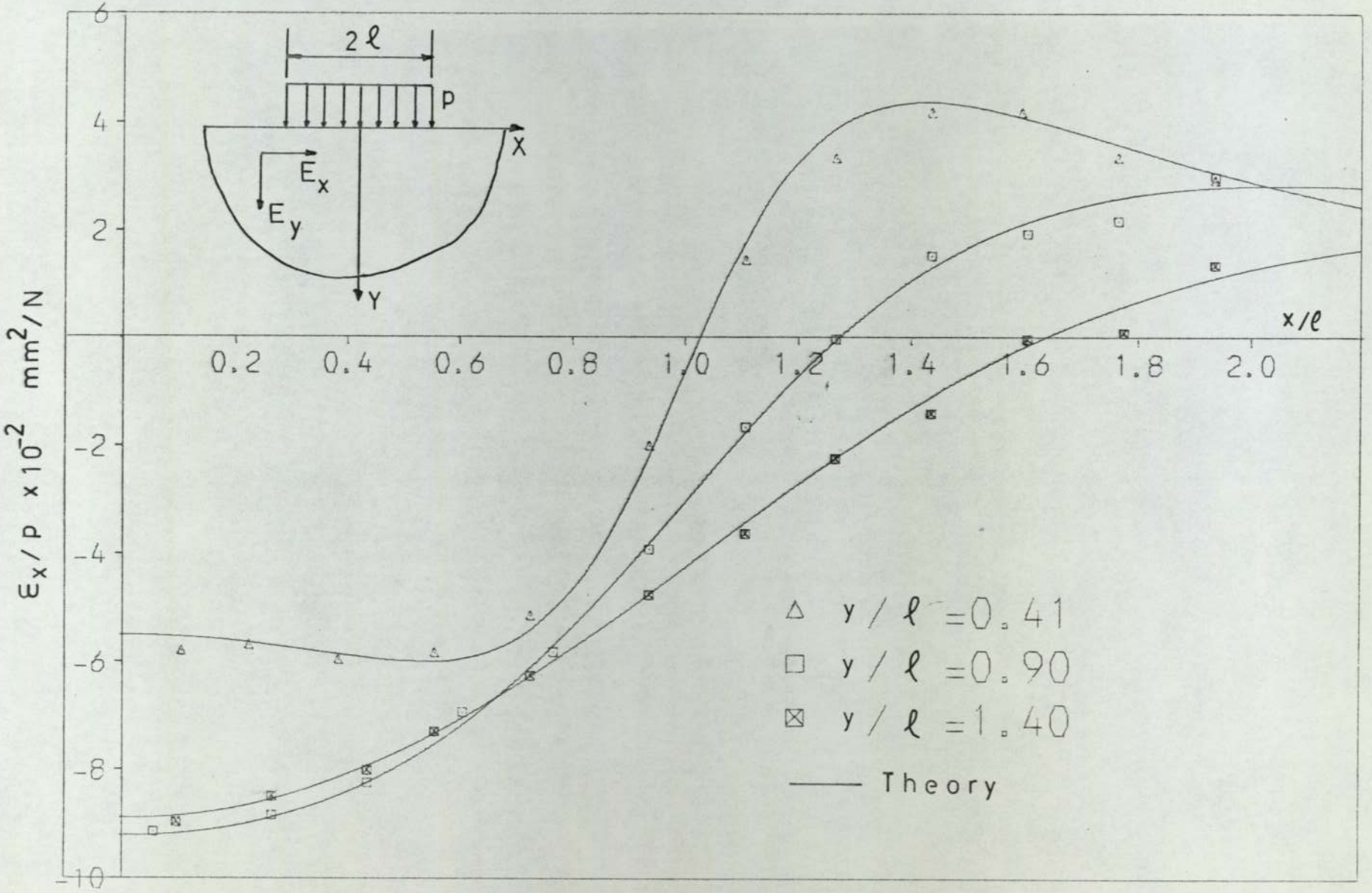

FIG. 9.12 HALF PLANE - U.D.L. - ε_x / p vs x/ℓ

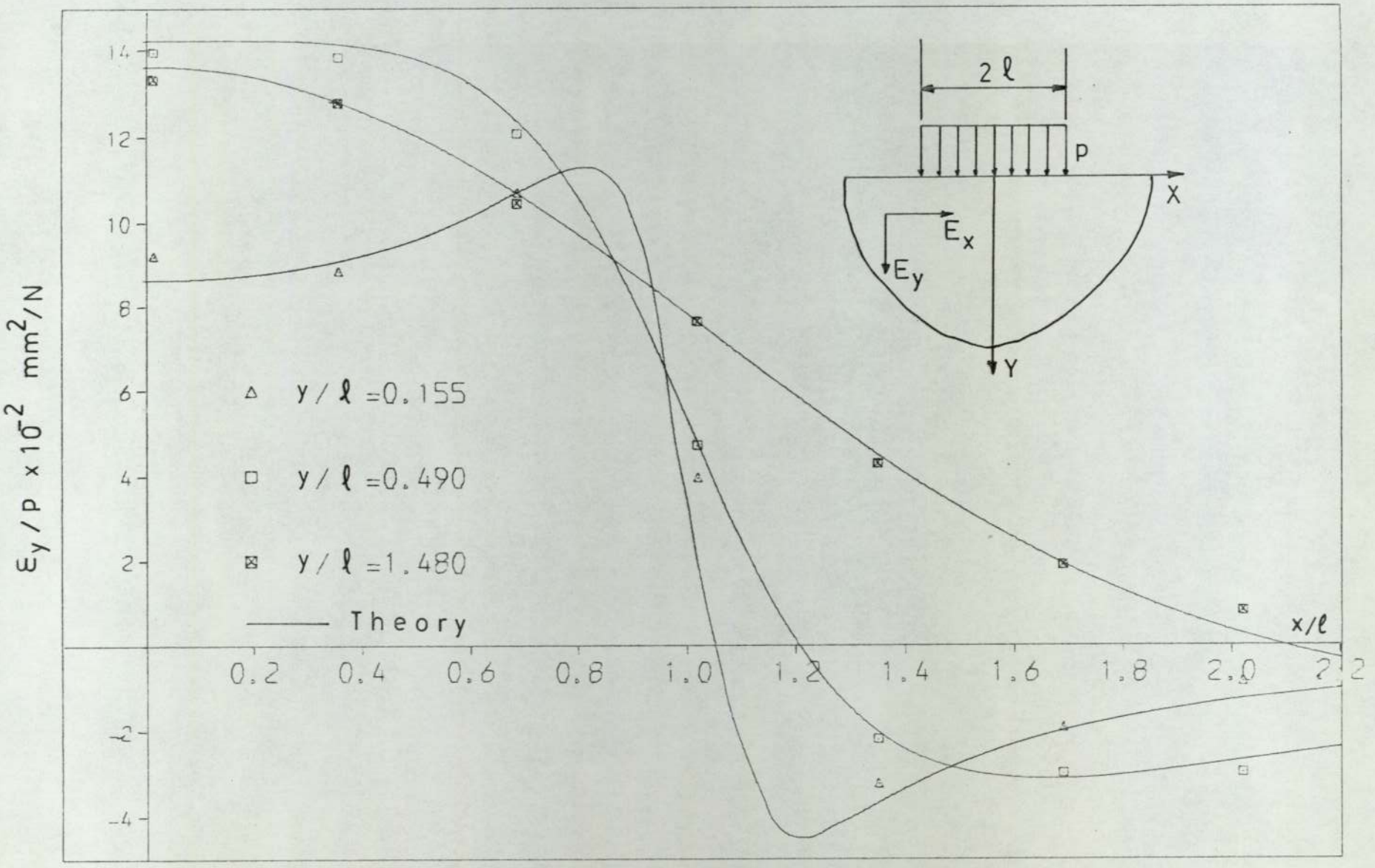

FIG.9.13 HALF PLANE - U.D.L. - ε_y / p vs x/ℓ

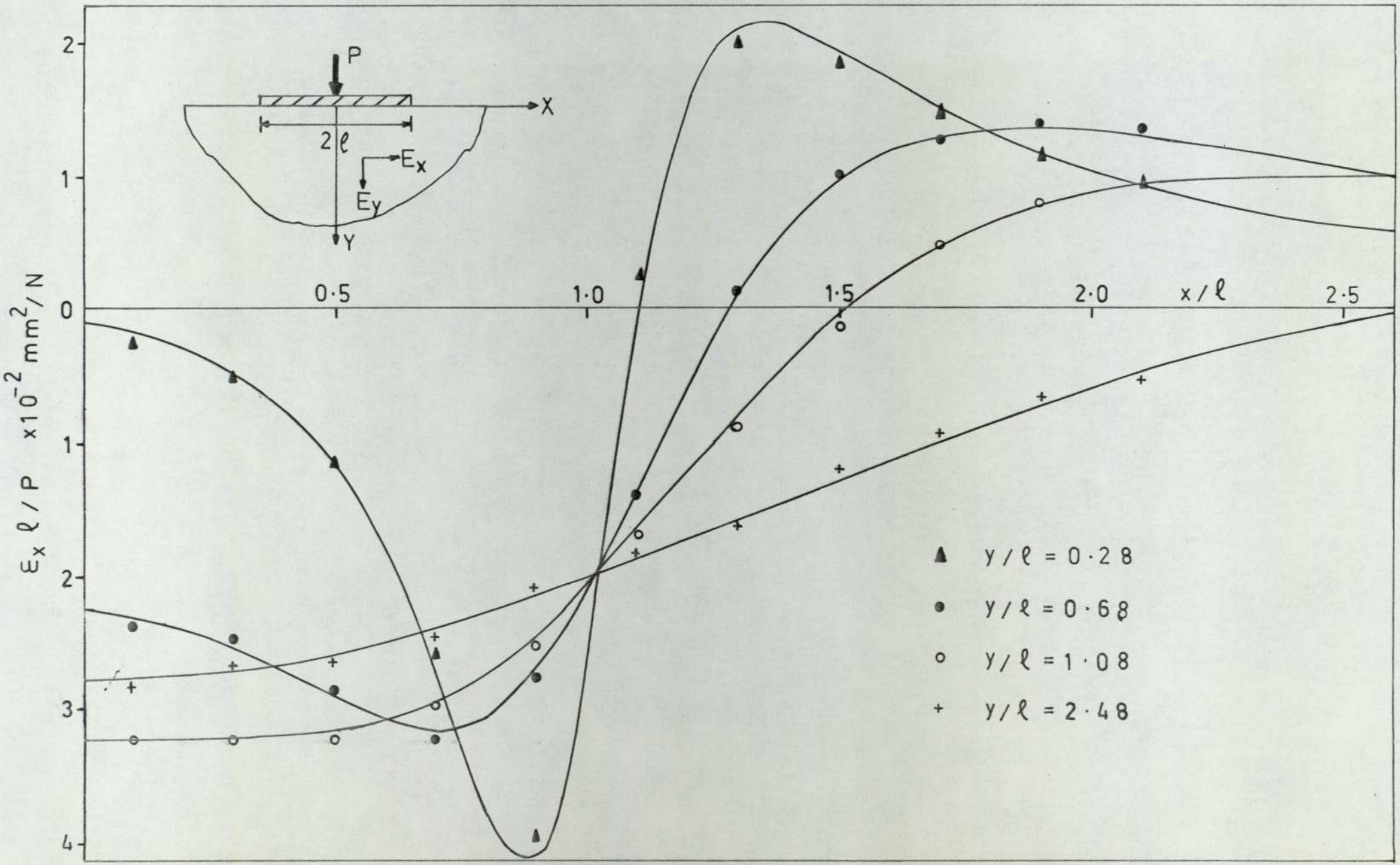

FIG.9.14 Half plane - Rigid punch - $\varepsilon_x \ell / P$ vs x/ℓ

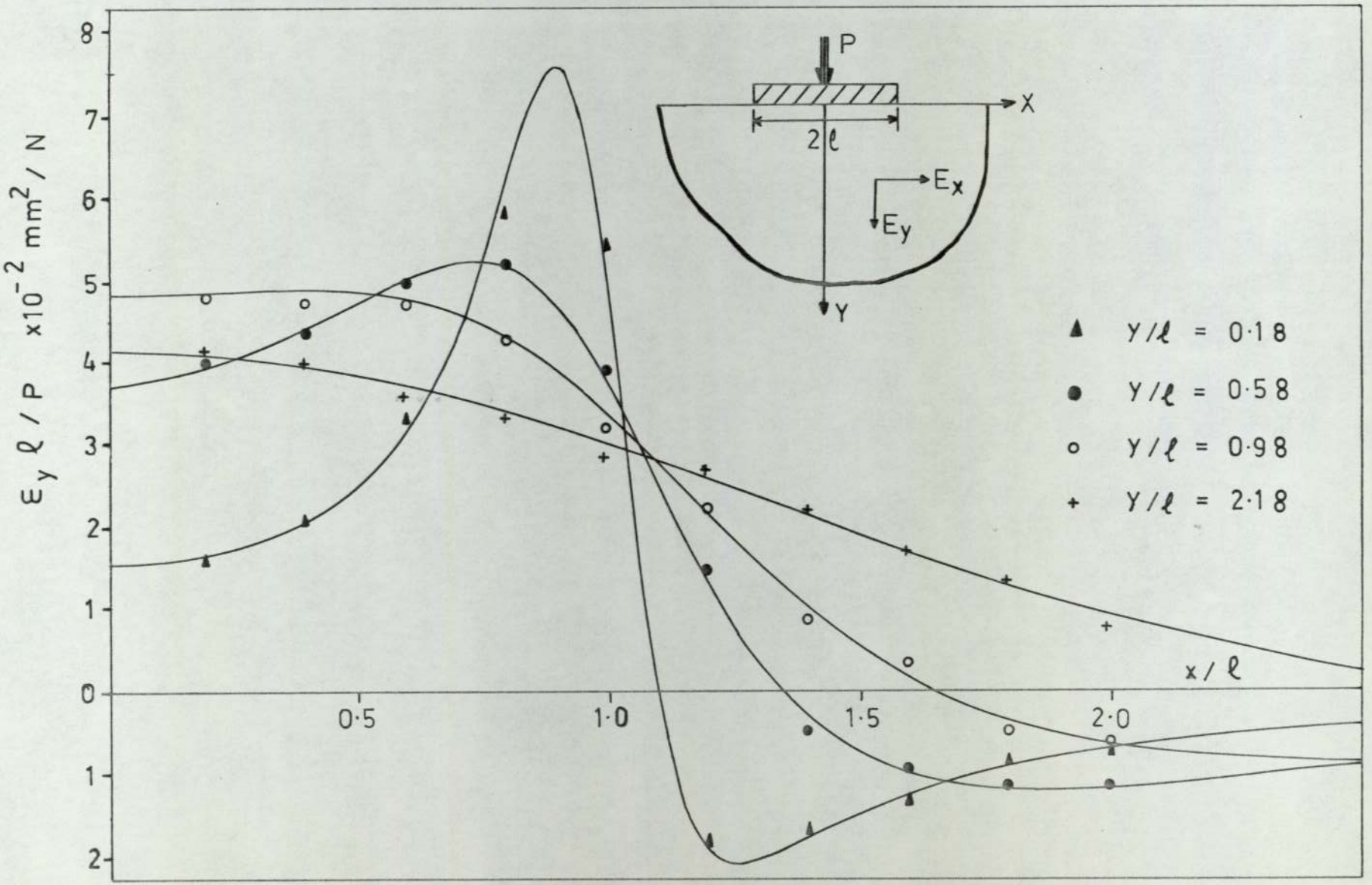

FIG·9.15 Half plane - Rigid punch - $\varepsilon_y \ell / P$ vs x / ℓ

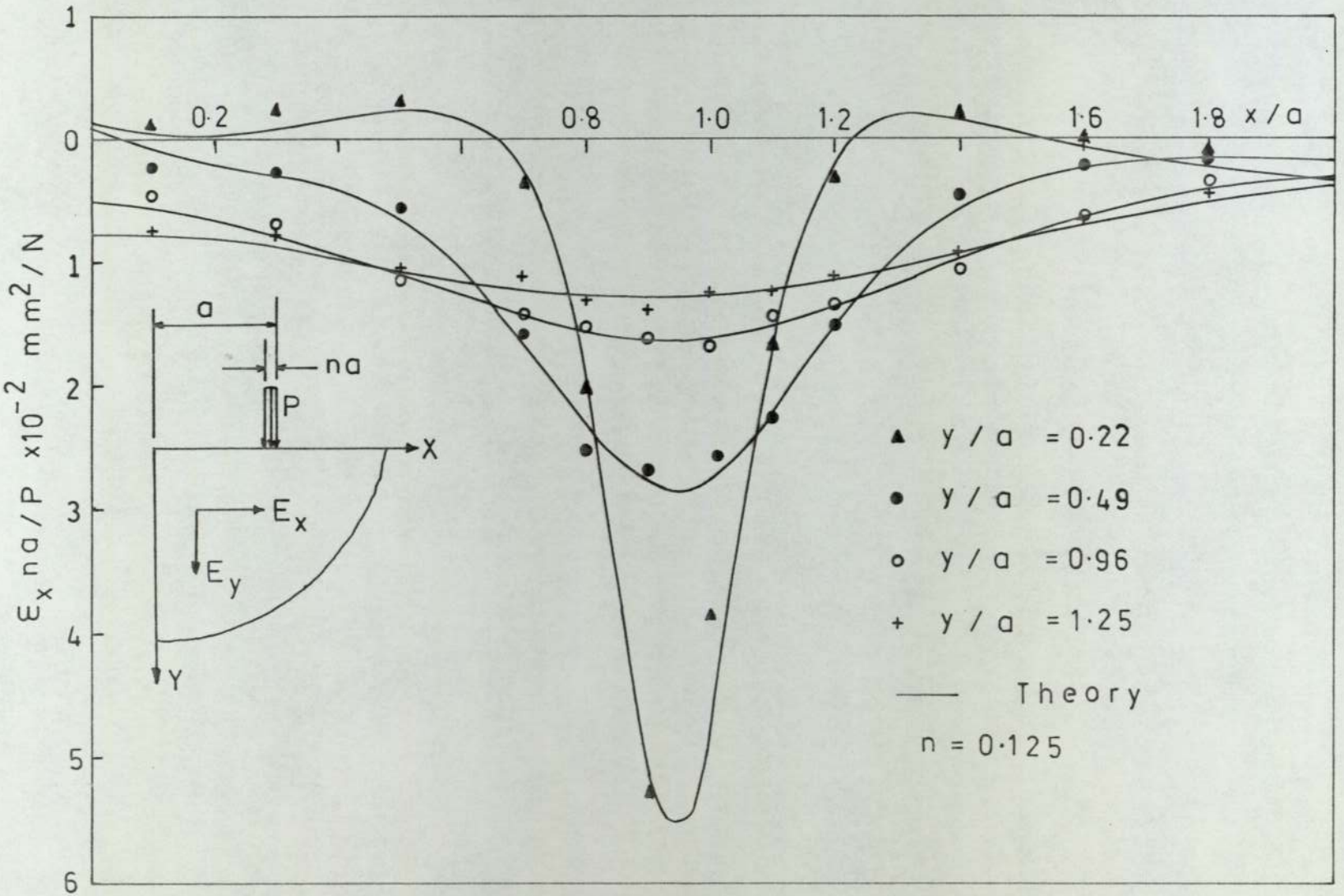

FIG.9.16 Quarter plane - Concentrated force - ε_x na/P vs x/a

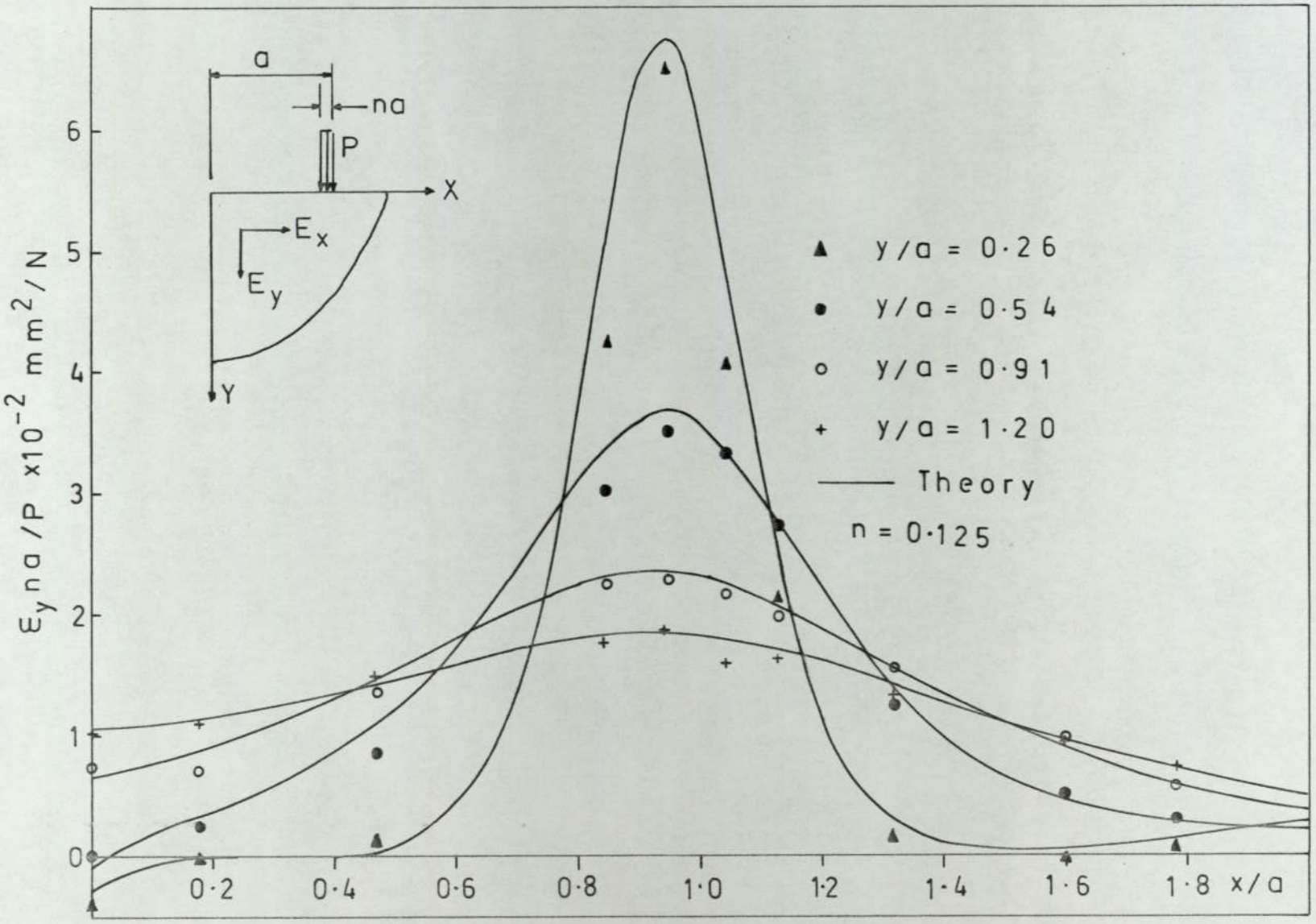

FIG. 9.17 Quarter plane - Concentrated force - ε_y na/P vs x/a

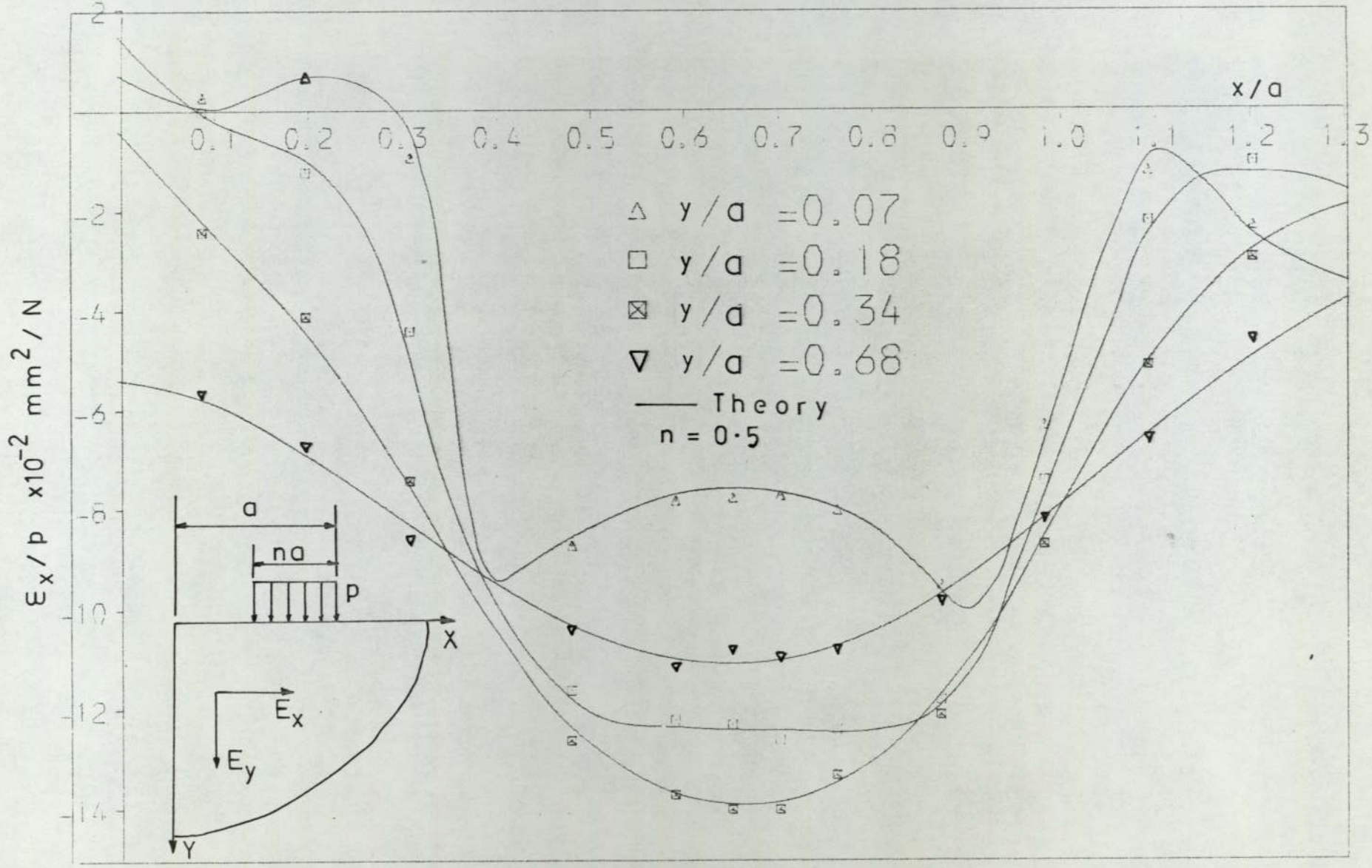

FIG 9.18 QUARTER PLANE - UNIFORMLY DISTRIBUTED LOAD - ε_x/p vs x/a

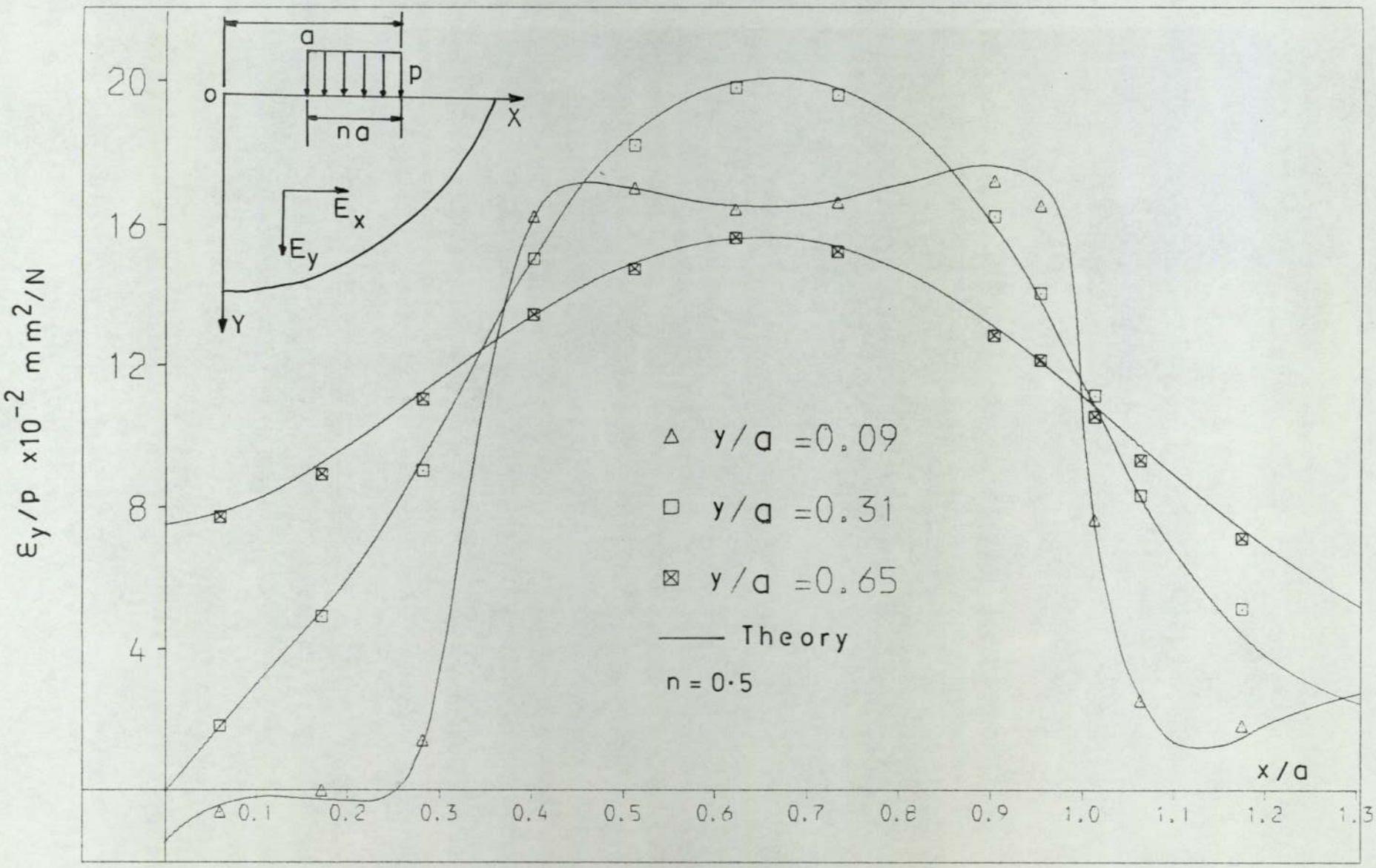

FIG.9.19 QUARTER PLANE -U.D.L. ε_y/p vs x/a

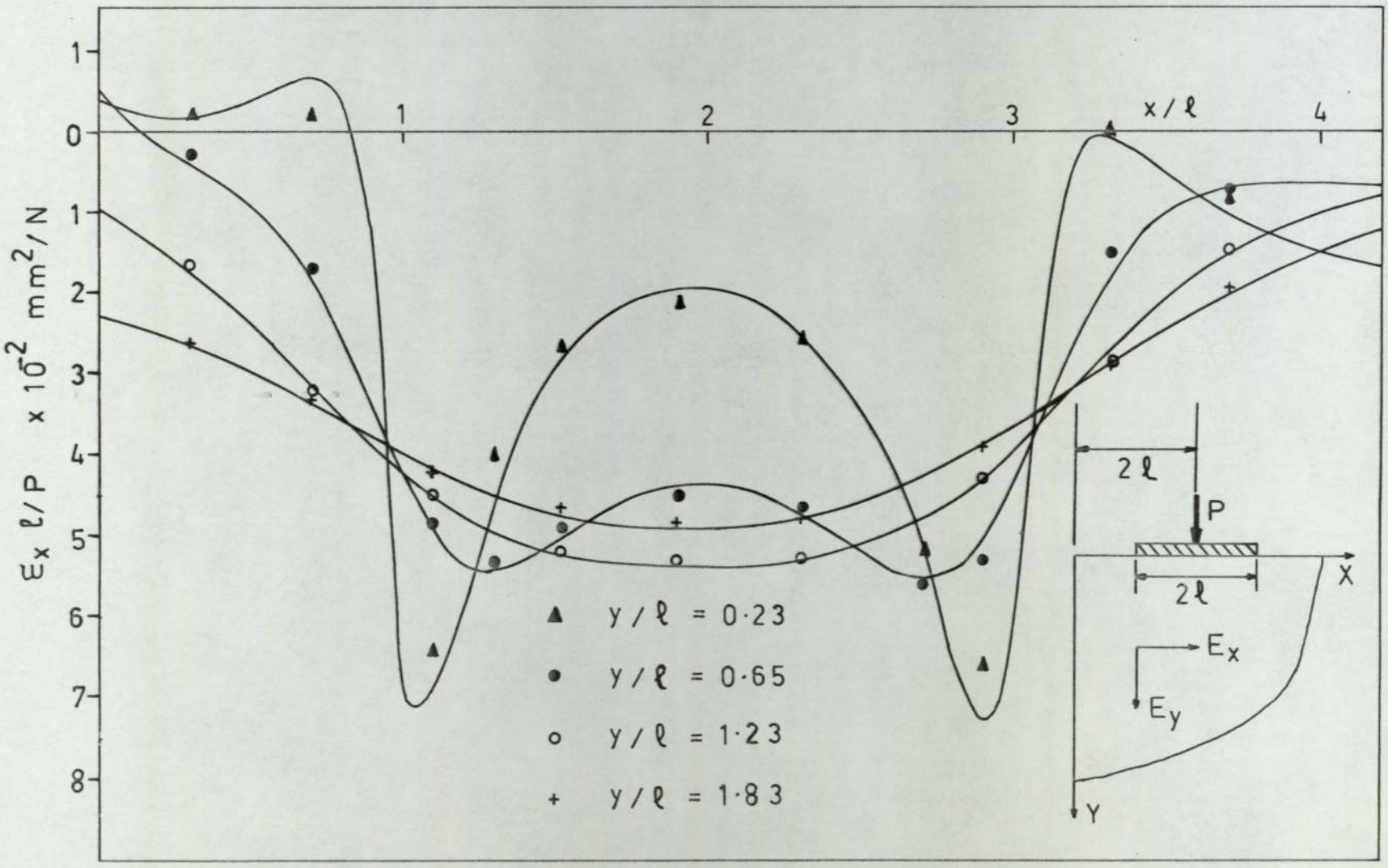

FIG.9.20 Quarter plane - Rigid punch - $\varepsilon_x\, \ell/P$ vs x/ℓ

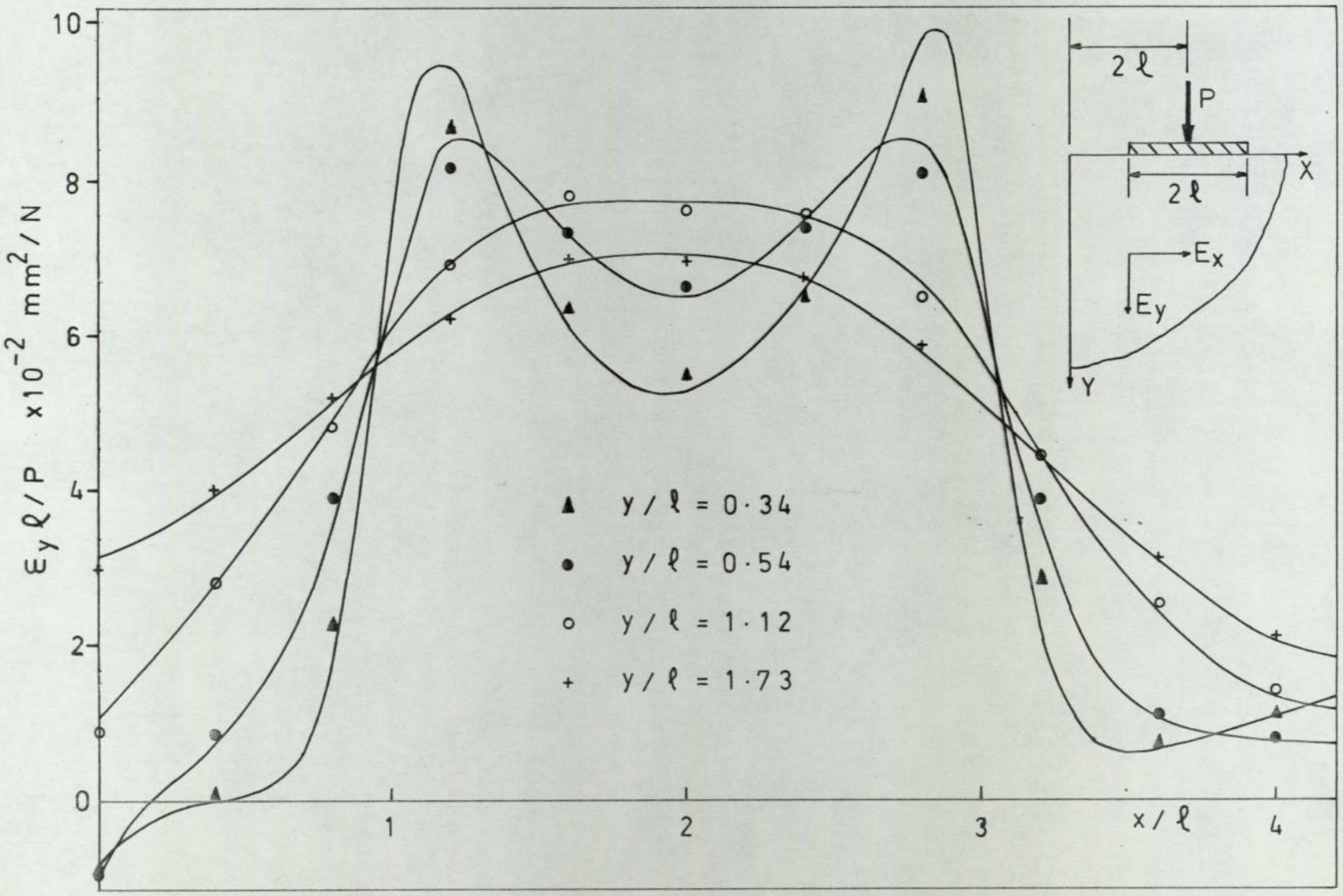

FIG.9.21 Quarter plane - $\varepsilon_y \ell / P$ vs x / ℓ

9.3) Plate stress tests.

A series of tests was carried out under plane stress conditions in order to investigate stress distributions in an orthotropic plate, whose boundaries can be approximated to those of a half-plane or a quarter-plane. The material used for the tests was a unidirectional glass-fibre reinforced polyester resin, henceforth referred to as a fibre-glass composite.

9.3.1) Constituent materials.

a) Glass. The fibre reinforcement was E-glass unidirectional cloth, type Y-996, supplied by Fothergill and Harvey Ltd.,

b) Resin. The resin used was preaccelerated Beetle Polyester resin 837, supplied by B.I.P. Chemicals Ltd., This type of resin requires the addition of a suitable peroxide catalyst to effect rapid gelation of room temperature. The catalyst used was Beetle catalyst 347 (methyl ethyl ketone peroxide). A curing time of approximately 45 min. was obtained with 0.1% by weight, of catalyst.

The physical properties of the fibre-glass reinforcement and resin, are listed in Table 9.4.

TABLE 9.4

	E kN/mm^2	ν	G kN/mm^2	Specific Gravity
E-glass*	70	0.2	29.16	2.55
Polyester** resin-837	4.1	0.33	1.54	1.19

* G.R.P. Parkyn (1970)

** B.I.P.Chemicals Ltd., Leaflet No.10.

9.3.2) Orthotropic material.

9.3.2.1) Moulding of fibre-glass composite.

A fibre-glass reinforced composite was moulded into the form of a plate, 3.5 mm thick, using a wooden mould 800 x 800 mm. Three layers of E-glass cloth were used and during placing of each layer, care was taken to avoid air being trapped between the fibres and the resin.

The plate was left in the mould under pressure for 24 hrs., after which it was removed and left for a week on a flat surface under a small pressure.

Square specimens (20 mm x 20 mm) were cut from the plate, for the determination of fibre and resin content (by volume).

The following average results were obtained from five tests:

$$v_f = 28.5\%, \quad v_r = 68.9\%, \quad v_v = 2.6\%,$$

where the subscripts f,r,v refer to fibre, resin and voids respectively.

The plate was then trimmed to a size of 700 mm x 700 mm.

9.3.2.2) Prediction of elastic constants.

As was discussed in Section 2.10, the elastic constants of composites can be predicted with a certain degree of accuracy from the properties of the constituent materials and their geometrical configuration. For the particular case of unidirectional fibre reinforced composites, we shall adopt the following notation:

The subscripts 'ℓ' and 't' denote the directions parallel (longitudinal) and normal (transverse) to the

9.3.2.2) contd.

direction of the fibres respectively, e.g. E_ℓ, E_t, $\nu_{\ell t}$, etc.

The longitudinal modulus E_ℓ was determined by the law of mixtures (equation 2.10- 1), while the transverse modulus E_t, the Poisson's ratio $\nu_{\ell t}$ and the shear modulus $G_{\ell t}$, were determined from the corresponding Tsai's equations (see Section 2.10). Since the composite was hand-layed, and, for a fibre volume fraction of 28.5%, a contiguity factor of 0.5 was considered.

The following values for the elastic constants were obtained:

$$E_\ell = 22.77 \text{ kN/mm}^2 \quad , \quad E_t = 8.9 \text{ kN/mm}^2 \ ,$$

$$\nu_{\ell t} = 0.255 \quad , \quad G_{\ell t} = 4.79 \text{ kN/mm}^2 .$$

Using the symmetry relation $\nu_{\ell t} E_t = \nu_{t\ell} E_\ell$, the value of $\nu_{t\ell}$ was found to be 0.099 (see also Table 9.5).

9.3.2.3) Experimental determination of elastic constants.

The elastic constants of the orthotropic composite were determined experimentally with specimens cut from the rectangular plate (the specimens were cut after the main tests had been carried out, so that the properties of the material actually tested were found).

Al-Khyatt (1974), using the same type of glass-cloth and resin, found that the values of E_ℓ and E_t for a unidirectional composite ($v_f = 0.3$), determined in compression, were 4% less than the corresponding values of the modulii determined in tension. Differences of this order of magnitude can be assumed insignificant, particularly in cases when the analysis of a problem is based on the

9.3.2.3) contd.

orthotropic elastic constants k_1 and k_2, which change by only 2%. Therefore, the elastic constants of the composite were determined in tension only.

1) Determination of $E_\ell, E_t, \nu_{\ell t}, \nu_{t\ell}$

Rectangular specimens (197 mm × 19 mm) were cut parallel (for the determination of E_ℓ, $\nu_{\ell t}$) and normal (for the determination of E_t, $\nu_{t\ell}$) to the direction of the fibres. Aluminium "end-pieces" (45 × 19 × 3 mm) were fixed on to the ends of the specimens with araldite adhesive in order to avoid stress concentrations and to obtain a uniform stress distribution over their width. The specimens were then subjected to static tensile loads in a Denison tension/compression machine.

The strains in the two principal directions were measured with electric strain gauges (Type GFLA-6; length: 6 mm; Gauge factor 2.16), connected to a Compulog Alpha 16 Computer. The strains were thus measured to an accuracy of 10^{-6}.

For each test, the principal strains were plotted against the applied load and the relations were found to be linear. From the ratio of their slopes, the corresponding Poisson's ratio was determined. The value of Poisson's ratio was employed to apply an area correction to the stress-strain curve, from the slope of which the corresponding Young's modulus was calculated (see Fig.9.22a and b).

From 14 tests (7 for each principal direction), the following average values were obtained (see also Table 9.5).

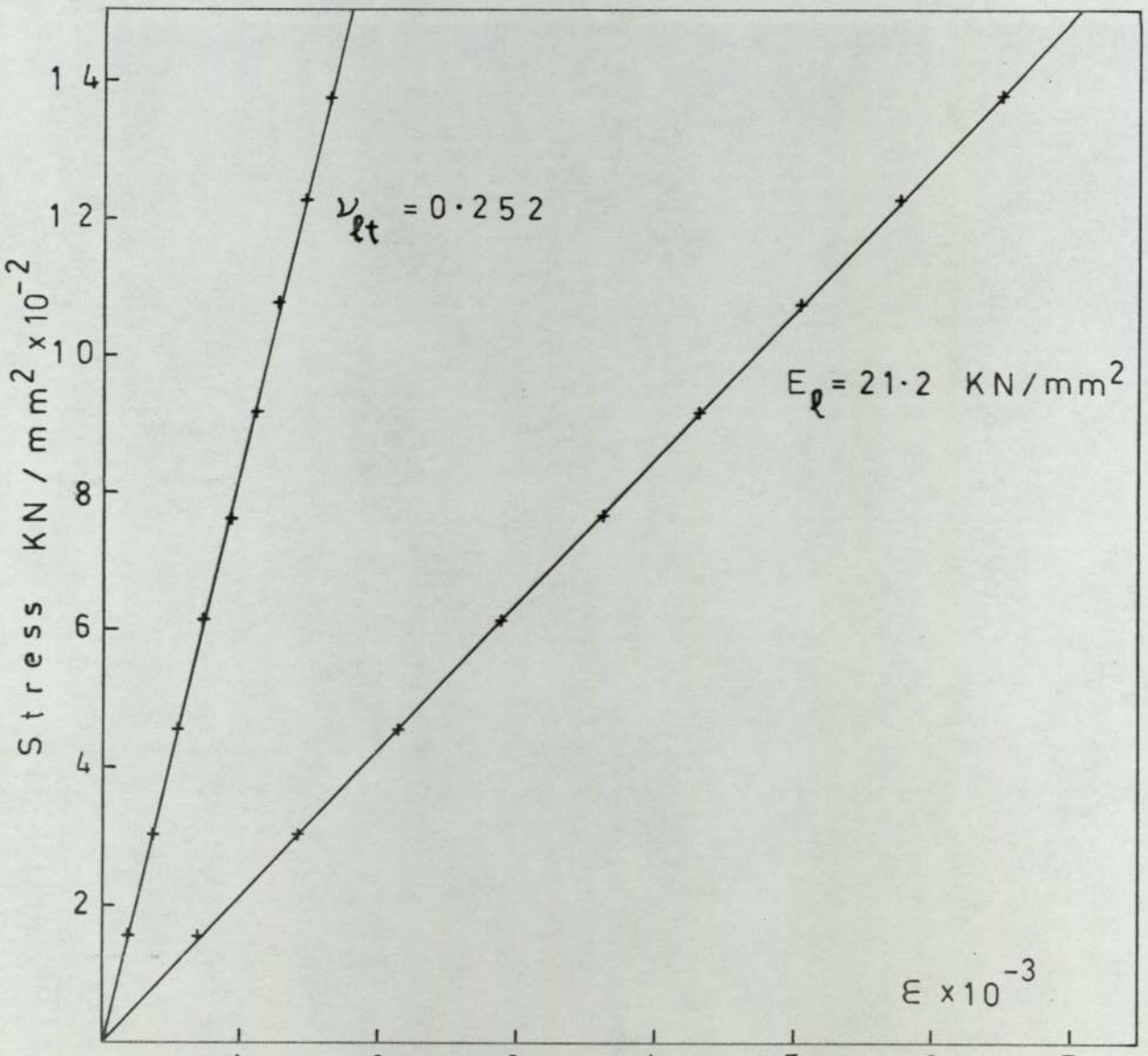

FIG. 9.22 a Stress vs strain - longitudinal direction

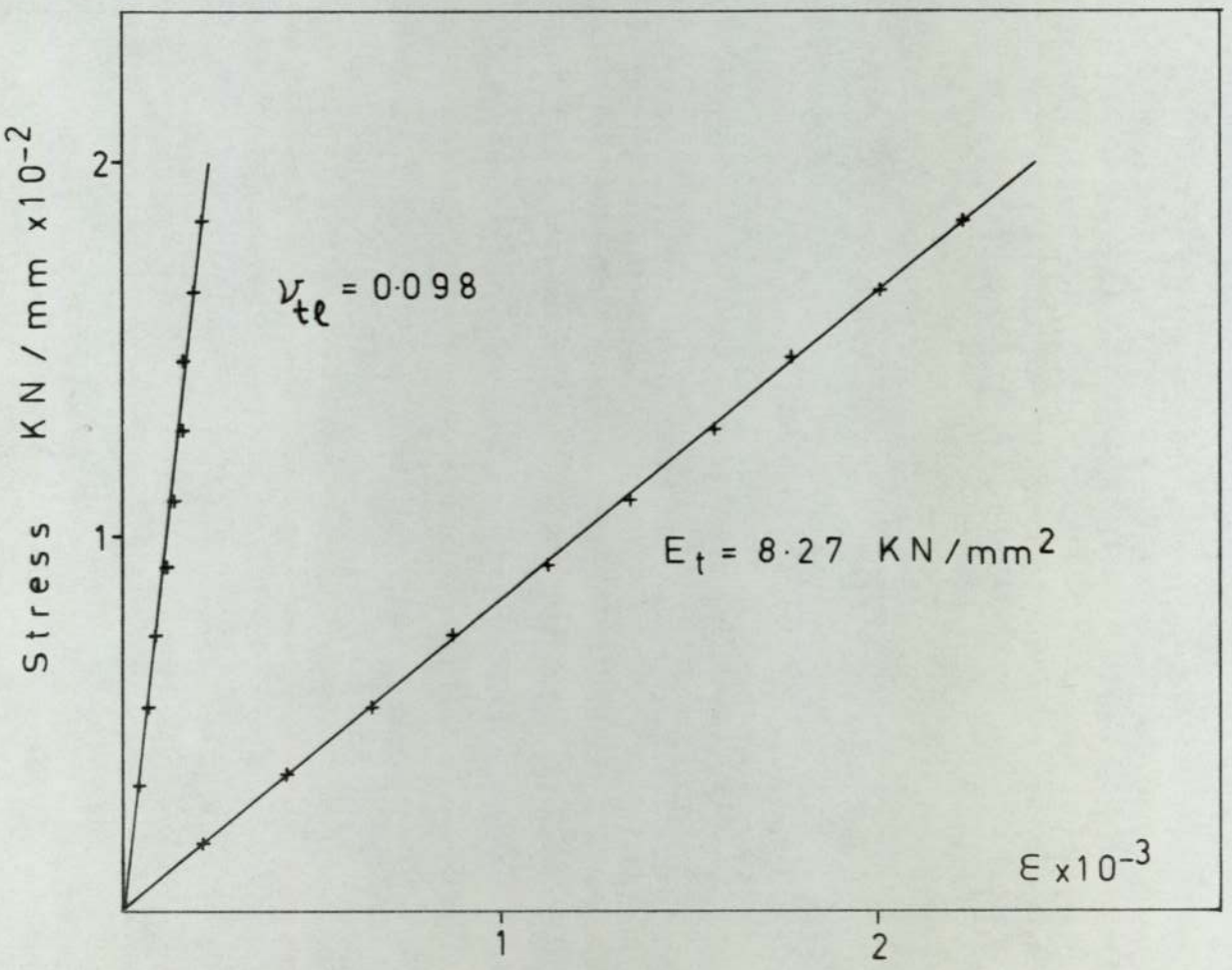

FIG· 9·22b Stress vs strain — transverse direction

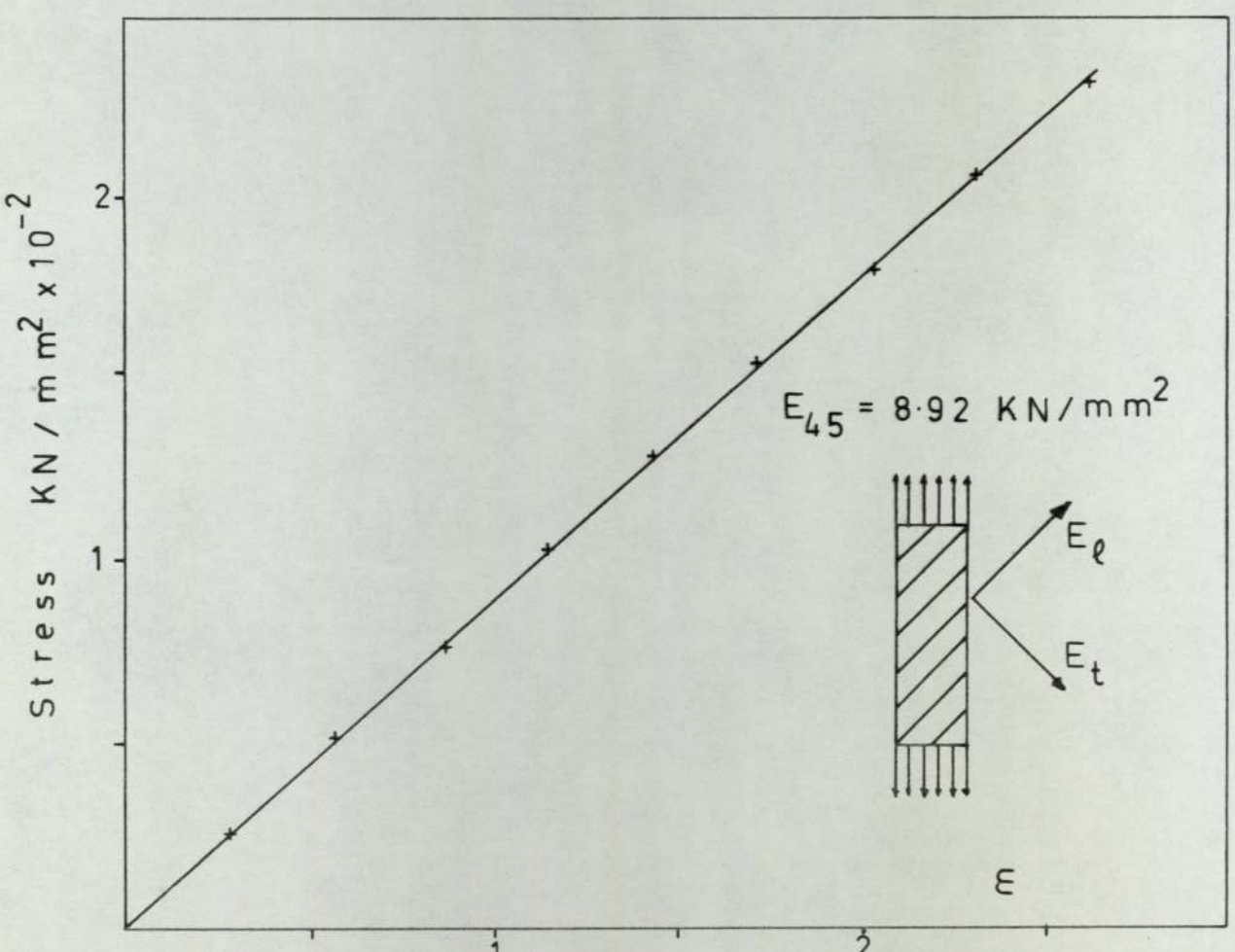

FIG. 9.23 Stress vs strain - 45° direction.

9.3.2.3) contd.

$E_\ell = 21.2$ kN/mm^2 $\qquad \nu_{\ell t} = 0.252$

$E_t = 8.27$ kN/mm^2 $\qquad \nu_{t\ell} = 0.098.$

It can be verified that the above results satisfy the symmetry condition:

$$\nu_{\ell t} E_t = \nu_{t\ell} E_\ell .$$

2) Determination of $G_{\ell t}$

Referring to the equations given in Appendix [1], for $\phi = 45°$, equation (A1-1) reduces to:

$$\frac{4}{E_{45}} = \frac{1-2\nu_{\ell t}}{E_\ell} + \frac{1}{E_t} + \frac{1}{G_{\ell t}}, \qquad 9.3\text{-}1$$

where E_{45} denotes the Young's modulus of the material in a direction inclined at 45° to the longitudinal axis. E_ℓ, E_t and $\nu_{\ell t}$ in equation (9.3-1) can be determined experimentally, as described in the previous paragraph. E_{45} can be found by subjecting specimens cut at 45° to the fibre direction, to a state of uniform tension. Then, the only unknown left in equation (9.3-1) is $G_{\ell t}$, which can be calculated.

The determination of E_{45} presents some problems, due to the fact that it is extremely difficult to subject off-angle specimens to pure tension. Pagano and Halpin (1968), investigated the influence of end-constraint and showed that if conventional clamping devices are used, the apparent Young's modulus E^*_ϕ determined in the tests, is related to the actual E_ϕ by the following relation:

$$E^*_\phi = E_\phi \left(\frac{1}{1-\chi} \right), \qquad 9.3\text{-}2$$

where

$$\chi = \frac{6\, c_{16}^2}{c_{11}\left(6c_{66}+c_{11}\frac{\ell^2}{h^2}\right)} . \qquad 9.3\text{-}3$$

9.3.2.3) contd.

2) contd.

c_{ij} are the elements of the compliance matrix (see equation 2.3-1); ℓ and h are the length and the half width of the spcimens respectively.

The magnitude of χ cannot be determined without a prior knowledge of the value of c_{ss} $(= 1/G_{\ell t})$, but its value would tend to zero as the ratio ℓ/h becomes large (see equation (9.3-3)). As a consequence $E^*_\phi \rightarrow E_\phi$.

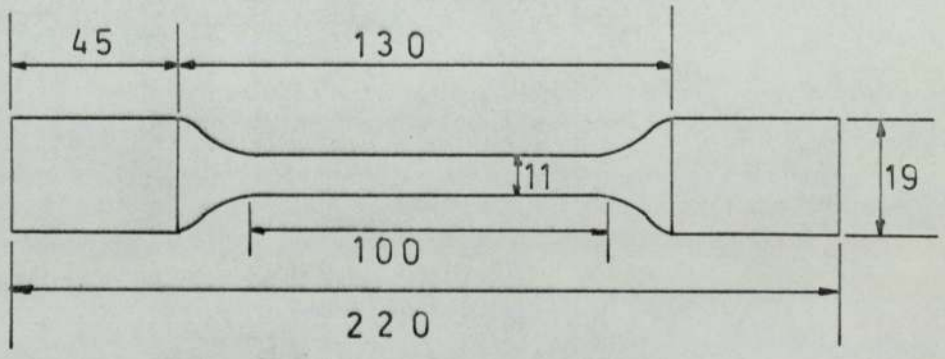

(All dimensions in mm).

Fig.9.24

Based on the above condition, the overall length of the specimens cut at 45° to the direction of the fibres, was increased to 220 mm. In addition, the specimens were machined as shown in Fig.9.24, to reduce their width to 11 mm. Thus, the ratio ℓ/h was increased to approximately 12. We could then assume that $\chi \approx 0$ and $E^*_\phi \approx E_\phi$.

The average result from seven tests was:

9.3.2.3) contd.

2) contd.

$E_{45} = 8.92$ kN/mm^2 (see Fig.9.23)

and from equation (9.3-1):

$G_{\ell t} = 3.29$ kN/mm^2 (see Table 9.5).

TABLE 9.5

	Theory	Experiment	Number of tests	S.D.
E_ℓ	22.77	21.20	7	± 0.4
E_t	8.90	8.27	7	± 0.3
$\nu_{\ell t}$	0.255	0.252	7	-
$\nu_{t\ell}$	0.099	0.098	7	-
$G_{\ell t}$	4.79	3.29	7	± 0.4

(All dimensional quantities in kN/mm^2)

ℓ_{11}	ℓ_{22}	ℓ_{12}	ℓ_{66}	k_1	k_2
0.0471	0.1209	-0.0118	0.3039	1.4609	0.4275

(All dimensional quantities in mm^2/kN).

9.3.3) Method of Testing.

Three different tests were carried out with the orthotropic composite plate, and are shown diagrammatically in Fig.9.25. In cases (a) and (b), the plate was suspended from points A_1 and A_2, while static loads were applied through a pin (3 mm in diameter) and hanger system at points A_0 for the "half-plane" problem, and point A_3 for the "quarter-plane" one. In both cases, the loads were applied in a direction normal to the direction of the fibres.

In case (c) (see Fig.9.25c), the plate was suspended from points A_2 and A_4, so that the load was applied in the direction of the fibres.

The strains at points in the vicinity of the loads were measured with electric strain gauges (Type: GFLA-3; length 3 mm; Gauge factor 2.13) positioned as shown in Fig.9.26a and 9.26b (see also Plate 9.12).At each point two strain gauges were used, one on each side of the plate and at right angles to each other, so that the strains could be measured in both X and Y-directions.

For each one of the tests, the plate was loaded in steps of 10 kg to a maximum of 120 kg and then unloaded, while readings of the strain gauges were taken by the Compulog Computer for each load increment. Each test was repeated three times.

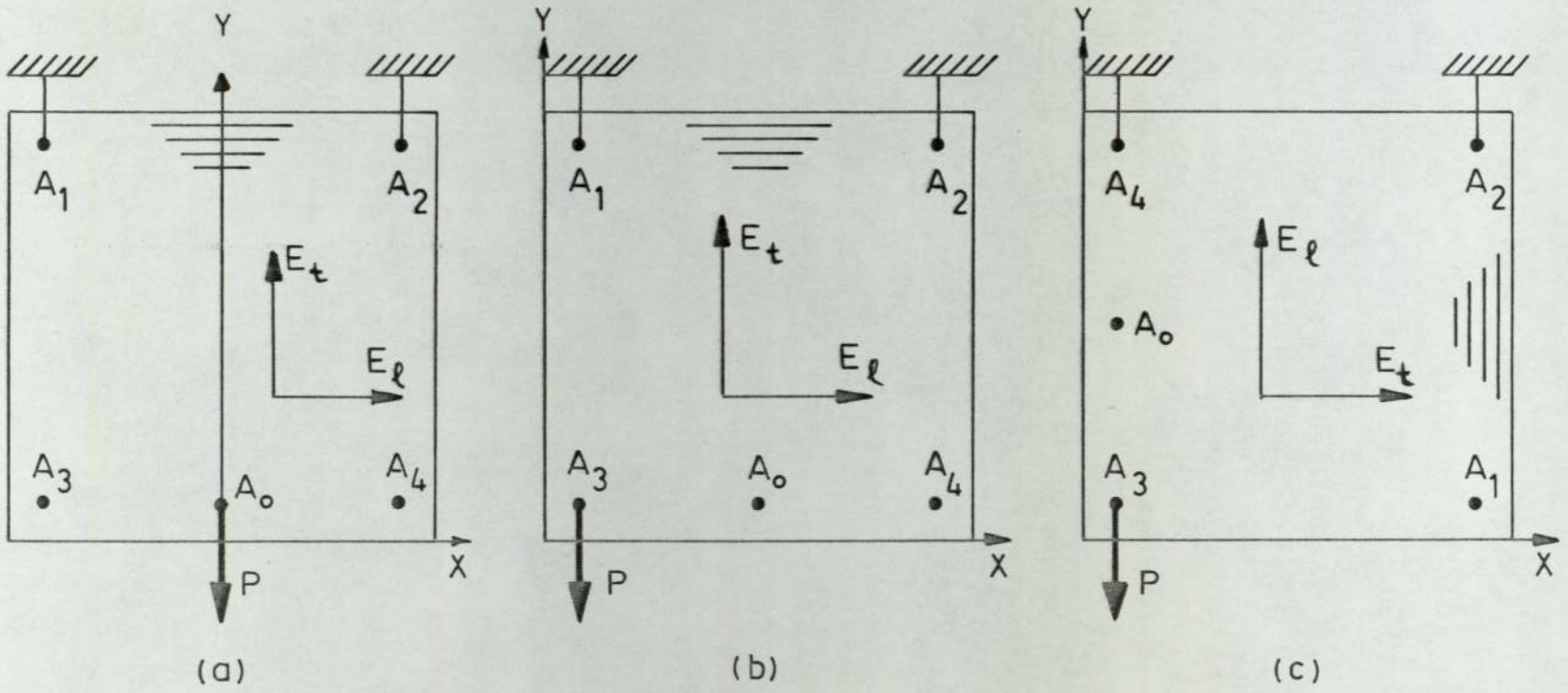

FIG. 9.25 Tests under plane stress conditions - fiber glass composite

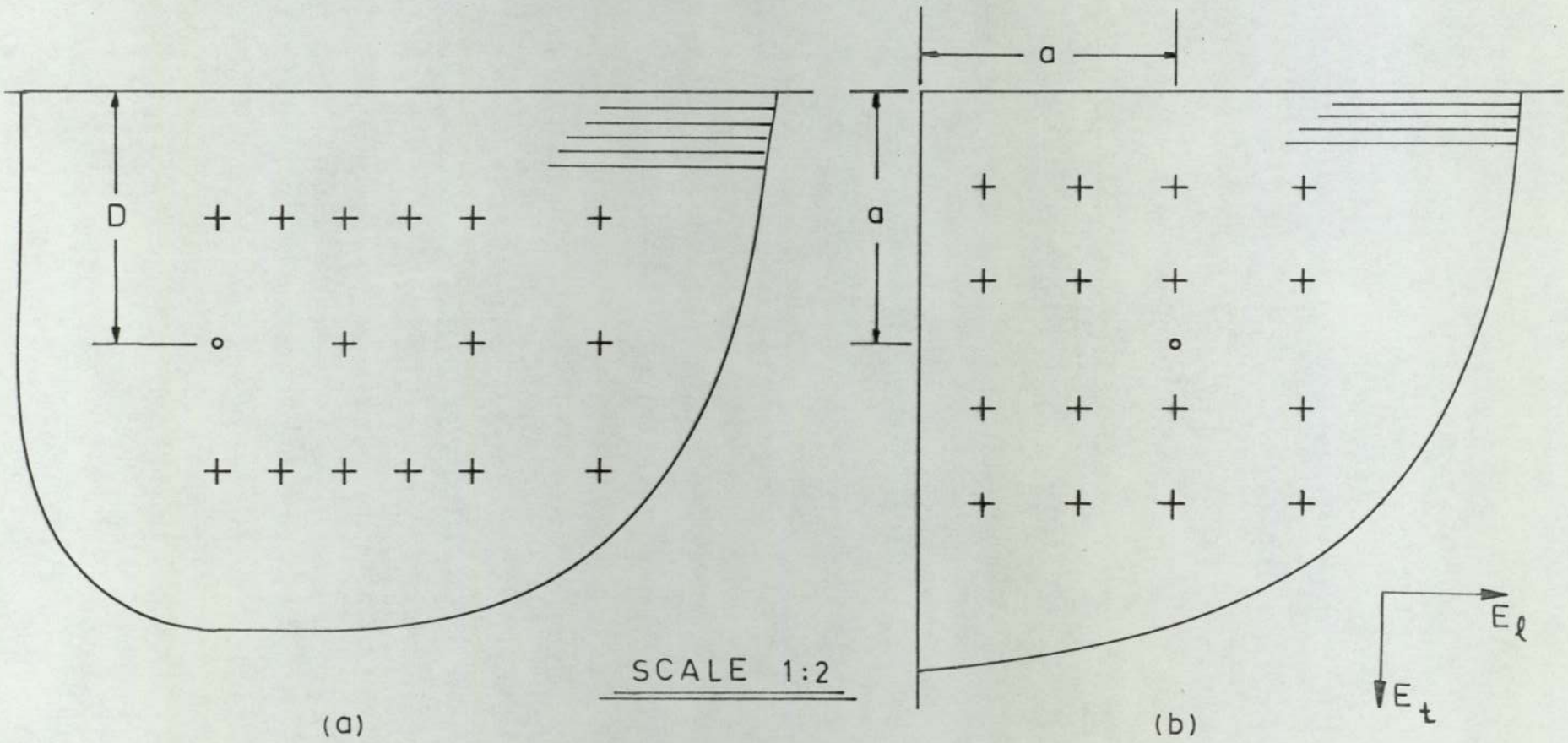

FIG. 9.26 Positions of strain gauges for half/quarter-plane tests

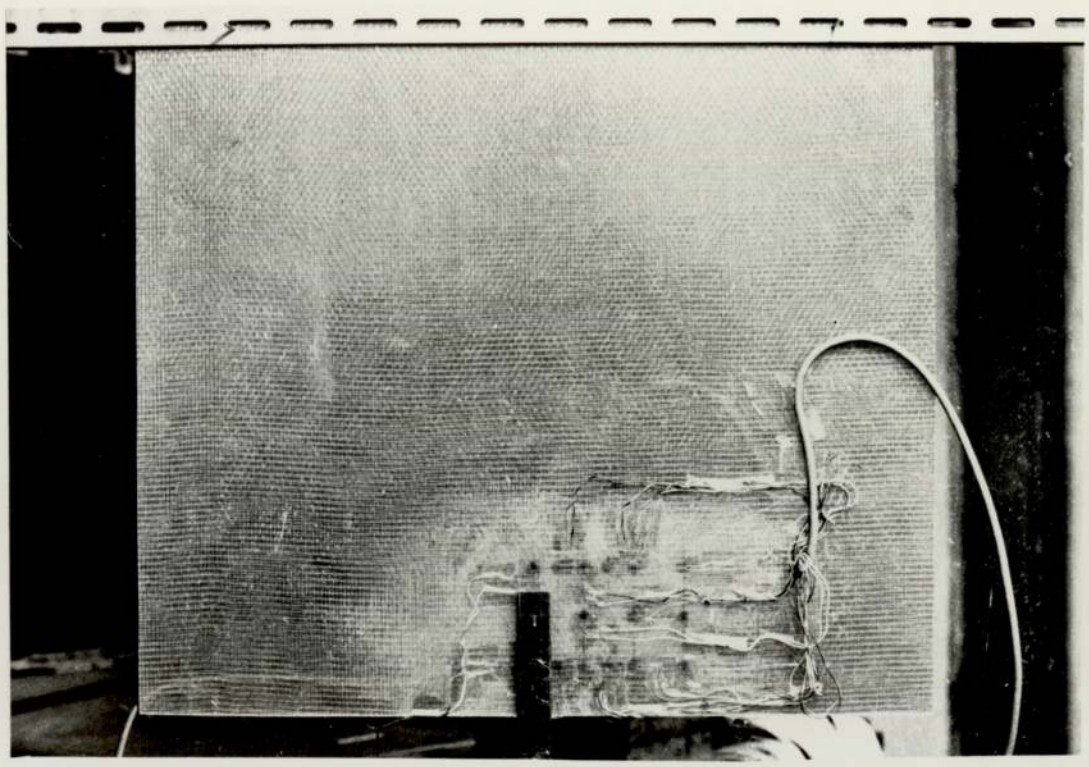

PLATE 9,12 Fibre-glass composite plate.

9.3.4) Analysis of results.

The strains ε_x and ε_y for each of the points considered, were plotted against the applied load. The relationship was found to be linear (a typical example is shown in Fig.9.27), although in some cases an origin correction was necessary. This form of non-linearity at the initial stages of loading indicated either that the plate was slightly curved in the unloaded state or a local non-linearity of the fibres.

During unloading, the strain-load curves were found to be identical to those of the loading stage, with no signs of creep (each test was carried out in approximately 20 min).

Heating of the strain gauges (which is a major problem when measuring strain on plastics, due to their low conductivity of heat) was minimized by using the Compulog Alpha 16 computer, with a reading time for each strain gauge of $\approx$ 0.1 sec. In addition, one "dummy" strain gauge was used with every four strain gauges on the material.

Each test was repeated three times and a remarkable consistency of results was observed. Average values for strain/load were used whenever necessary.

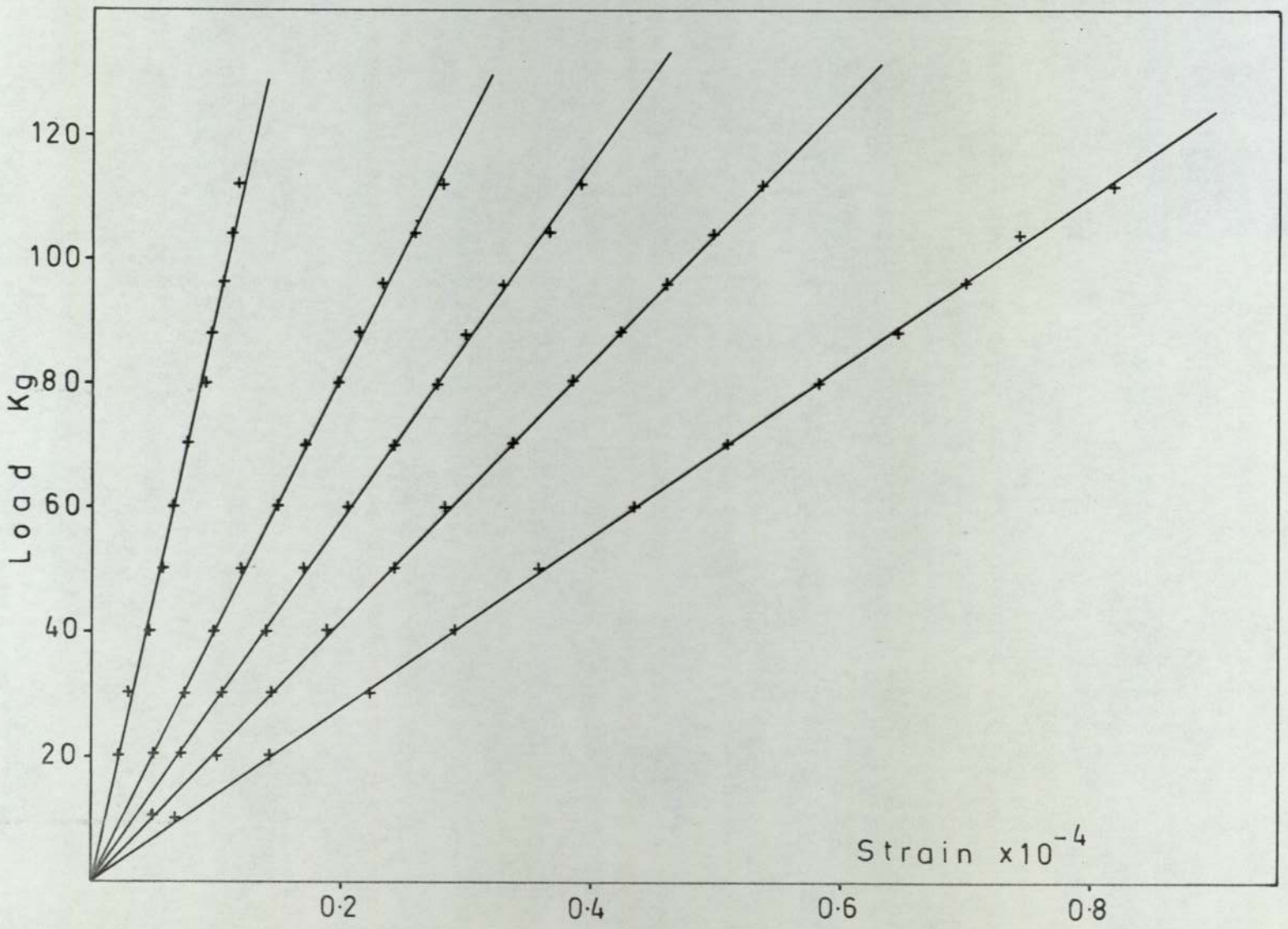

FIG. 9.27. A typical set of load/strain curves.
Plane stress tests.

9.3.5) Presentation of results.

The strains ε_x/P and ε_y/P at a point, were used in conjunction with the elastic constants of the material to determine the direct stress components at that point (the stresses were determined in dimensionless form, e.g. σ_x a/P, where P is load per unit thickness).

Theoretical values for the stresses were obtained through equation (4.7-3) for the half-plane problem and equation (6.6-1) for the quarter-plane one. These values were plotted against $\bar{x}$ for various values of $\bar{y}$ and are shown in Fig.9.28, 9.29 (half-plane) and Fig.9.30-9.33 (quarter-plane). The experimental results were marked on the same graphs for comparison.

Referring to Fig.9.28 and 9.29 (half-plane problem) we observe that for $\bar{x} > 0.3$ and $y > 1.5$ there is good correlation between theory and experiment. For $\bar{x} < 0.3$ and $0.5 < \bar{y} < 1.5$ the experimental results deviate from the theoretical curves, as it would be expected for points in the vicinity of a concentrated force. The stress component σ_x, which attains high values at points near the boundary of the half-plane diminishes very rapidly with $\bar{y}$ and for $\bar{y} > 1.5$ it becomes relatively insignificant.

We now refer to Fig.9.30-9.33 for the quarter-plane problem. The correlation between theory and experiment is somewhat inferior compared to that of the half-plane problem, but the pattern of stress distribution indicated by the experimental results is correct.

A point worth noticing is the development of relatively high stresses in the X-direction, at points near the Y = 0 boundary of the quarter plane, when the

9.3.5) contd.

longitudinal axies of the unidirectional composite coincides with the direction of the applied load (see Figure.9.32).

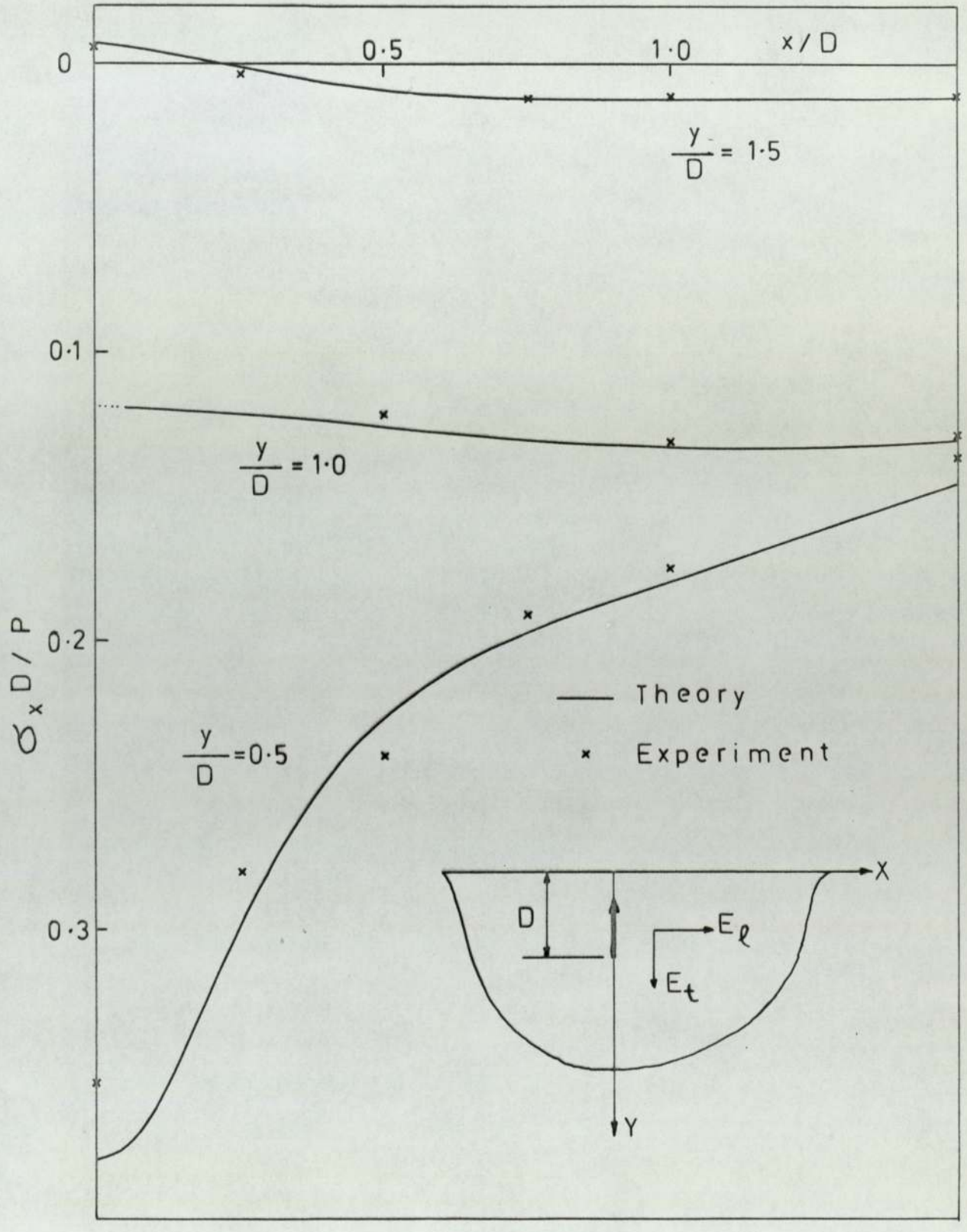

FIG.9.28 σ_x D/P vs x/D

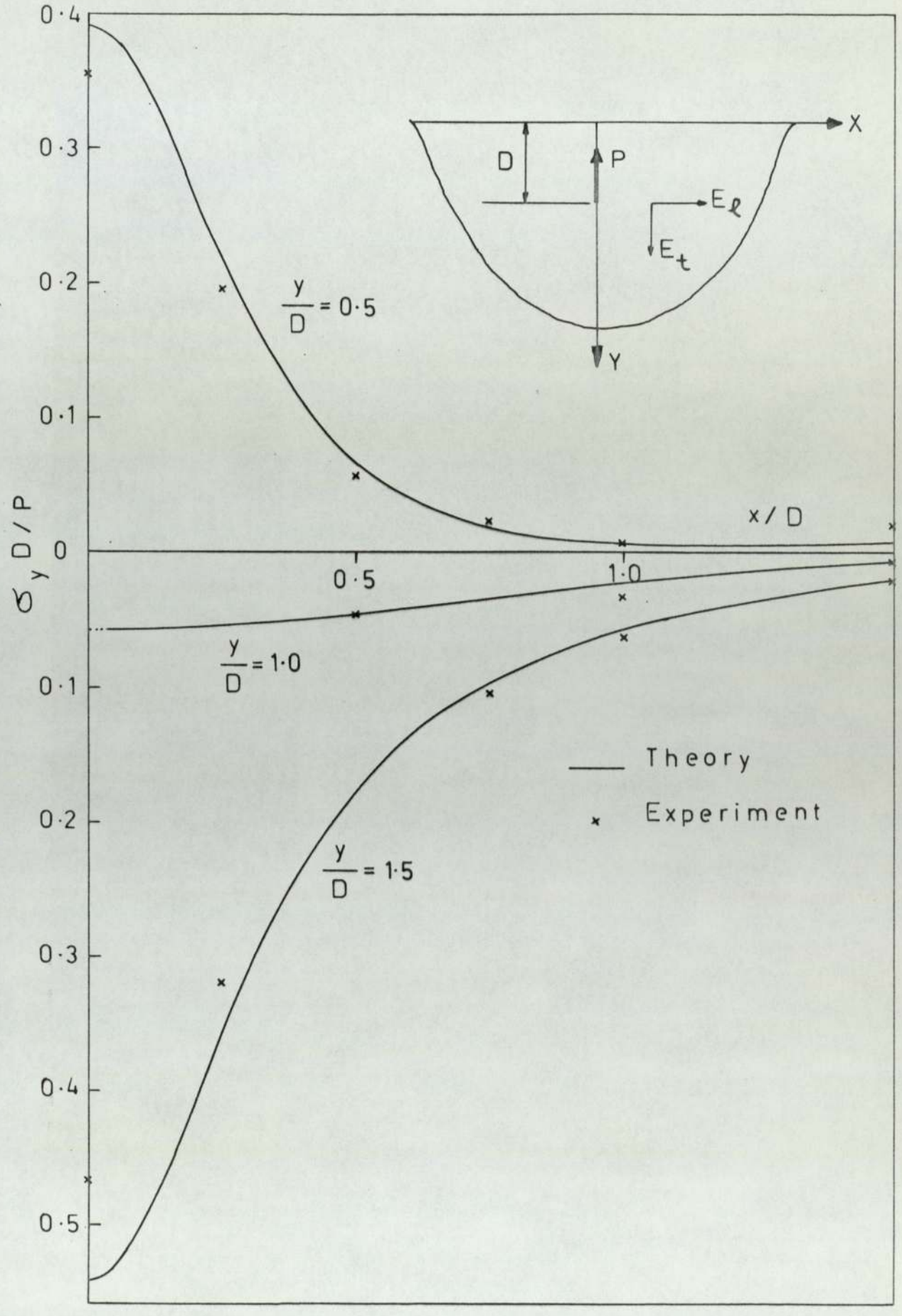

FIG.9.29 σ_y D/P vs x/D

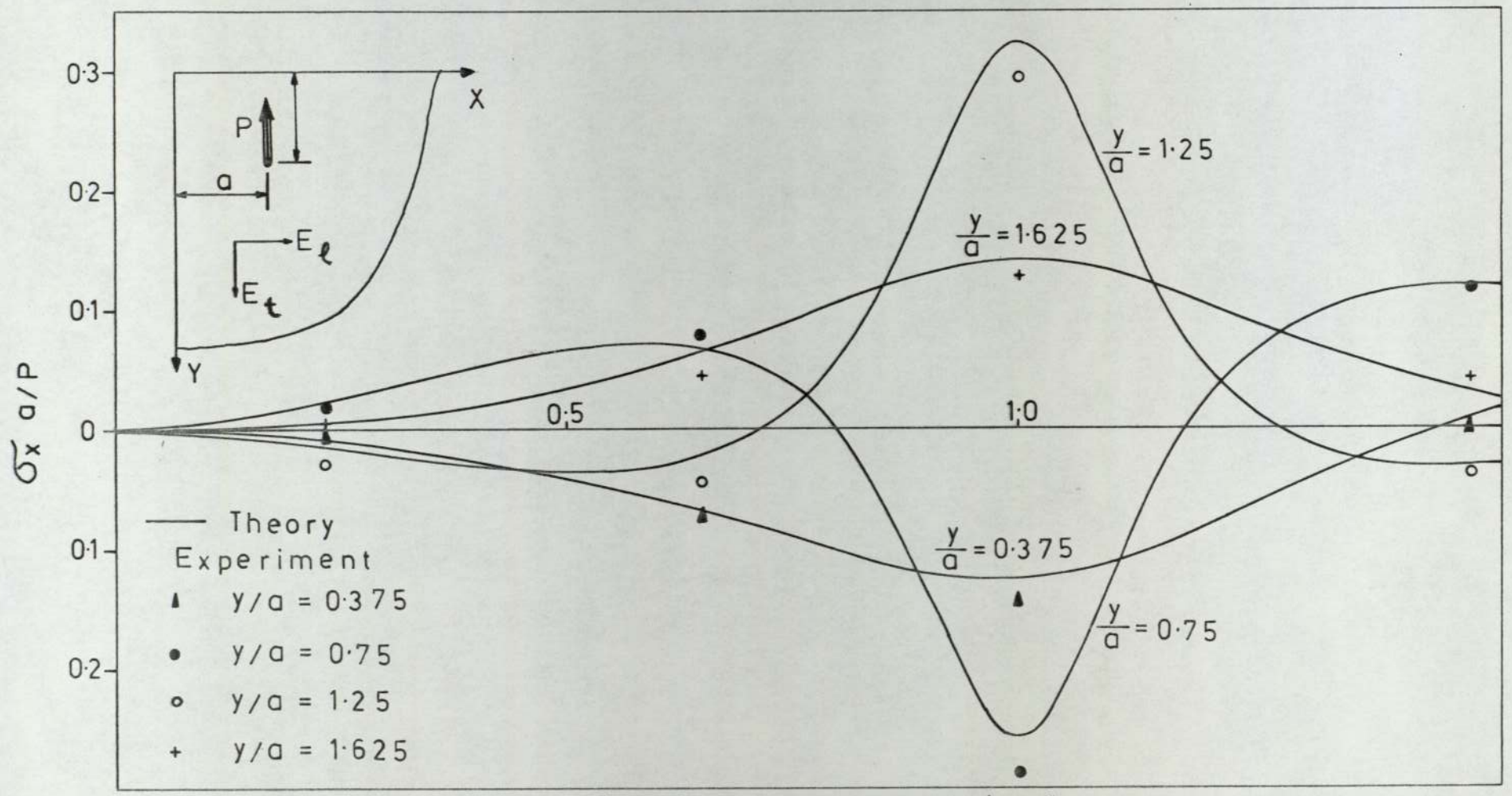

FIG. 9.30 Quarter plane — Interior concentrated force

σ_x a/P vs x/a

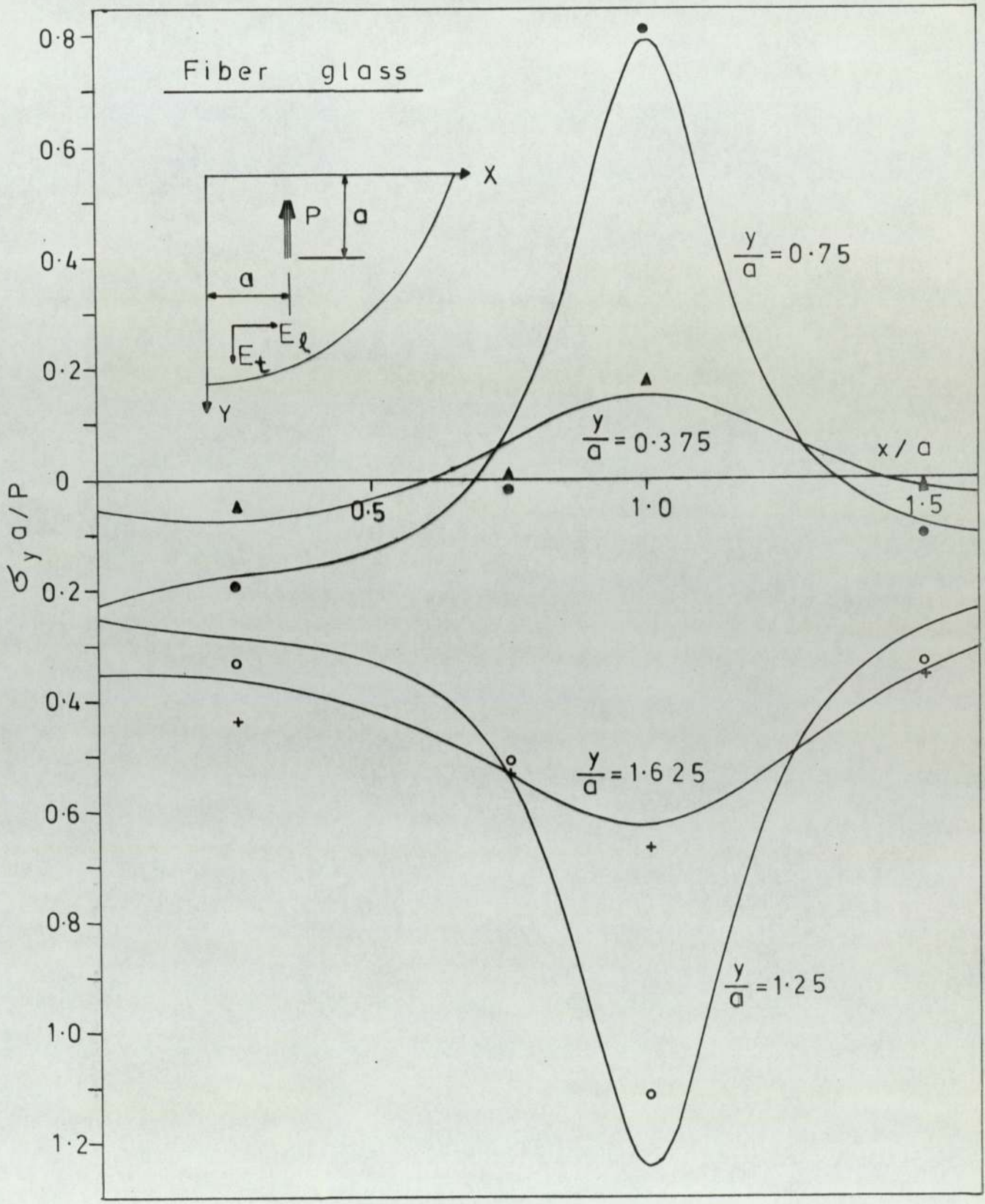

FIG. 9.31 Quarter plane – Interior concentrated force
σ_y a/P vs x/a

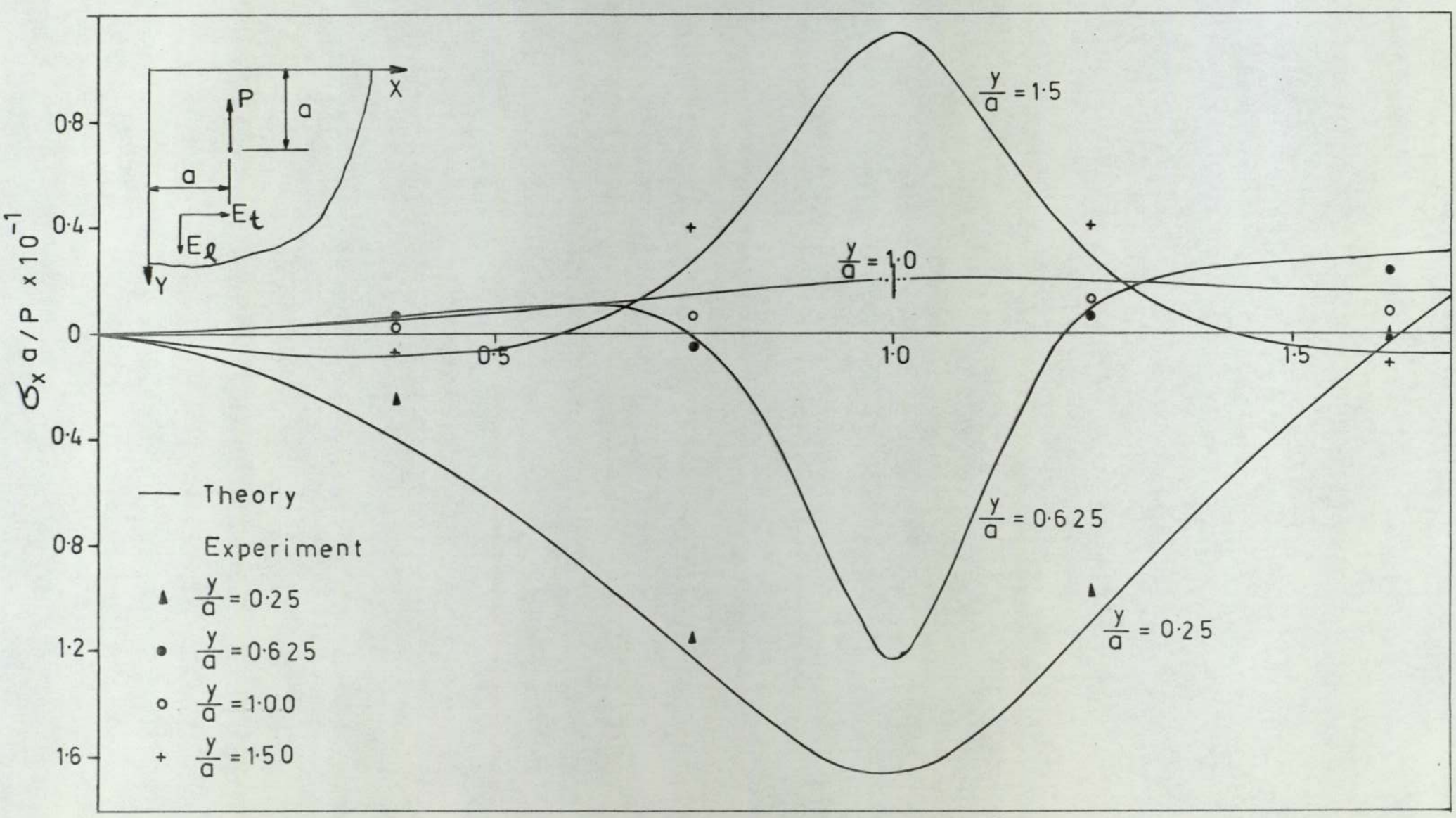

FIG. 9.32 Quarter plane — Concentrated force — σ_x a/P vs x/a

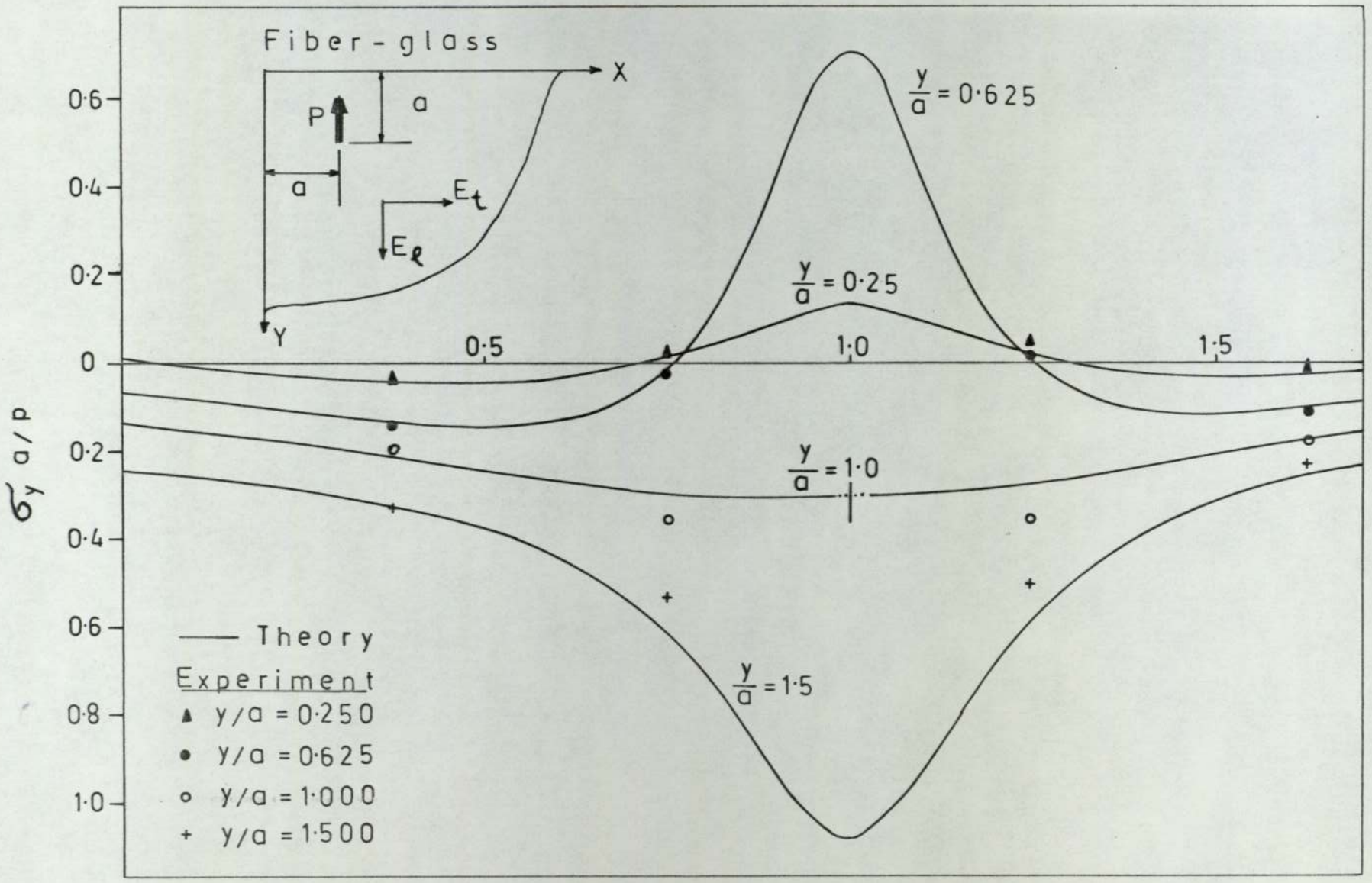

Fig.9.33 Quarter plane — Concentrated force — σ_y a/P vs x/a

APPENDIX 1.

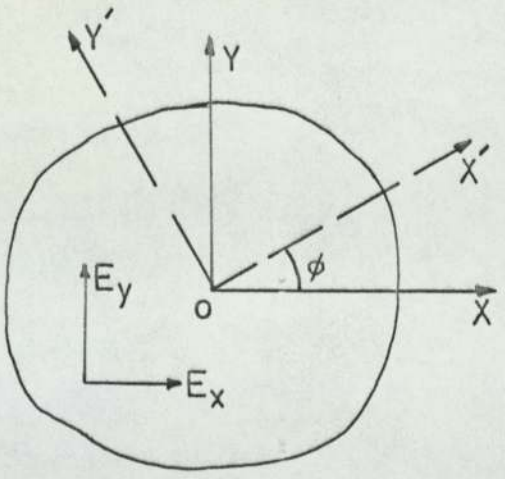

Fig.A1.1

The engineering elastic constants of an orthotropic body index plane stress, in the X'Y' coordinate system (see Fig.A1.1) are given in terms of the constants in the XY system, by the following relations:

$$\frac{1}{E_{x'}} = \frac{\cos^4\phi}{E_x} + \left(\frac{1}{G_{xy}} - \frac{2\nu_{xy}}{E_x}\right) \sin^2\phi \cos^2\phi + \frac{\sin^2\phi}{E_y} , \qquad \text{A1-1}$$

$$\frac{1}{E_{y'}} = \frac{\sin^4\phi}{E_x} + \left(\frac{1}{G_{xy}} - \frac{2\nu_{xy}}{E_x}\right) \sin^2\phi \cos^2\phi + \frac{\cos^2\phi}{E_y} , \qquad \text{A1-2}$$

$$\frac{1}{G'_{xy}} = \left(\frac{1}{E_x} + \frac{1}{E_y} + \frac{2\nu_{xy}}{E_x}\right) \sin^2\phi + \frac{\cos^2 2\phi}{G_{xy}} , \qquad \text{A1-3}$$

$$\nu'_{xy} = E_x \left[\frac{\nu_{xy}}{E_x} - \frac{1}{4}\left(\frac{1}{E_x} + \frac{1}{E_y} + \frac{2\nu_{xy}}{E_x} - \frac{1}{G_{xy}}\right) \sin^2 2\phi\right] , \qquad \text{A1-4}$$

APPENDIX 2.

The symbols which refer to the new orientation of the coordinate axes are denoted by a dash (') e.g. k_1', k_2' etc.

It can be verified that the elastic constants ℓ_{12} and ℓ_{66} remain unaltered, while ℓ_{11} and ℓ_{22} are replaced by ℓ_{22} and ℓ_{11} respectively

As a consequence:

$$\rho_1' = \rho_1 \frac{\ell_{22}}{\ell_{11}} \quad , \quad \rho_2' = \rho_2 \left(\frac{\ell_{22}}{\ell_{11}}\right)^2 \qquad \text{A2-1}$$

and

$$(k_1')^2 = \frac{\ell_{22}}{\ell_{11}} k_1^2, \quad (k_2')^2 = \frac{\ell_{22}}{\ell_{11}} k_2^2 \; . \qquad \text{A2-2}$$

From equation (2.6-4) we have:

$$\frac{\ell_{22}}{\ell_{11}} = \frac{1}{k_1^2 k_2^2} \; . \qquad \text{A2-3}$$

Substituting (A2-3) into (A2-2), and since $k_1, k_2 > 0$:

$$k_1' = \frac{1}{k_2} \quad , \quad k_2' = \frac{1}{k_1} \qquad \text{A2-4}$$

APPENDIX 3.

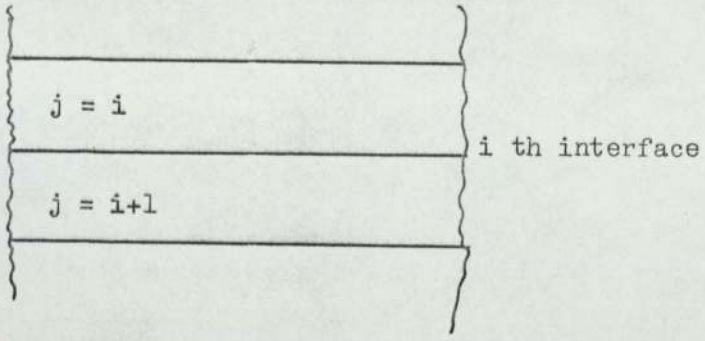

Fig.A3.1.

The displacements of u^j, v^j of a point (x_i, y_i) of the j^{th} layer on the i^{th} interface are given by:

$$\left[u^j\right]_{y_i} = \ell^j_{11} \int \sigma_x \, dx + \ell^j_{12} \int \sigma_y \, dx + f(x), \qquad \text{A3-1}$$

$$\left[v^j\right]_{y_i} = \ell^j_{12} \int \sigma_x \, dy + \ell^j_{22} \int \sigma_y \, dy + f(y),$$

where i = 1 ... n and j = i, i + 1.

The functions f(x) and f(y), which are assumed to represent rigid body rotations, can be excluded from the following equations since they do not affect the subsequent analysis (see equation 5.4-9).

Substituting the expressions for the stresses σ_x and σ_y from equation (5.4-1) into (A3-1), we have

$$\left[u^j\right]_{y_i} = \underset{\sim}{U}^j \, \underset{\sim}{\mathcal{L}}^j \sin(\lambda x), \qquad \text{A3-2a}$$

$$\left[v^j\right]_{y_i} = \underset{\sim}{V}^j \, \underset{\sim}{\mathcal{L}}^j \cos(\lambda x), \text{ for } i = 1 \ldots n, \; j = i, i+1,$$

where

$$\mathcal{Y}^j = \left\{ \left(\frac{\alpha_j^2 e^j_{11} - \lambda^2 e^j_{12}}{\lambda} \right) \begin{bmatrix} e^{\alpha_j y_i}; & e^{-\alpha_j y_i} \end{bmatrix} ; \left(\frac{\beta_j^2 e^j_{11} - \lambda^2 e^j_{12}}{\lambda} \right) \begin{bmatrix} e^{\beta_j y_i}; & e^{-\beta_j y_i} \end{bmatrix} \right\}$$

$$\mathcal{Y}^j = \left\{ \left(\frac{\alpha_j^2 e^j_{12} - \lambda^2 e^j_{22}}{\alpha_j} \right) \begin{bmatrix} e^{\alpha_j y_i}; & e^{-\alpha_j y_i} \end{bmatrix} ; \left(\frac{\beta_j^2 e^j_{12} - \lambda^2 e^j_{22}}{\beta_j} \right) \begin{bmatrix} e^{\beta_j y_i}; & e^{-\beta_j y_i} \end{bmatrix} \right\}$$

A3-2b

APPENDIX 4.

The elements of the $\underline{A}$ matrix are given by the following expressions:

$$a_{11} = \frac{1}{\Delta}\left[-2\alpha\beta \quad +(\alpha+\beta)\beta\, e^{-\alpha}\, e^{\beta} \quad + (\alpha-\beta)\beta e^{-\alpha}\, e^{-\beta}\right],$$

$$a_{12} = -\frac{\lambda}{\Delta}\left[-2\beta \quad +(\alpha+\beta)e^{-\alpha}\, e^{\beta} \quad - (\alpha-\beta)e^{-\alpha}\, e^{-\beta}\right],$$

$$a_{13} = \frac{1}{\Delta}\left[-2\alpha\beta\, e^{-\alpha} \quad +(\alpha+\beta)\beta e^{-\beta} \quad + (\alpha-\beta)\beta\, e^{\beta}\right].$$

$$a_{14} = -\frac{\lambda}{\Delta}\left[-2\beta\, e^{-\alpha} \quad +(\alpha+\beta)e^{-\beta} \quad - (\alpha-\beta)e^{\beta}\right],$$

$$a_{21} = -\frac{1}{\Delta}\left[2\alpha\beta \quad -(\alpha+\beta)\beta e^{\alpha} e^{-\beta} \quad - (\alpha-\beta)\beta e^{\alpha}\, e^{\beta}\right],$$

$$a_{22} = \frac{\lambda}{\Delta}\left[-2\beta \quad +(\alpha+\beta)e^{\alpha} e^{-\beta} \quad - (\alpha-\beta)e^{\alpha}\, e^{\beta}\right],$$

$$a_{23} = -\frac{1}{\Delta}\left[2\alpha\beta\, e^{\alpha} \quad -(\alpha+\beta)\beta\, e^{\beta} \quad - (\alpha-\beta)\beta\, e^{-\beta}\right].$$

$$a_{24} = \frac{\lambda}{\Delta}\left[-2\beta\, e^{\alpha} \quad +(\alpha+\beta)\, e^{\beta} \quad - (\alpha-\beta)\, e^{-\beta}\right],$$

$$a_{31} = \frac{1}{\Delta}\left[-2\alpha\beta \quad +(\alpha+\beta)\alpha e^{\alpha} e^{-\beta} \quad - (\alpha-\beta)\alpha e^{-\alpha} e^{-\beta}\right],$$

$$a_{32} = -\frac{\lambda}{\Delta}\left[-2\alpha \quad +(\alpha+\beta)e^{\alpha} e^{-\beta} \quad + (\alpha-\beta)e^{-\alpha} e^{-\beta}\right],$$

$$a_{33} = \frac{1}{\Delta}\left[-2\alpha\beta\, e^{-\beta} \quad +(\alpha+\beta)\alpha e^{-\alpha} \quad - (\alpha-\beta)\alpha\, e^{-\alpha}\right],$$

$$a_{34} = -\frac{\lambda}{\Delta}\left[-2\alpha\, e^{-\beta} \quad +(\alpha+\beta)e^{-\alpha} \quad + (\alpha-\beta)e^{\alpha}\right],$$

$$a_{41} = -\frac{1}{\Delta}\left[2\alpha\beta \quad -(\alpha+\beta)\alpha e^{-\alpha}\, e^{\beta} \quad + (\alpha-\beta)\alpha e^{\alpha} e^{\beta}\right],$$

$$a_{42} = \frac{\lambda}{\Delta}\left[-2\alpha \quad +(\alpha+\beta)e^{-\alpha} e^{\beta} \quad + (\alpha-\beta)e^{\alpha} e^{\beta}\right],$$

$$a_{43} = -\frac{1}{\Delta}\left[2\alpha\beta e^{\beta} \quad -(\alpha+\beta)\alpha\, e^{\alpha} \quad + (\alpha-\beta)\alpha\, e^{-\alpha}\right],$$

$$a_{44} = \frac{\lambda}{\Delta}\left[-2\alpha e^{\beta} \quad +(\alpha+\beta)e^{\alpha} \quad + (\alpha-\beta)\, e^{-\alpha}\right], \qquad \text{A4-1}$$

where

$$\Delta = \lambda^2 \left\{ 8\alpha\beta + (\alpha-\beta)^2 \left[e^{\alpha+\beta} + e^{-(\alpha+\beta)} \right] - (\alpha+\beta)^2 \left[e^{\alpha-\beta} + e^{+(\alpha-\beta)} \right] \right\} . \qquad A4-2$$

The elements of the $\underline{A}'$ matrix are given by:

$$a'_{21} = \frac{\beta' e^{\alpha'}}{\lambda^2(\alpha'-\beta')} , \quad a'_{22} = - \frac{\alpha' e^{\beta'}}{\lambda^2(\alpha'-\beta')} ,$$

$$a'_{41} = - \frac{e^{\alpha'}}{\lambda^2(\alpha'-\beta')} , \quad a'_{42} = \frac{e^{\beta'}}{\lambda^2(\alpha'-\beta')} . \qquad A4-3$$

APPENDIX 5.

For the F-functions to be convergent it must be shown that:

$$\left[\frac{2}{\pi}\ \frac{(\ell nk_1-\ell nk_2)}{(k_1-k_2)}\right]^2 k_1k_2 < 1. \qquad \text{A5-1}$$

The above inequality is simultaneously satisfied if:

$$\left[\frac{\ell nk_1-\ell nk_2}{k_1-k_2}\right]^2 k_1k_2 < 1. \qquad \text{A5-2}$$

Let

$$\alpha = \frac{k_1}{k_2} \text{ and } \beta = \ell n\ \frac{k_1}{k_2}. \qquad \text{A5-3}$$

Then, for $k_1 > k_2 > 0$,

$$\alpha > 1 \quad \text{and} \quad \beta > 0. \qquad \text{A5-4}$$

Inequality (A5-2) can be written as follows:

$$\alpha^2 - (2+\beta^2)\alpha + 1 > 0 \qquad \text{A5-5}$$

or

$$\left[\alpha - \left(1 + \frac{\beta^2}{2} + \frac{\beta}{2}\sqrt{\beta^2+4}\right)\right]\left[\alpha - \left(1 + \frac{\beta^2}{2} - \frac{\beta}{2}\sqrt{\beta^2+4}\right)\right] > 0 \qquad \text{A5-6}$$

Now, since

$$1 + \frac{\beta^2}{2} > \frac{\beta}{2}\sqrt{\beta^2+4} > 0, \qquad \text{A5-7}$$

inequality (A5-5) is simultaneously satisfied if

$$\alpha > 1 + \frac{\beta^2}{2} + \frac{\beta}{2}\sqrt{\beta^2+4}. \qquad \text{A5-8}$$

We can write A5-8 in the following form:

$$\alpha = e^{\beta} = 1 + \beta + \frac{\beta^2}{2!} + \frac{\beta^3}{3!} + \ldots > 1 + \frac{\beta^2}{2} + \frac{\beta}{2}\sqrt{\beta^2+4}\ , \quad \text{A5-8}$$

which reduces to:

$$\beta + \frac{\beta^3}{3!} + \ldots > \frac{\beta}{2}\sqrt{\beta^2+4}. \qquad \text{A5-9}$$

Finally, considering the first two terms of the series (equation A5-9), it can be shown that (A5-9) reduces to:

$$\frac{\beta^2}{9} + \frac{4}{3} > 1 \qquad \text{A5-10}$$

which is true for all values of β.

REFERENCES

REFERENCES.

1) ACUM,W.E.A. and L.FOX, 1951 "Computation of load stresses in a three-layer elastic system". Geotechnique, Vol.II,No.4.

2) AKÖZ,A.Y. and T.R.TAUCHERT, 1973. "Plane deformation of an orthotropic elastic semispace subject to distributed surface loads". J.Appl.Mech. Vol.95.

3) Aℓ-KHAYATT, Q.J. 1974. "The structural properties of glass fibre reinforced plastics". Ph.D.Thesis. The University of Aston in Birmingham, England.

4) BAKER,B.R. 1964. "Closed forms for the stresses in a class of orthotropic wedges." J.Appl.Mech. Paper 64-WA/APM-5.

5) BARDEN,L. 1963. "Stresses and displacements in a cross-anisotropic soil". Geotechnique. Vol.13, No.3.

6) BENTHEM,J.P. 1963. "On the stress distribution in anisotropic infinite wedges". Quart.Appl.Math. Vol.21.

7) BERRY,D.S. 1960. "An elastic treatment of ground movement due to mining".I.Isotropic ground.J.Mech.Phys.Solids.Vol.8.

8) BERRY,D.S. 1961. "An elastic treatment of ground movement due to mining". II. Transversely isotropic ground. J.Mech.Phys. Solids. Vol.9.

9) BERRY,D.S. and T.W.SALES. 1962. "An elastic treatment of ground movement due to mining". III. Three dimensional problem. Transversely isotropic ground. J.Mech.Phys.Solids.Vol.10.

10) BIOT,M.A. 1935. "Effect of certain discontinuities on the pressure distribution in a loaded soil". Physics. Vol.6. No.12.

11) BORESI,A.P. 1965. "Elasticity in engineering mechanics." Prentice-Hall.

12) BRILLA,J. 1962. "Contact problems of an elastic anisotropic half-plane". Revue de Mechanique appliquee.Vol.VII,No.3.

13) BURMISTER,D.M. 1943. "The theory of stresses and displacements in layered systems and applications to the design of airport runways". Proc.23rd Annual Meeting of the Highway Research Board.

14) BURMISTER,D.M. 1945. "The general theory of stresses and displacements in layered systems, III". J.Appl.Phys. Vol.16, No.2; No.3; No.5.

15) CALCOTE,L.R. 1969. "The analysis of laminated composite structures". Van Nostrand Reinhold Co.

16) CAROTHERS,S.D. 1912. Proc.Roy.Soc. Edinburgh, Sect.A, Vol.23.

17) CAROTHERS,S.D. 1920. "Plane strain: the direct determination of stress". Proc.Roy.Soc. (London) Ser.A Vol.97.

18) CHARRIER,I.M. and M.J.SUDLOW. 1973. "Structure-properties relationships for short-fibre composites". Fibre Science and Technology, Vol.6, No.4.

19) CHEN,C.H. and S.CHENG. 1967. "Mechanical properties of fibre reinforced composites". J.Comp.Mat. Vol.1.

20) CHEN,C.H. and S.CHENG, 1970. "Mechanical properties of anisotropic fibre-reinforced composites". J.Appl.Mech. Vol.37.

21) CHURCHILL,R.V. 1941. "Fourier series and boundary value problems". McGraw-Hill, New York.

22) CONWAY,H.D. 1953a. "Some problems of orthotropic plane stress". J.Appl.Mech. Vol.20.

23) CONWAY,H.D. 1953b. "The stress distributions induced by concentrated loads acting in isotropic and orthotropic half-planes". J.Appl.Mech. Vol.20.

24) CONWAY,H.D. 1955a. "Further problems in orthotropic plane stress". J.Appl.Mech. Vol.22.

25) CONWAY,H.D. 1955b. "The indentation of an orthotropic half-plane". ZAMP. Vol.VI.

26) CONWAY,H.D. 1955c. "Stress distributions in orthotropic strips". J.Appl.Mech. Vol.22.

27) CONWAY,H.D. 1955d. "Note on the orthotropic half-plane subjected to concentrated loads". J.Appl.Mech. Vol.22.

28) CONWAY,H.D. 1967. "The indentation of an orthotropic half-plane having inclined principal axes". J.Appl.Mech. Vol.34.

29) DIETZ,A.G.H. 1965. "Composite Materials". Edgar Marburg Lecture. A.S.T.M.

30) DOBIE,W. 1948. "Electric resistance strain gauges". E.V.P.

31) DURELLI,A.J. 1967. "Applied stress analysis". Prentice-Hall.

32) EKVALL,J.C. 1961. "Elastic properties of orthotropic mono filament laminates". ASME Paper 61-AV-56, Aviation Conference, Los Angeles.

33) FILON,L.N.G. 1902. "On an approximate solution for the bending of a beam of rectangular cross-section under any system of load, with special reference to points of concentrated or discontinuous loading". Trans.Roy.Soc. Ser.A, Vol.201.

34) FLAMANT, 1892. Compt.Rend. Vol.114.

35) FLUGGE,W.(Ed) (1962). "Handbook of Engineering Mechanics." McGraw-Hill, New York.

36) FOYE,R.L. 1972. "The transverse Poisson's ratio of composites". J.of Comp.Materials. Vol.6.

37) GERRARD,C.M. 1967. "Stresses and displacements in layered cross-anisotropic elastic systems". Proc.5th Aust.- New Zealand Conf.Soil Mech.Fndn.Eng.

38) GERRARD,C.M. and W.J.HARRISON, 1970. "Stresses and displacements in a loaded orthorombic half-space". C.S.I.R.O. Aust.Div.App.Geomech.Tech. Paper No.9.

39) GERRARD,C.M. and W.J.HARRISON, 1971. "The analysis of a loaded half-space comprised of anisotropic layers". C.S.I.R.O. Aust.Div.App.Geomech.Tech.Paper No.10.

40) GIRKMANN,K., 1943. "Angriff von Einzellasten in der striefenformigen Scheibe". Ingenieur Archiv. Vol.13.

41) GODFREY,D.E.R. 1955. "Generalized plane stress in an elastic wedge under isolated loads". Quart.J.Mech.Appl.Math.,Vol.8.

42) GOODMAN,J.R. and J.BODRIG, 1970. "Orthotropic elastic properties of wood". Proc.ASCE. J.Struct.Div. ST.11.

43) GREEN,A.E. and G.I.TAYLOR, 1939. "Stress systems in aelotropic plates I". Proc.Roy.Soc.Sec.A. Vol.173.

44) GREEN,A.E. 1939. "Stress systems in aelotropic plates II". Proc.Roy.Soc.Ser.A. Vol.173.

45) GREEN,A.E. and W.ZERNA, 1954. "Theoretical Elasticity". Oxford University Press.

46) HARR,M.E. 1966."Foundations of theoretical soil mechanics." McGraw-Hill.

47) HARRINGTON,W.J. and T.W.TING, 1971, "The existence an uniqueness of solution to certain wedge problems". J.Elasticity Vol.1.

48) HASHIN,Z. 1960. "On the determinations of Airy polynomial stress functions." Bull.Res.Counc.of Israel.Vol.8 C

49) HASHIN,Z. 1967. "Plane anisotropic beams". J.Appl.Mech. Vol.34.

50) HASHIN,Z. and B.W.ROSEN, 1964. "The elastic moduli of fibre-reinforced materials". J.Appl.Mech. Vol.31.

51) HEARMON,R.F.S. 1946. "The elastic constants of anisotropic materials". Reviews of Modern Physics. Vol.18, No.3.

52) HEARMON,R.F.S. 1961. "Applied anisotropic elasticity". Oxford University Press.

53) HETÈNYI,M. 1960. "A method of solution for the elastic quarter-plane". J.Appl.Mech. Vol.27.

54) HETÈNYI,M. 1970. "A general solution for the elastic quarter space". J.Appl.Mech. Vol.37.

55) HOFFMAN,O. 1967. "The brittle strength of orthotropic materials". J.Comp.Mat. Vol.1.

56) HOLISTER,G.S. 1967. "Experimental stress analysis and methods". Cambridge University Press.

57) HOLISTER,G.S. and C.THOMAS, 1966. "Fibre reinforced materials". Elsevier Publ. Co., London.

58) HOLLIDAY,L. 1966. "Composite materials" Elsevier Publ.Co.,

59) HOOLEY,R.F. and P.D.HIBBERT, 1967. "Stress concentration in timber beams". Proc.ASCE.J.Struct.Div. ST.2

60) HOWLAND,R.C.J. 1929. "Stress systems in an infinite strip". Proc.Roy.Soc.(London). Ser.A.Vol.124.

61) ISENBERG,J. and S.ADHAM, 1970. "Analysis of orthotropic reinforced concrete structures". Proc.ASCE.J.Struct.Div. ST12.

62) IYENGAR,K.T.S.R. 1962. "A Fourier-integral solution for the elastic quarter-plane". J.Franklin Inst. 272.

63) JAEGER,J.C. 1956. "Elasticity fracture and flow". Metheun

64) KAMADA,T. 1966. "On the simple tension of an anisotropic semi-infinite plate with partially stiffened edge". J.Appl.Mech. Vol.33.

65) KUO,S.S. 1972. "Computer applications of numerical methods". Addison-Wesley.

66) LANG,H.A. 1956. "The affine transformation for orthotropic plane stress and plane strain problems". J.Appl.Mech. Vol.23.

67) LEKHNITSKII,S.G. 1963. "Theory of elasticity of an anisotropic elastic body". Holden-Day, San Fransisco.

68) LEMCOE,M.M. 1960. "Stresses in layered elastic solids". J.Eng.Mech.Div.Proc. of the A.S.C.E. E.M.4.

69) LEMPRIERE,B.M. 1968. "Poisson's ratio in orthotropic materials". A.I.A.A.Journal. Vol.6, No.11.

70) LEVY,M., 1898. Compt.Rend. Vol.126.

71) LOVE,A.E.H. 1906. "A treatise on the mathematical theory of elasticity". Cambridge University Press.

72) MAJUMDAR,S. and P.V.McLOUGHLIN Jr. 1973. "Upper bounds to in-plane shear strength of unidirectional fibre-reinforced composites". J.Appl.Mech.Vol.95.

73) MICHELL,J.H. 1900. "The stress distribution in an aelotropic solid with an infinite plane boundary". Proc.London Math.Soc. Vol.32.

74) MICHELL,J.H. 1902. Proc.London Math,Soc. Vol.34.

75) MILNE-THOMSON, 1962. "Antiplane elastic systems". Spring-Verlag, Berlin.

76) MILNE-THOMSON, 1968. "Plane elastic systems". Springer, Berlin.

77) MOODY,W.I. 1961, "A method of solution for the elastic quarter plane". Discussion. J.Appl.Mech. Vol.28.

78) MUSKHELISHVILI,N.I. 1953. "Some basic problems of the mathematical theory of elasticity". Groningen, Noordhoff.

79) NEUBERT,H.K.P. 1967, "Strain gauges: kinds and uses". Macmillan.

80) OGORKIEWICZ,R.M. 1970. "Mechanical behaviour of fibre composites". G.R.P. Ed.B.Parkyn.

81) OGORKIEWICZ,R.M. 1973. "Orthotropic characteristics of glass-fibre-epoxy laminates under plane stress". J.Mech.Eng.Science Vol.15, No.2.

82) OKUBO,H. 1940. "The stress distribution in a semi-infinite domain having a plane boundary and compressed by a rigid body". Z.Angew.Math.Mech.Bd. 20, Nr.5.

83) OKUBO,H. 1941. "Stress systems in an aelotropic rectangular plate". Z.Angew.Math.Mech.Bd. Vol.21, Nr.3.

84) OKUBO,H. 1951. "On the two-dimensional problem of a semi-infinite elastic body compressed by an elastic plane". Quart.J.Mech. and Appl.Math. Vol.IV, Pt.3.

85) PAGANO,N.J. and J.C.HALPIN, 1968. "Influence of end constraint in the testing of anisotropic bodies". J.Comp.Mat. Vol.2, No.1.

86) PICKERING,D.J. 1970. "Anisotropic elastic parameters for soil". Geotechnique Vol.20, No.3.

87) PICKETT,G. 1938. Proc.18th annual meeting Highway Research Board Vol.18, pt.II.

88) PICKETT,G. 1944. "Application of the Fourier method to the solution of certain boundary problems in the theory of elasticity". J.Appl.Mech. Vol.66.

89) POTITSKY,H. 1961. "A method of solution for the elastic quarter-plane". Discussion J.Appl.Mech. Vol.28.

90) POULOS,H.G. 1967. "Stresses and displacements in an elastic layer underlain by a rough rigid base". Geotechnique. Vol.17, No.4.

91) POULOS,H.G. and E.H.DAVIS, 1974. "Elastic solutions for soil and rock mechanics". J.Wiley and Sons Inc.

92) REYNOLDS,H.R. 1961. "Rock Mechanics". Lockwood.

93) ROSEN,B.W, DOW,N.F. and Z.HASHIN, 1964. "Mechanical properties of fibrous composites". NASA CR-31.

94) SADOWSKY,M. 1928. "Zweidimensionale probleme der Elastizitatstheorie". Z.Angew. Math.Mech. 8.

95) SAHA,S, MUKHERJEE,S. and C.C.CHAO, 1972. "Concentrated forces in semi-infinite anisotropic media". J.Comp.Mat. Vol.6.

96) SALAMON,M.D. 1968. "Elastic moduli of stratified rock mass". Int.J.Rock Mech.Min.Science. Vol.5.

97) SCOTT,J.R. 1965. "Physical testing of rubbers". Maclaren.

98) SELVADURAI,A.P.S. 1973. "Bending of an infinite beam resting on a porous elastic medium". Geotechnique.Vol.23, No.3.

99) SELVADURAI,A.P.S. and N.MOUTAFIS, 1975. "Some generalized results for an orthotropic elastic quarter-plane". Applied Scientific Research, Vol.30, No.6.

100) SEN,B. 1954. "Note on two-dimensional indentation problems of a non-isotropic semi-infinite elastic medium". ZAMP Vol.V.

101) SLIKER,A. 1972. "Measuring Poisson's ratios in wood". Experimental mechanics. Vol.12, No.5.

102) SMITH,C.S. 1974. "Applications of fibre reinforced composites in marine technology". Composites-Standards, Testing and Design. National Physical Laboratory Conference.

103) SNEDDON,I.N. 1951. "Fourier transforms" McGraw-Hill, New York.

104) SPENCER,A.J.M. 1972. "Deformations of fibre-reinforced materials". Clarendon Press, Oxford.

105) STERNBERG,E. and W.T.KOITER, 1958. "The wedge under a concentrated couple: A paradox in the two dimensional theory of elasticity". J.Appl.Mech. Vol.25.

106) SUN,C.T. 1973. "Incremental deformations in orthotropic laminated plates under initial stress". J.Appl.Mech. Vol.95.

107) THOMASON,P.F. 1973. "Stress distribution in a wedge for boundary conditions approximating to the rake-face loads of a metal cutting tool". J.Mech.Eng.Science.Vol.15, No.3.

108) TIMOSHENKO,S.P. and J.N.GOODIER, 1970. "Theory of elasticity". McGraw-Hill, New York.

109) TRANTER,C.J. 1948. "The use of the Mellin transform in finding the stress distribution in an infinite wedge". Q.J.Mech.Appl.Math.Vol.1.

110) TSAI,S.W. 1964. "Structural behaviour of composite materials". NASA CR-71.

111) TSAI,S.W. 1968. "Composite materials workshop". Technomic Publ.Co. Stanford, Conn.

112) UESHITA,K. and G.C.MEYERHOFF, 1967. "Deflection of multilayer soil systems". J.Soil Mech.Fndns.Div. ASCE, Vol.93 No.SM5.

113) VERSTRAETEN,J. 1967. "Stresses and displacements in elastic layered systems". Proc.2nd Int.Conf.Struct.Design of Asphalt Pavements. University of Michigan.

114) WENDT,F.W. et al.1967. "Mechanics of composite materials". Proc.5th Symp.on Naval Struct.Mech. Pergamon Press,Oxford.

115) WHIFFIN,A.C. and N.W.LISTER, 1962. "The application of elastic theory to flexible pavements." Int.Conf. of Struct. Design of Asphalt Pavements. University of Michigan.

116) WHITNEY,J.M. 1967. "Elastic moduli of unidirectional composites with anisotropic filaments". J.Comp.Mat. Vol.1.

117) WHITNEY,J.M. and M.B.RILEY, 1966. "Elastic properties of fibre reinforced composite materials". AIAA Journal.

118) WU,E. and R.L.THOMAS, 1968. "Off-axis test of a composite". J.Comp.Mat. Vol.2, No.4.

119) YU,C.J. 1973. "Local effects of a concentrated load applied to orthotropic beams".J.Franklin Inst. Vol.296, No.3.